Louisiana Transportation Research Center

Technical Assistance Report 15-01TA-C

Evaluation of Cores from I-10 between Acadian Thruway and College Drive

by

Tyson Rupnow, Ph.D., P.E.
Zachary Collier, E.I.
Amar Raghavendra, P.E.

LTRC

4101 Gourrier Avenue | Baton Rouge, Louisiana 70808
(225) 767-9131 | (225) 767-9108 fax | www.ltrc.lsu.edu

TECHNICAL REPORT STANDARD PAGE

1. Report No.	2. Government Accession No.	3. Recipient's Catalog No.
FHWA/LA.15/15-01TA-C		

4. Title and Subtitle	5. Report Date
Evaluation of Cores from I-10 Between Acadian Thruway and College Drive	6. Performing Organization Code LTRC Project Number: 15-01TA-C SIO Number: DOTLT1000064
7. Author(s) Tyson Rupnow, Ph.D., P.E., Zachary Collier, E.I., and Amar Raghavendra, P.E.	8. Performing Organization Report No.
9. Performing Organization Name and Address Louisiana Transportation Research Center 4101 Gourrier Avenue Baton Rouge, LA 70808	10. Work Unit No. 11. Contract or Grant No.
12. Sponsoring Agency Name and Address Louisiana Department of Transportation and Development P.O. Box 94245 Baton Rouge, LA 70804-9245	13. Type of Report and Period Covered **Technical Assistance** **November 2015** 14. Sponsoring Agency Code

15. Supplementary Notes
Conducted in Cooperation with the U.S. Department of Transportation, Federal Highway Administration

16. Abstract
This technical assistance report documents the investigation conducted by the Louisiana Transportation Research Center (LTRC) of the cored concrete from Eastbound and Westbound I-10 between Acadian Thruway and College Drive in Baton Rouge, LA. The top 3-4 inches of the cores in highly distressed areas were difficult to obtain. The petrographic analysis showed that there are no signs of alkali carbonate reaction (ACR). Alkali silica reaction (ASR) was present, but not significant enough to cause the distress observed. The petrographic analysis showed that the highly distressed areas contained excessive air content, averaging 17 percent, in the top 3-4 inches of the pavement. This excessive air content leads to a weaker concrete and, when combined with the shrinkage cracking, can lead to spalling of the affected areas. Potential remedies include partial depth patching, full depth patching with a panel replacement or hydroblasting the top 3-4 inches of the section and completing a bonded overlay.

17. Key Words	18. Distribution Statement
	Unrestricted. This document is available through the National Technical Information Service, Springfield, VA 21161.

19. Security Classif. (of this report)	20. Security Classif. (of this page)	21. No. of Pages	22. Price

Evaluation of Cores from I-10 between Acadian Thruway and College Drive

by

Tyson Rupnow, Ph.D., P.E.
Zachary Collier, E.I.
Amar Raghavendra, P.E.

Louisiana Transportation Research Center
4101 Gourrier Avenue
Baton Rouge, LA 70808

LTRC Project No. 15-01TA-C

conducted for

Louisiana Department of Transportation and Development
Louisiana Transportation Research Center

February 2016

ABSTRACT

This technical assistance report documents the investigation conducted by the Louisiana Transportation Research Center (LTRC) of the cored concrete from Eastbound and Westbound I-10 between Acadian Thruway and College Drive in Baton Rouge, LA. The top 3-4 inches of the cores in highly distressed areas were difficult to obtain. The petrographic analysis showed that there are no signs of alkali carbonate reaction (ACR). Alkali silica reaction (ASR) was present, but not significant enough to cause the distress observed. The petrographic analysis showed that the highly distressed areas contained excessive air content, averaging 17 percent, in the top 3-4 inches of the pavement. This excessive air content leads to a weaker concrete and, when combined with the shrinkage cracking, can lead to spalling of the affected areas. Potential remedies include partial depth patching, full depth patching with a panel replacement or hydroblasting the top 3-4 inches of the section and completing a bonded overlay.

TABLE OF CONTENTS

INTRODUCTION

This report will detail the condition of cores taken from East and Westbound I-10 between Acadian Thruway and College Drive. The cores were being investigated due to visible surface cracking and spalling in select areas.

OBJECTIVE AND SCOPE

The objective of the study was to determine and document the extent and cause of cracking and spalling noted in a section of Eastbound I-10 between Acadian Thruway and College Drive. To meet the objective, eight cores were obtained for petrographic analysis. An additional five pavement cores from the affected area and two median barrier wall cores were also obtained to further clarify the results from the petrographic analysis.

METHODOLOGY

LTRC Concrete Research Laboratory personnel obtained eight cores, four in each direction, (see Figure 1) with assistance of District personnel in April 2015 with five additional cores being obtained in July 2015. The cores were photographed and sent to the petrographer for analysis. A petrographic analysis was conducted according to ASTM C856 and ASTM C1723.

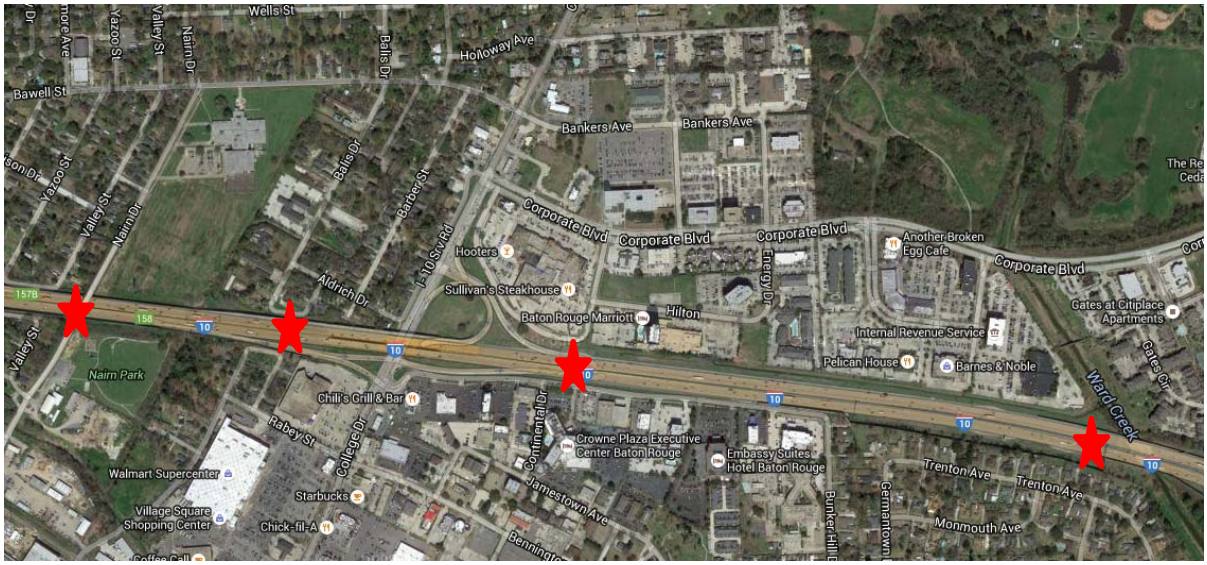

Figure 1
Core locations

DISCUSSION OF RESULTS

This section will provide a brief overview of the petrographic analysis results.

Core Conditions

The cores were retrieved to about a 16-inch depth. In general, intact cores were difficult to obtain in the highly distressed areas. The cores showed high distress limited to the top 3-4 inches. The pavement thickness exceeded 16 inches in most places.

Petrographic Results

The results from the petrographic analysis showed that there is no ACR occurring in the samples. The cracking exhibited by the pavement was most likely due to shrinkage cracking. ASR is present in the cores, but is localized around the sand particles and is not in a sufficient quantity to cause the deterioration that the Department is seeing in the pavement. The initial report showed that in the affected areas exhibiting a large amount of spalling, the entrained air content was significantly higher than the surrounding concrete. The cracking is attributed to shrinkage cracks most likely due to the moderate aggregate gradation.

The deterioration is attributed to excessive air content. The petrographic report notes that the top 3-4 inches generally average 17 percent air content with mid-slab air content in the normal range. Figure 2 shows the distribution of air void content by volume. Note that the excessive air void content exceeds 15 percent. This will make the concrete very weak and susceptible to deterioration. Figure 3 shows the same results but limits it to the top, middle, and bottom portion of the pavement.

Figures 4 and 5 show the images for pavement core number 1. Note that in these images the sample is polished, colored black, and the voids are then filled with a white paste to show the contrasting air void distribution. Note that Figure 4 shows the top and bottom sections while Figure 5 shows the sections in more detail. The results show that the concentration of air is extremely high in the distressed top 5 inches of the pavement core.

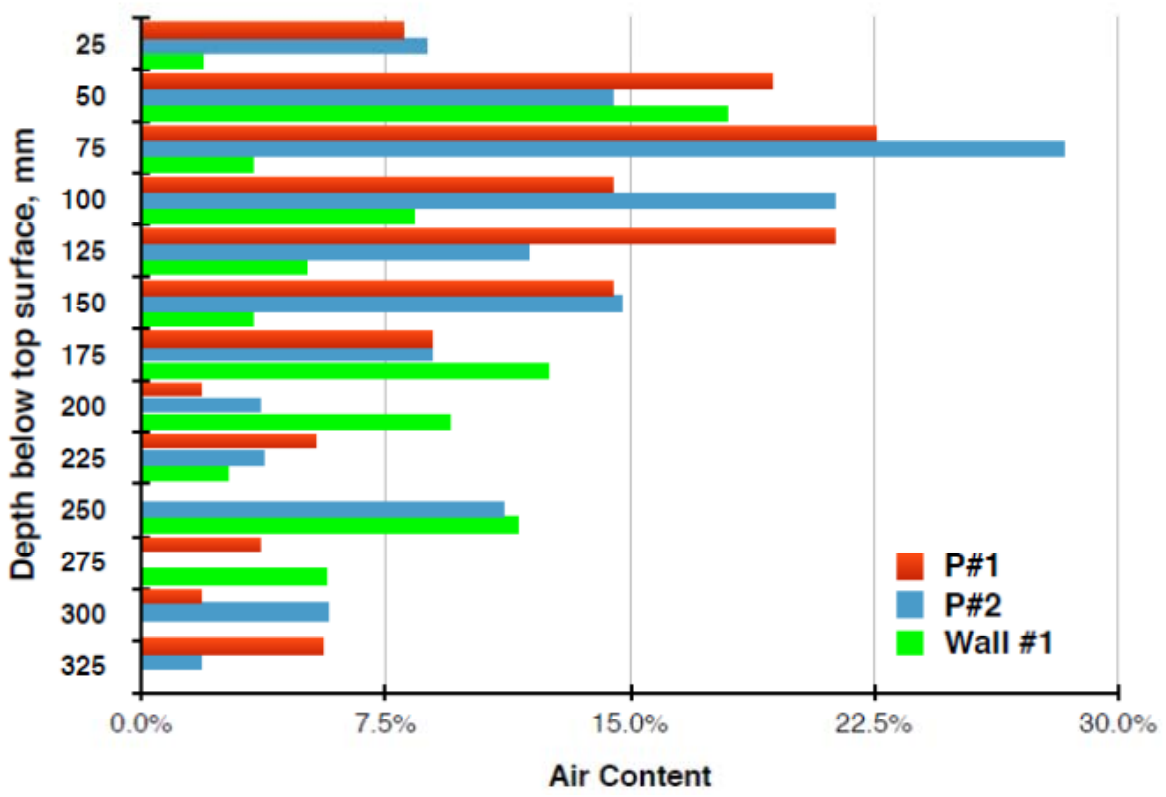

Figure 2
Distribution of air void content

Measured Parameters	P#1 Top	P#1 Middle	P#2 Top	P#2 Middle	Wall #1 Top	Wall #1 Middle
Aggregate Stops	218	290	229	257	249	261
Paste Stops (S_p)	80	80	71	104	78	71
Air Stops (S_a)	61	15	60	19	24	30
Total Stops (S_t)	359	385	360	380	351	362
Calculated Parameters	**P#1 Top**	**P#1 Middle**	**P#2 Top**	**P#2 Middle**	**Wall #1 Top**	**Wall #1 Middle**
Traverse Length (T_t; in.)	26.9	28.9	27.0	28.5	26.3	27.2
Traverse Length (T_t; mm)	427	458	428	452	418	431
Aggregate Content	60.7%	75.3%	63.6%	67.6%	70.9%	72.1%
Paste Content (p)	22.3%	20.8%	19.7%	27.4%	22.2%	19.6%
Air Content (A)	17.0%	3.9%	16.7%	5.0%	6.8%	8.3%
Paste-Air Ratio (p/A)	1.3	5.3	1.2	5.5	3.3	2.4

Note: Analysis done via the Point-Count Method (Method B) in ASTM C457 using a stepping distance of 1.905 mm (0.075 in.) at 125x magnification.

Figure 3
Air void contents for the top, middle, and bottom of cores

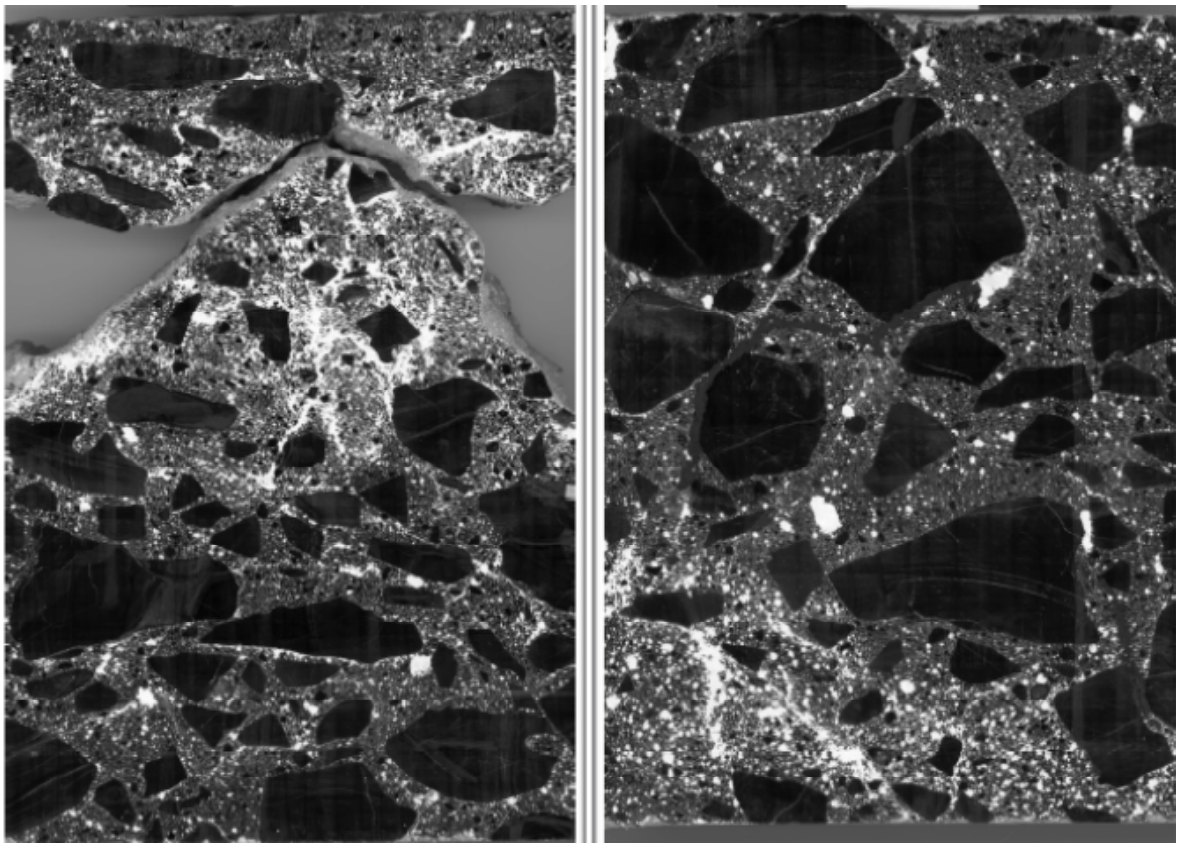

Figure 4
Pavement number 1 core; Left: top, Right: bottom

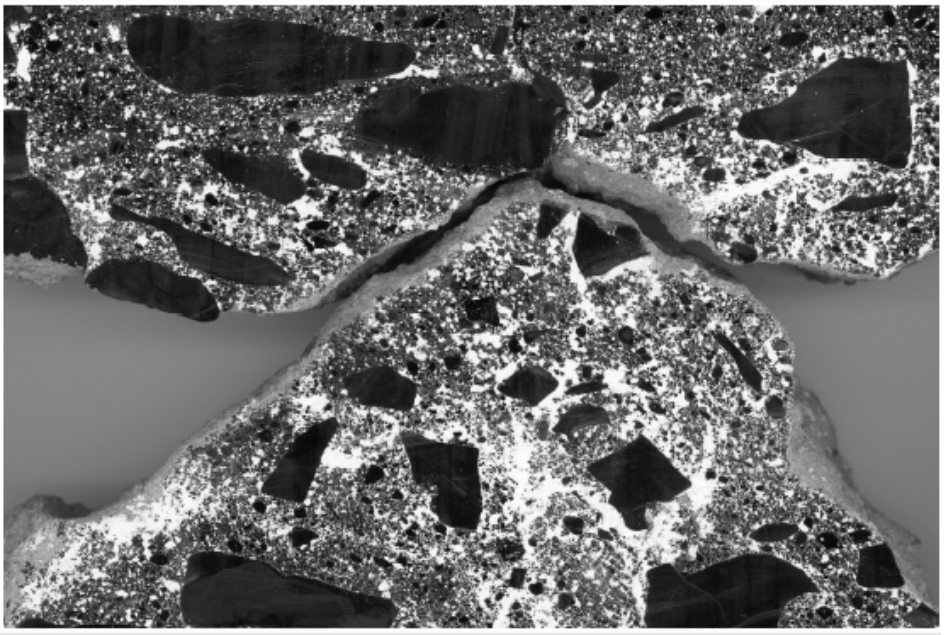

Figure 5
Top section of pavement number 1 core enhanced showing excessive air content

Figures 6 and 7 show the images for pavement core number 2. Note that for these images the sample is polished, colored black, and the voids are then filled with a white paste to show the contrasting air void distribution. Note that Figure 6 shows the top included with the middle section of the core, while Figure 7 shows the top distressed section in more detail. The results show that the concentration of air is extremely high in the distressed top 5 inches of the pavement core. Further elaboration on the results is included in the Appendix of this report, which contains the report from the petrographer.

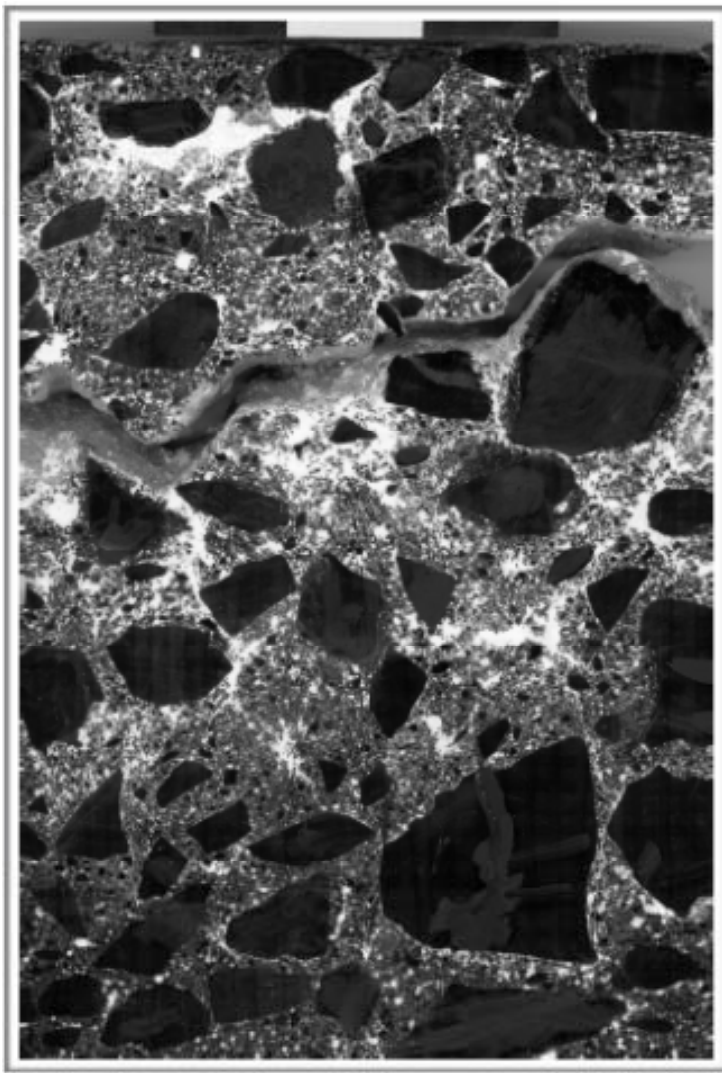

Figure 6
Top and middle section of pavement core number 2

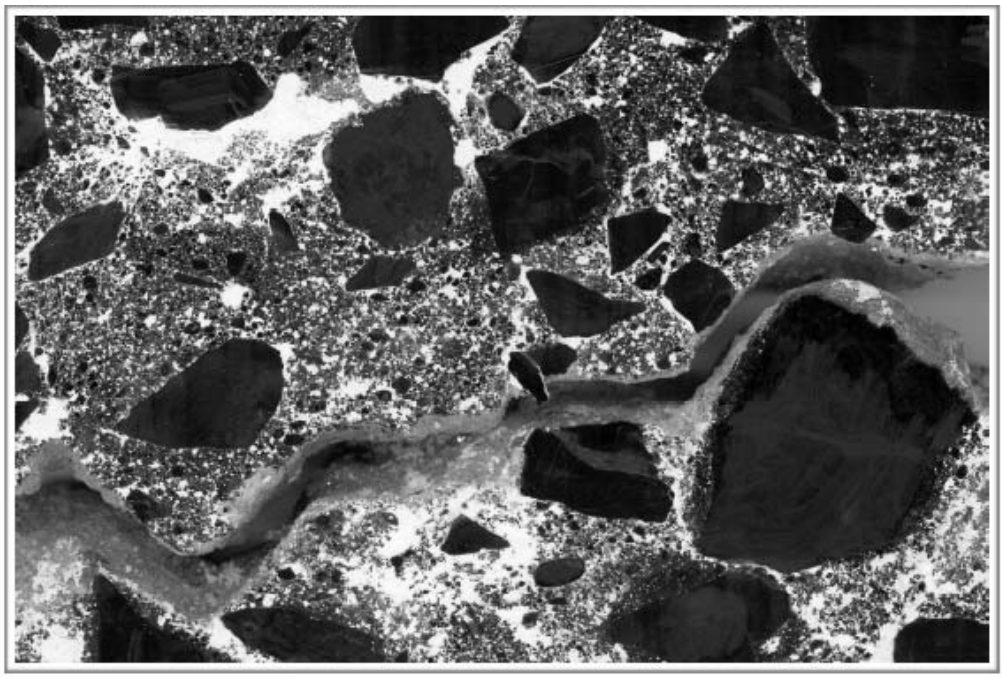

Figure 7
Top of pavement core number 2 enhanced showing excessive air void concentration

The excessive air content in the top sections of these cores can most likely be attributed to construction practices. If it were an admixture incompatibility issue, the authors believe that department personnel would see a far greater area in distress. It is the authors' opinion that the vibrators were set for the 14-inch thick pavement design with a certain paving speed, but the as constructed pavement thickness generally exceeds 16 inches. The combination of excess pavement thickness and vibrator settings most likely ensured that the excess air voids were not vibrated out of the pavement surface during the consolidation of the fresh concrete pavement as it was constructed.

Possible remedies for this section include partial depth patching of the affected areas, full depth patching of the affected areas, or hydroblasting the entire section to remove the top 3-4 inches and completing a bonded concrete overlay. Of the options, the most cost-effective solution is probably the full depth patching to include whole panel replacement of the affected panels.

CONCLUSIONS

The petrographic analysis of the cores showed that the distress is due to excessive air void contents generally located within the top 3-4 inches of the pavement surface in select areas. This is most likely due to a consolidation issue during construction. Possible remedies include full panel replacement, partial depth patching, and hydroblasting the entire section and completing a bonded overlay.

APPENDIX

Petrographic Investigation of Concrete Cores From Cracked Pavement Slabs Located on Interstate 10 in Baton Rouge, Louisiana

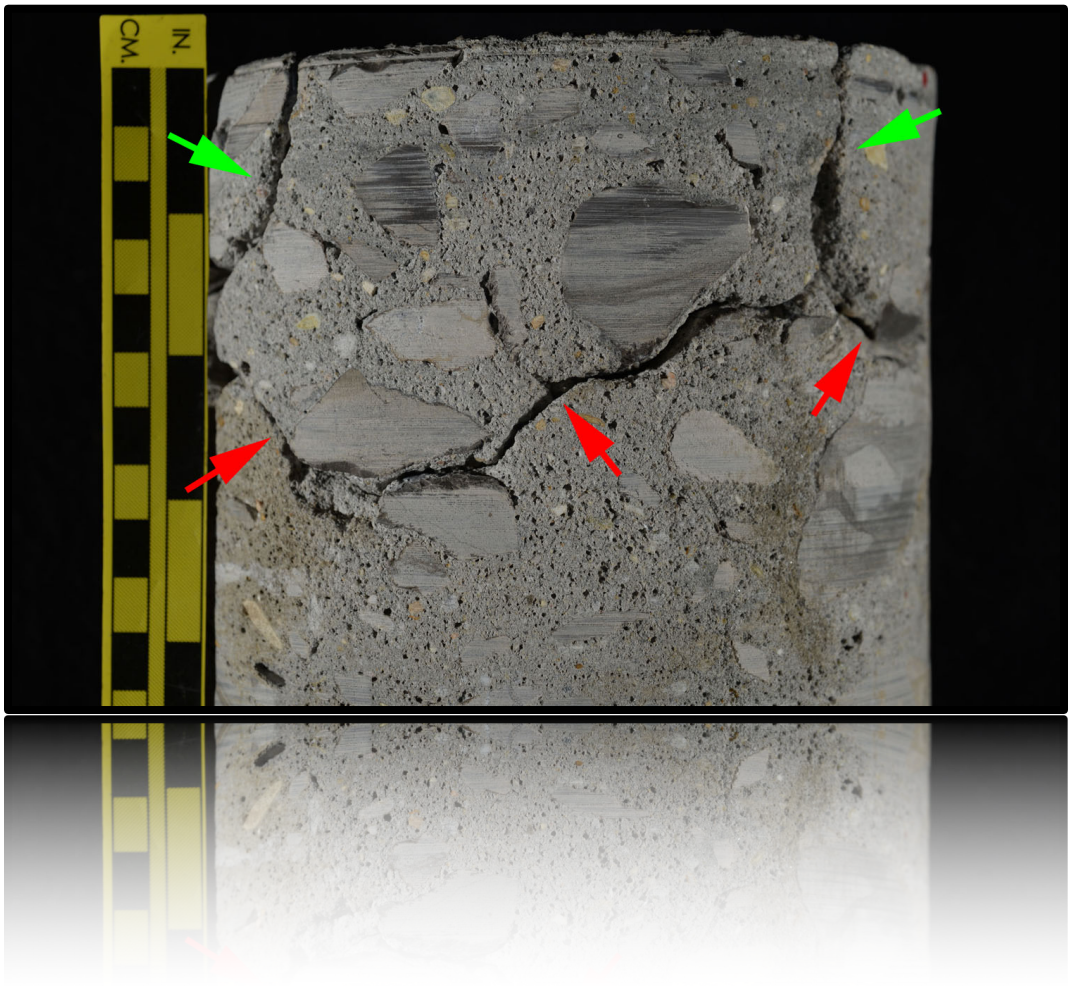

Prepared for: Mr. Tyson D. Rupnow, Ph.D., P.E.
Louisiana Transportation Research Center
Baton Rouge, Louisiana

Prepared by: David Rothstein, Ph.D., P.G., FACI
Report No.: DRP15.1293

6 September 2015

DRP Consulting, Inc. 3200 Carbon Place #104 Boulder, CO 80301
www.drpcinc.com

EXECUTIVE SUMMARY

Eight (8) concrete cores extracted from cracked pavement slabs on Interstate Highway 10 located in Baton Rouge, Louisiana are subjects of petrographic examination to assess the occurrence of delaminations and cause (s) of pattern cracking. In addition, three (3) cores are subjects of enhanced contrast and point count measurements of air content determinations from the top and middle portions of each core.

The findings from this scope of work indicate that cracking and delamination of the affected pavement cores are from mechanisms other than a durability mechanism such as alkali-silica reaction (ASR) or alkali-carbonate reaction (ACR). Although seven of the eight cores examined petrographically show evidence of very minor ASR, no evidence of cracking or microcracking due to ASR was observed. The delaminations appear linked to high air contents at the tops of the cores rather than any progressive deterioration mechanism.

Observations from this scope of work indicate that the concrete represented by the cores is made with similar materials. The paste consists of hydrated portland cement with no fly ash, slag cement or other supplemental cementitious materials observed. The hydration is normal. The coarse aggregate is a crushed dolomitic limestone with a nominal top size of 38 mm (1 ½ in.). The coarse aggregate is somewhat gap-graded. The fine aggregate is a siliceous natural sand that consists primarily of quartz and quartzite with minor amounts of granitic rocks and chert.

All the cores are purposefully air entrained and most of them contain 4-6% air, based on visual estimations (the first eight cores were not subject to point count or image analysis). Two of the cores (EB #2 and EB#3) contain 7-9% air, again based on visual estimations. Abbreviated point count analyses combined with enhanced contrast image analysis on two delaminated pavement cores (P#1 and P#2) indicated very high air contents (~ 17%) at the tops of the cores.

Most of the cores show linear cracks that strike across the top surfaces of the cores and cut sub-vertically into the cores. The cracks pass mostly around aggregate particles and are consistently free of secondary deposits. These properties are consistent with the cracks forming from shrinkage. The gap grading of the coarse aggregate and high sand content of the concrete mixtures are factors that promote susceptibility to shrinkage cracking.

1.0 INTRODUCTION

Mr. Tyson D. Rupnow, Ph.D., P.E. of the Louisiana Transportation Research Center **(LTRC**) located in Baton Rouge, Louisiana requested DRP Consulting, Inc. (**DRP**) to investigate the condition of concrete represented by cores extracted from cracked pavement slabs on Interstate Highway 10 located in Baton Rouge, Louisiana. The purpose of the examinations was to determine the cause(s) of the cracking and in particular determine if the concrete was cracked due to alkali-aggregate reaction (AAR). **DRP** performed petrographic examinations of cores from other pavements for **LTRC** and found the cracking was linked to alkali-carbonate reaction (ACR) involving the coarse aggregate. In addition, minor alkali-silica reaction (ASR) was observed involving cherts in the fine aggregate in these cores.

On 16 April 2015 **DRP** received eight (8) concrete cores from **LTRC** and on 22 April 2015 **DRP** received authorization to perform the scope of work outlined below. After completion of the optical microscopy (OM) examinations on all eight cores and examination using scanning electron microscopy with energy-dispersive x-ray spectrometry (SEM/EDS) on several cores, **DRP** notified Mr. Tyson by email on 26 May 2015 that none of the cracking was linked to AAR. In fact, no evidence of cracking or microcracking due to ACR was observed in any of the cores. While seven (7) of the eight (8) cores showed evidence of ASR, it was only associated with minor deposits of gel in voids and no cracking or microcracking was observed in association with ASR. Mr. Rupnow requested that **DRP** suspend activities until **LTRC** could acquire cores from other areas where severe cracking and delamination of pavements was observed. **DRP** received three (3) additional cores on 11 August 2015. In order to stay within the budget approved for the project, **DRP** performed abbreviated microscopical point counts and enhanced contrast image analyses of these cores to determine if high air contents at the tops of the cores were present and possible causes of the pavement delaminations. **Table 1** summarizes information regarding the identification and testing of these cores. No information was provided regarding the project specifications for the concrete, the concrete mix design, or the results of testing during construction.

Table 1. Summary of core identifications and testing schedule.

DRP No.	Client ID	Condition	Testing
19YD7483	EB #1	Cracked pavement slab core	Petrographic Examination (ASTM C856/C1723)
19YD7484	EB #2	Cracked pavement slab core	Petrographic Examination (ASTM C856/C1723)
19YD7485	EB #3	Cracked pavement slab core	Petrographic Examination (ASTM C856/C1723)
19YD7486	EB #4	Cracked pavement slab core	Petrographic Examination (ASTM C856/C1723)
19YD7487	WB #1	Cracked pavement slab core	Petrographic Examination (ASTM C856/C1723)
19YD7488	WB #2	Cracked pavement slab core	Petrographic Examination (ASTM C856/C1723)
19YD7489	WB #3	Cracked pavement slab core	Petrographic Examination (ASTM C856/C1723)
19YD7490	WB #4	Cracked pavement slab core	Petrographic Examination (ASTM C856/C1723)
19YD7679	P#1	Delaminated pavement slab core	Air Content Determination
19YD7680	P#2	Delaminated pavement slab core	Air Content Determination
19YD7681	Wall #1	Intact wall core	Air Content Determination

2.0 SCOPE OF WORK

The testing involved petrographic analysis of the first eight (8) cores using OM according to ASTM C856 [**1**] supplemented with SEM/EDS analyses as described in ASTM C1723 [**2**]. The hardened air content was measured for the last three (3) cores using enhanced contrast image analysis and the modified point count method as described in ASTM C457 [**3**]. However, the image analysis and point count analyses were focused on the top ~ 75 mm (3 in.) and the middle ~ 75 mm (3 in.) of the cores. The point counts were abbreviated and involved counting ~ 350 points in the top and ~ 350 points in the middle of each section of the analyzed cores.

This report summarizes the findings of this scope of work. *Appendices A-H* contain the notes, photographs and photomicrographs from the petrographic examinations. *Appendix I* contains the results of the hardened air content determinations. *Appendix J* describes the procedures used to complete these tests.

1 *Standard Practice for Petrographic Examination of Hardened Concrete.* Annual Book of ASTM Standards, Vol. 4.02., ASTM C856-11.

2 *Standard Guide for Examination of Hardened Concrete Using Scanning Electron Microscopy,* Annual Book of ASTM Standards, Vol. 4.02, ASTM C1723-10.

3 *Standard Test Method for Microscopical Determination of Parameters of the Air-Void System in Hardened Concrete*, Annual Book of ASTM Standards, Vol. 4.02, ASTM C457-11.

3.0 FINDINGS

The following findings are relevant to the concrete represented by the cores.

3.1 ***Orientation, Dimensions & As-Received Condition*** All the cores are vertical in orientation save the wall core, which is horizontal. The cores span from finished surfaces (or a formed surface on the wall core) to saw-cut surfaces, representing partial thicknesses of the sampled elements slabs. The first eight slab cores are 80 mm (3 ⅛ in.) in diameter and ~ 325 mm (~ 13 in.) long. The last two slab cores are 100 mm (4 in.) in diameter and ~ 350 mm (14 in.) long. The wall core is 100 mm (4 in.) in diameter and 255 mm (~ 10 in.) long. The cores are hard and compact and lack embedded steel. Most of the cores showed worn top surface that exposed coarse aggregate particles.

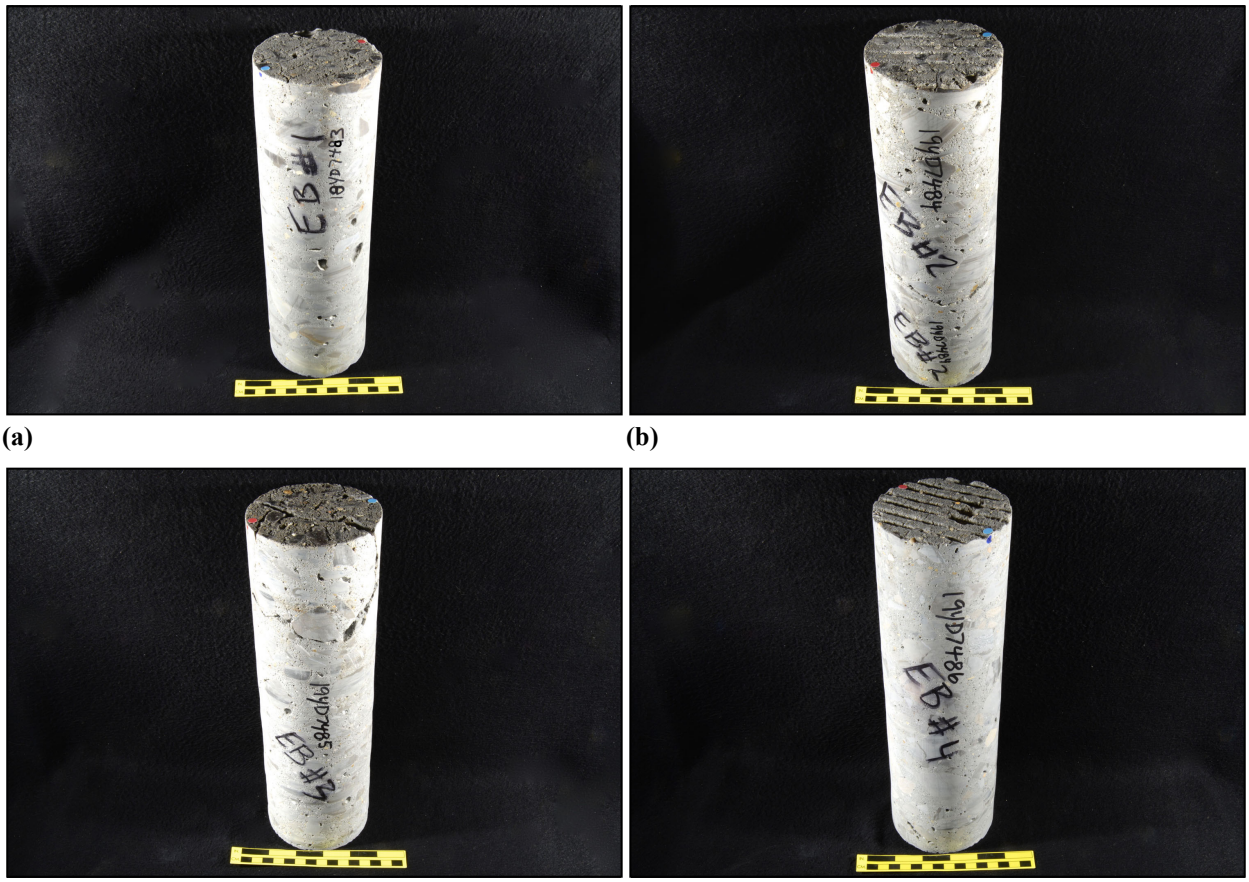

(a) **(b)**

(c) **(d)**

Figure 1. Photographs showing the top and sides of the eastbound cores in their as-received condition. (a) Core EB #1. (b) Core EB #2. (c) Core EB #3. (d) Core EB #4. The yellow scale bar is ~ 150 mm (6 in.) long.

(e) (f)

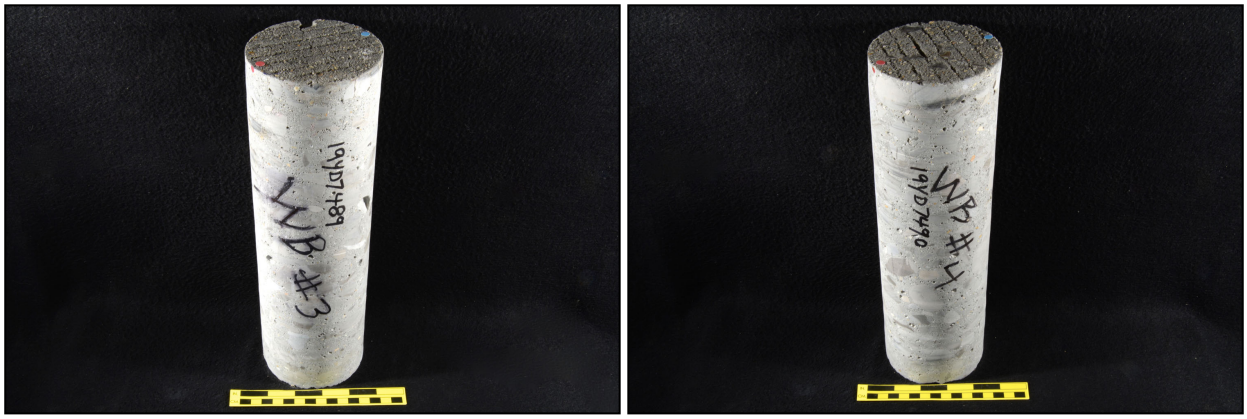

(g) (h)

(i) (j)

Figure 1 (cont'd). Photographs showing the top and sides of the westbound cores in their as-received condition and the other two pavement cores that showed significant delaminations. (e) Core WB #1. (f) Core WB #2. (g) Core WB #3. (h) Core WB #4. (i) Core P#1. (j) Core P#2. The yellow scale bar is ~ 150 mm (6 in.) long. See *Appendix I* for photographs of Core Wall #1 in as-received condition.

3.2 ***Components: Paste*** The paste fraction of all eight cores subjected to petrographic examination consists of hydrated cement with no fly ash, slag cement or other supplemental cementitious materials observed (**Figure 2)**. The hydration is normal with relict and residual cement grains (RRCG) that consist primarily of belite rimmed by interstitial aluminate and ferrite observed most commonly. Some variations in the abundance of RRCG, the size and abundance of calcium hydroxide crystals, paste color and other optical properties indicate minor variations in the water and cementitious materials content.

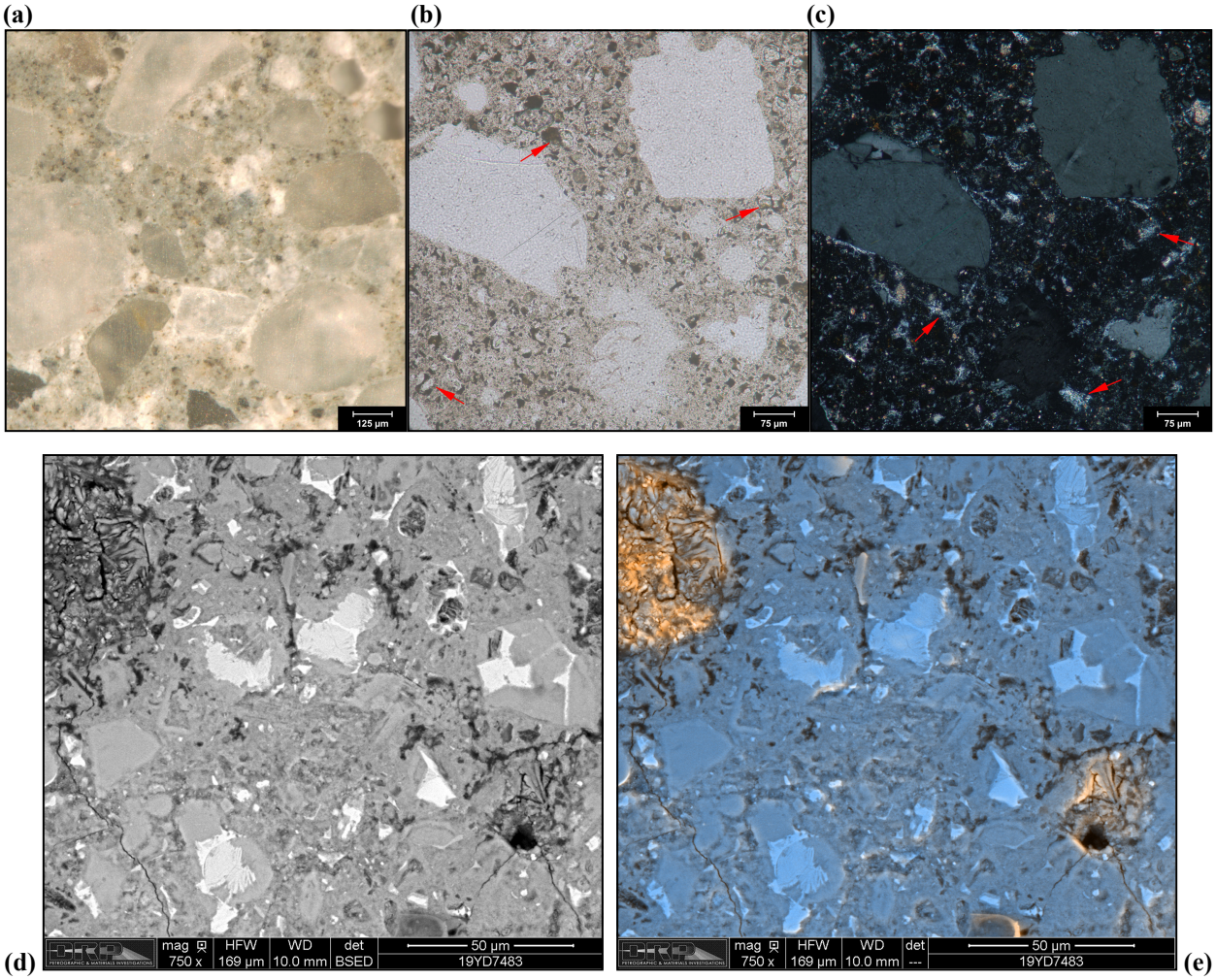

Figure 2. Examples of paste properties in Core EB #1. (a) Reflected light photomicrograph of the polished surface showing detail of paste color and texture in the middle of the core. Transmitted light photomicrographs of thin section showing detail of paste in (b) plane-polarized and (c) cross-polarized light. The red arrows in (b) indicate RRCG and in (c) the red arrows indicate coarse calcium hydroxide. (d) Backscatter electron micrograph and (e) combined backscatter and secondary electron micrograph showing detail of paste microstructure. The white and very light gray areas in (d) are RRCG.

3.3 ***Components: Air*** All the cores from the fist set of eight are air-entrained with air contents that ranged from an estimated 4-6% except Core EB #2 and Core EB #3, which contain an estimated 7-9% air (**Figure 3**). Note that in the first eight cores air contents were estimated visually but were not measured by point count methods as outlined in ASTM C457. Many of the cores in the first set of eight contained large voids typical of incomplete consolidation, entrapped air or water voids. In particular, Core EB #3 showed numerous large voids in the top 55 mm (2 ⅛ in.) where extensive cracking and delamination of the concrete was observed, as discussed below.

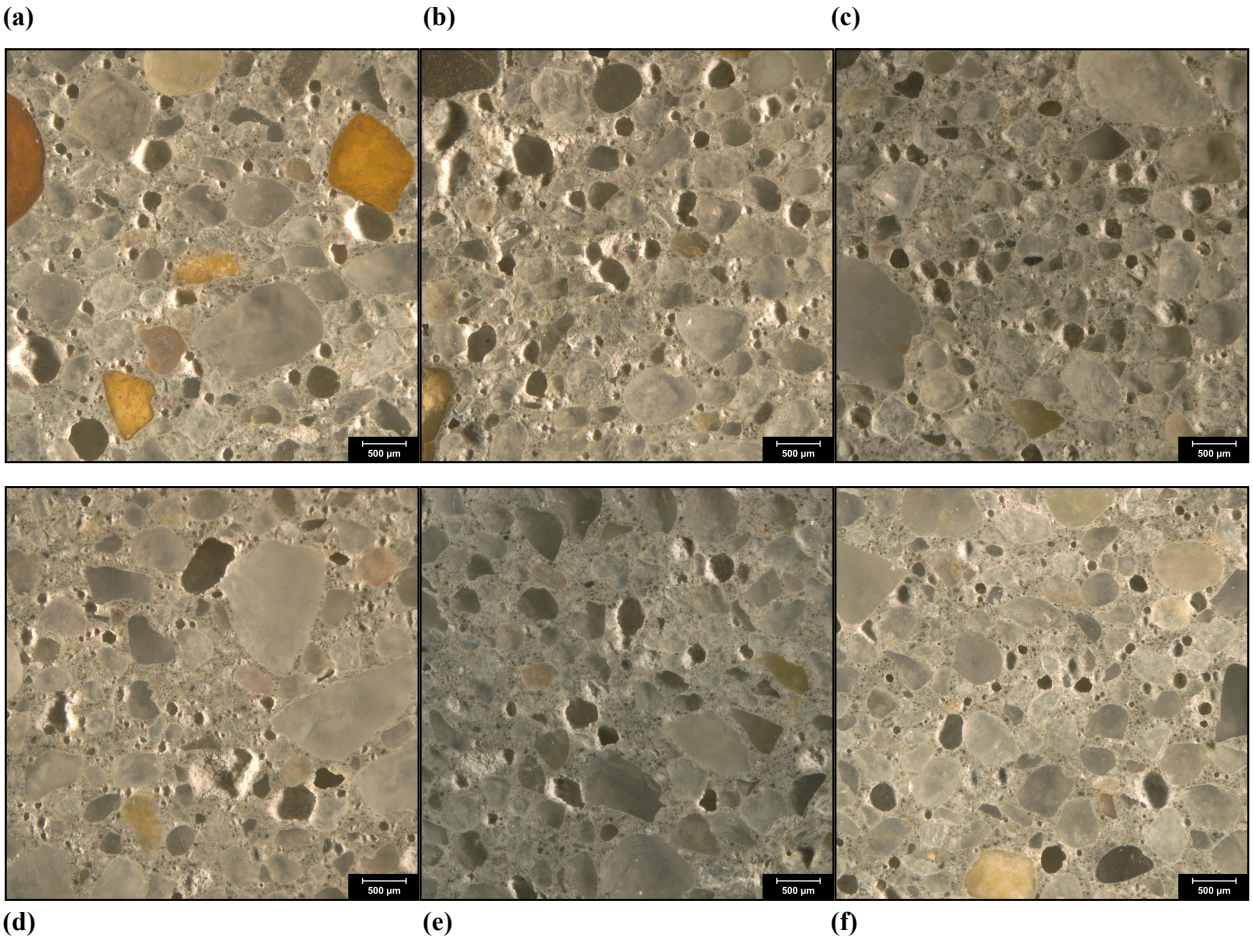

Figure 3. Reflected light photomicrographs of polished slabs showing examples of entrained air voids. (a) Core EB #1. (b) Core EB #2. (c) Core EB #3. (d) Core WB #2. (e) Core WB #3. (f) Core WB #4.

3.4 ***Delamination & Air*** The consolidation of the concrete represented by the first eight cores ranges from moderate to good. Several cores showed large voids near the top surface and consolidation voids on the sides of the core. However, no link was observed between these large voids and distress or cracking in the cores except in Core EB #3, where extensive cracking and delamination was observed in the top 55 mm (2 ⅛ in.) of the core. This is shown in more detail in *Section 3.6 Cracking and Microcracking.*

Core P#1 and Core P#2 contained zones of extremely high air (~ 17%) at the top of the cores and much lower air (4-5%) in the middle (**Figure 4**). The zones of high air coincide approximately with the depth of delaminations observed in these cores. Core Wall #1 did not show elevated air near its outer surface and was not delaminated.

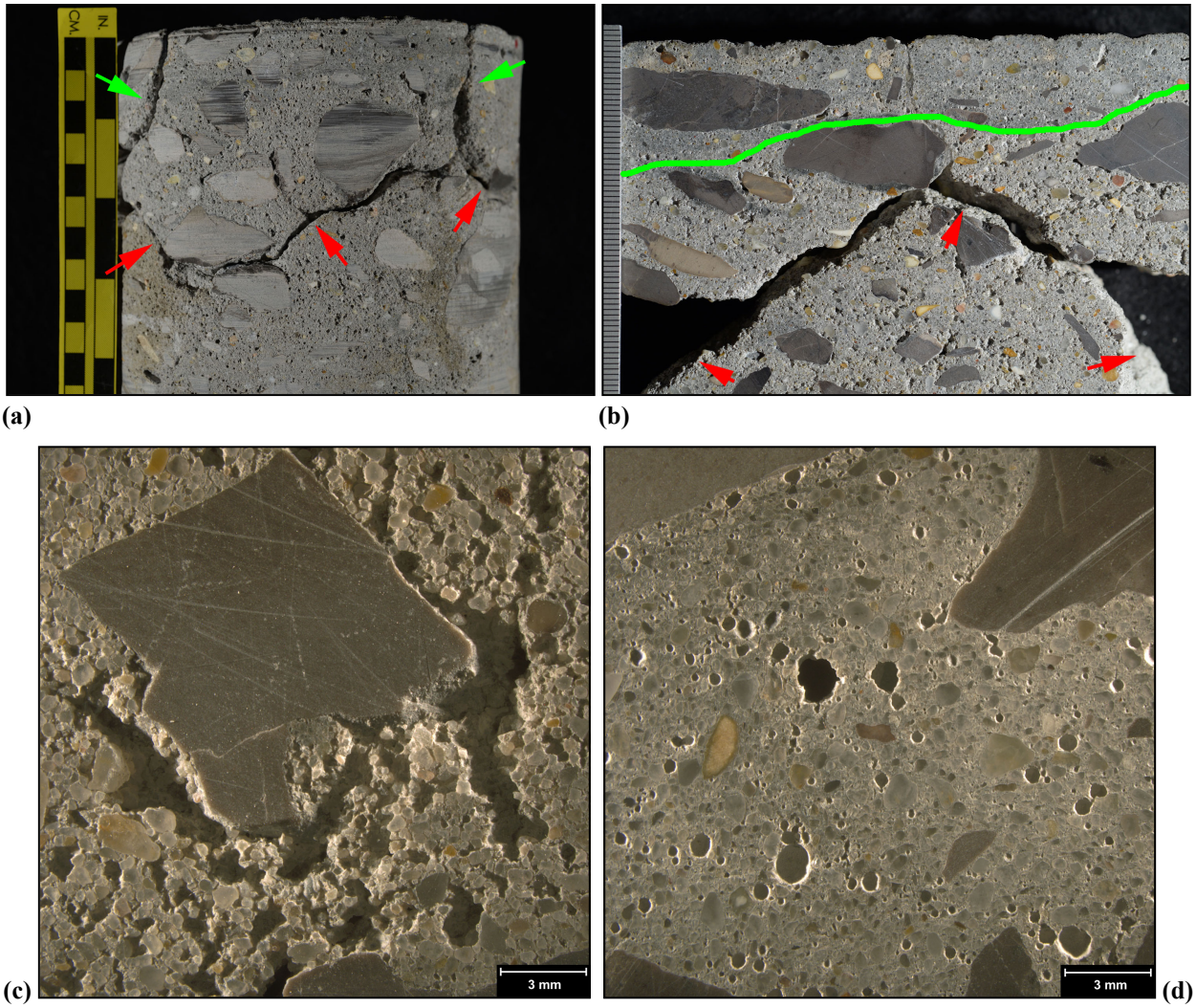

Figure 4. (a) Photograph of the side of Core P#1 near the top of the core. The red arrows show sub-horizontal crack along which the core delaminated. The green arrows indicate sub-vertical cracks. (b) Photograph of the polished surface of Core P#1 showing section near the top of the core. The green line separates a zone of significantly lower air content than the zone below it; on average the concrete has ~ 17% air. The red arrows highlight the delamination crack. Reflected light photomicrographs of the polished surface of Core P#1 showing detail of voids (c) at the top and (d) in the middle of the core.

3.5 ***Components: Aggregates*** All the cores contains similar aggregates that consist of a crushed limestone coarse aggregate with a nominal top size of 38.5 mm (1 ½ in.) and fine aggregate that consists of a natural siliceous sand (**Figure 6**). The coarse aggregate is a dolomitic limestone very similar to that observed to be susceptible to ACR in previous investigations. The rocks are hard and competent. The limestone is medium brown in color with patches of euhedral dolomite rhombs and other patches of amorphous, clay-rich material. In the present cores these rocks commonly show prominent reaction rims but at most only very minor internal microcracking and no significant microcracking of the paste around the aggregate. The coarse aggregate commonly shows marked gap grading with a paucity of intermediate sized particles and an abundance of sand. The sand is siliceous in composition and consists primarily of quartz and quartzite with minor amounts of granitic rocks and chert. Many of the components present in the sand are potentially susceptible to ASR. Very minor ASR was observed in seven of the eight cores subjected to petrographic examination, as discussed in more detail below, but no evidence of cracking or distress was linked to ASR. No potentially deleterious components, such as clay lumps, friable particles, coal, lignite or excessive fines were observed.

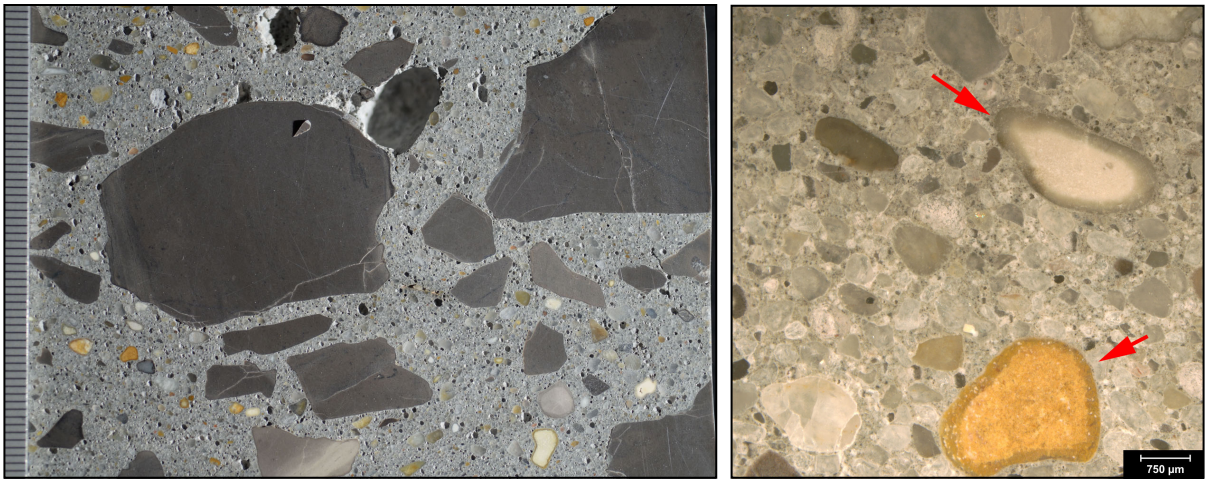

(a) **(b)**

Figure 6. (a) Photograph and (b) reflected light photomicrograph of polished surface of Core EB #3 showing coarse and fine aggregate, respectively. The scale is in millimeters in (a). The red arrows in (b) indicate particles of chert.

3.6 ***Cracking and Microcracking*** Most of the cores showed linear cracks on their top surfaces. The cracks are typical of drying shrinkage as they cut sub-vertically from the top surface, cutting primarily around aggregate particles and lacking significant secondary deposits save calcium carbonate (**Figure 7**). These cracks were typically 250-500 µm (10-20 mil) wide and most commonly cut to depths of ~ 9.5 mm (⅜ in.) below the top surface of the core. A few cores showed sub-vertical cracks that cut to depths of 15-25 mm (⅝-1 in.). These also cut around aggregates and lack secondary deposits. Core EB #1 showed a sub-horizontal crack subjacent to the top surface but was not delaminated.

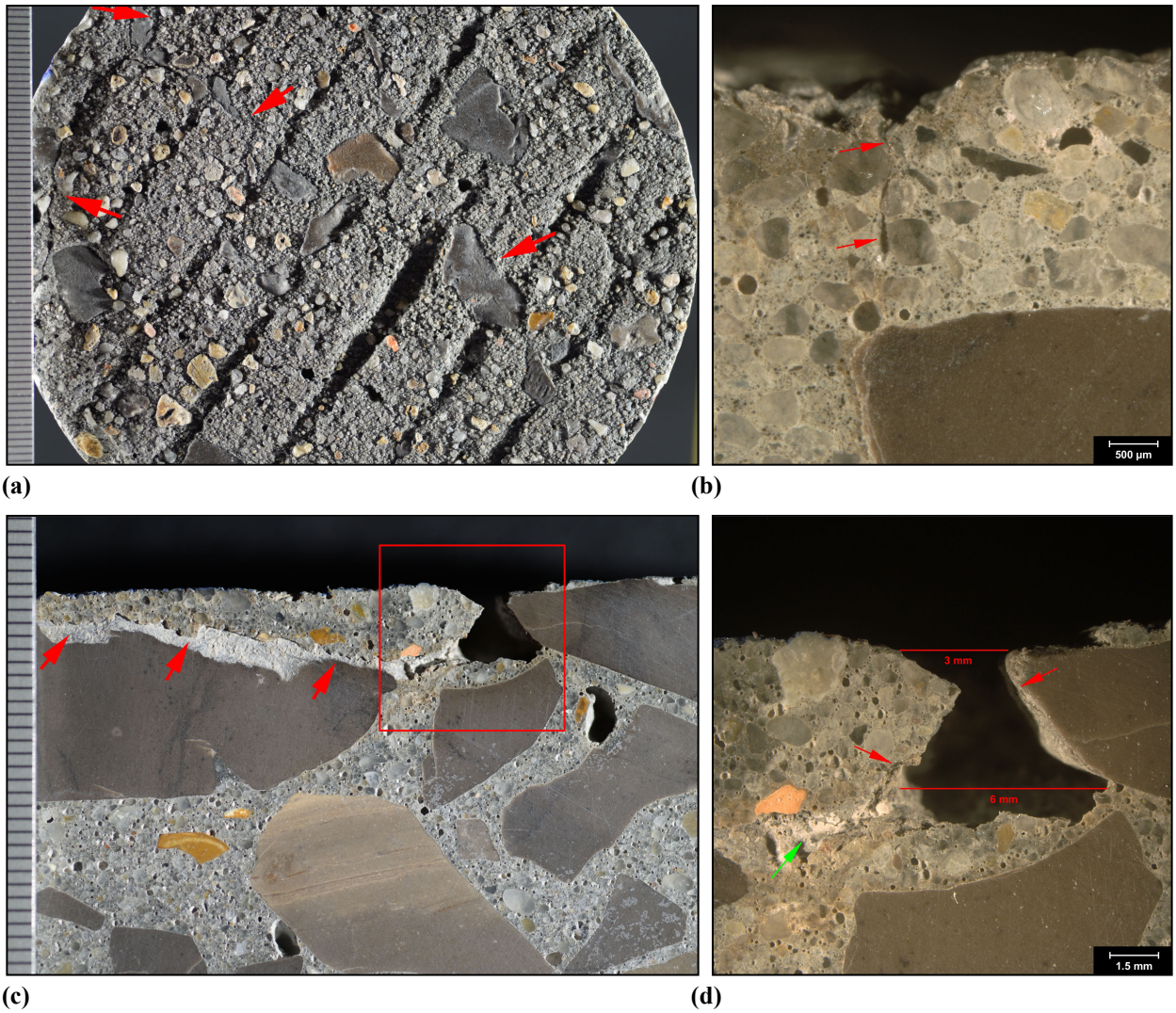

(a) (b)

(c) (d)

Figure 7. (a) Photograph of the top of Core WB #4 showing triple point hairline cracks (red arrows) on a worn tined surface. (b) Reflected light photomicrograph of polished surface of Core WB #4 showing sub-vertical microcrack (red arrows) at the top surface that represents an extension of the hairline crack observed on the top surface. (c) Photograph of the top of the polished surface of Core EB #1 showing a sub-horizontal crack (red arrows) subjacent to the top surface. The red box shows the approximate area of (b) where red arrows indicate a large void (width measured by red bars) and the green arrow shows the sub-horizontal crack.

Core EB #3 Core EB #3 showed the most prominent cracking in the eight cores that were examined petrographically (**Figure 8**). The core was received with several cracks that were open when the core was received (precluding measurement of their widths). A sub-horizontal crack cut through the full width of the core at ~ 55 mm (2 ⅛ in.) below the top surface. Above this sub-horizontal a complex network of cracks, hairline cracks and microcracks cut through the paste in orientations that range from sub-horizontal to oblique to sub-vertical. These cracks and microcracks cut predominantly around aggregate particles and lack secondary deposits. In Core EB #3 microcracking was observed throughout the thickness of the core. These microcracks lacked secondary deposits, were most commonly oriented obliquely and cut around aggregate particles.

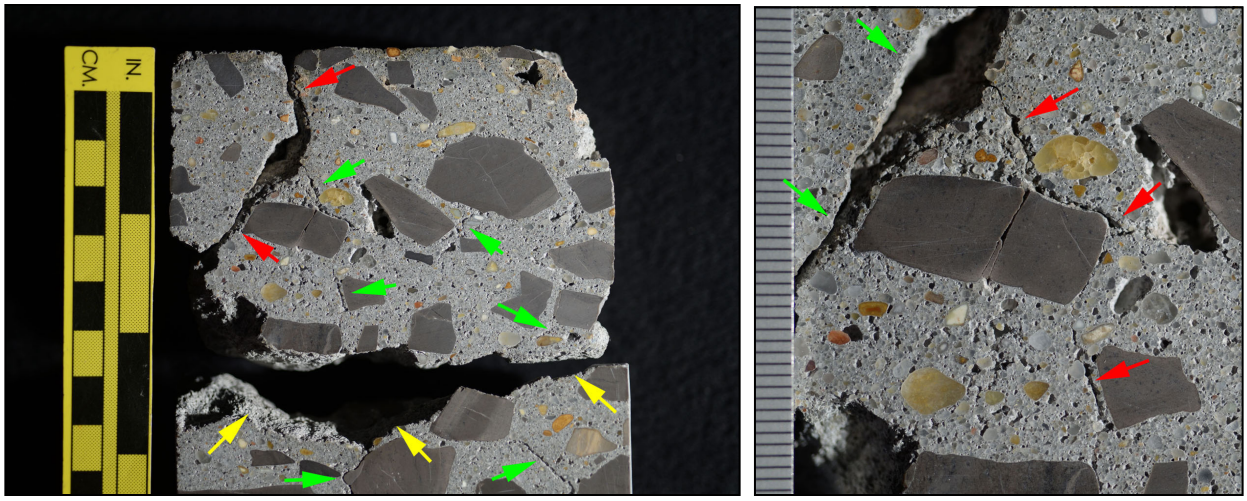

(a) **(b)**

Figure 8. (a) Photographs of the polished surface of Core EB #3 showing overview and detail, respectively of cracking at the top of the core. In (a) the yellow arrows indicate the main sub-horizontal crack along which the core delaminated. The red arrows in (a) indicate a sub-vertical crack which, combined with the sub-horizontal crack, cut the core into three pieces. The green arrows indicate oblique cracks that cut through the paste both above and below the sub-horizontal crack.

Core P #1, Core P#2 As mentioned above, these two cores showed major delaminations that correlate with the presence of very high air.

3.7 ***Secondary Deposits—Carbonation*** The cores show negligible carbonation based on phenolphthalein staining and thin section microscopy (**Figure 9**). Voids are generally free of secondary deposits.

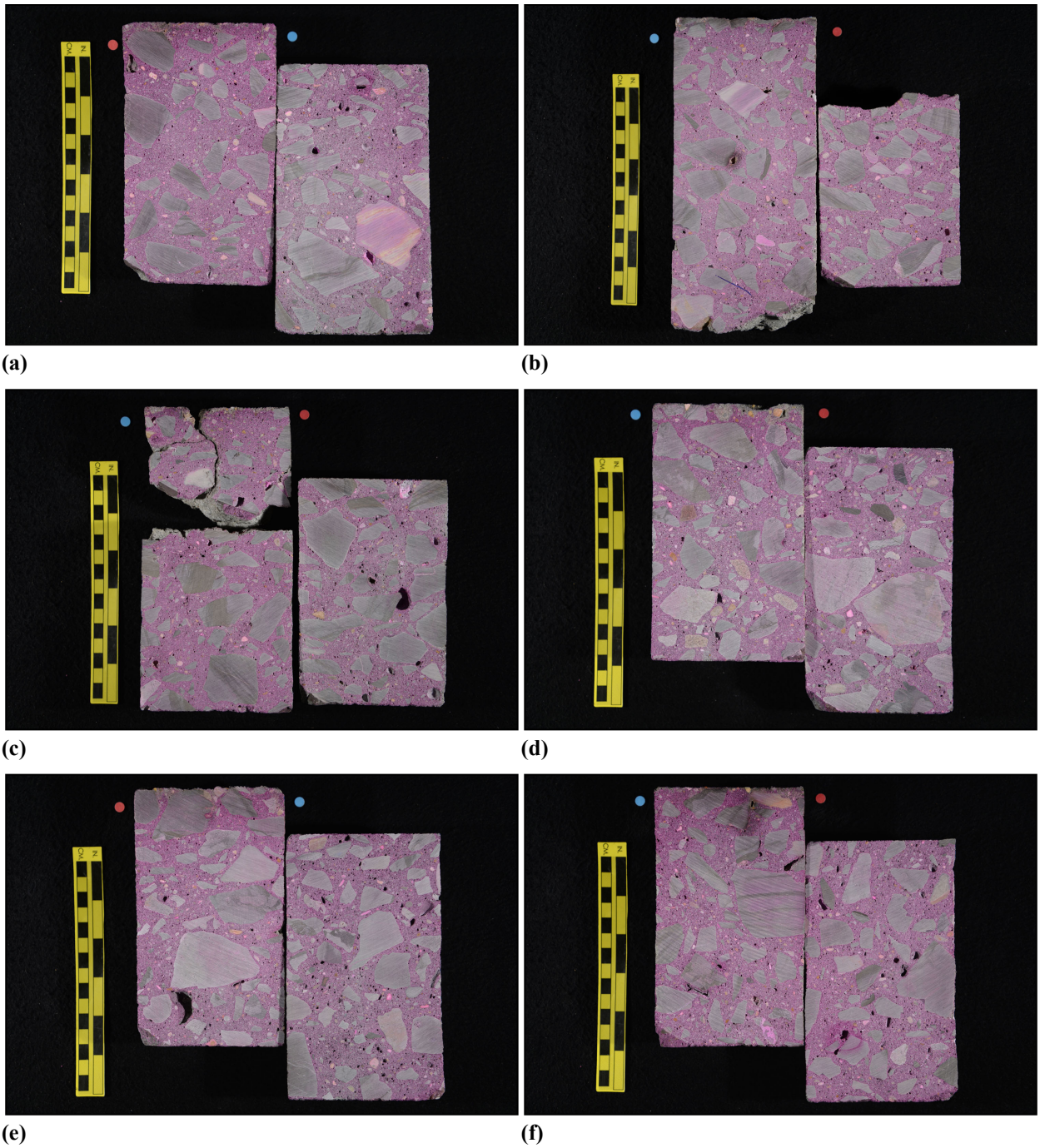

Figure 9. Photographs of the phenolphthalein stained surfaces. (a) Core EB #1. (b) Core EB #2. (c) Core EB #3. (d) Core EB #4. (e) Core WB #1. (f) Core WB #2. The yellow scale bar is ~ 150 mm (6 in.) long.

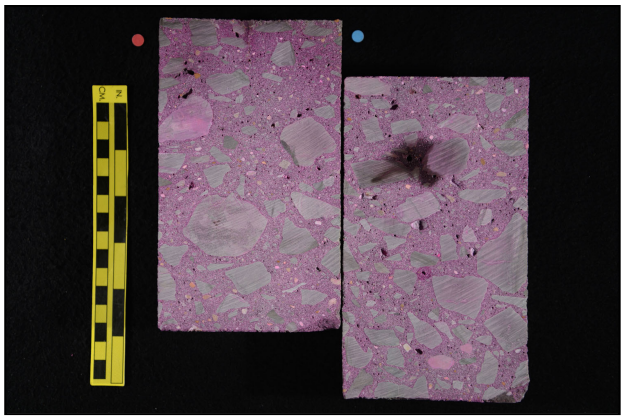

(g)

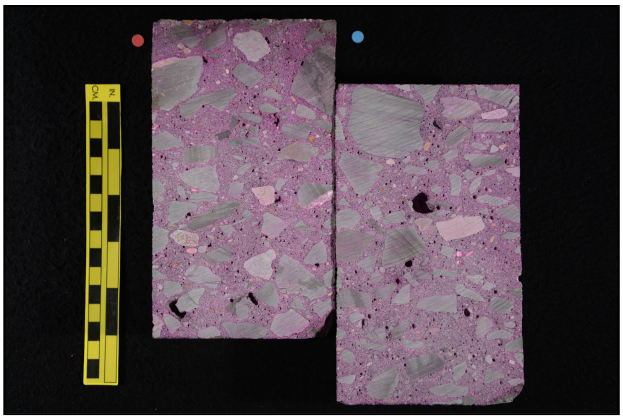

(h)

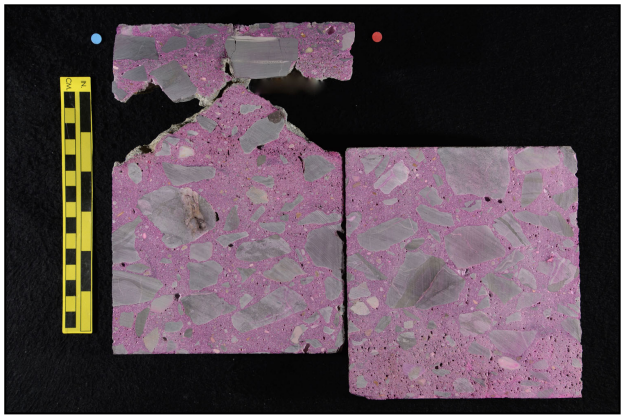

(i)

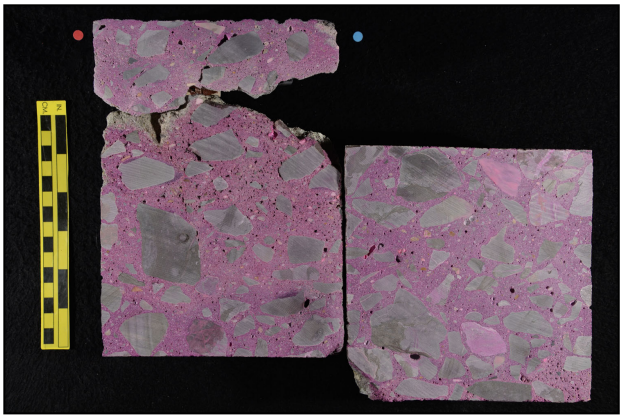

(j)

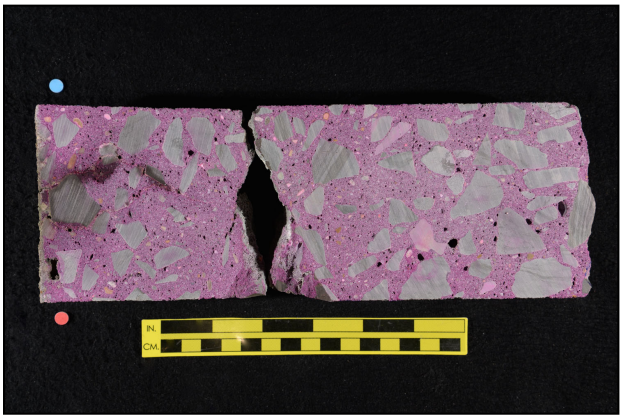

(k)

Figure 9 (cont'd). Photographs of the phenolphthalein stained surfaces. (g) Core WB #3. (h) Core WB #4. (i) Core P#1. (jd) Core P #2. (k) Core Wall #1. The yellow scale bar is ~ 150 mm (6 in.) long.

3.8 ***Secondary Deposits—Alkali-Silica Reaction (ASR)*** Seven of the eight cores examined petrographically show trace to very minor ASR; Core WB #1 is the sole core lacking deposits of gel. In all cases deposits of gel were observed in voids, most commonly adjacent to or near particles of limestone in the coarse aggregate (**Figure 10**). SEM/EDS analysis of these deposits confirm they consist of ASR gel, most commonly with calcium as the dominant cation in the gel **(Figure 11**).

(a)

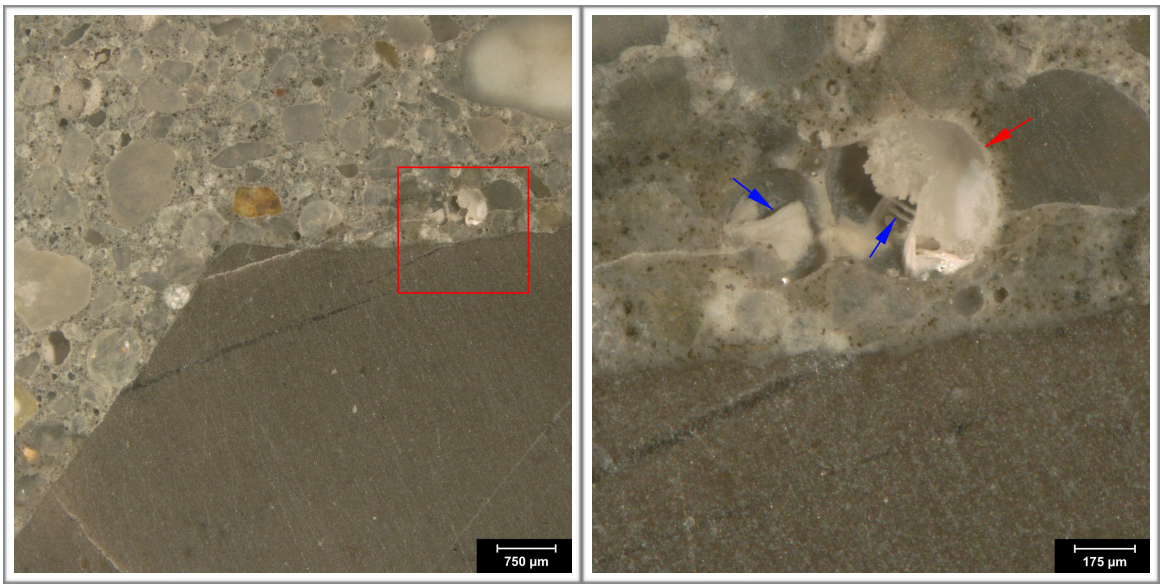

(b)

Figure 10. Reflected light photomicrographs of polished surface of Core EB #1 showing (a) overview and (b) detail of gel deposits in void next to a coarse aggregate particle about 85 mm (3 ⅜ in.) below the top surface. The red square in (a) shows the approximate area of (b) where the red arrow indicates a gelatinous deposit and blue arrows indicate more crystalline deposits.

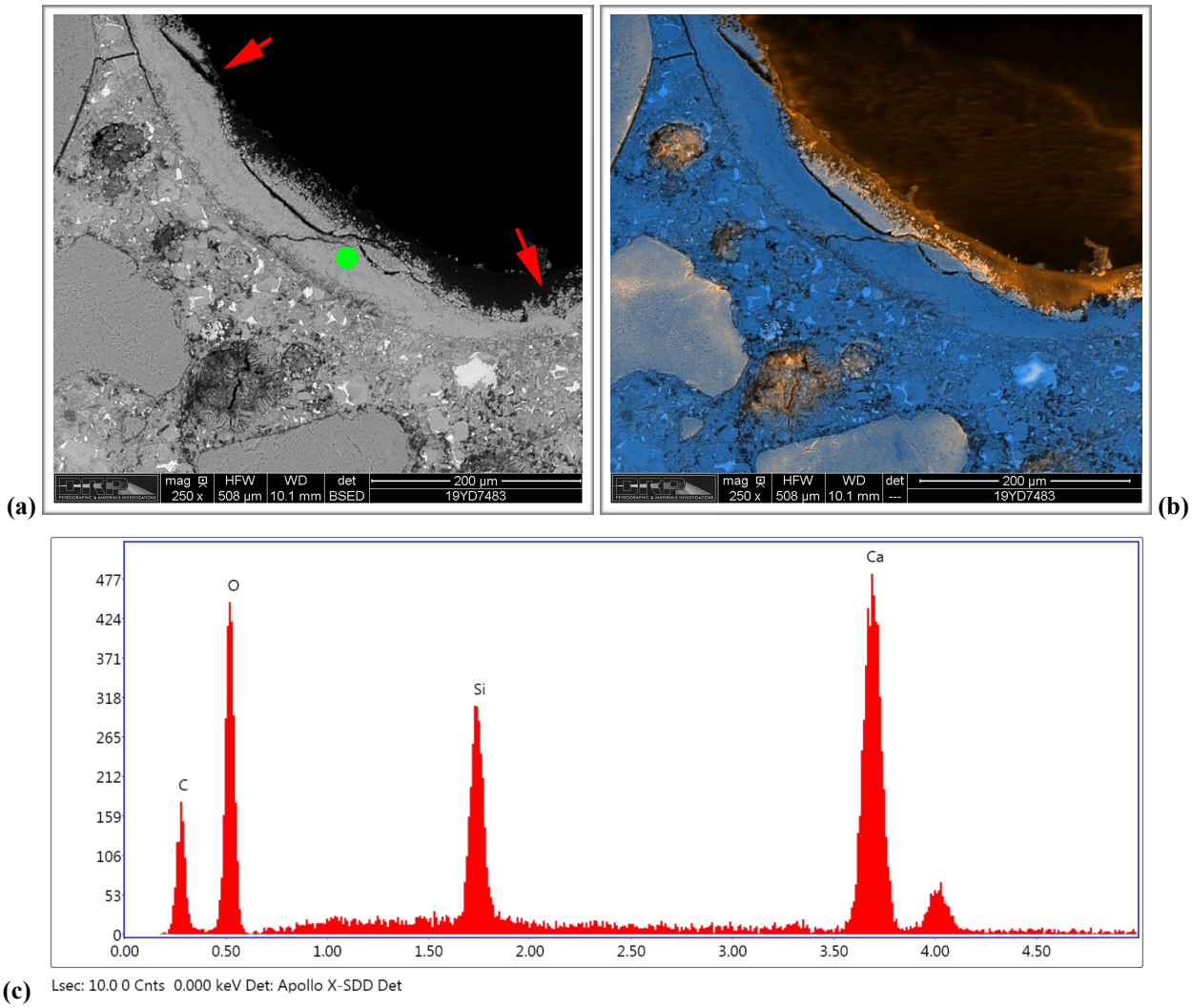

Figure 11. (a) Backscatter electron (BSE) and (b) combined backscatter/secondary electron (BSE/SE) micrograph of polished surface of Core EB #1 showing detail of void lined with gel.

3.9 ***Secondary Deposits—Ettringite*** Minor deposits of ettringite were observed in voids in all of the cores. No microcracking or distress was associated with these deposits.

4.0 CONCLUSIONS

The findings described above indicate that the concrete represented by the cores is made with similar materials. The paste consists of hydrated portland cement with no fly ash, slag cement or other supplemental cementitious materials observed. The hydration is normal. The coarse aggregate is a crushed dolomitic limestone with a nominal top size of 38 mm (1 ½ in.). The coarse aggregate is somewhat gap-graded. The fine aggregate is a siliceous natural sand that consists primarily of quartz and quartzite with minor amounts of granitic rocks and chert.

All the cores are purposefully air entrained and most of them contain 4-6% air, based on visual estimations (the first eight cores were not subject to point count or image analysis). Two of the cores (EB #2 and EB#3) contain 7-9% air, again based on visual estimations. Abbreviated point count analyses combined with enhanced contrast image analysis on two delaminated pavement cores (P#1 and P#2) indicated very high air contents (~ 17%) at the tops of the cores.

Most of the cores show linear cracks that strike across the top surfaces of the cores and cut sub-vertically into the cores. The cracks pass mostly around aggregate particles and are consistently free of secondary deposits. These properties are consistent with the cracks forming from shrinkage. The gap grading of the coarse aggregate and high sand content of the concrete mixtures are factors that promote susceptibility to shrinkage cracking.

Although seven of the eight cores examined petrographically show evidence of very minor ASR, no evidence of cracking or microcracking due to ASR was observed. In addition, while some reaction rims were observed on the coarse aggregate particles, no evidence of distress related to ACR was observed in any core. No evidence of distress related to any other progressive deterioration mechanisms was observed in any core.

These findings indicate that cracking and delamination of the affected pavement cores are from mechanisms other than a durability mechanism. The delaminations appear linked to extremely high air contents at the tops of the cores.

This concludes work performed on this project to date.

David Rothstein, Ph.D., P.G. FACI

LTRC Cracked Pavement Core Petrography

Appendices

1. RECEIVED CONDITION

ORIENTATION	Vertical core taken through highway pavement slab measures 100 mm (~ 4 in.) in diameter and 325 mm (~ 12 ¾ in.) long (**Figure A1, A2**).
SURFACES	The top surface worn with exposed coarse aggregate particles that are worn smooth (**Figure A3**) and the bottom surface is a saw cut such that the core represents a partial thickness of the pavement slab.
GENERAL CONDITION	The concrete is hard and compact and rings lightly when sounded with a hammer.

2. EMBEDDED OBJECTS

GENERAL	None observed.

3. CRACKING

MACROSCOPIC	A hairline crack was observed on the polished surface that cuts sub-vertically from the top of the core to ~ 25 mm (1 in.; **Figure A4**). The crack is free of secondary deposits and cuts around aggregate particles. Subjacent to the top surface and adjacent to a large void at the top of the core (see below) the polished surface shows a gap between a coarse aggregate particle and the paste (**Figure A5**). The paste along this interface is white and has a very granular texture.
MICROSCOPIC	No significant microcracking was observed.

4. VOIDS

VOID SYSTEM	Concrete is air-entrained (**Figure A6**) and contains 4-6% air by visual estimation (not determined following ASTM C457). A large, irregularly shaped void is present at the top of the polished surface. The void is ~ 3 mm (⅛ in.) across at the top of the core and has a tear-drop shape on the polished surface, such that it is ~ 6 mm (¼ in.) across about 6 mm (¼ in.) below the top surface (**Figure A7**).
VOID FILLINGS	Voids are commonly lined with ettringite.

5. COARSE AGGREGATE

PHYSICAL PROPERTIES	Crushed quarry rock with 38 mm (1 ½ in.) nominal top size (**Figure A8**). The rocks are hard and competent. The particles are sub-equant to tabular in shape with sub-angular to sub-round edges. The grading and distribution are relatively even. The sand is very fine.
ROCK TYPES*	The aggregate is carbonate in composition and consists of brown dolomitic limestone. The limestone is massive and dense; most particles lack significant sedimentary features. Occasional particles that are light brown to tan in color show coarse lenses of calcite, some bioclastic material and infilled vugs as well as subtle laminations of carbonaceous or clay-rich material.
OTHER FEATURES	No deleterious coatings or incrustations observed. No low w/c mortar coatings observed. Occasional particles show very internal microcracking that appears more consistent with the processing of the aggregate than alkali-carbonate reaction (ACR).

**Modal abundance based on visual estimation.*

6. FINE AGGREGATE

PHYSICAL PROPERTIES	Natural sand consists of rocks that are hard and competent (**Figure A9**). The particles are sub-equant to tabular in shape with sub-round to sub-angular edges. The grading and distribution are relatively even.
ROCK TYPES	The sand is siliceous in composition and consists primarily of quartz and quartzite with minor amounts of granitic rocks and chert.
OTHER FEATURES	No deleterious coatings or incrustations observed and no low w/c mortar coatings observed. Occasional particles of cherts show evidence of ASR with reaction rims and microcracks that cut into the paste.

7. PASTE OBSERVATIONS

POLISHED SURFACE	Paste is gray (Munsell 2.5Y/6/1) to dark gray (2.5Y/4/1), has a smooth texture and sub-vitreous luster (**Figure A10**). The paste is hard (Mohs 3.5-4). The paste is mottled grayish brown (2.5Y/6/4) to light gray (2.5Y/7/1) for 2-4 mm (80-160 mil) from the top surface.
FRESH FRACTURE	Fracture surface is light gray, has a hackly texture and a sub-vitreous luster. The fracture cuts primarily through aggregate particles (**Figure A11**). No significant secondary deposits were observed though minor deposits of ettringite commonly line voids.
THIN SECTION*	The paste contains hydrated portland cement; no fly ash, slag cement or other SCM were observed. The hydration is normal with 4-8% RRCG that consist mostly of interstitial ferrite and aluminate with occasional grains of belite (**Figure A12, Figure A13**). CH makes up 10-17% of the paste, is fine to medium-grained and evenly distributed.

** Abbreviations as follows: RRCG = relict and residual cement grains; SCM = supplemental cementitious materials; CH = calcium hydroxide; ITZ = interfacial transition zone. Modal abundances are based on visual estimations.*

8. SECONDARY DEPOSITS

PHENOLPHTHALEIN	Entire surface stains purple (**Figure A14**).
DEPOSITS	Minor carbonation observed at the top of the core and in irregularly distributed zones in the paste in thin section. Minor deposits of ettringite observed in voids. Trace to minor deposits of ASR gel observed in rare voids, most commonly next to limestone particles (**Figure A15**).

FIGURES

(a)

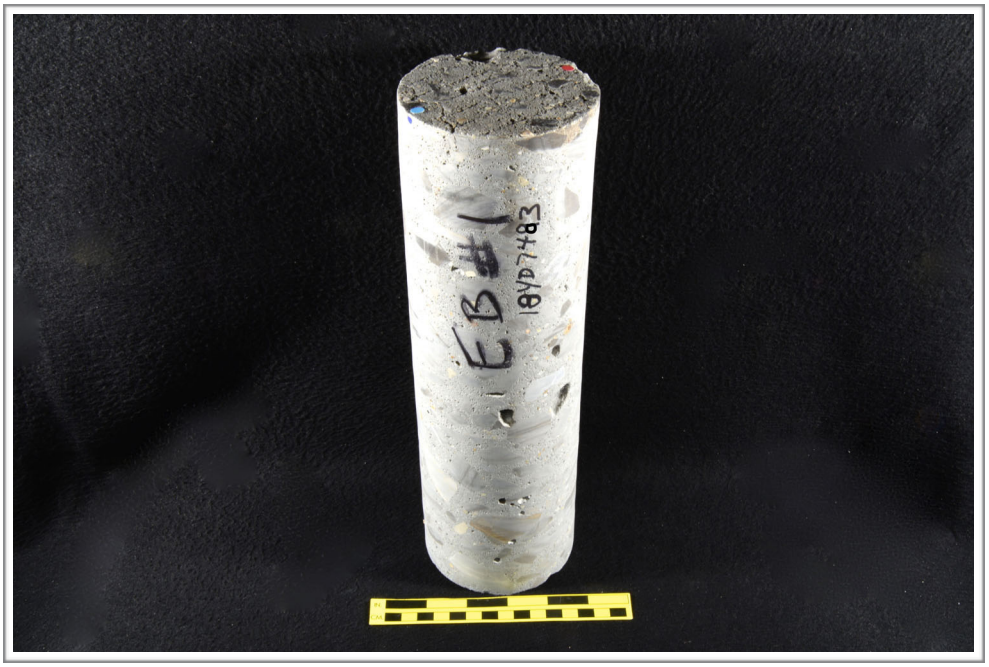

(b)

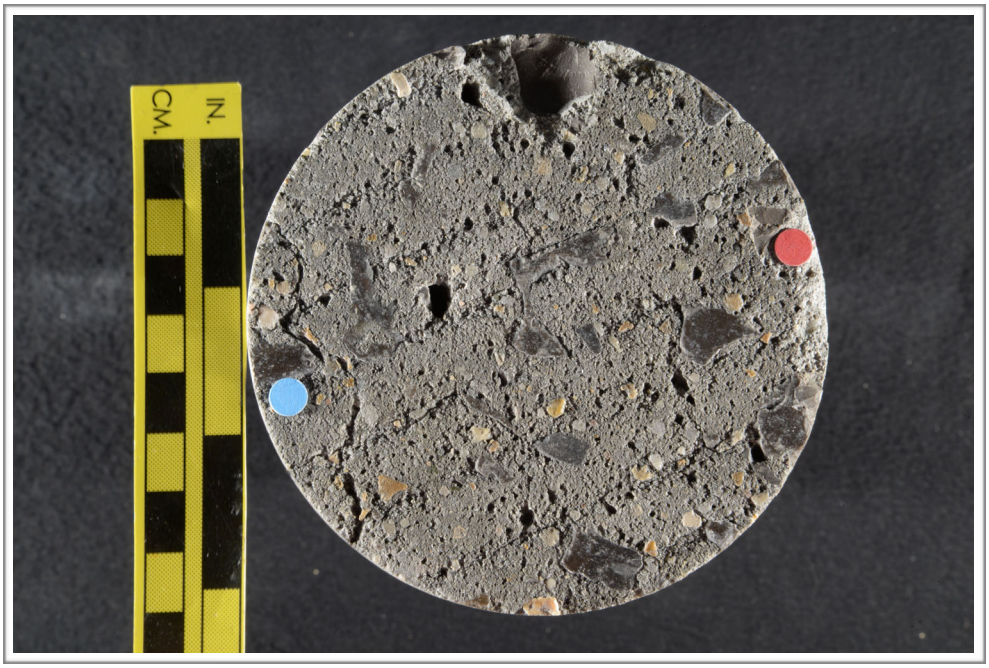

Figure A1. Photographs showing (a) oblique view of the top and side of the core with identification labels and (b) the top of the core. The red and blue dots in (a) show the orientation of the saw cuts used to prepare the sample.

(c)

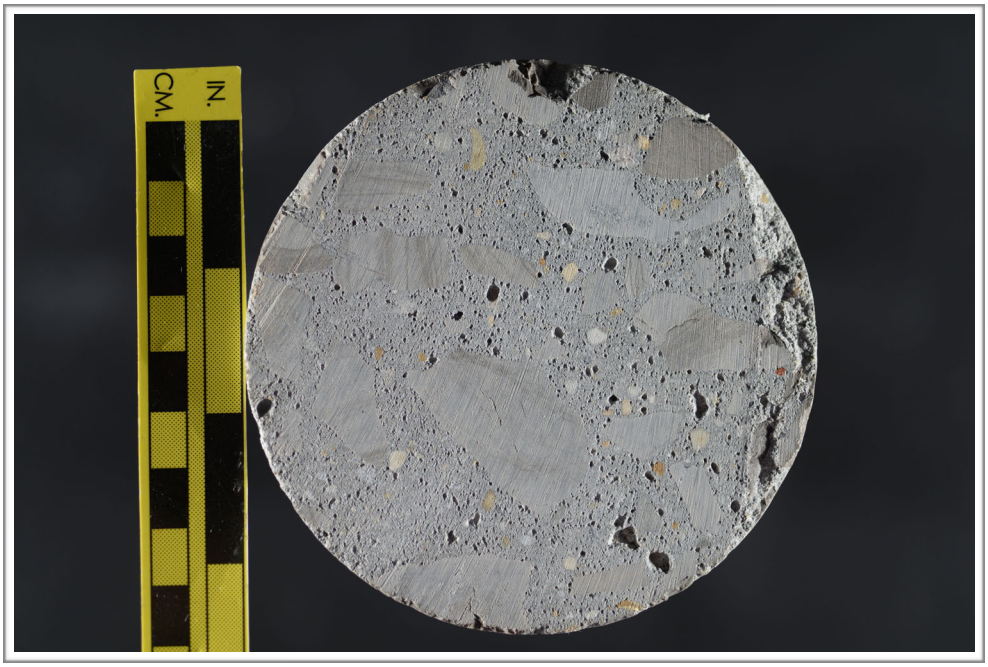

Figure A1 (cont'd). (c) Photograph showing the bottom of the core.

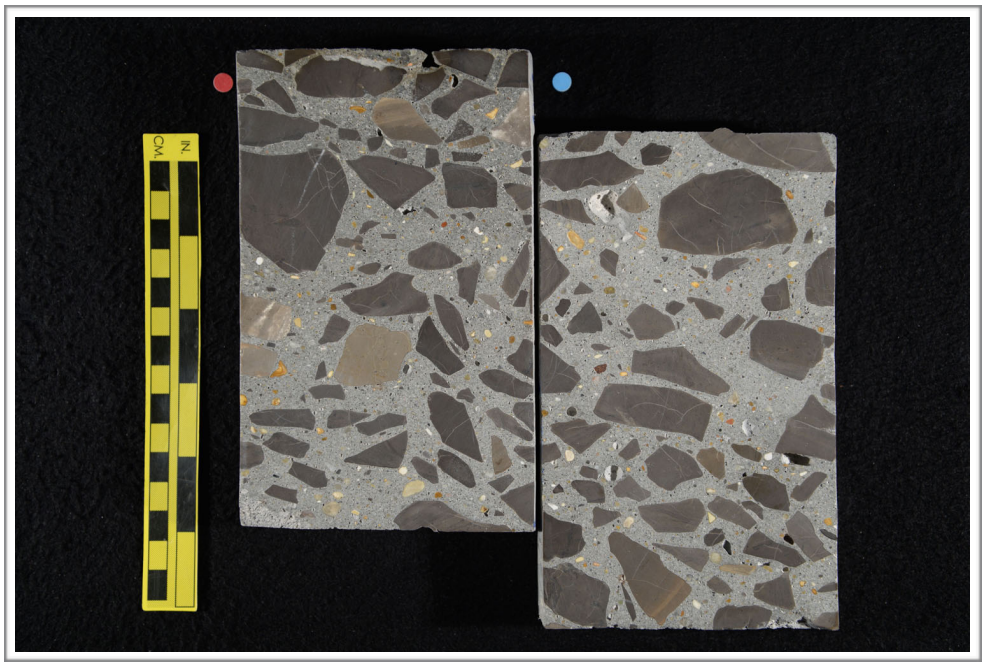

Figure A2. Photograph showing the polished surface of the core.

Figure A3. Photograph showing detail of the top surface of the core; scale in millimeters.

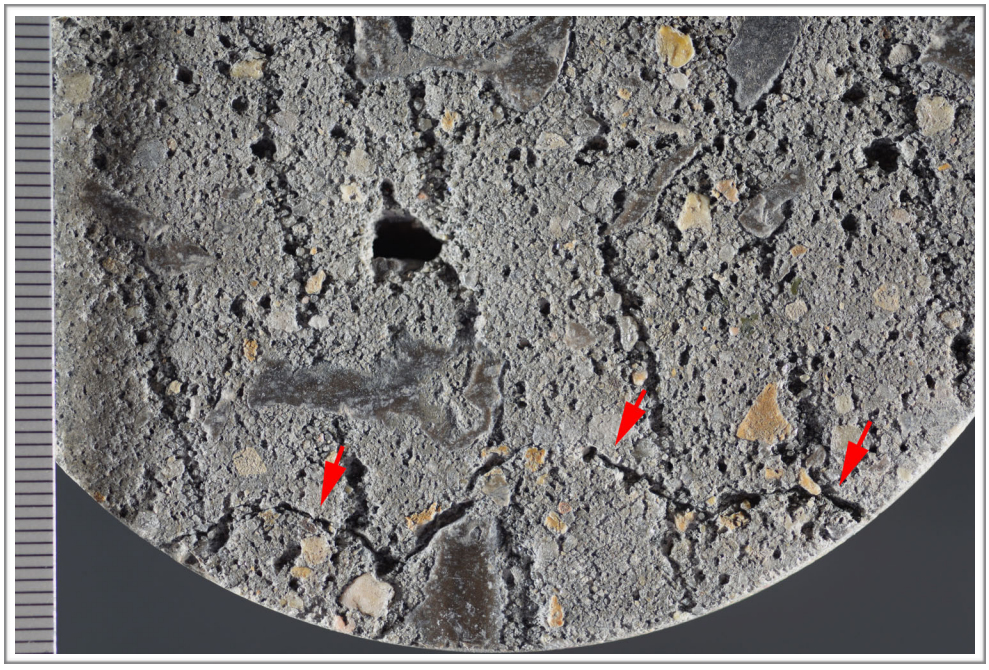

Figure A4. Photograph showing crack (red arrows) on the top surface; scale in millimeters.

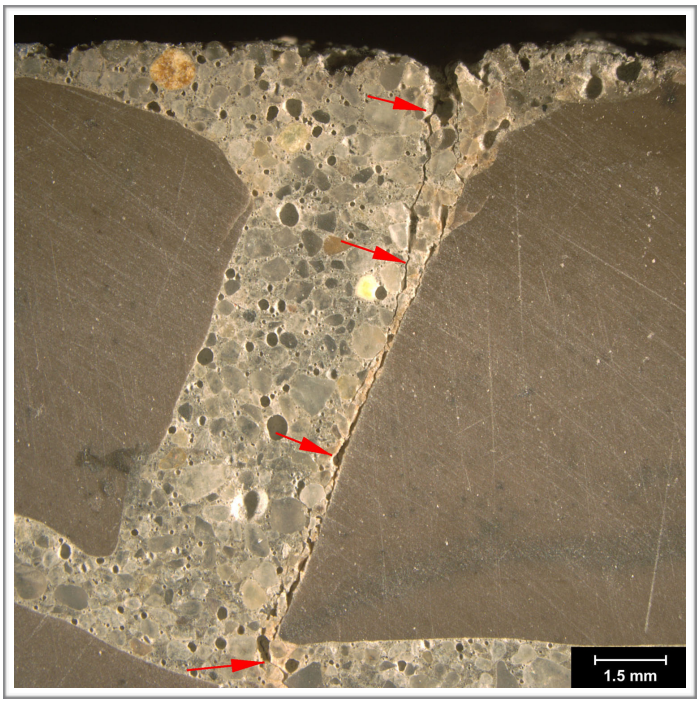

Figure A4 (cont'd). (b) Reflected light photomicrograph of the polished surface showing hairline crack (red arrows) at the top of the core.

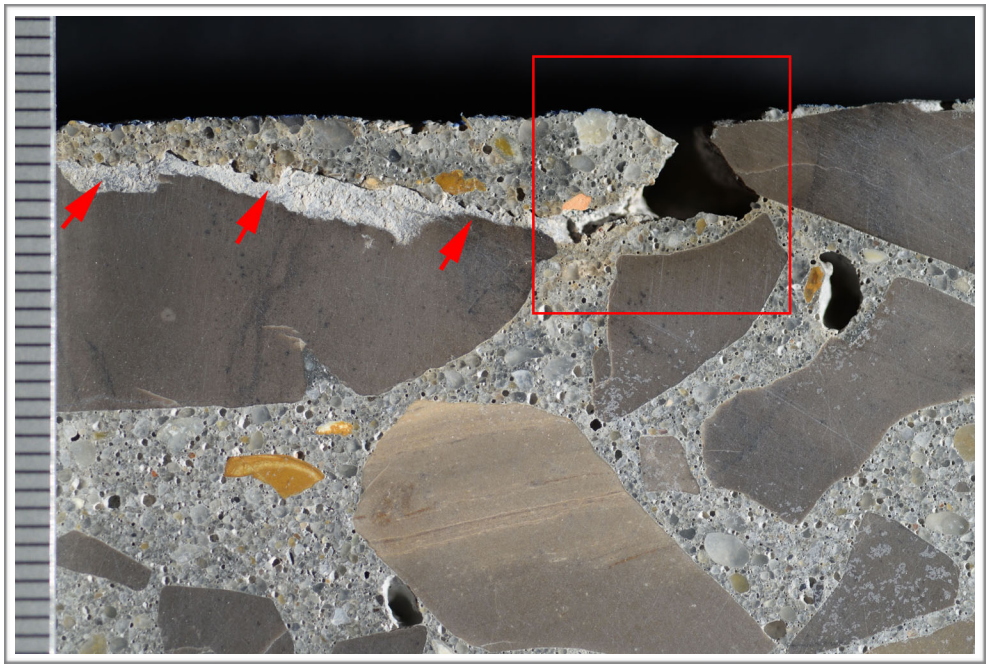

Figure A5. Reflected light photomicrograph of the polished surface showing vertical microcrack (red arrows) at the top of the core. The red box shows the approximate area of Figure A7.

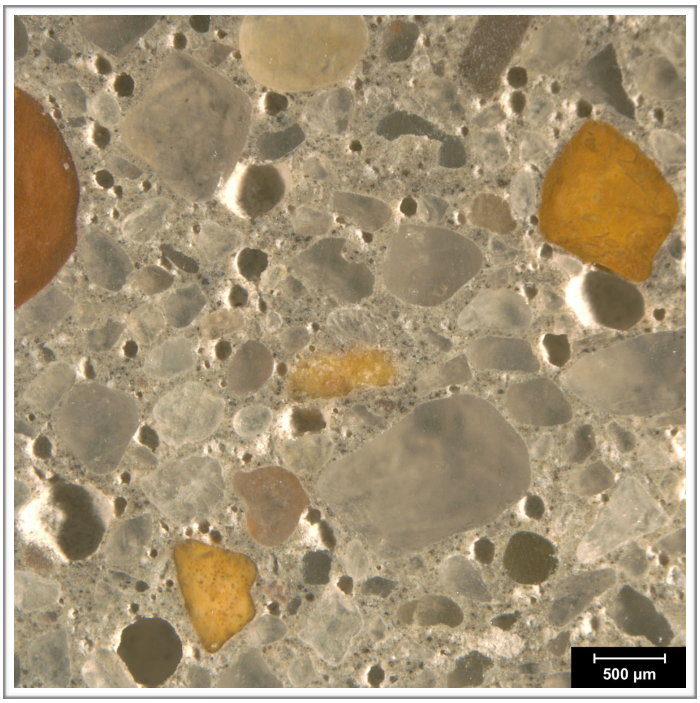

Figure A6. Reflected light photomicrograph of the polished surface entrained air voids (dark circles).

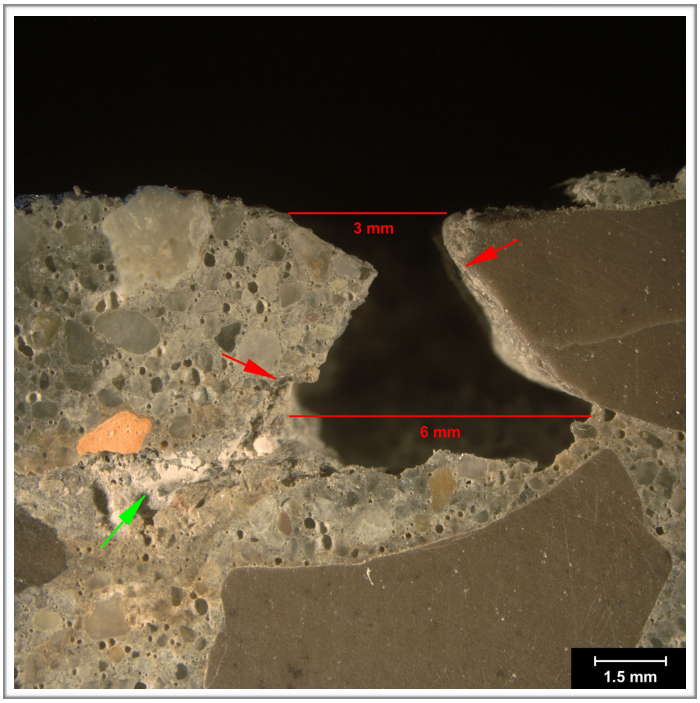

Figure A7. Reflected light photomicrograph of polished surface showing tear-drop shaped void (red arrows and bars) at the top of the core. The green arrow highlights crack.

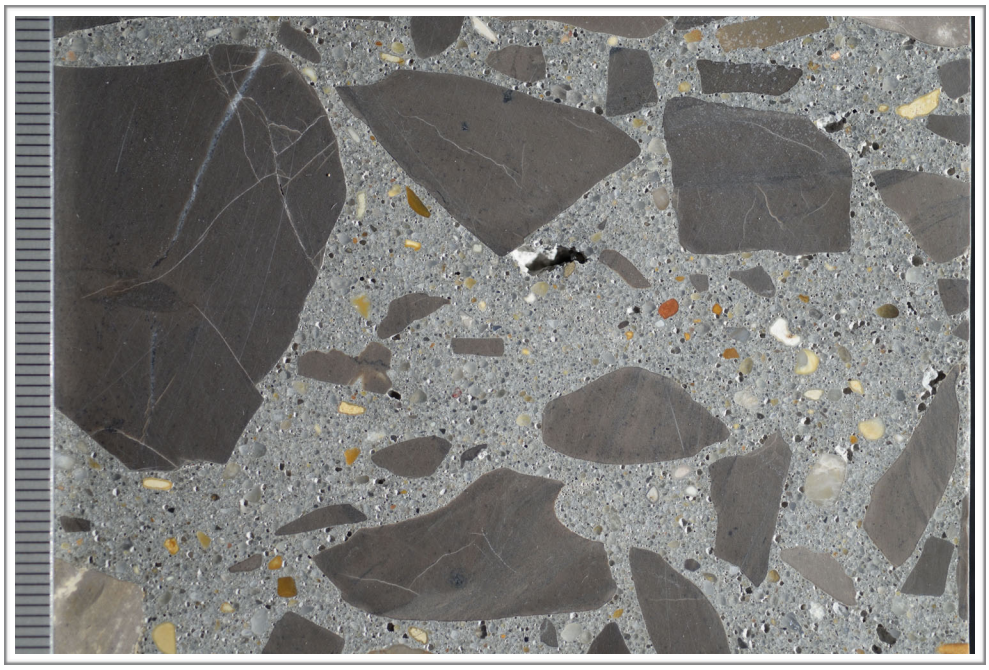

Figure A8. Photograph of the polished surface showing coarse aggregate; scale in millimeters.

Figure A9. Reflected light photomicrograph of polished surface showing the fine aggregate.

(a)

(b)

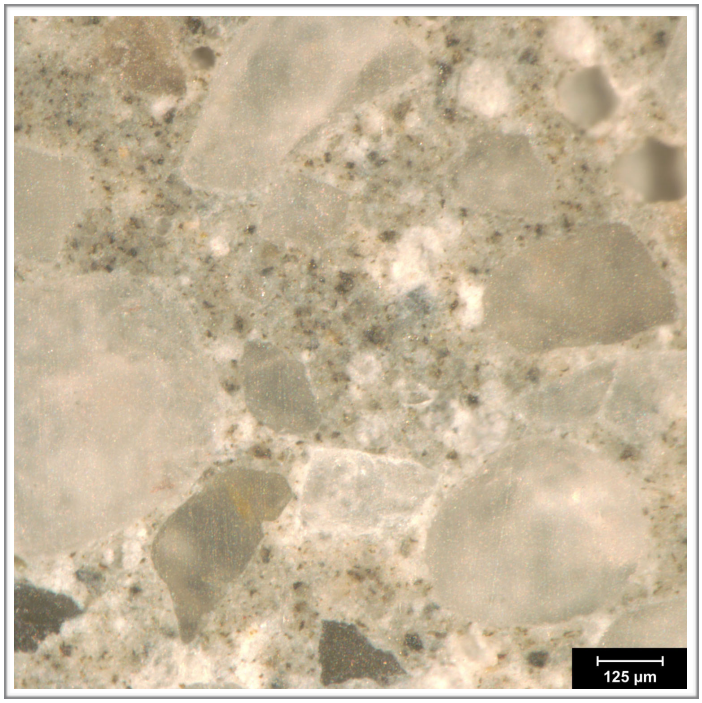

Figure A10. (a) Photograph of polished surface showing overview of paste at the top of the core. The scale is in millimeters. (b) Reflected light photomicrograph showing detail of paste color, texture and luster in the middle of the core.

(a)

(b)

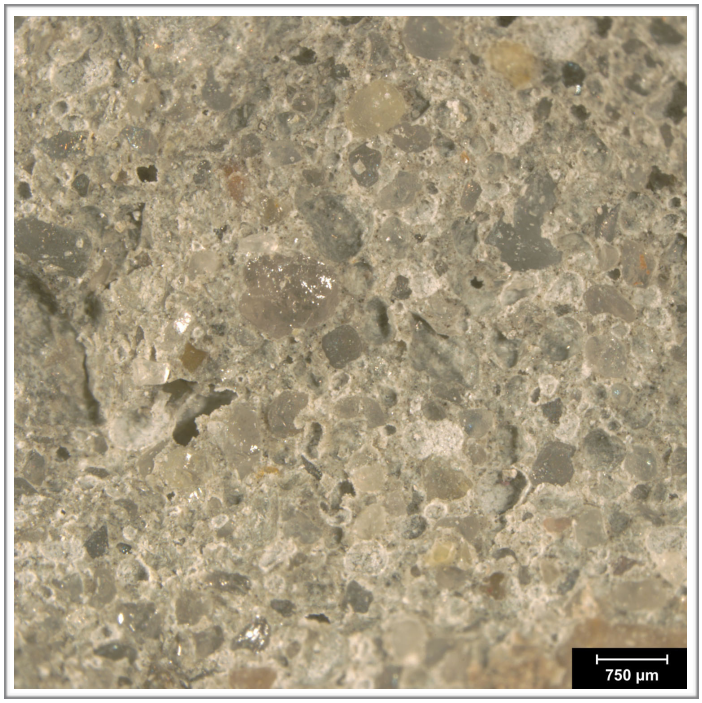

Figure A11. (a) Photograph and (b) reflected light photomicrograph of the fresh fracture surface. The scale in (a) is in millimeters.

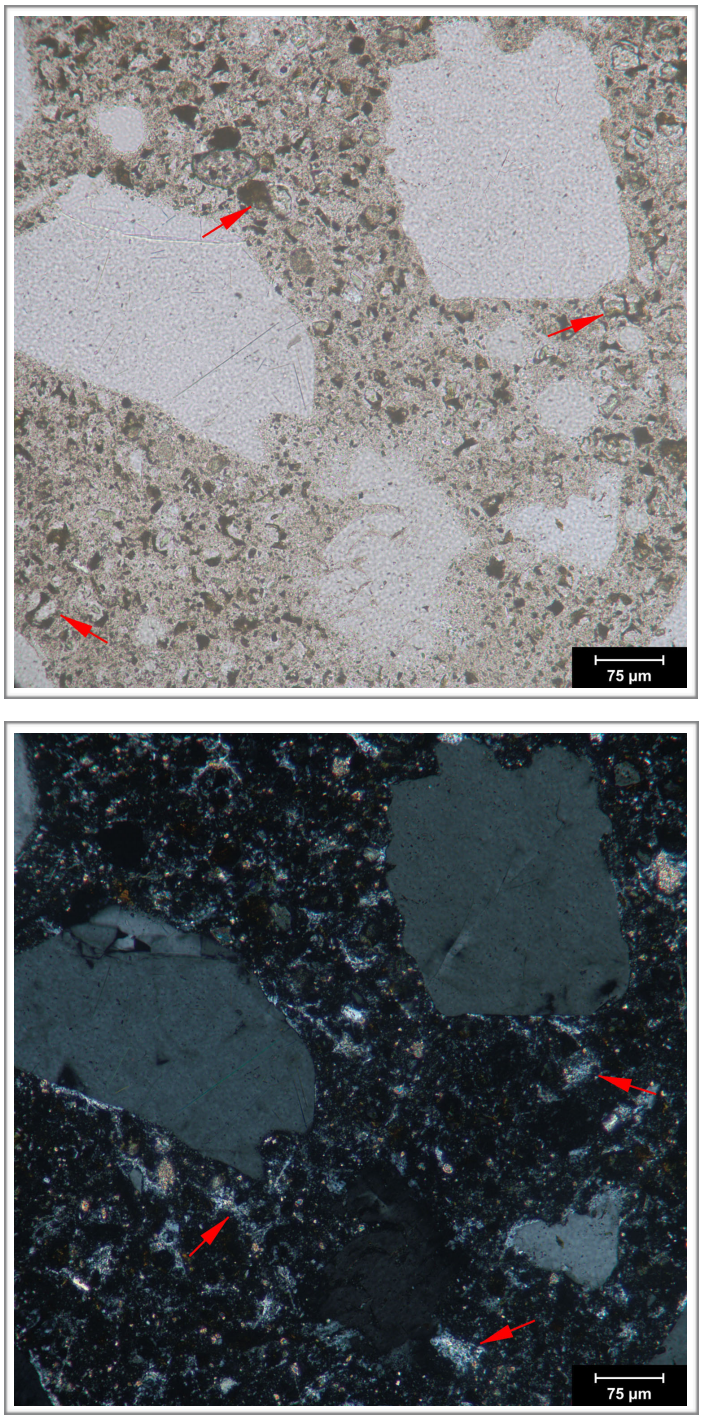

Figure A12. Transmitted light photomicrographs of thin section from the concrete core showing detail of paste in (a) plane-polarized and (b) cross-polarized light. The red arrows indicate RRCG in (a) and coarse calcium hydroxide in (b).

(a)

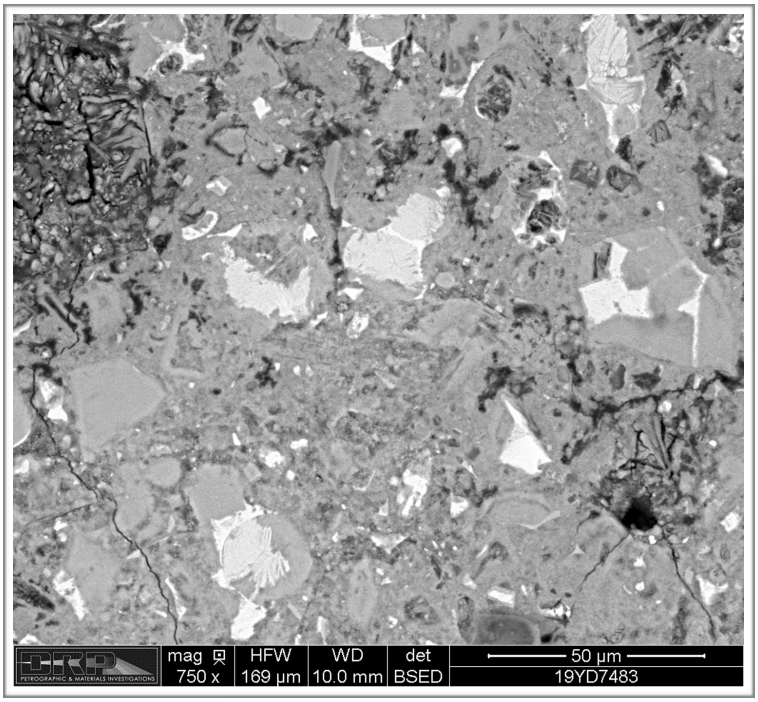

(b)

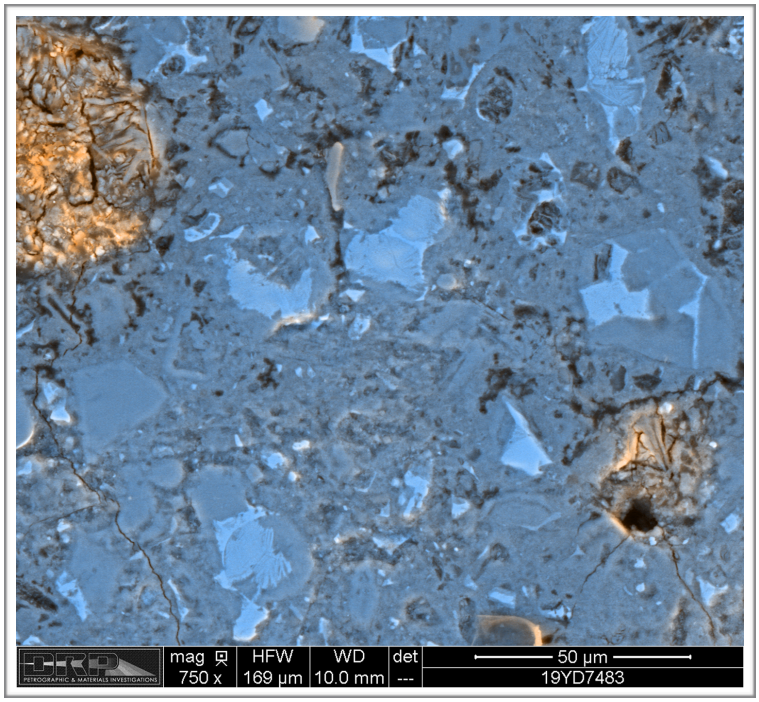

Figure A13. (a) Backscatter electron (BSE) and (b) combined backscatter/secondary electron (BSE/SE) micrograph of polished surface showing detail of paste. The white areas in (a) represent relict and residual cement grains.

(a)

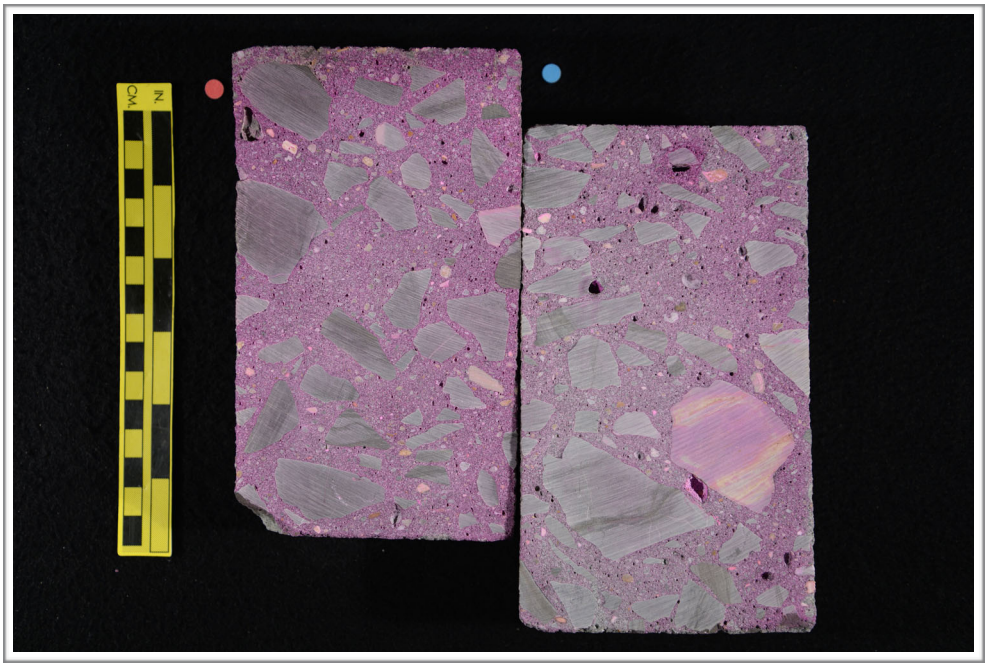

(b)

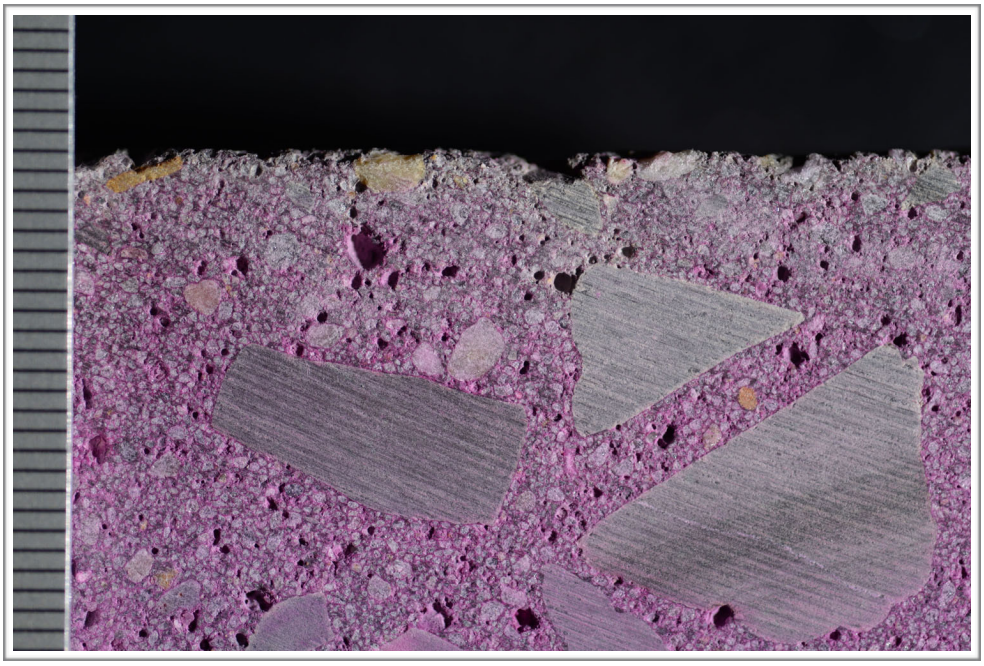

Figure A14. Photographs showing (a) overview of phenolphthalein stained surface and (b) detail of surface near the top of the core. Scale in millimeters in (b).

(a)

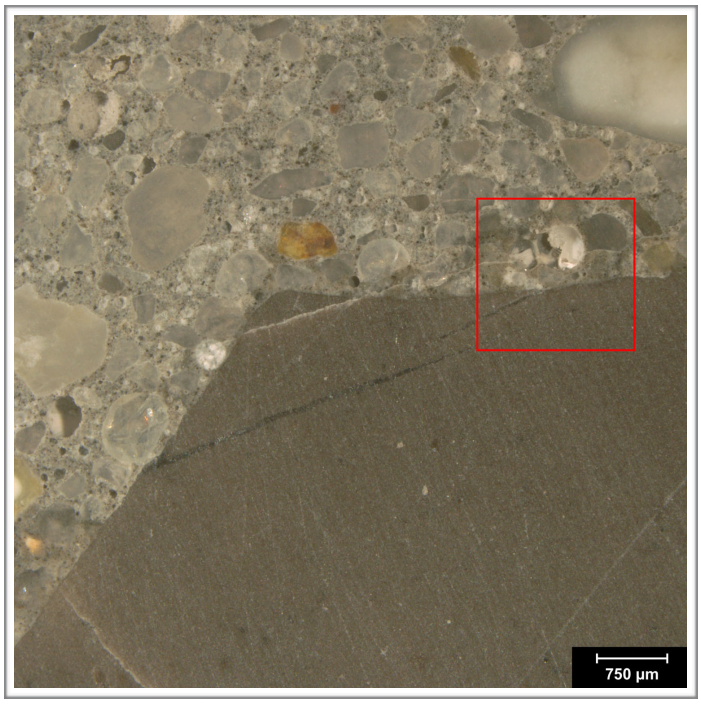

(b)

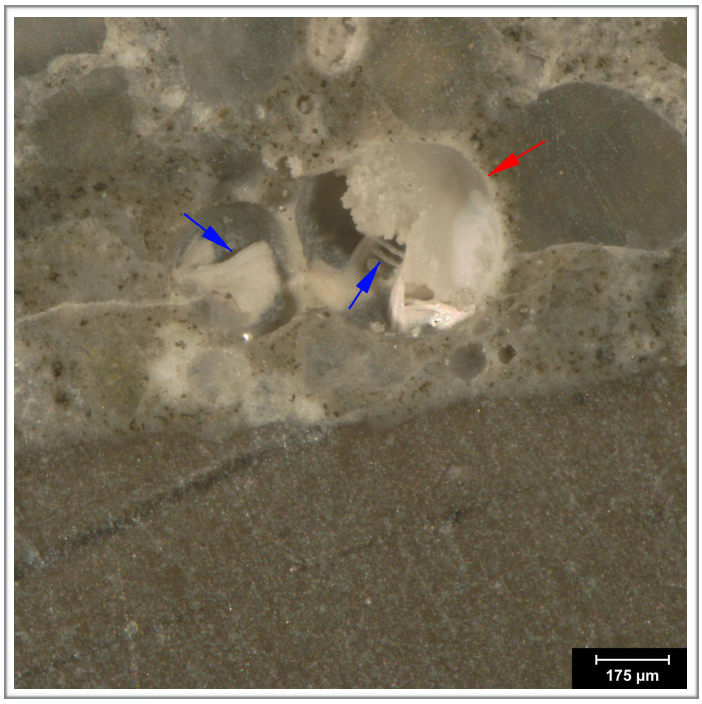

Figure A15. Reflected light photomicrographs of polished surface showing (a) overview and (b) detail of gel deposits in void next to a coarse aggregate particle about 85 mm (3 ⅜ in.) below the top surface. The red square in (a) shows the approximate area of (b) where the red arrow indicates a gelatinous deposit and blue arrows indicate more crystalline deposits.

(c)

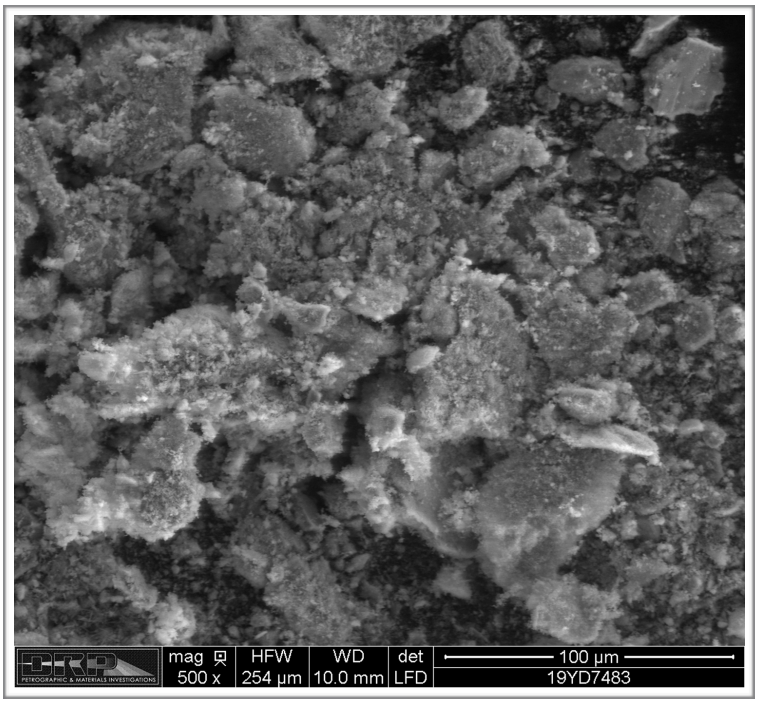

(d)

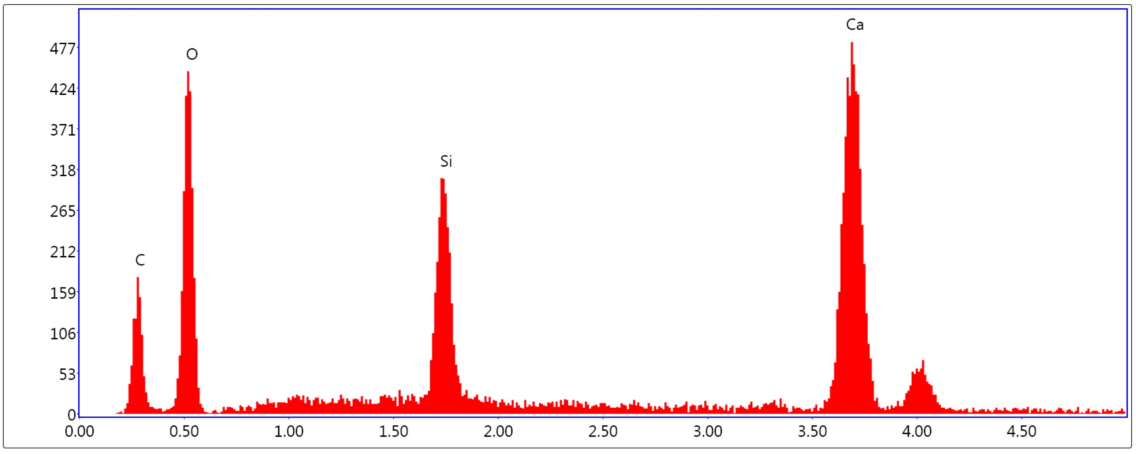

Figure A15 (cont'd). (c) Secondary electron micrograph of gel deposits scraped from voids shown in (b) and placed on carbon tape. (d) EDS spectrum of deposit indicating composition typical of ASR gel.

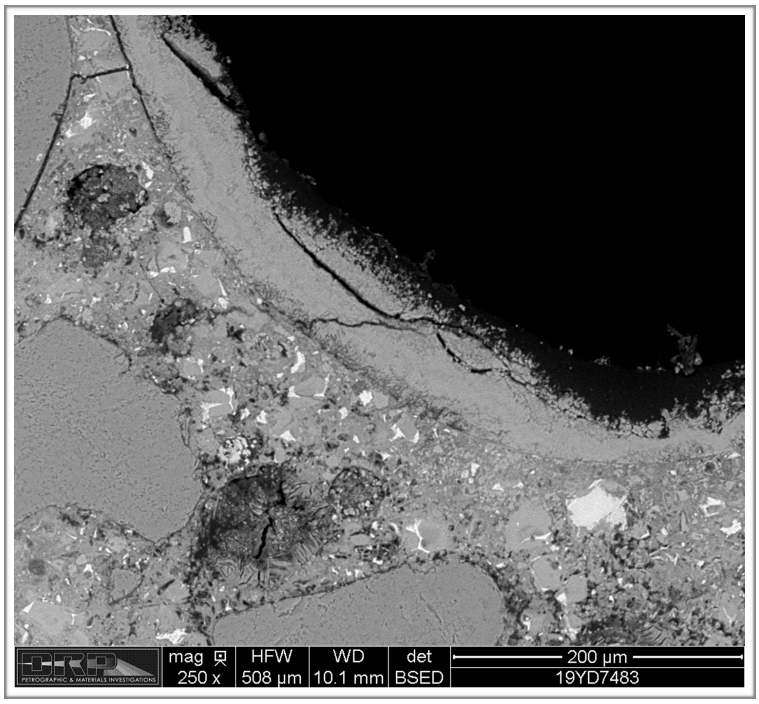

(a)

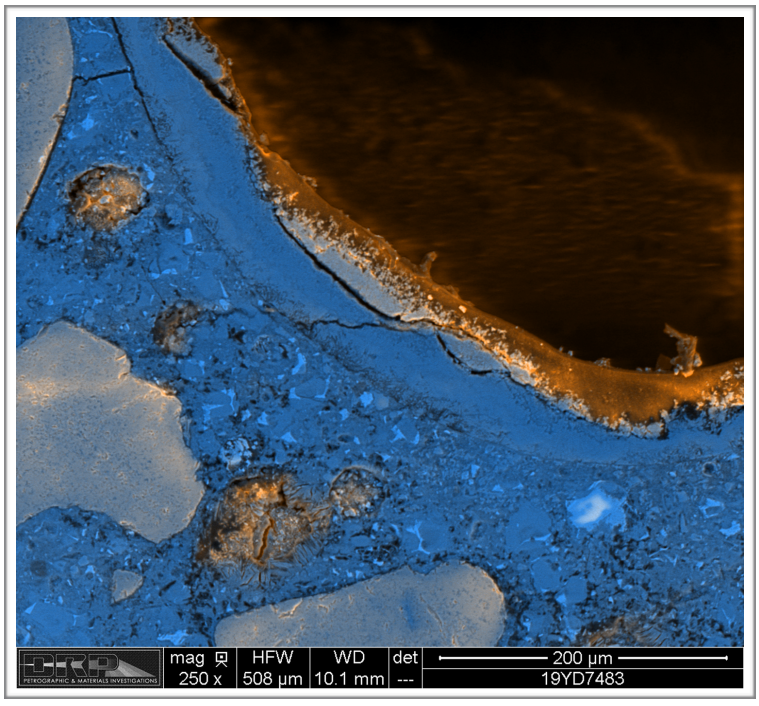

(b)

Figure A16. (a) Backscatter electron (BSE) and (b) combined backscatter/secondary electron (BSE/SE) micrograph of polished surface showing detail of void with gel.

(c)

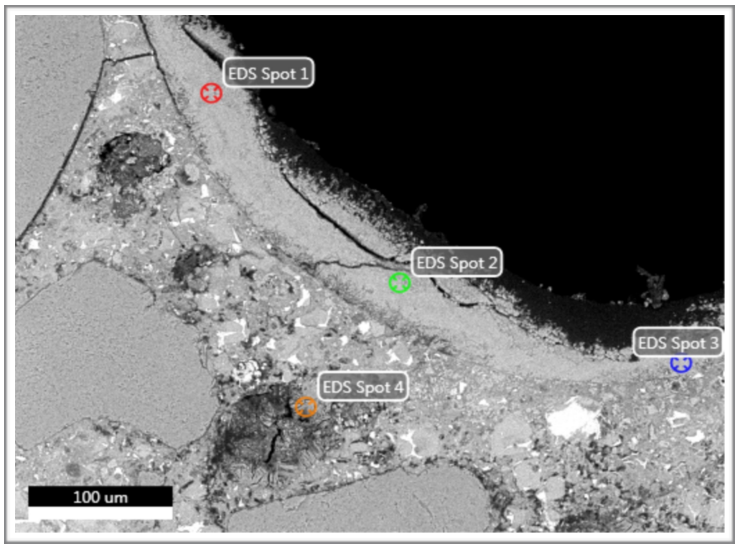

(d)

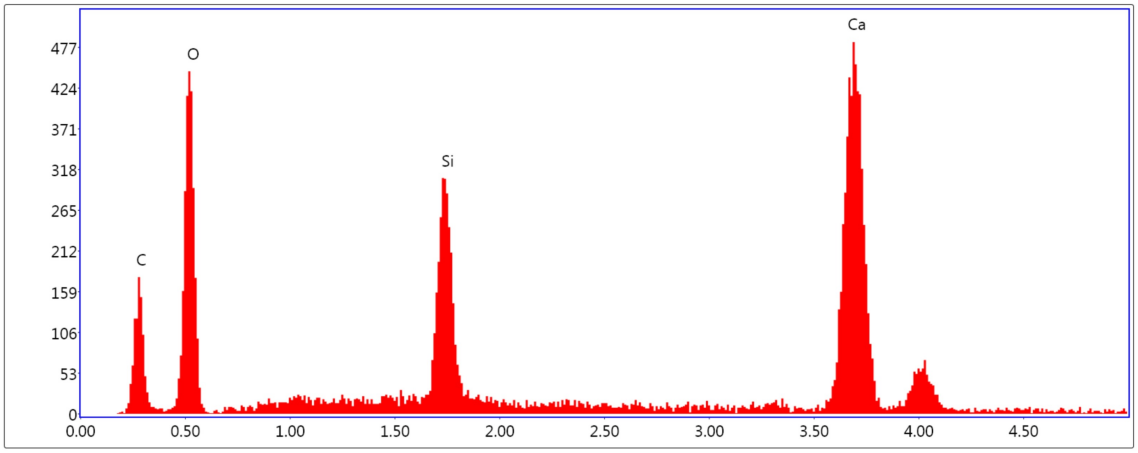

Lsec: 10.0 0 Cnts 0.000 keV Det: Apollo X-SDD Det

(e)

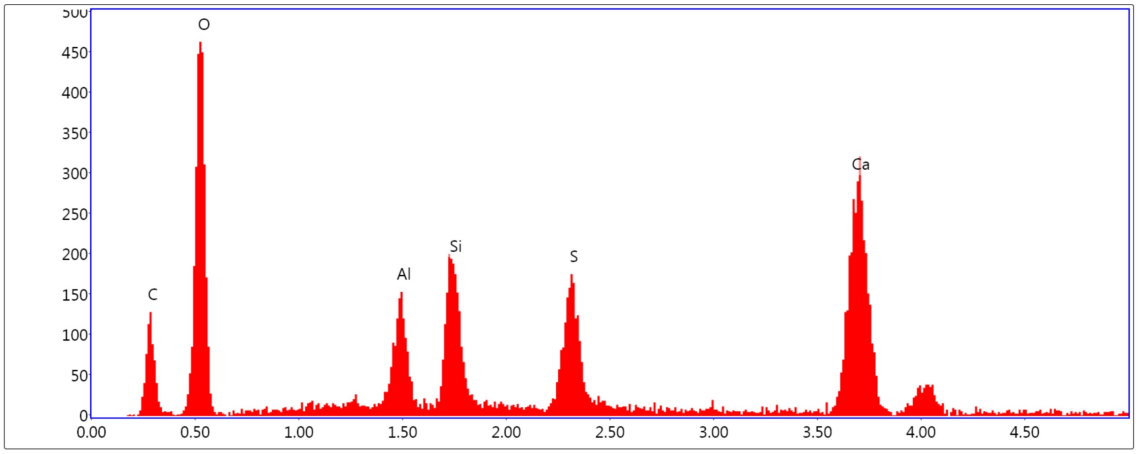

Lsec: 10.0 0 Cnts 0.000 keV Det: Apollo X-SDD Det

Figure A16 (cont'd). BSE micrograph showing location of EDS analyses in gel deposit shown in (a) and (b). The EDS spectrum shown in (d) is from EDS Spot 2 and is typical of ASR gel and Spots 1-3. The spectrum shown in (e) is from EDS Spot 4 and is typical of ettringite.

1. RECEIVED CONDITION

ORIENTATION	Vertical core taken through highway pavement slab measures 100 mm (~ 4 in.) in diameter and 330 mm (~ 13 in.) long (**Figure B1, B2**).
SURFACES	The top surface has a worn tined texture and exposed coarse aggregate particles that are worn smooth (**Figure B3**) and the bottom surface is a saw cut such that the core represents a partial thickness of the pavement slab.
GENERAL CONDITION	The concrete is hard and compact and rings lightly when sounded with a hammer. The core was received in two pieces with the break at 180-210 mm (7 ⅛- 8 ¼ in.).

2. EMBEDDED OBJECTS

GENERAL	None observed.

3. CRACKING

MACROSCOPIC	A linear crack cuts across the top surface of the core; the crack is up to ~ 500 µm (20 mil) wide and has a strike length of 30 mm (1 ⅛ in.) on the surface (**Figure B4**). On the polished surface the crack cuts sub-vertically to a depth of ~ 9.5 mm (⅜ in.). The crack cuts around aggregate particles and is free of secondary deposits. A hairline crack that is ~ 100 µm (4 mil) wide cuts obliquely through the paste for ~ 12.5 mm (½ in.) about 125 mm (5 in.) below the top surface (**Figure B5**). The crack cuts around aggregate particles and is free of secondary deposits.
MICROSCOPIC	No significant microcracking was observed.

4.VOIDS

VOID SYSTEM	Concrete is air-entrained (**Figure B6**) and contains 7-9% air by visual estimation (not determined following ASTM C457). The core is moderately well consolidated with a few voids up to 9.5 mm (⅜ in.) across observed throughout the core, including one ~ 6 mm (¼ in.) below the top surface.
VOID FILLINGS	Voids are commonly lined with ettringite. Rare voids contain gel.

5. COARSE AGGREGATE

PHYSICAL PROPERTIES	Crushed quarry rock with 38 mm (1 ½ in.) nominal top size (**Figure B7**). The rocks are hard and competent. The particles are sub-equant to tabular in shape with sub-angular to sub-round edges. The grading and distribution are relatively even. The sand is very fine.
ROCK TYPES*	The aggregate is carbonate in composition and consists of brown dolomitic limestone similar to that in Core #1. The limestone is massive and dense; most particles lack significant sedimentary features.
OTHER FEATURES	No deleterious coatings or incrustations observed. No low w/c mortar coatings observed. Occasional particles show very internal microcracking that appears more consistent with the processing of the aggregate than alkali-carbonate reaction (ACR).

**Modal abundance based on visual estimation.*

6. FINE AGGREGATE

PHYSICAL PROPERTIES	Natural sand consists of rocks that are hard and competent (**Figure B8**). The particles are sub-equant to tabular in shape with sub-round to sub-angular edges. The grading and distribution are relatively even.
ROCK TYPES	The sand is siliceous in composition and consists primarily of quartz and quartzite with minor amounts of granitic rocks and chert.
OTHER FEATURES	No deleterious coatings or incrustations observed and no low w/c mortar coatings observed. Occasional particles of chert show evidence of ASR with reaction rims and microcracks that cut into the paste.

7. PASTE OBSERVATIONS

POLISHED SURFACE	Paste is gray (Munsell 2.5Y/6/1) to dark gray (2.5Y/4/1), has a smooth texture and sub-vitreous luster (**Figure B9**). The paste is hard (Mohs 3.5-4). The paste is slightly mottled light gray to grayish brown in the top 2-4 mm (80-160 mil).
FRESH FRACTURE	Fracture surface is light gray, has a hackly texture and a sub-vitreous luster. The fracture cuts primarily through aggregate particles (**Figure B10**). No significant secondary deposits were observed though minor deposits of ettringite commonly line voids.
THIN SECTION*	The paste contains hydrated portland cement; no fly ash, slag cement or other SCM were observed. The hydration is normal with 4-8% RRCG that consist mostly of interstitial ferrite and aluminate with occasional grains of belite (**Figure B11**). CH makes up 10-17% of the paste, is fine to medium-grained and evenly distributed.

** Abbreviations as follows: RRCG = relict and residual cement grains; SCM = supplemental cementitious materials; CH = calcium hydroxide; ITZ = interfacial transition zone. Modal abundances are based on visual estimations.*

8. SECONDARY DEPOSITS

PHENOLPHTHALEIN	Entire surface stains purple (**Figure B12**).
DEPOSITS	Minor carbonation observed at the top of the core and in irregularly distributed zones in the paste in thin section. Minor deposits of ettringite observed in voids. Trace to minor deposits of ASR gel observed in rare voids, most commonly next to limestone particles (**Figure B13, Figure B14**).

FIGURES

(a)

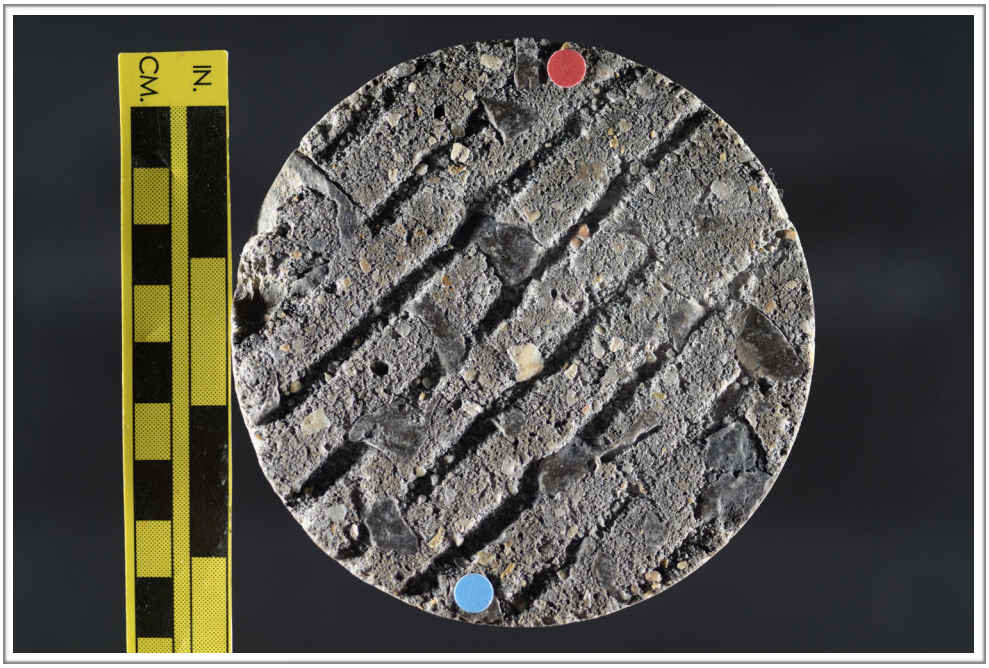

(b)

Figure B1. Photographs showing (a) oblique view of the top and side of the core with identification labels and (b) the top of the core. The red and blue dots in (a) show the orientation of the saw cuts used to prepare the sample.

(c)

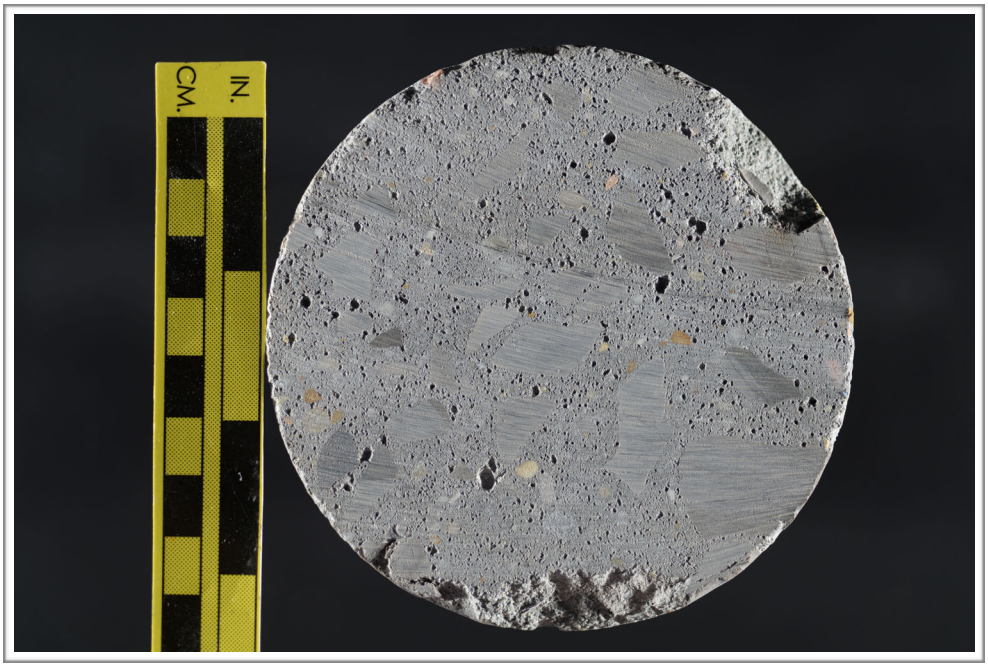

Figure B1 (cont'd). (c) Photograph showing the bottom of the core.

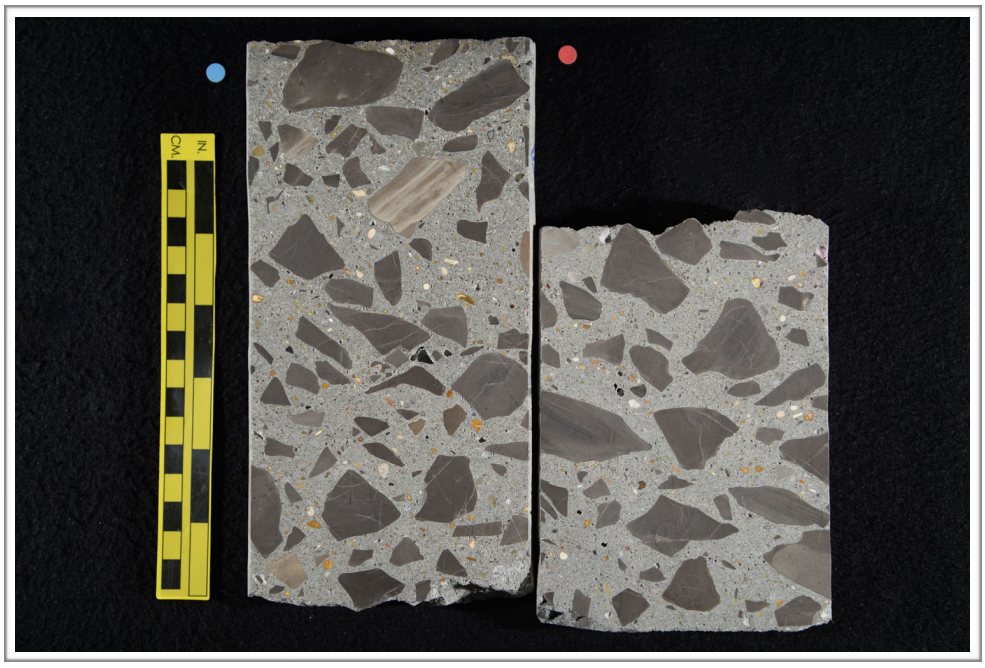

Figure B2. Photograph showing the polished surface of the core.

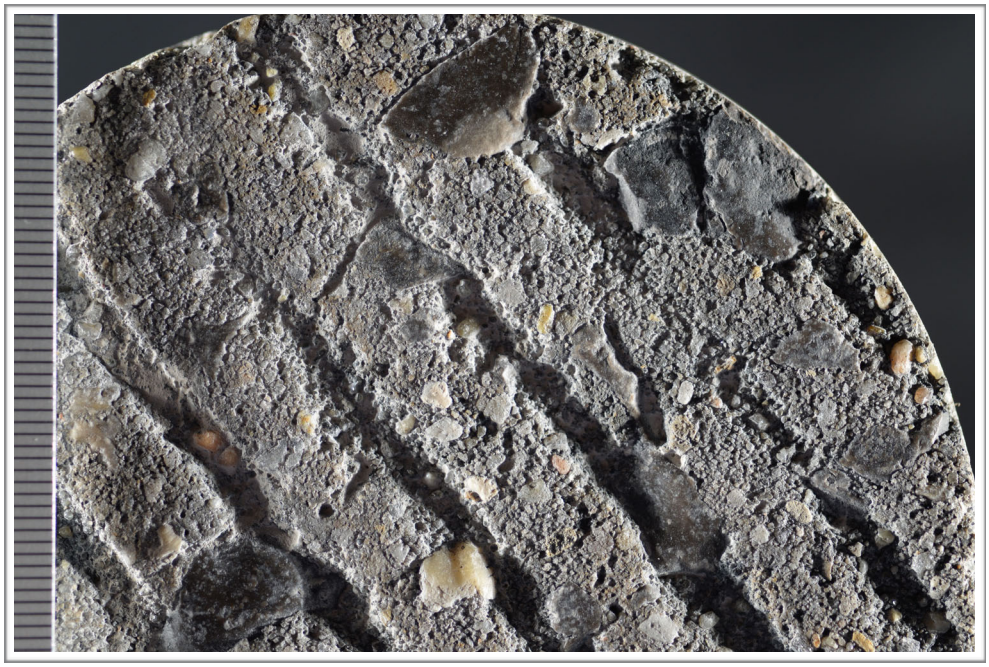

Figure B3. Photograph showing detail of the top surface of the core; scale in millimeters.

Figure B4. Photograph showing crack (red arrows) on the top surface; scale in millimeters.

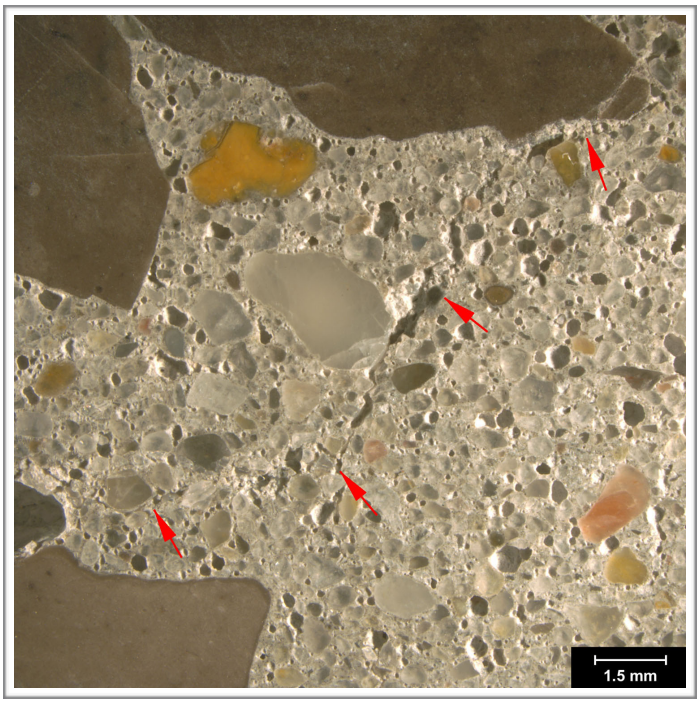

Figure B5. Reflected light photomicrograph of the polished surface showing hairline crack (red arrows) about 125 mm (5 in.) below the top surface.

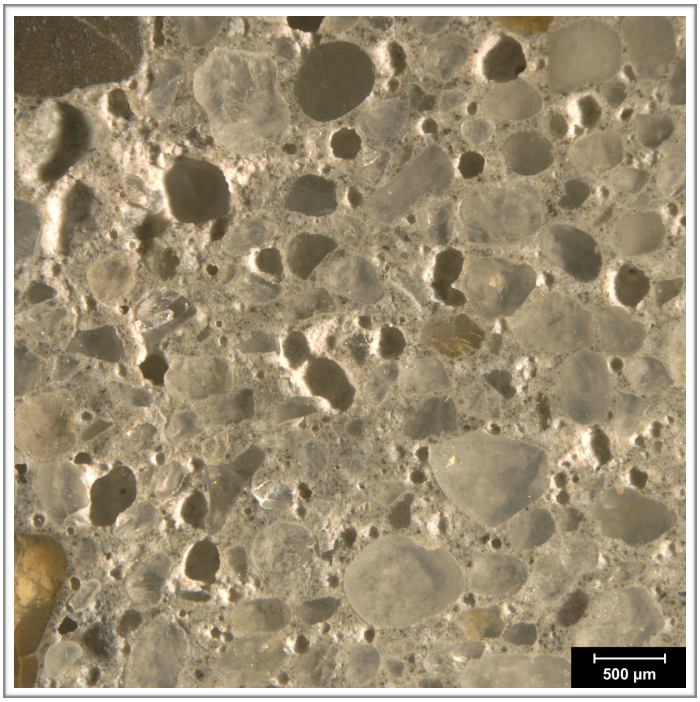

Figure B6. Reflected light photomicrograph of the polished surface showing entrained air voids (dark circles).

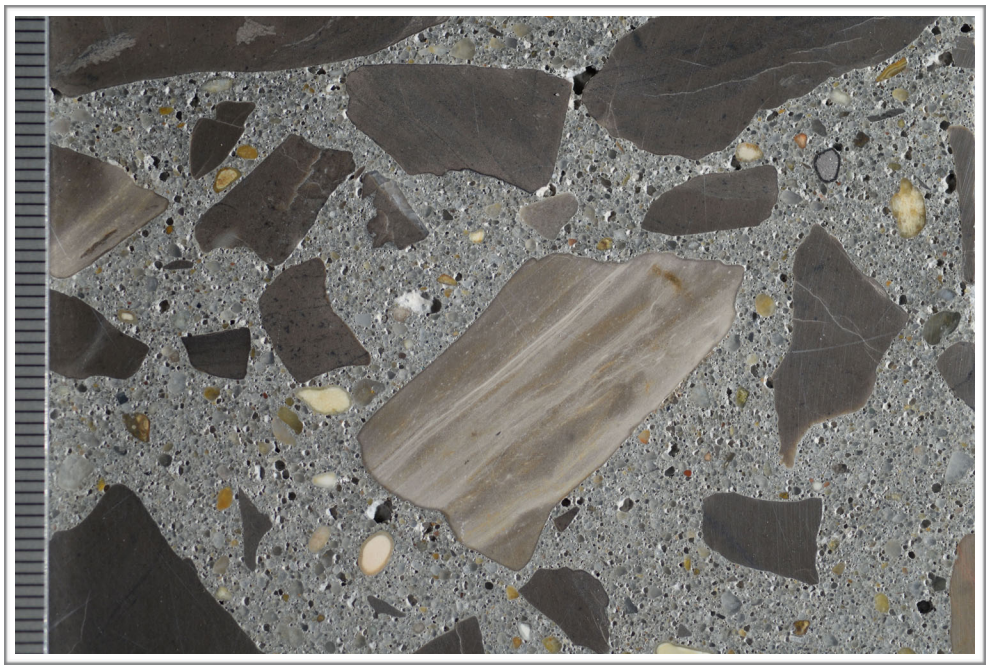

Figure B7. Photograph of the polished surface showing coarse aggregate; scale in millimeters.

Figure B8. Reflected light photomicrograph of polished surface showing the fine aggregate.

(a)

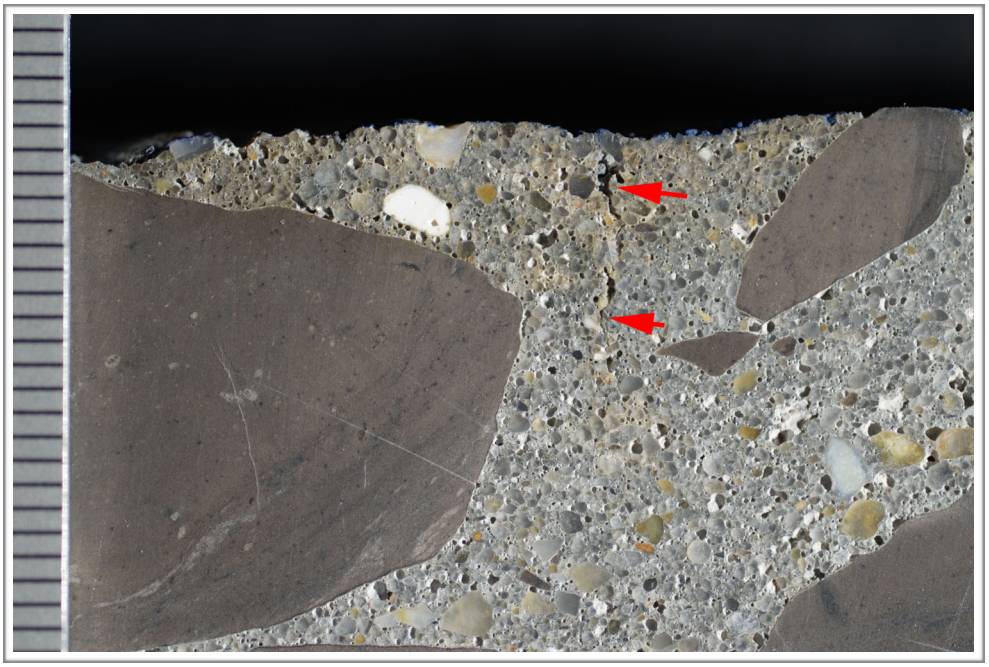

(b)

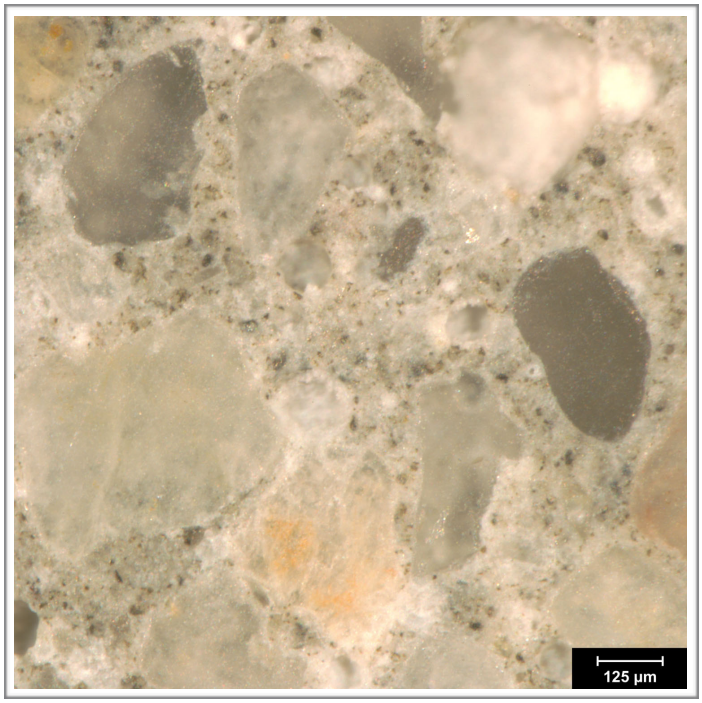

Figure B9. (a) Photograph of polished surface showing overview of paste at the top of the core. The scale is in millimeters; the red arrows indicate the hairline crack that cut across the top surface. (b) Reflected light photomicrograph showing detail of paste color, texture and luster in the middle of the core.

(a)

(b)

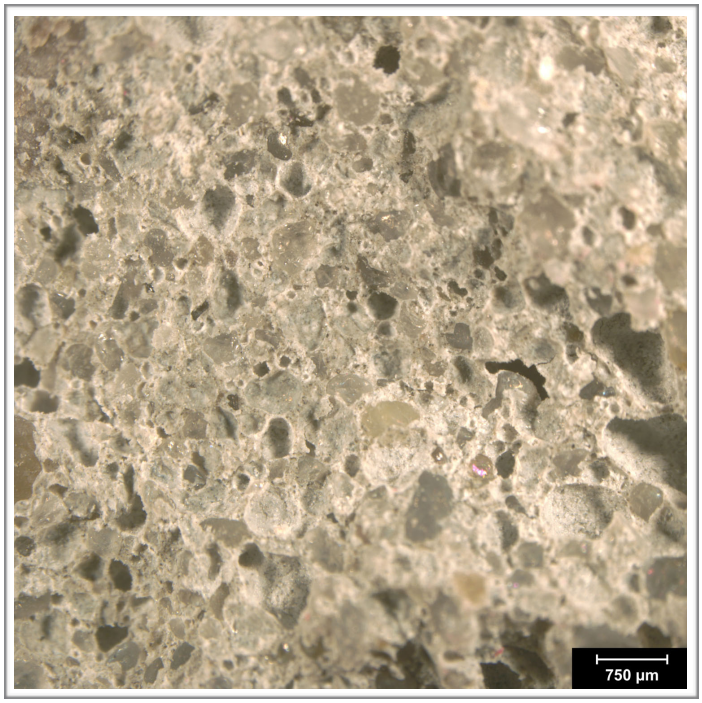

Figure B10. (a) Photograph and (b) reflected light photomicrograph of the fresh fracture surface. The scale in (a) is in millimeters.

(a)

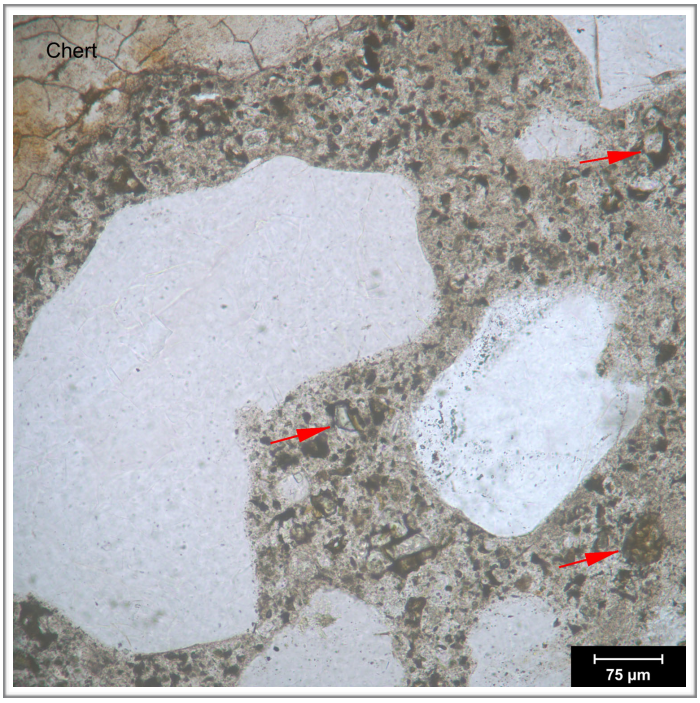

(b)

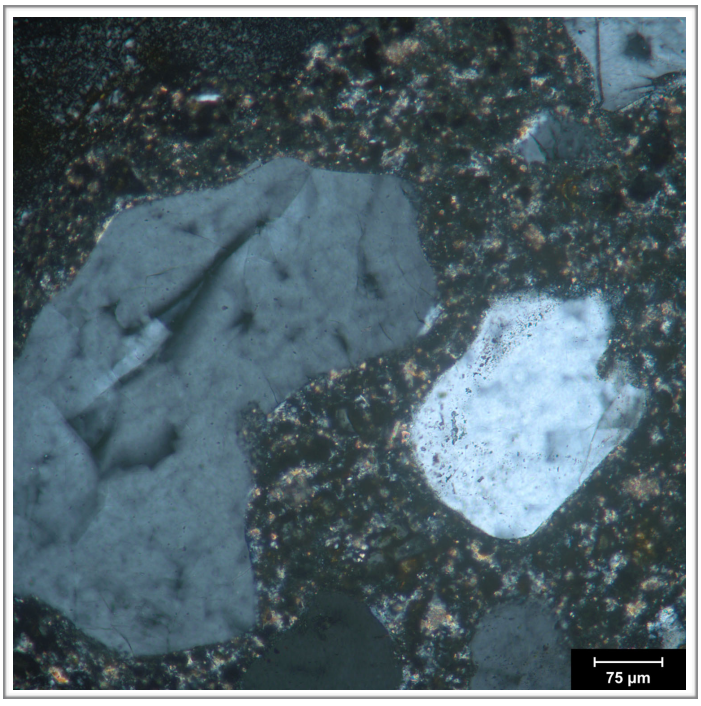

Figure B11. Transmitted light photomicrographs of thin section showing detail of paste in (a) plane-polarized and (b) cross-polarized light. The red arrows indicate RRCG in (a).

(a)

(b)

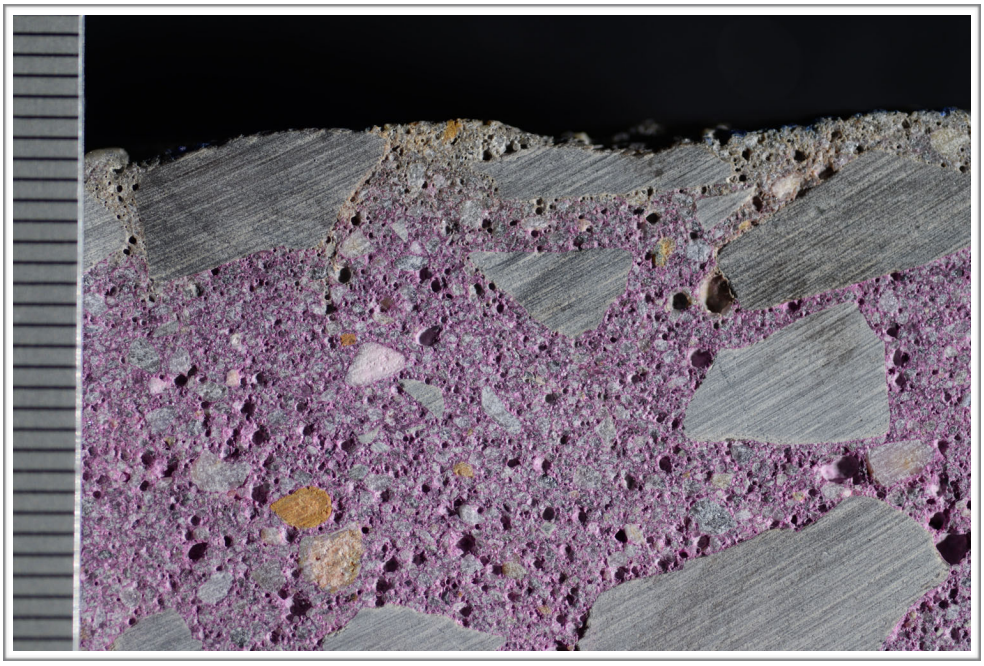

Figure B12. Photographs showing (a) overview of phenolphthalein stained surface and (b) detail of surface near the top of the core. Scale in millimeters in (b).

(a)

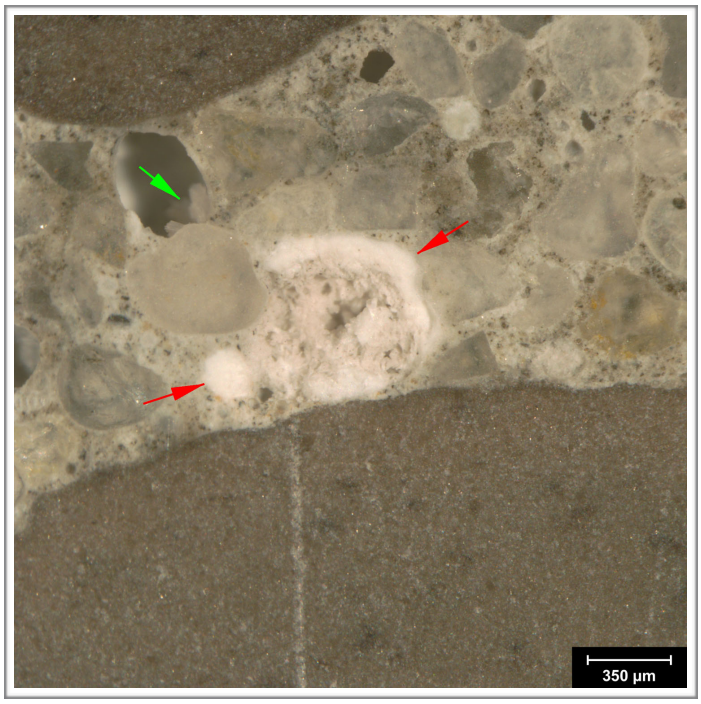

(b)

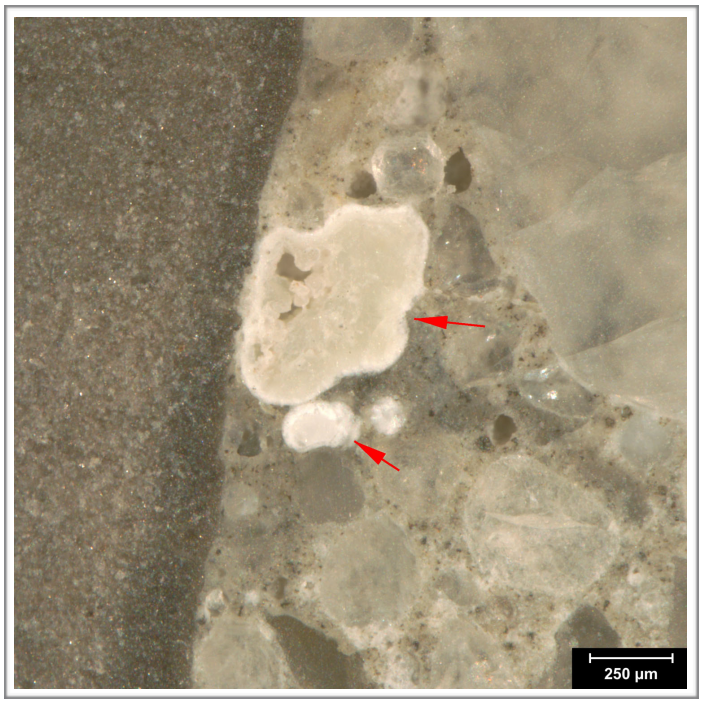

Figure B13. Reflected light photomicrographs of polished surface showing secondary deposits in voids (a) 35 mm (1 ⅜ in.) and (b) 220 mm (8 ⅝ in.) below the top surface. In (a) the red arrows indicate gelatinous deposits and the green arrow indicates a more crystalline deposit. In (b) the red arrow highlights a crystalline deposit.

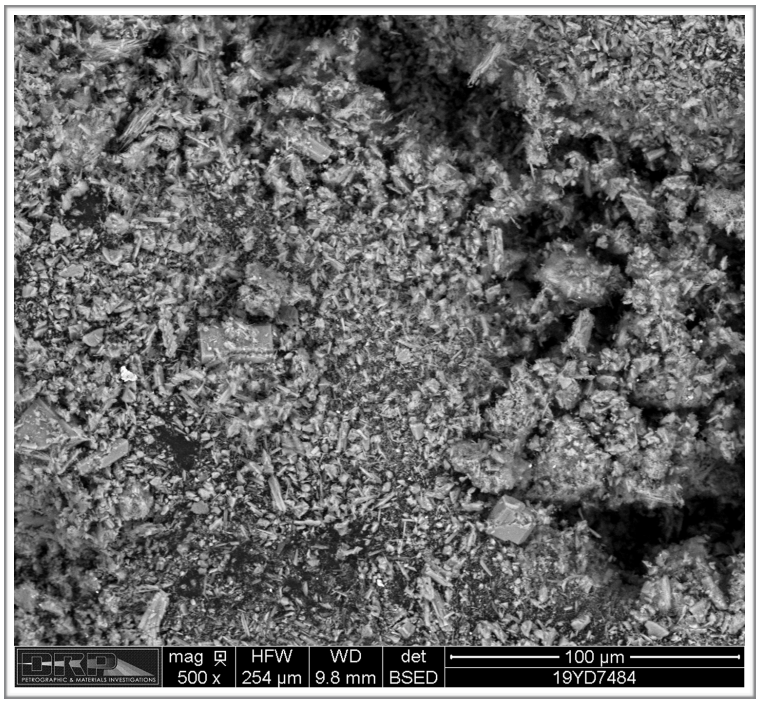

(a)

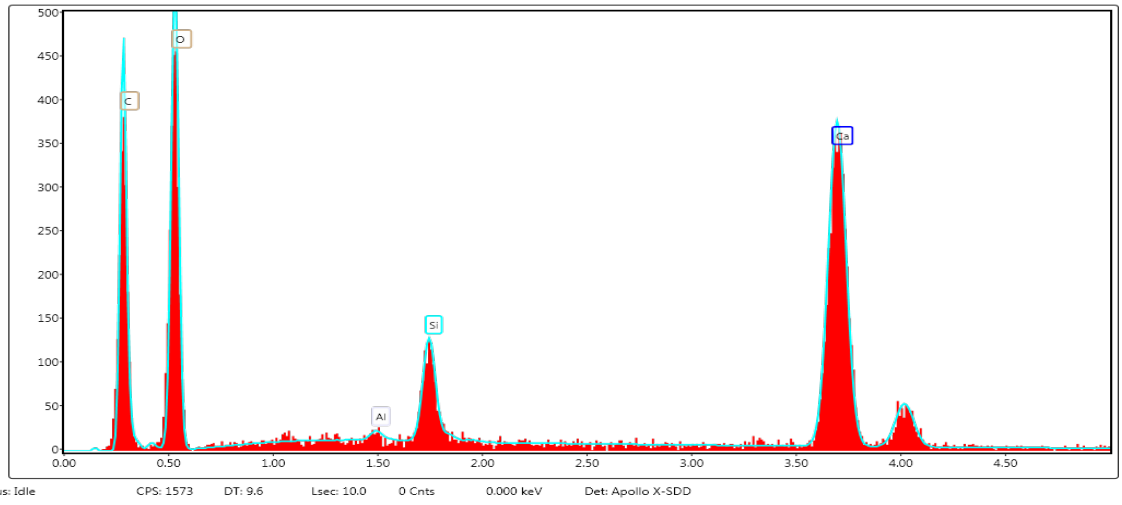

(b)

Figure B14. (a) Backscatter electron micrograph of gel deposits scraped from void shown in B13 (a) and placed on carbon tape. (b) EDS spectrum of deposit indicating composition typical of ASR gel.

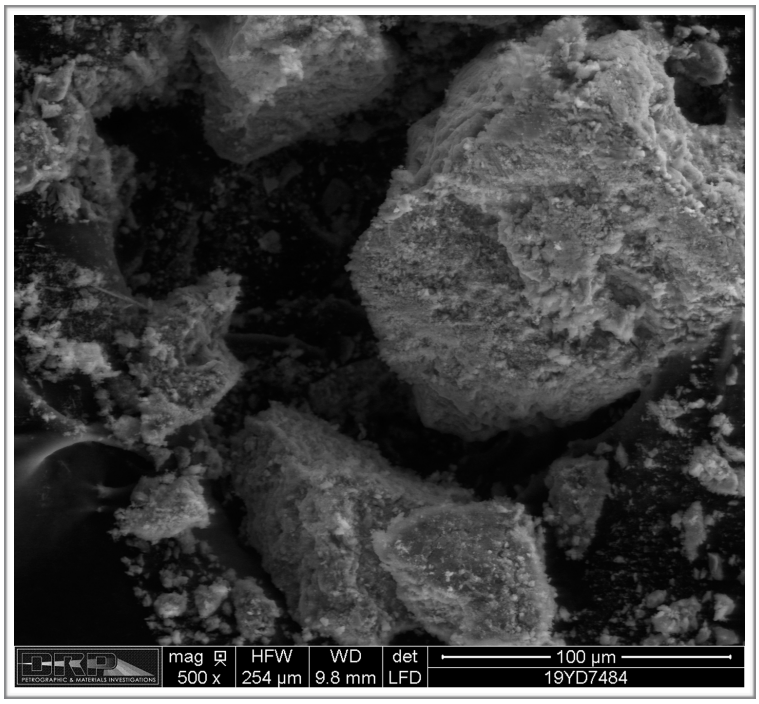

(a)

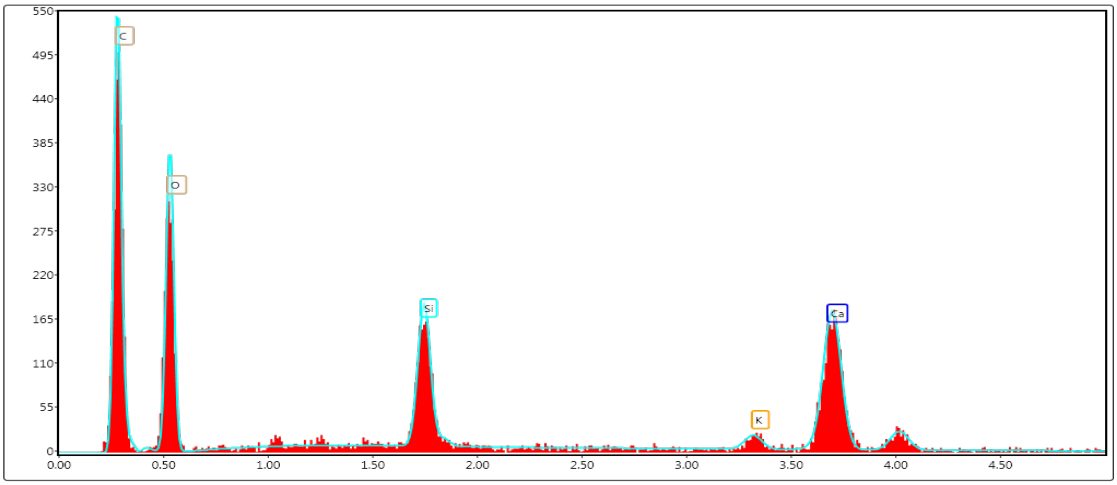

(b) Status: Idle CPS: 1284 DT: 10.5 Lsec: 10.0 0 Cnts 0.120 keV Det: Apollo X-SDD

Figure B15. (a) Backscatter electron micrograph of gel deposits scraped from void shown in B13 (b) and placed on carbon tape. (b) EDS spectrum of deposit indicating composition typical of ASR gel.

1. RECEIVED CONDITION

ORIENTATION	Vertical core taken through highway pavement slab measures 100 mm (~ 4 in.) in diameter and 330 mm (~ 13 in.) long (**Figure C1, C2**).
SURFACES	The top surface has a worn tined texture and exposed coarse aggregate particles that are worn smooth (**Figure C3**) and the bottom surface is a saw cut such that the core represents a partial thickness of the pavement slab.
GENERAL CONDITION	The concrete is hard and compact and rings lightly when sounded with a hammer. The core was received in three pieces. There is a horizontal break that cuts cross the core in two about 55 mm (2 ⅛ in.) below the top surface. The top piece is in turn cut in two by a sub-vertical crack (**Figure C4**).

2. EMBEDDED OBJECTS

GENERAL	None observed.

3. CRACKING

MACROSCOPIC	Two open cracks cut the core in three pieces as described above. These cracks cut primarily around aggregate particles and lack significant secondary deposits. On the polished surface there is a complex network of cracks and hairline cracks that splay from the main vertical crack and cut obliquely through the paste from ~ 25 mm (1 in.) to 38 mm (1 ½ in.) below the top surface where they cut sub-horizontally and then sub-vertically to the main horizontal crack (**Figure C5**). Numerous cracks ranging from 100-250 µm wide strike sub-horizontally to obliquely across the polished surface about 50 mm (2 in.) below the top of the core. A sub-vertical microcrack cuts from the main horizontal crack at ~ 50 mm (2 in.) depth to a depth of ~ 125 mm (5 in.). The crack cuts around aggregate particles and is free of secondary deposits (**Figure C6**).
MICROSCOPIC	Numerous microcracks were observed nested within the network of irregular cracking in the top 50 mm (2 in.). Some of these intersect or are next to voids with gelatinous deposits but the microcracks are free of secondary deposits (**Figure C7**). Occasional microcracks were observed throughout the remainder of the core; these are typically 25-100 µm (1-4 mil) wide and range up to 19 mm (¾ in.) long (**Figure C8**). These cut around aggregate particles and are free of secondary deposits. Many of these microcracks have irregular, undulating walls and variable widths.

4. VOIDS

VOID SYSTEM	Concrete is air-entrained (**Figure C9**) and contains 7-9% air by visual estimation (not determined following ASTM C457). The core is poorly consolidated in the top 55 mm (2 ⅛ in.) where several large, irregularly shaped voids ranging from 12.5-25 mm (½-1 in.) across were observed (**Figure C10**).
VOID FILLINGS	Voids are commonly lined with ettringite. Rare voids contain gel.

5. COARSE AGGREGATE

PHYSICAL PROPERTIES	Crushed quarry rock with 38 mm (1 ½ in.) nominal top size (**Figure C11**). The rocks are hard and competent. The particles are sub-equant to tabular in shape with sub-angular to sub-round edges. The grading and distribution are relatively even. The sand is very fine.
ROCK TYPES*	The aggregate is carbonate in composition and consists of brown dolomitic limestone similar to that in Core #1. The limestone is massive and dense; most particles lack significant sedimentary features.
OTHER FEATURES	No deleterious coatings or incrustations observed. No low w/c mortar coatings observed. Occasional particles show internal microcracking that is concentrated near the edge of the particle and cuts into the paste, but the particles lack significant reaction rims.

**Modal abundance based on visual estimation.*

6. FINE AGGREGATE

PHYSICAL PROPERTIES	Natural sand consists of rocks that are hard and competent (**Figure C12**). The particles are sub-equant to tabular in shape with sub-round to sub-angular edges. The grading and distribution are relatively even.
ROCK TYPES	The sand is siliceous in composition and consists primarily of quartz and quartzite with minor amounts of granitic rocks and chert.
OTHER FEATURES	No deleterious coatings or incrustations observed and no low w/c mortar coatings observed. Occasional particles of chert show evidence of ASR with reaction rims and microcracks that cut into the paste.

7. PASTE OBSERVATIONS

POLISHED SURFACE	Paste is gray (Munsell 2.5Y/6/1) to dark gray (2.5Y/4/1), has a smooth texture and sub-vitreous luster (**Figure C13**). The paste is hard (Mohs 3.5-4). The paste is slightly discolored to pale yellow brown in discrete zones that up to 3 mm (⅛ in.) thick in the top 12.5 mm (½ in.) of the core.
FRESH FRACTURE	Fracture surface is light gray, has a hackly texture and a sub-vitreous luster. The fracture cuts primarily through aggregate particles (**Figure C14**). No significant secondary deposits were observed though minor deposits of ettringite commonly line voids.
THIN SECTION*	The paste contains hydrated portland cement; no fly ash, slag cement or other SCM were observed. The hydration is normal with 4-8% RRCG that consist mostly of interstitial ferrite and aluminate with occasional grains of belite (**Figure C15**). CH makes up 10-17% of the paste, is fine to medium-grained and evenly distributed.

** Abbreviations as follows: RRCG = relict and residual cement grains; SCM = supplemental cementitious materials; CH = calcium hydroxide; ITZ = interfacial transition zone. Modal abundances are based on visual estimations.*

8. SECONDARY DEPOSITS

PHENOLPHTHALEIN	Entire surface stains purple (**Figure C16**).
DEPOSITS	Minor carbonation observed at the top of the core and in irregularly distributed zones in the paste in thin section. Minor deposits of ettringite observed commonly in voids. Minor deposits of ASR gel observed in voids (**Figure C17-Figure C19**). No evidence of cracking or microcracking due to ASR observed.

FIGURES

(a)

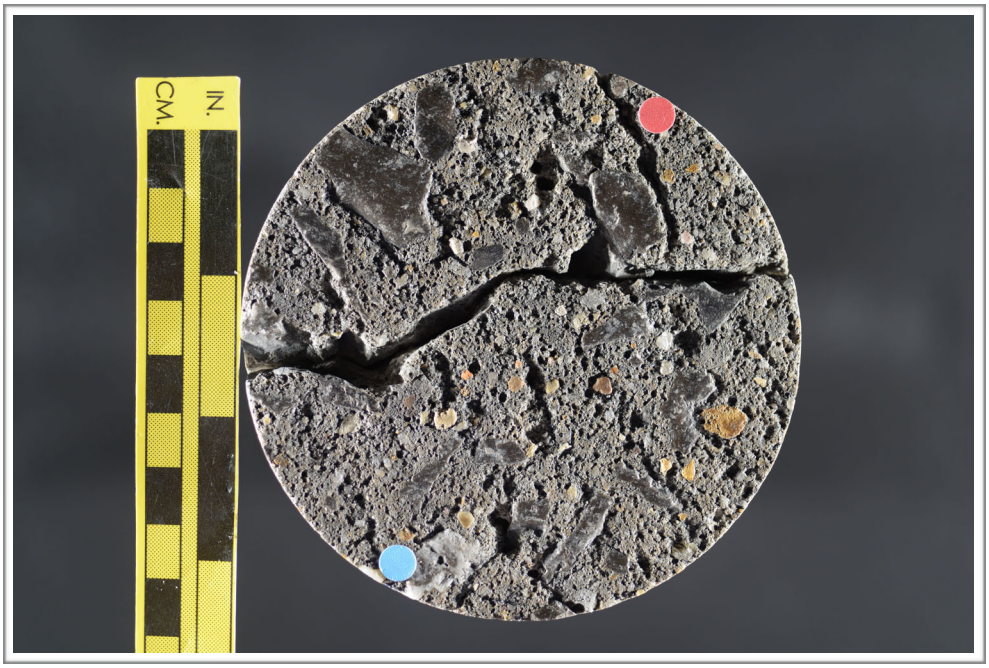

(b)

Figure C1. Photographs showing (a) oblique view of the top and side of the core with identification labels and (b) the top of the core. The red and blue dots in (a) show the orientation of the saw cuts used to prepare the sample.

(c)

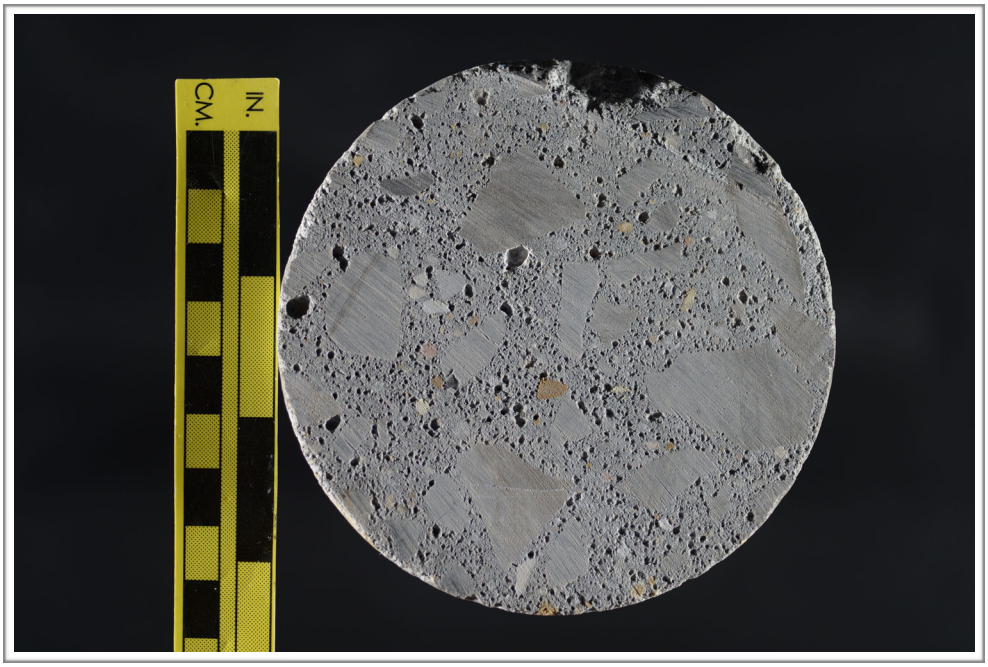

Figure C1 (cont'd). (c) Photograph showing the bottom of the core.

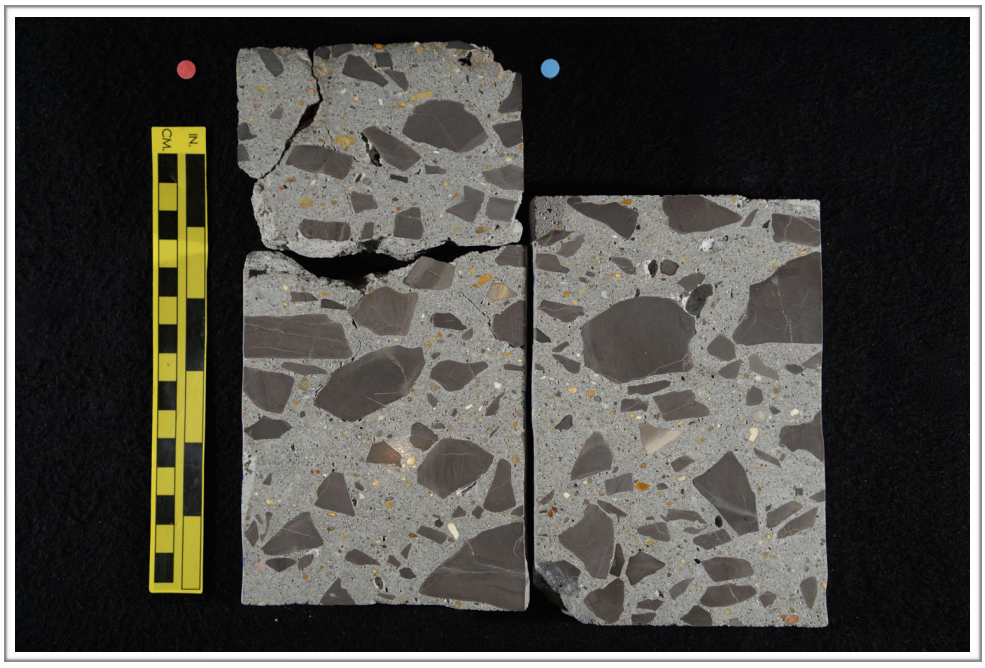

Figure C2. Photograph showing the polished surface of the core.

Figure C3. Photograph showing detail of the top surface of the core; scale in millimeters.

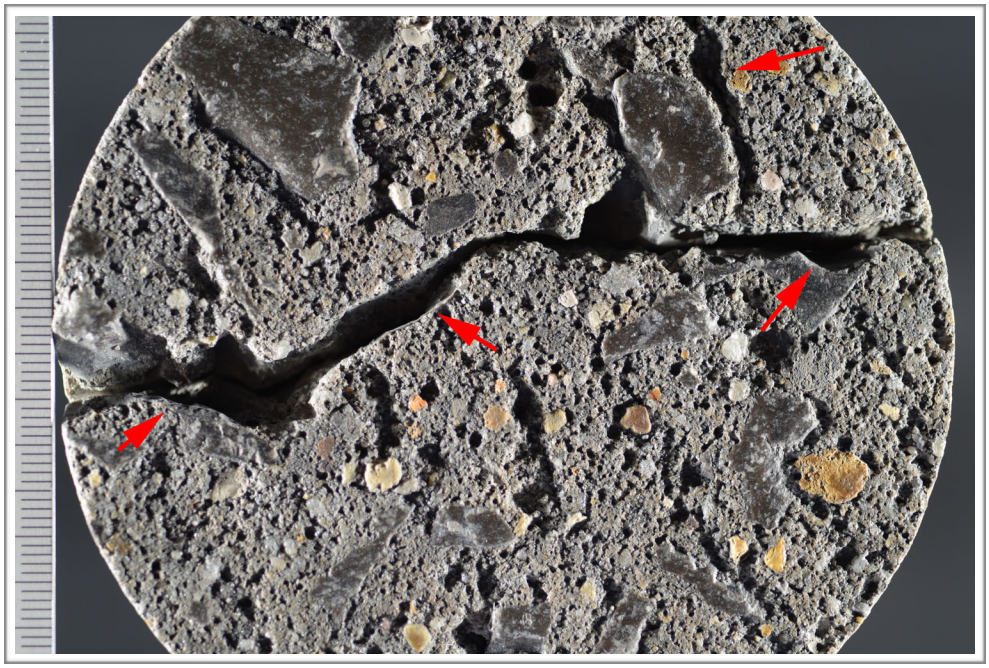

Figure C4. Photograph showing cracks (red arrows) on the top surface; scale in millimeters.

(a)

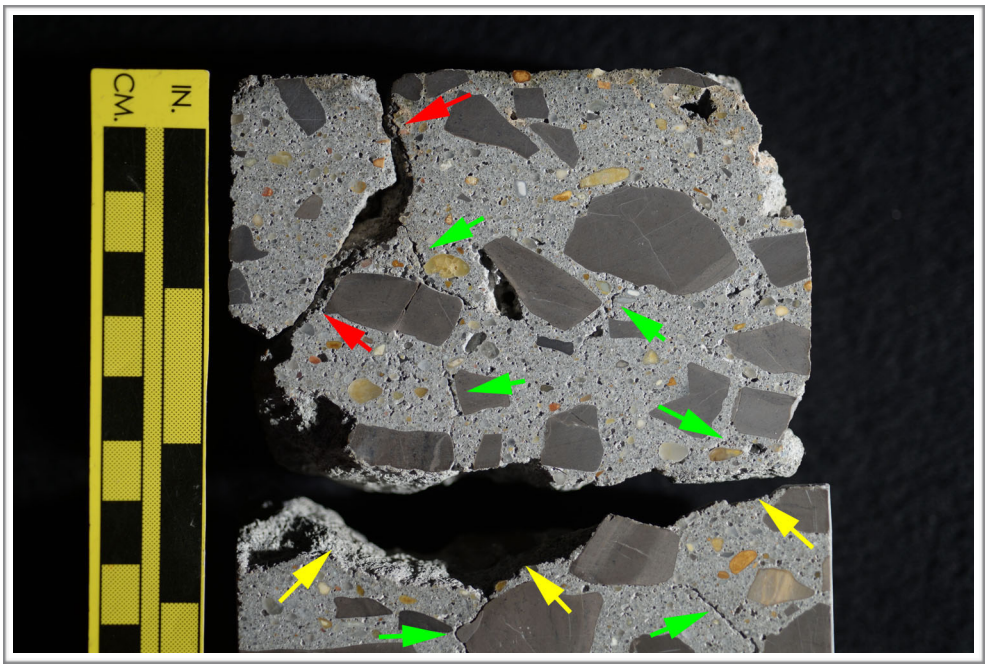

(b)

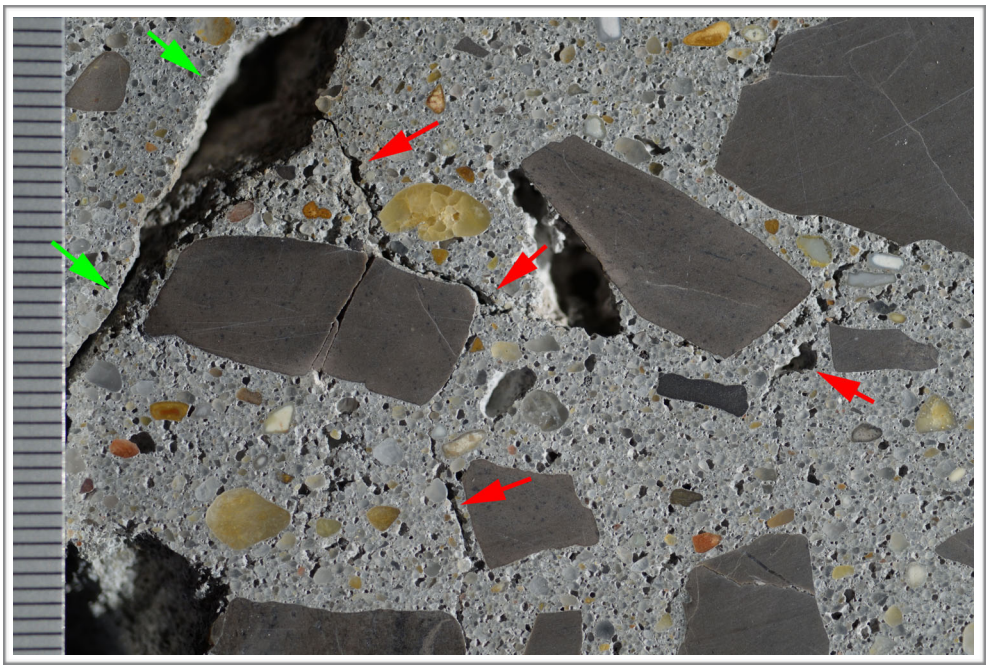

Figure C5. Photograph of the polished surface showing (a) overview and (b) detail of cracking near the top of the core. In (a) the yellow arrows indicate main horizontal crack that cut core in two and the red arrows indicate the main sub-vertical crack that cut the top piece in two pieces. The green arrows indicate smaller cracks. In (b) the green arrows indicate the main crack and the red arrows show smaller cracks. The scale is in millimeters in (b).

(a)

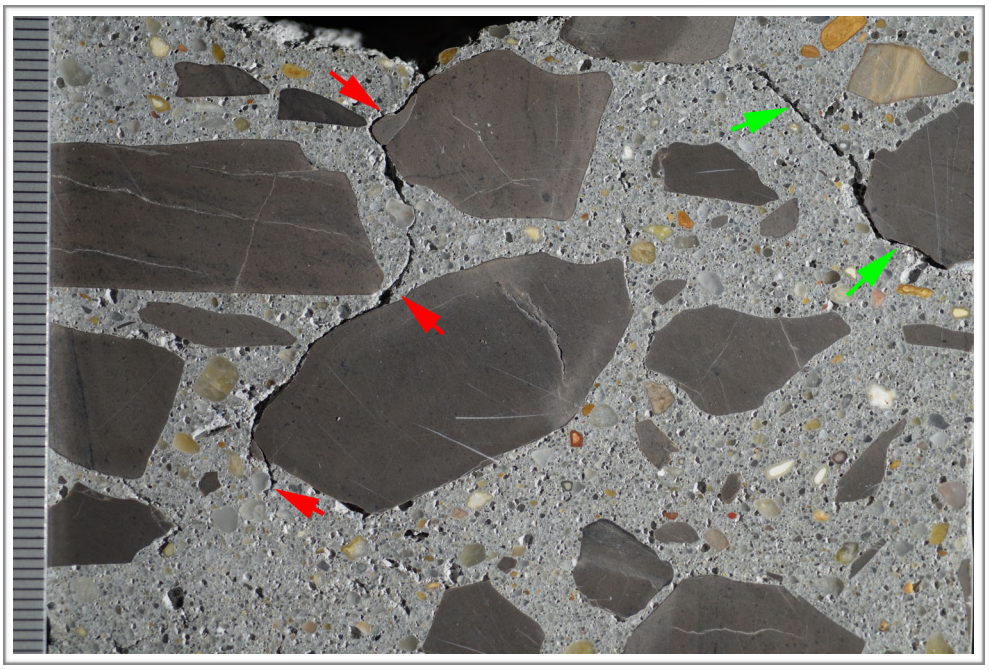

(b)

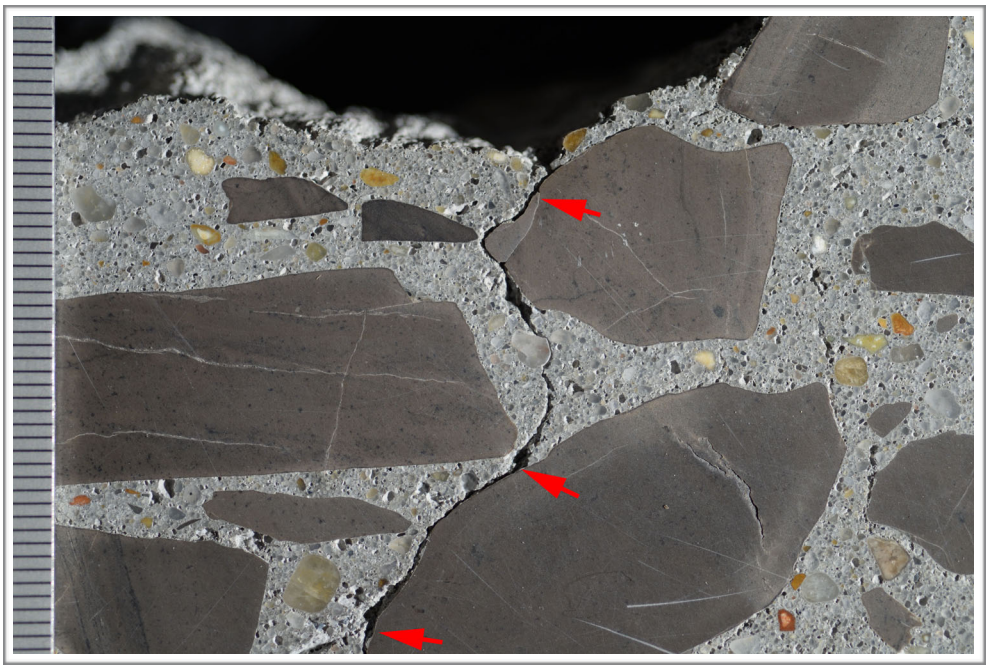

Figure C6. Photographs showing (a) overview and (b) detail of cracking below the main sub-horizontal crack about 50 mm (2 in.) below the top surface. The red arrows indicate the sub-vertical crack that from the horizontal crack. The green arrows in (a) indicate an oblique crack. The scale is in millimeters in both photos.

(a)

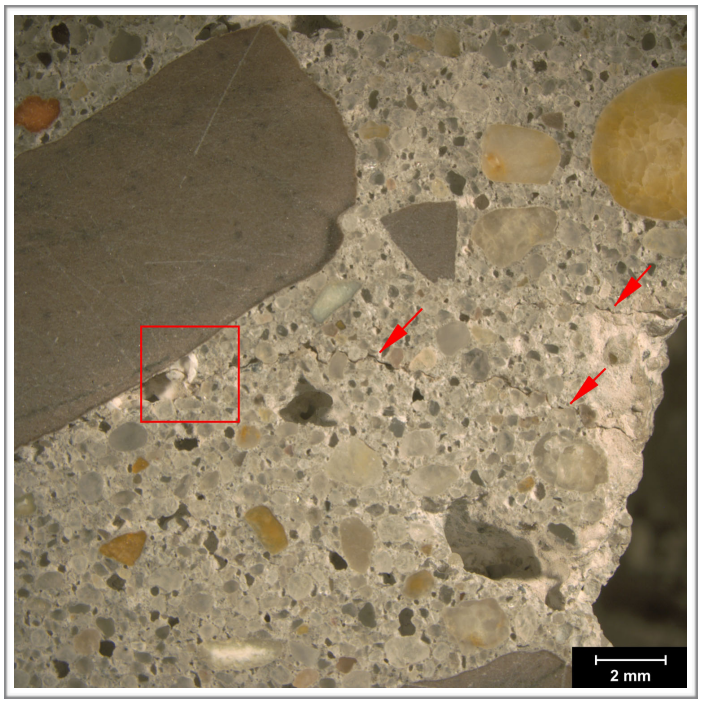

(b)

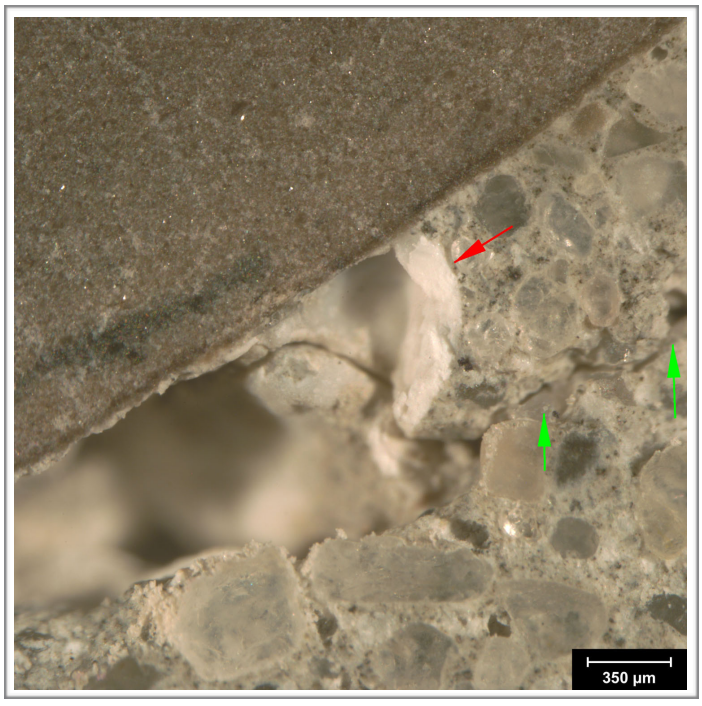

Figure C7. Reflected light photomicrographs of the polished surface showing (a) overview and (b) detail of microcracks about 38 mm (1 ½ in.) below the top surface. In (a) the red arrows indicate sub-horizontal microcracks that intersect a void next to a limestone particle that contains gelatinous deposits. The red box in (a) shows the approximate area of (b), where the red arrow indicates the deposit and the green arrows indicate a microcrack.

(a)

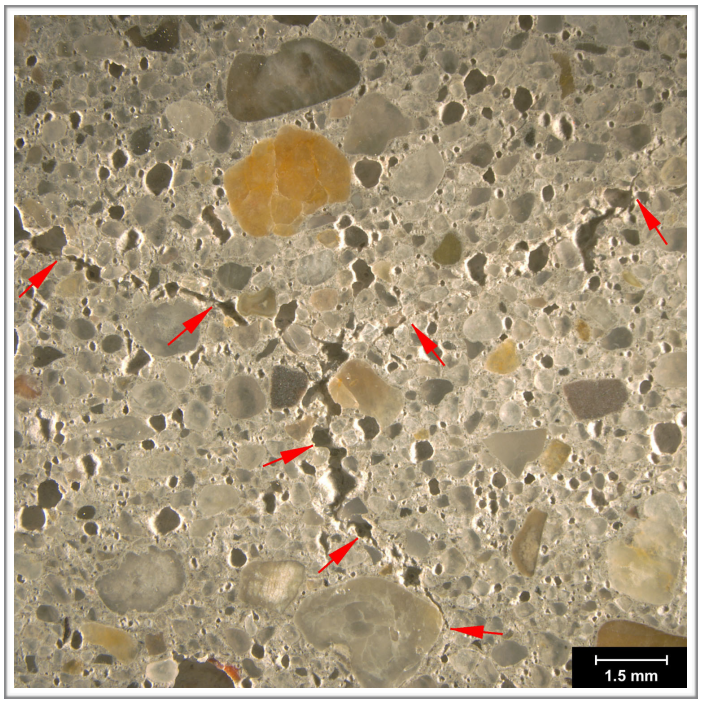

(b)

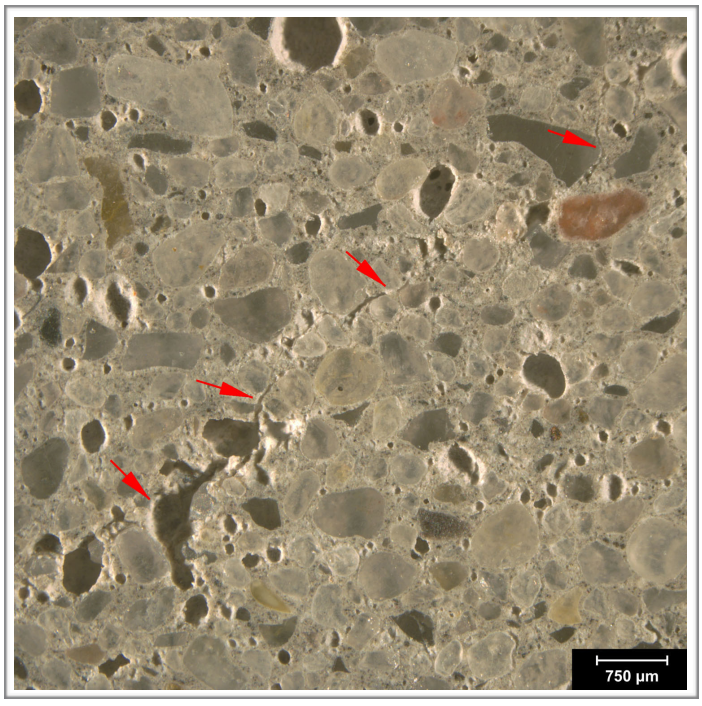

Figure C8. Reflected light photomicrographs of the polished surface showing microcracks (red arrows) about (a) 145 mm (5 ¾ in.) and (b) 150 mm (6 in.) below the top surface.

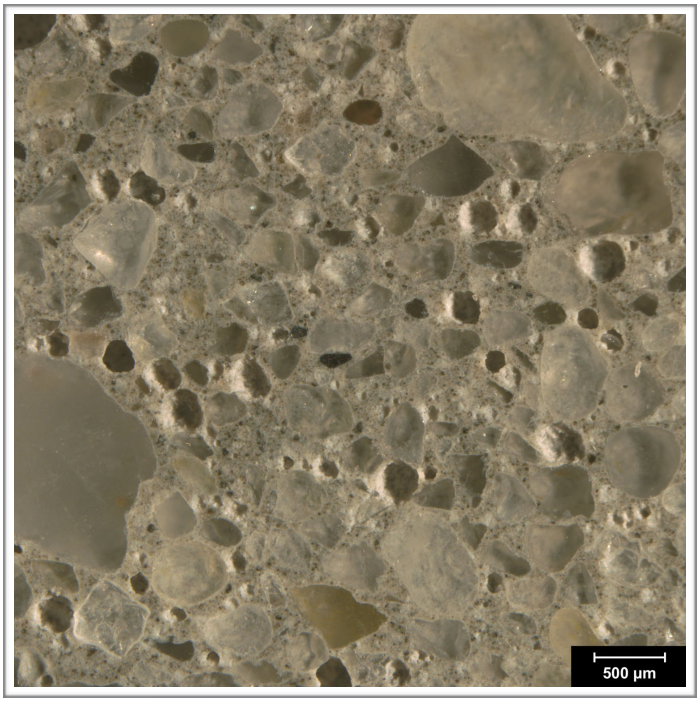

Figure C9. Reflected light photomicrograph of the polished surface showing entrained air voids (dark circles).

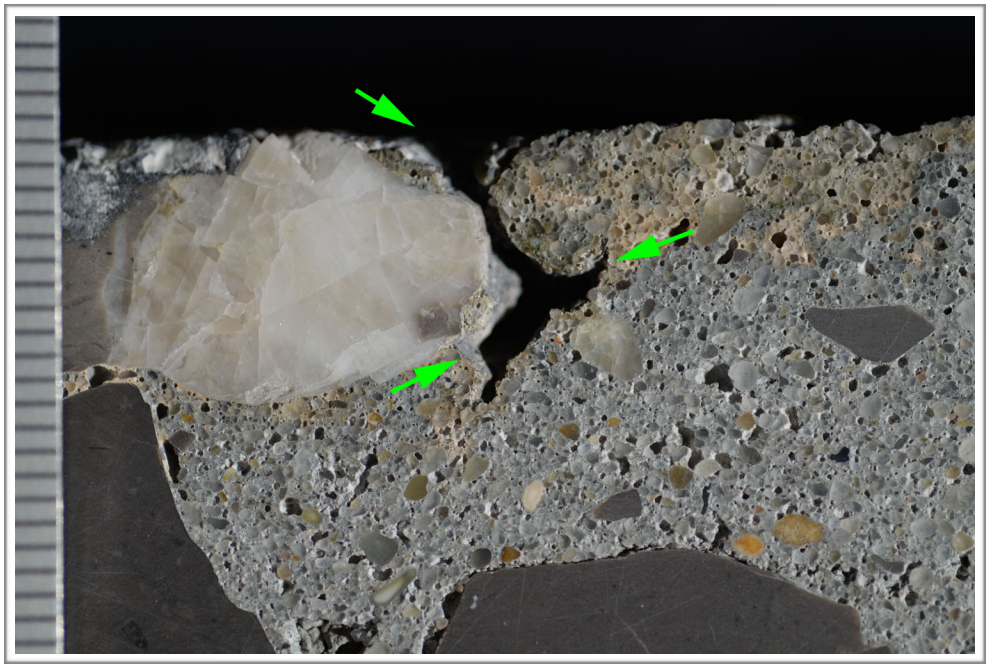

Figure C10. Photograph of the polished surface showing irregular void (green arrows) at the top of the core; scale in millimeters.

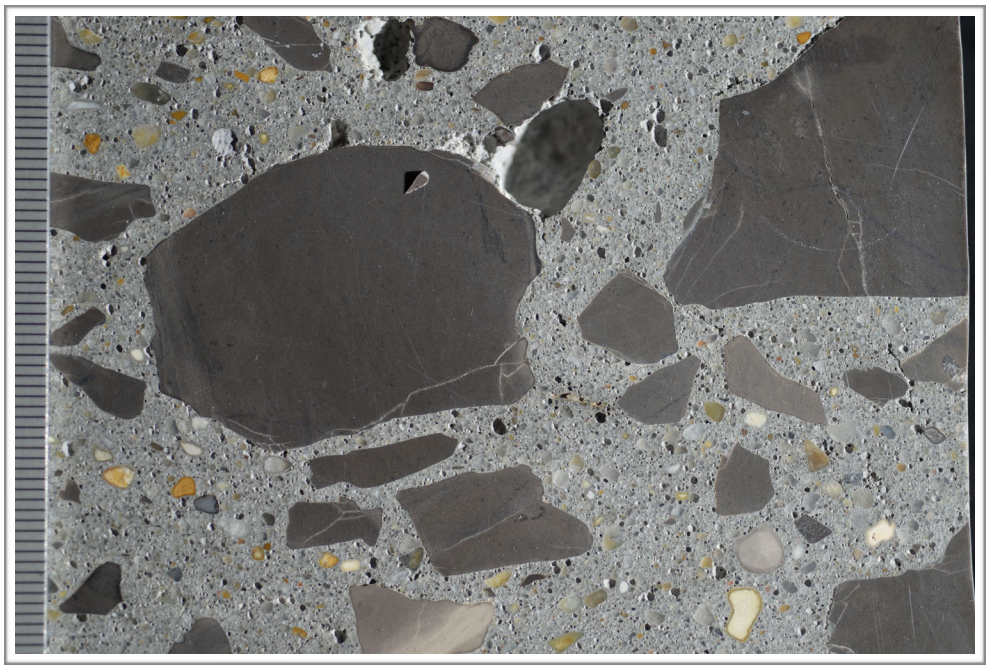

Figure C11. Photograph of the polished surface showing coarse aggregate; scale in millimeters.

Figure C12. Reflected light photomicrograph of polished surface showing the fine aggregate.

(a)

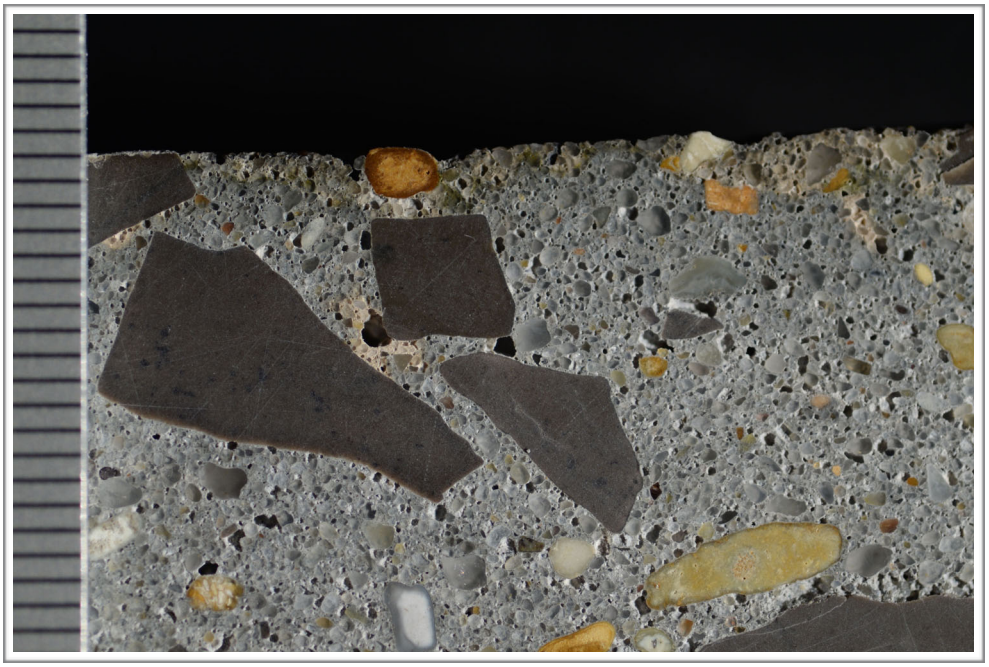

(b)

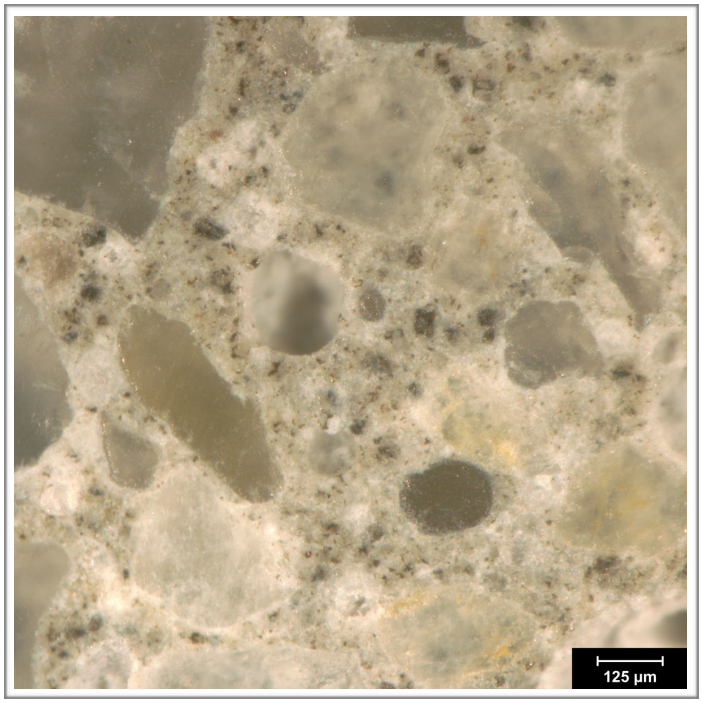

Figure C13. (a) Photograph of polished surface showing overview of paste at the top of the core. The scale is in millimeters; the red arrows indicate the hairline crack that cut across the top surface. (b) Reflected light photomicrograph showing detail of paste color, texture and luster in the middle of the core.

(a)

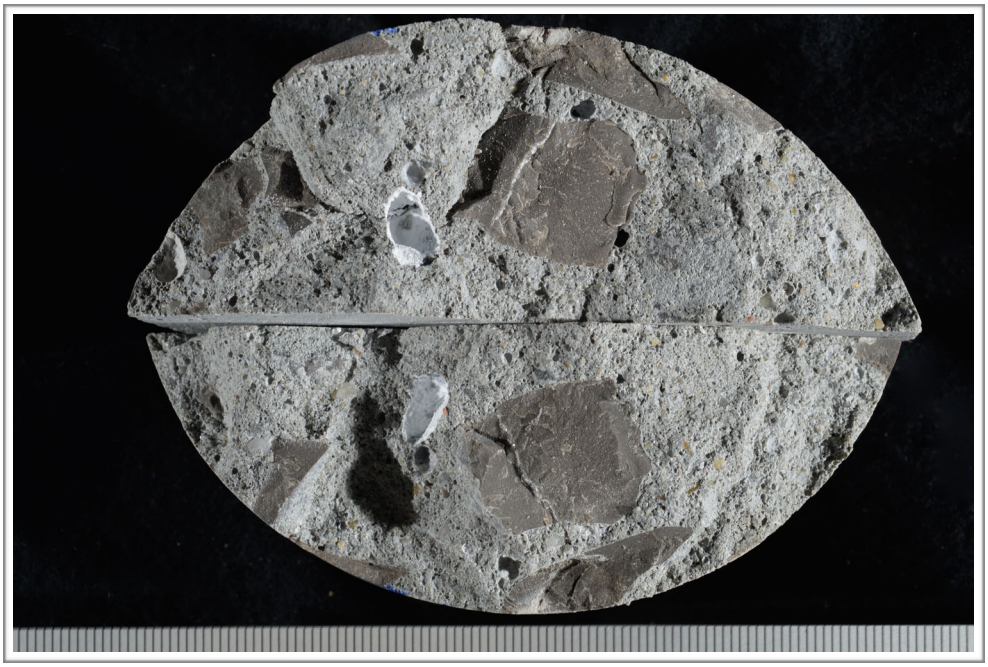

(b)

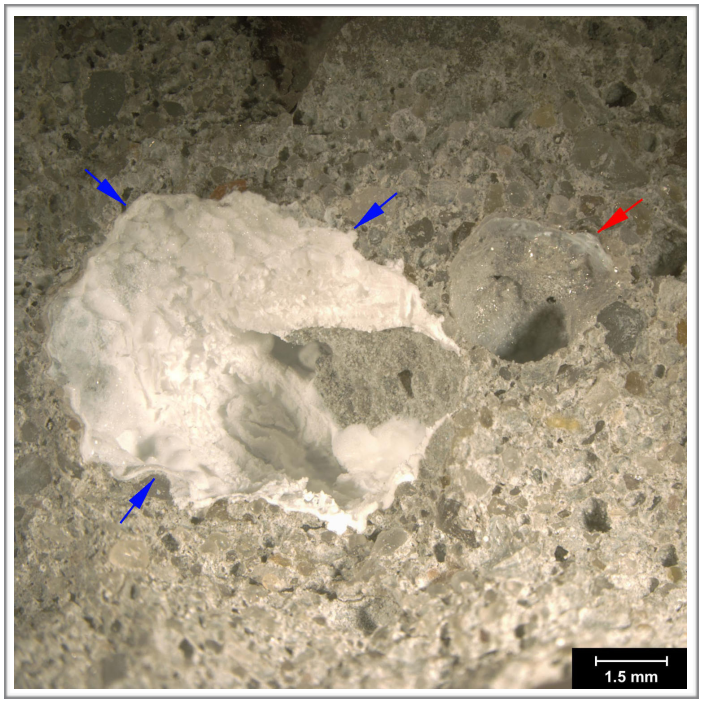

Figure C14. (a) Photograph and (b) reflected light photomicrograph of the fresh fracture surface. The scale in (a) is in millimeters. In (b) the blue arrows indicate white gelatinous deposit in a void and the red arrow indicates a clear gel.

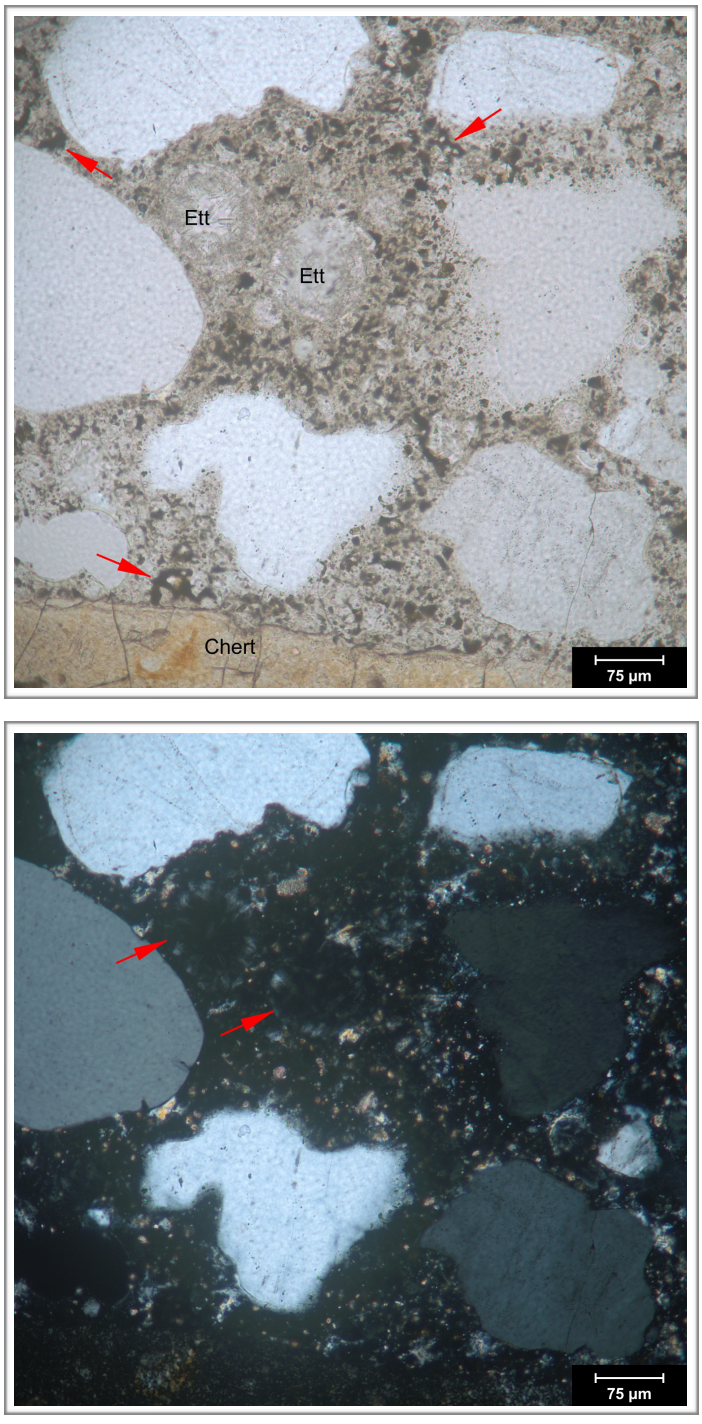

Figure C15. Transmitted light photomicrographs of thin section from the concrete core showing detail of paste in (a) plane-polarized and (b) cross-polarized light. The red arrows indicate RRCG in (a) and coarse calcium hydroxide in (b). Ett indicates voids with ettringite.

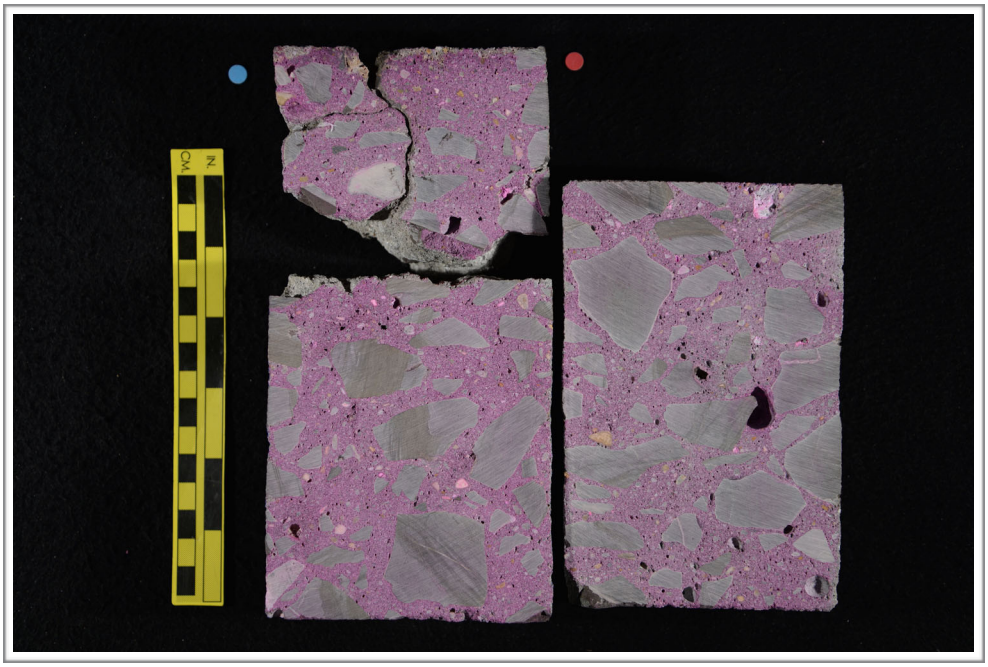

(a)

(b)

Figure C16. Photographs showing (a) overview of phenolphthalein stained surface and (b) detail of surface near the top of the core. Scale in millimeters in (b).

(a)

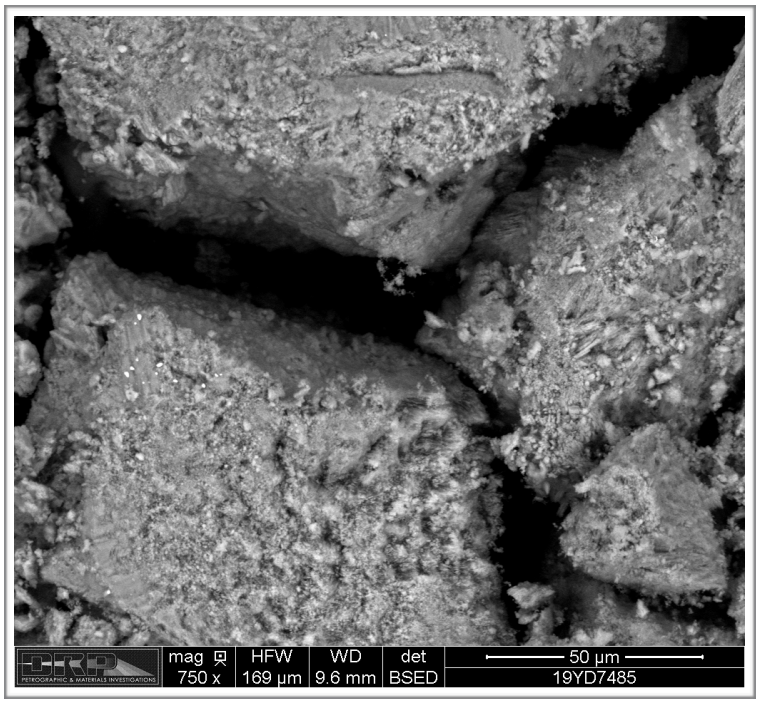

(b)

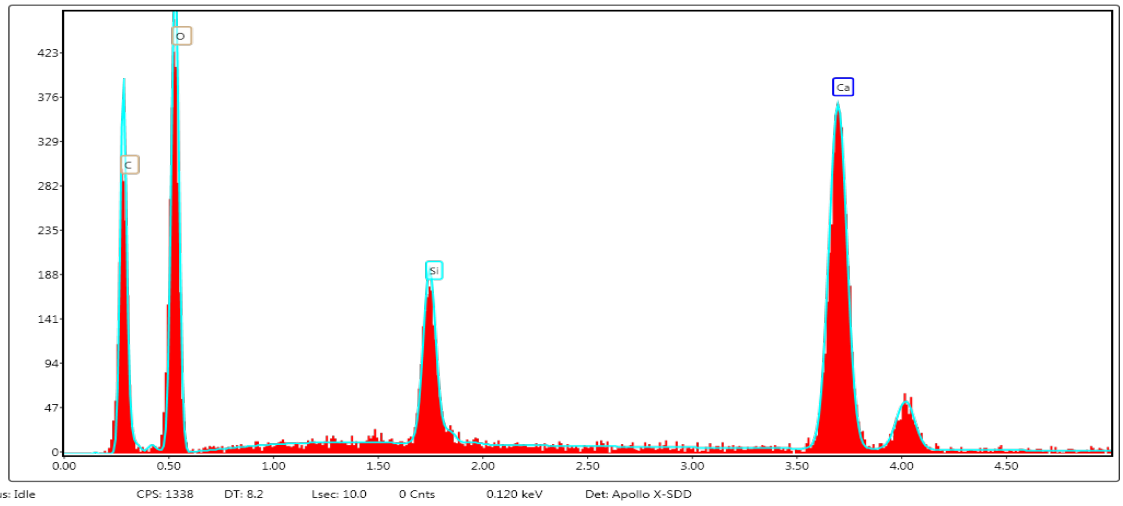

Figure C17. (a) Backscatter electron micrograph of gel deposits scraped from void shown in C7(b) and placed on carbon tape. (b) EDS spectrum of deposit indicating composition typical of ASR gel.

(a)

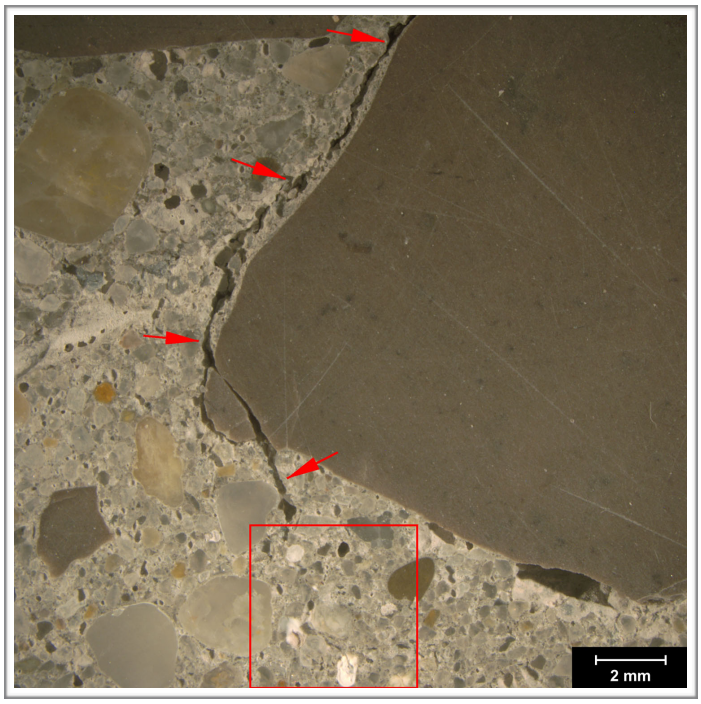

(b)

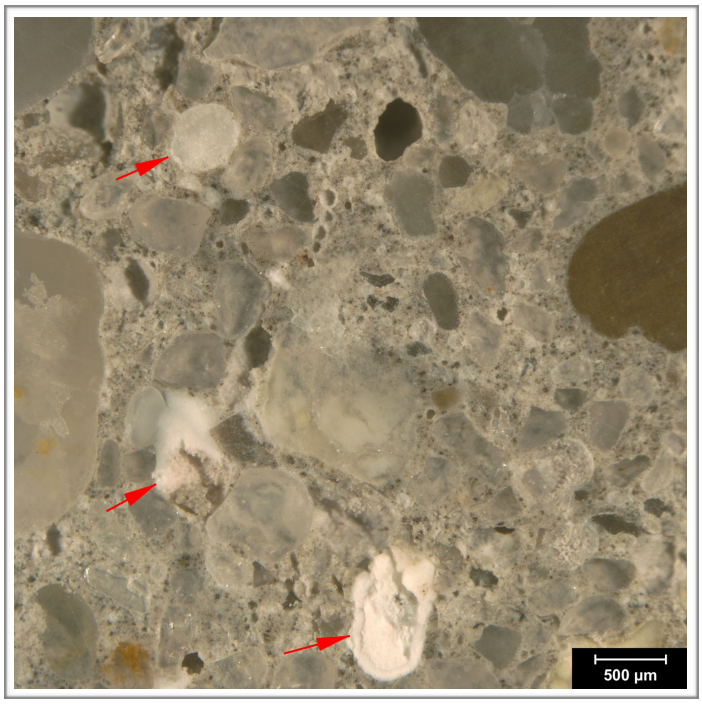

Figure C18. Reflected light photomicrographs of polished surface showing (a) overview and (b) detail of deposits in voids about 115 mm (4 ½ in.) below the top surface. In (a) the red arrows indicate cracks and the red box shows the area of (b), where the red arrow indicates gel in voids.

(a)

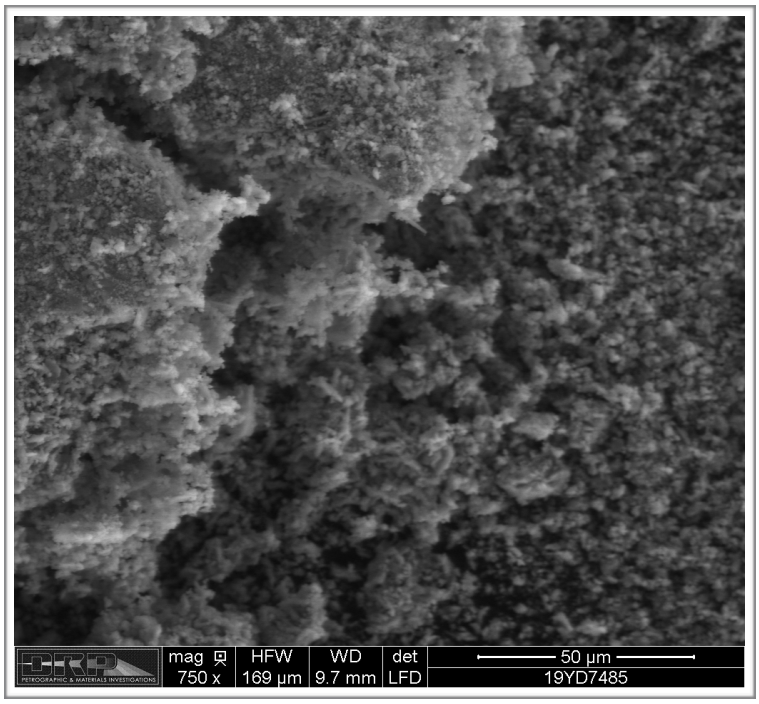

(b)

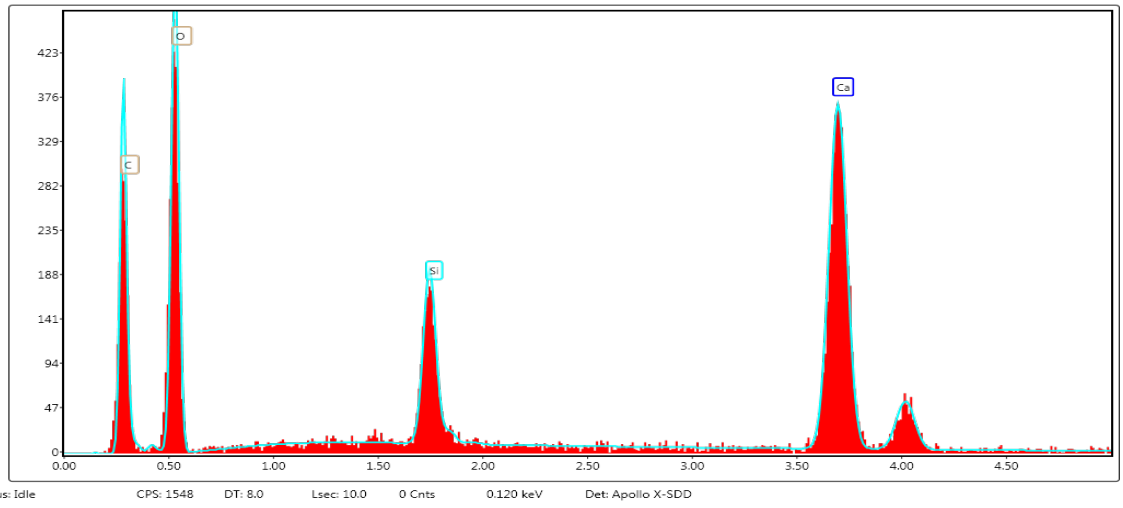

Figure C19. (a) Backscatter electron micrograph of gel deposits scraped from void shown in C18(b) and placed on carbon tape. (b) EDS spectrum of deposit indicating composition typical of ASR gel.

1. RECEIVED CONDITION

ORIENTATION	Vertical core taken through highway pavement slab measures 100 mm (~ 4 in.) in diameter and 325 mm (~ 13 in.) long (**Figure D1, D2**).
SURFACES	The top surface shows minor wear; the tines are largely intact but a few coarse aggregate particles are exposed and worn smooth and a few irregular tine grooves are present (**Figure D3**). The bottom surface is a saw cut such that the core represents a partial thickness of the pavement slab.
GENERAL CONDITION	The concrete is hard and compact and rings lightly when sounded with a hammer. The core was received intact in one piece.

2. EMBEDDED OBJECTS

GENERAL	None observed.

3. CRACKING

MACROSCOPIC	None observed except for minor internal hairline cracks in coarse aggregate particles. These do not propagate into the paste.
MICROSCOPIC	A microcrack that is ~ 75 µm (3 mil) wide cuts sub-vertically from the top surface to ~ 3 mm (⅛ in.); the crack is free of secondary deposits and cuts around an aggregate particle (**Figure D4**). No other microcracking was observed.

4. VOIDS

VOID SYSTEM	Concrete is air-entrained (**Figure D5**) and contains 4-6% air by visual estimation (not determined following ASTM C457). The core is moderately well consolidated with only a few large voids that measure 6-9.5 mm (¼-⅜ in.) across observed.
VOID FILLINGS	Voids are commonly lined with ettringite. Rare voids contain gel.

5. COARSE AGGREGATE

PHYSICAL PROPERTIES	Crushed quarry rock with 38 mm (1 ½ in.) nominal top size (**Figure D6**). The rocks are hard and competent. The particles are sub-equant to tabular in shape with sub-angular to sub-round edges. The grading and distribution are relatively even. The sand is very fine.
ROCK TYPES*	The aggregate is carbonate in composition and consists of brown dolomitic limestone as well as tan to light brown limestones that show laminations and evidence of bioturbation as well as some oolitic limestones.
OTHER FEATURES	No deleterious coatings or incrustations observed. A few minor low w/c mortar coatings observed. Occasional particles show internal cracking and microcracking; these do not propagate into the paste.

**Modal abundance based on visual estimation.*

6. FINE AGGREGATE

PHYSICAL PROPERTIES	Natural sand consists of rocks that are hard and competent (**Figure D7**). The particles are sub-equant to tabular in shape with sub-round to sub-angular edges. The grading and distribution are relatively even.
ROCK TYPES	The sand is siliceous in composition and consists primarily of quartz and quartzite with minor amounts of granitic rocks and chert.
OTHER FEATURES	No deleterious coatings or incrustations observed and no low w/c mortar coatings observed. Particles of chert typically show reaction rims but no microcracking or deposits of gel are associated with them.

7. PASTE OBSERVATIONS

POLISHED SURFACE	Paste is gray (Munsell 2.5Y/6/1) to dark gray (2.5Y/4/1), has a smooth texture and sub-vitreous luster (**Figure D8**). The paste is hard (Mohs 3.5-4). The paste is dark gray for up to 3 mm (⅛ in.) from the top of the core.
FRESH FRACTURE	Fracture surface is light gray, has a hackly texture and a sub-vitreous luster. The fracture cuts primarily around aggregate particles (**Figure D9**). No significant secondary deposits were observed though minor deposits of ettringite commonly line voids.
THIN SECTION*	The paste contains hydrated portland cement; no fly ash, slag cement or other SCM were observed. The hydration is normal with 4-8% RRCG that consist mostly of interstitial ferrite and aluminate with occasional grains of belite (**Figure D10**). CH makes up 10-17% of the paste, is fine to medium-grained and evenly distributed.

** Abbreviations as follows: RRCG = relict and residual cement grains; SCM = supplemental cementitious materials; CH = calcium hydroxide; ITZ = interfacial transition zone. Modal abundances are based on visual estimations.*

8. SECONDARY DEPOSITS

PHENOLPHTHALEIN	Entire surface stains purple (**Figure D11**).
DEPOSITS	Minor carbonation observed at the top of the core and in irregularly distributed zones in the paste in thin section. Minor deposits of ettringite observed commonly in voids. Minor deposits of ASR gel observed in voids (**Figure D12, D13**). No evidence of cracking or microcracking due to ASR observed.

FIGURES

(a)

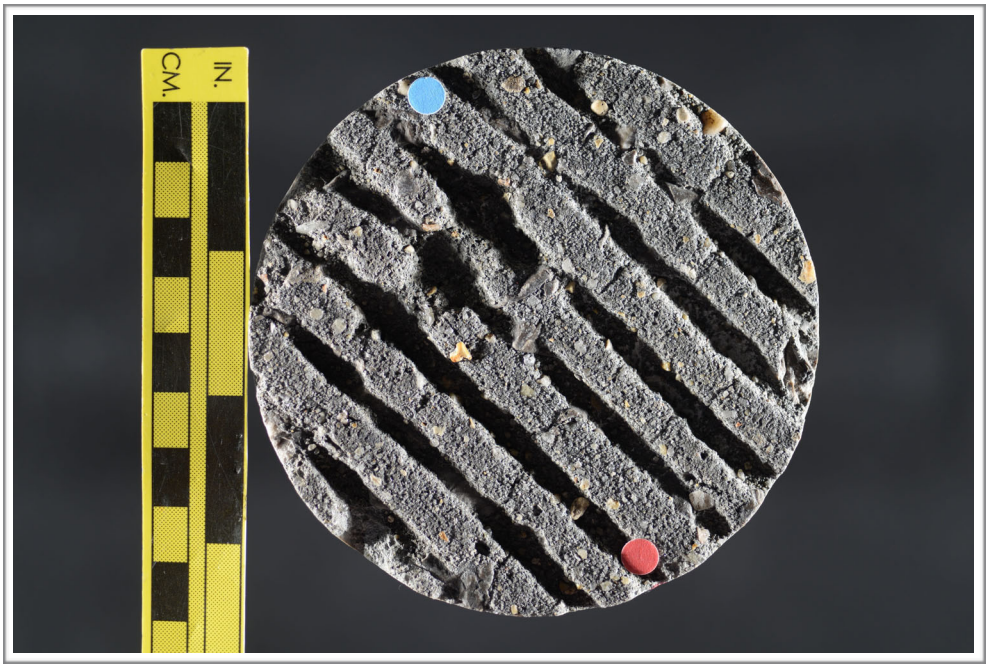

(b)

Figure D1. Photographs showing (a) oblique view of the top and side of the core with identification labels and (b) the top of the core. The red and blue dots in (a) show the orientation of the saw cuts used to prepare the sample.

(c)

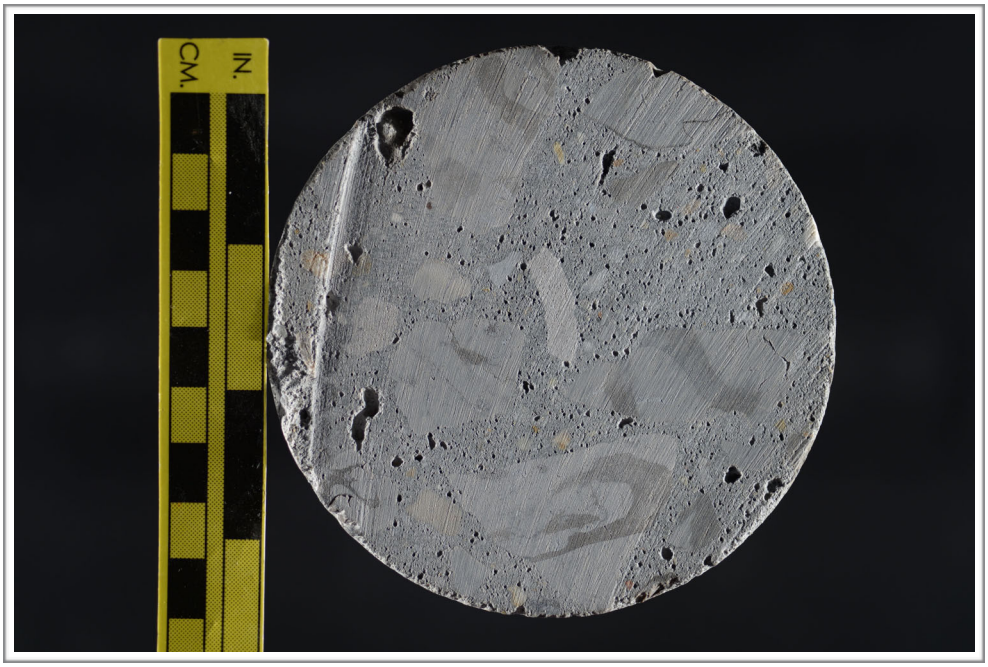

Figure D1 (cont'd). (c) Photograph showing the bottom of the core.

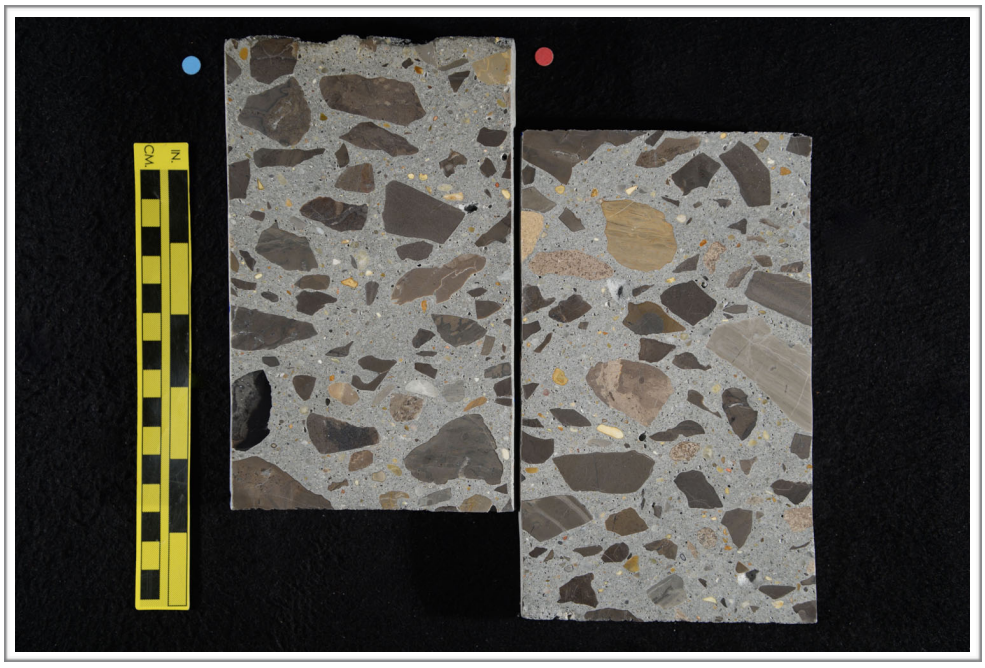

Figure D2. Photograph showing the polished surface of the core.

(a)

(b)

Figure D3. Photographs showing detail of the top surface of the core; scale in millimeters in both photos.

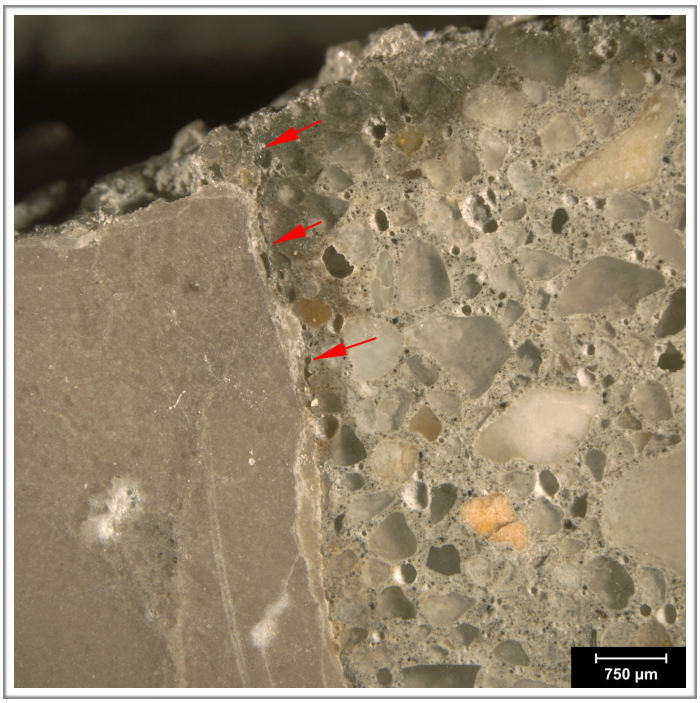

Figure D4. Reflected light photomicrograph of the polished surface showing microcrack (red arrows) at the top of the core.

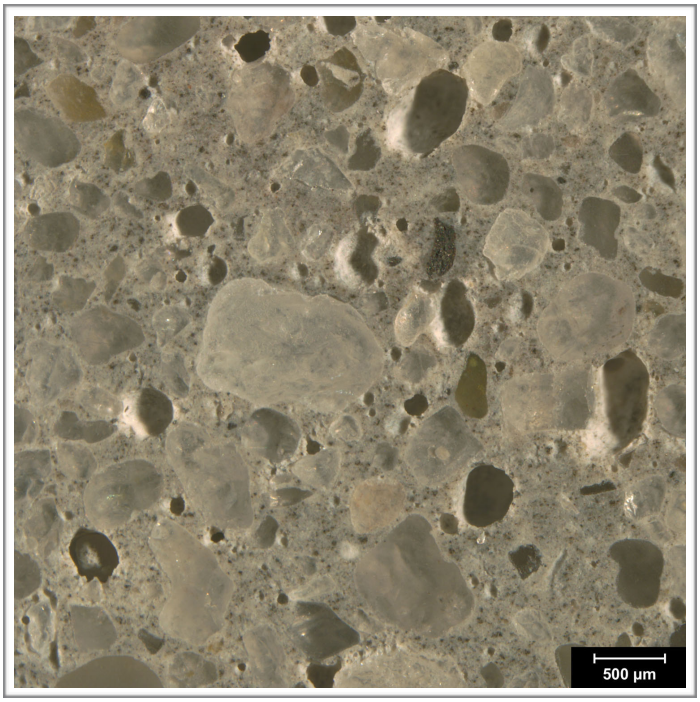

Figure D5. Reflected light photomicrograph of the polished surface showing entrained air voids (dark circles).

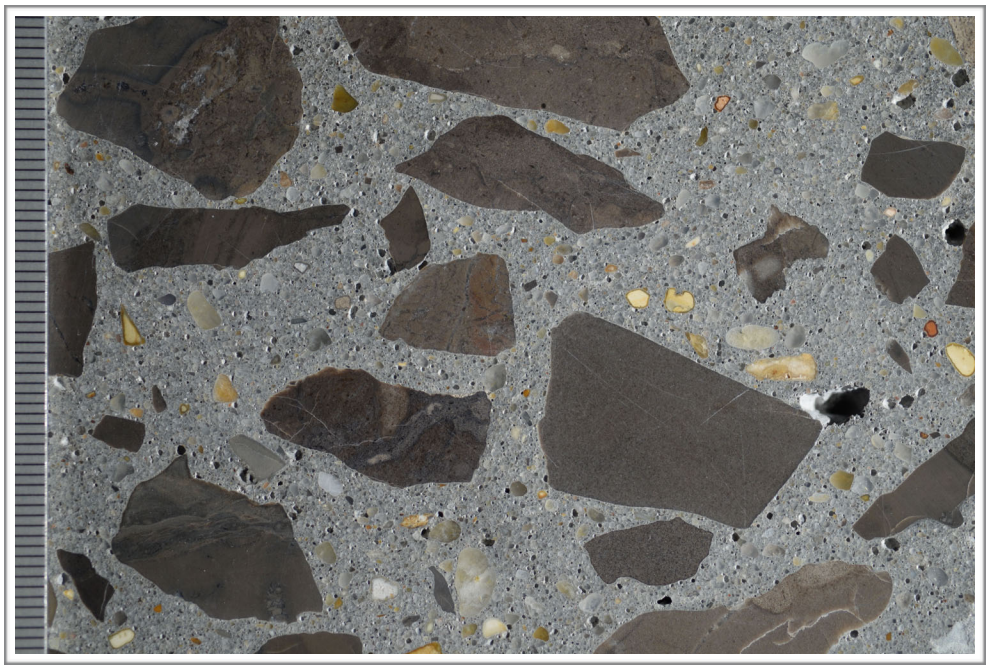

Figure D6. Photograph of the polished surface showing coarse aggregate; scale in millimeters.

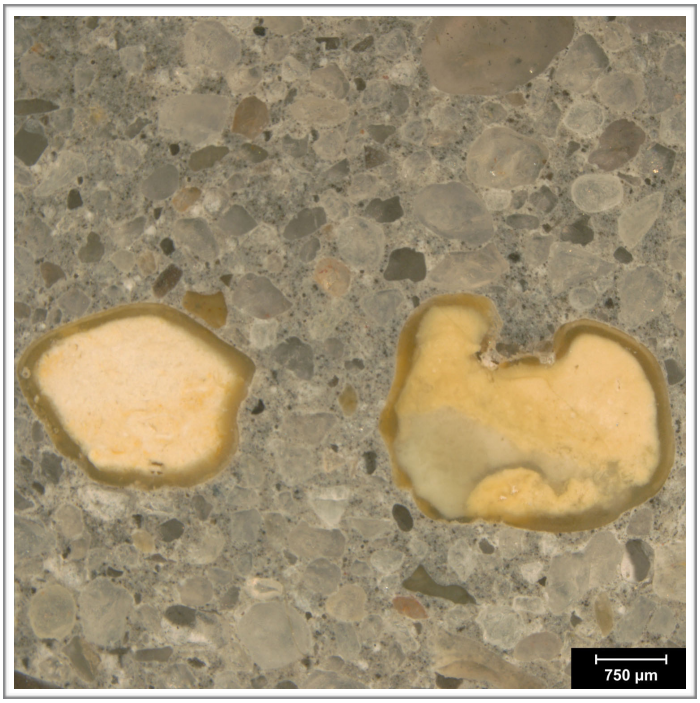

Figure D7. Reflected light photomicrograph of polished surface showing the fine aggregate.

(a)

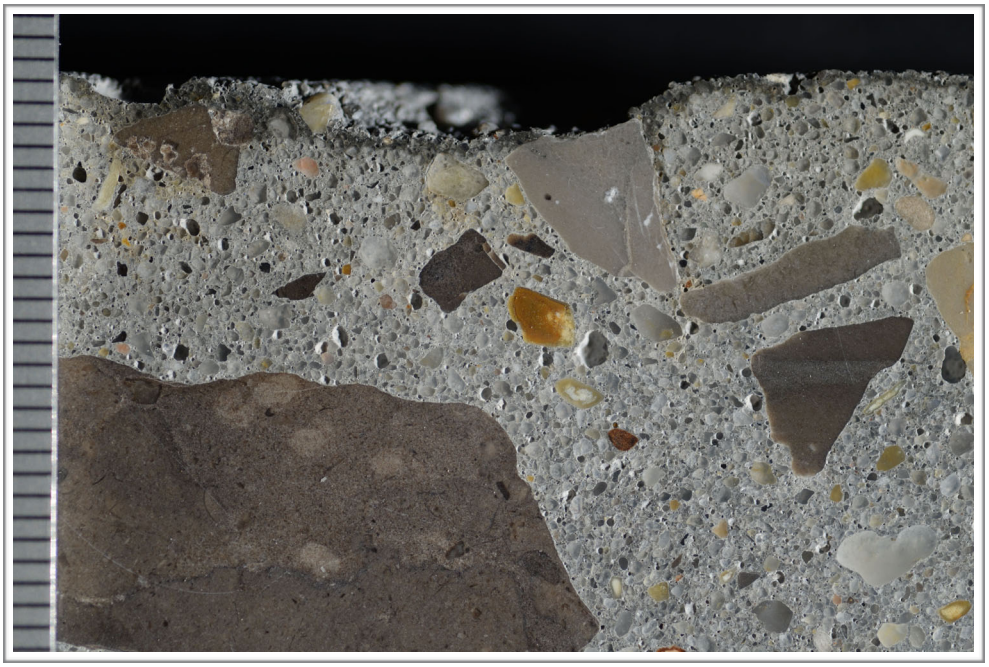

(b)

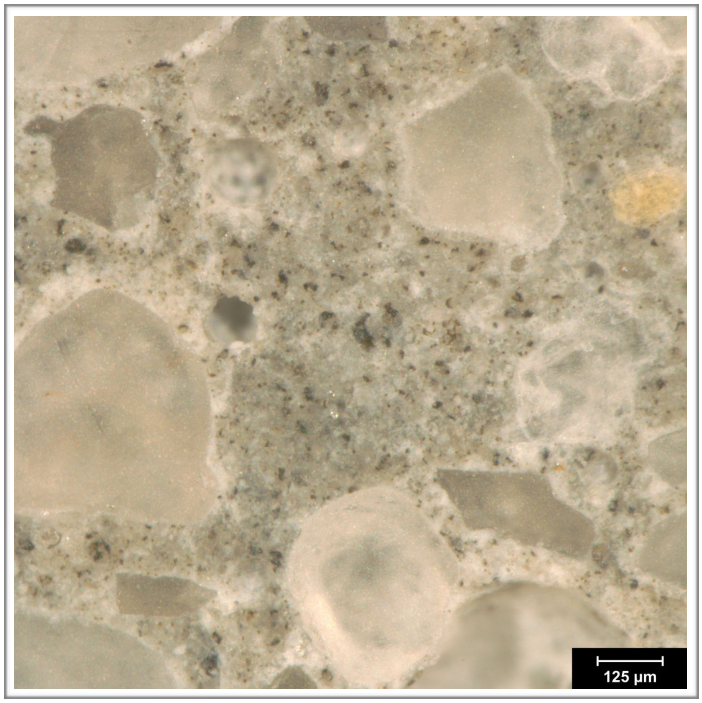

Figure D8. (a) Photograph of polished surface showing overview of paste at the top of the core. The scale is in millimeters. (b) Reflected light photomicrograph showing detail of paste color, texture and luster in the middle of the core.

(a)

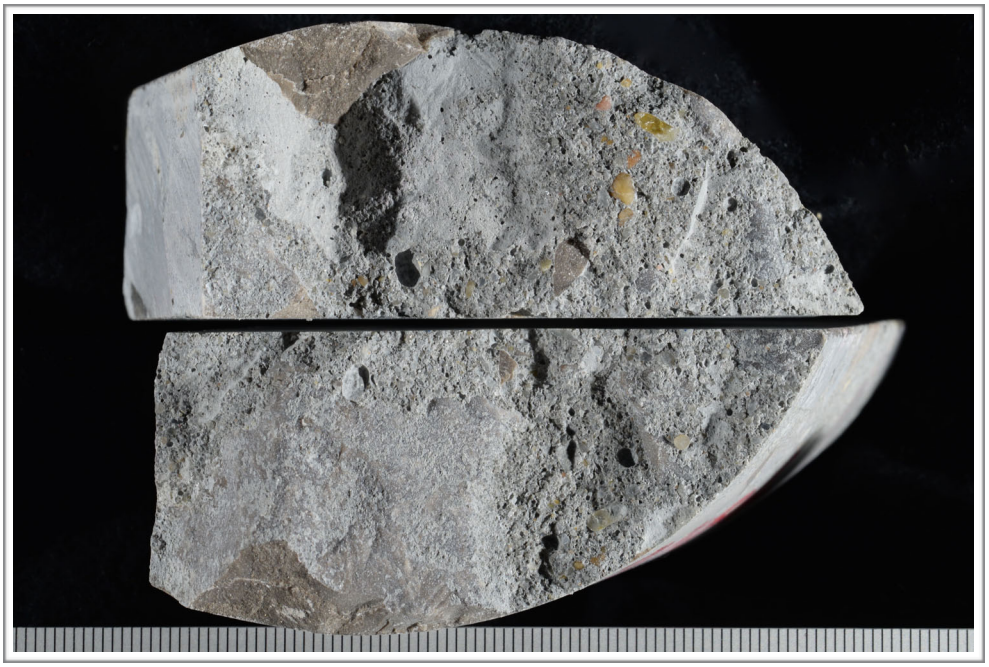

(b)

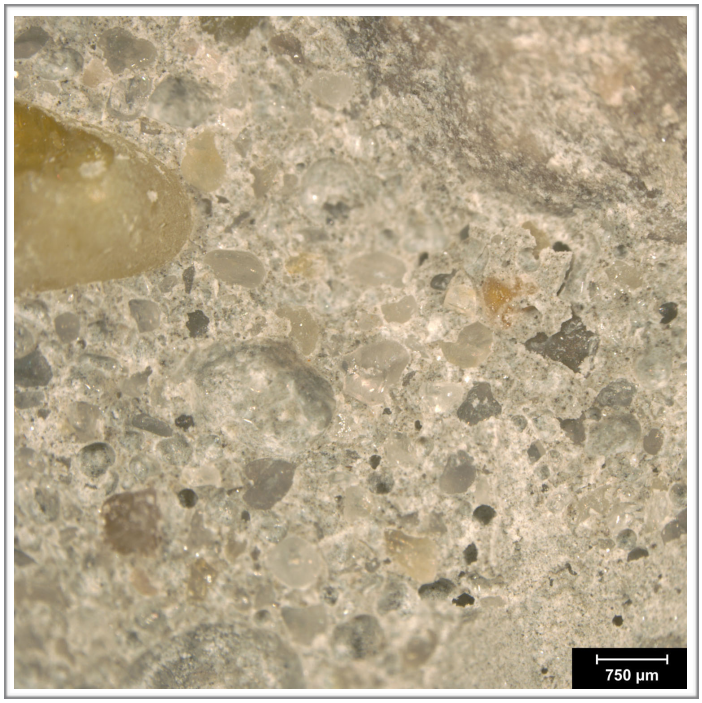

Figure D9. (a) Photograph and (b) reflected light photomicrograph of the fresh fracture surface. The scale in (a) is in millimeters.

(a)

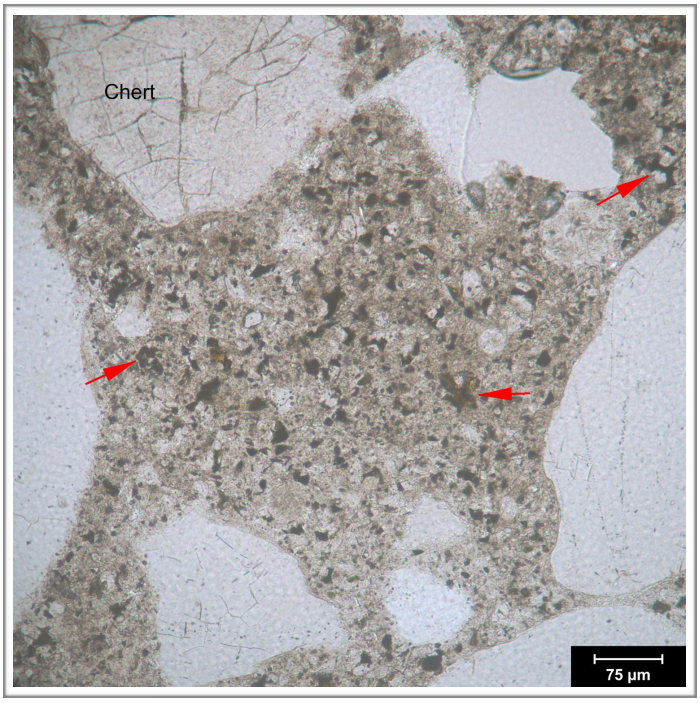

(b)

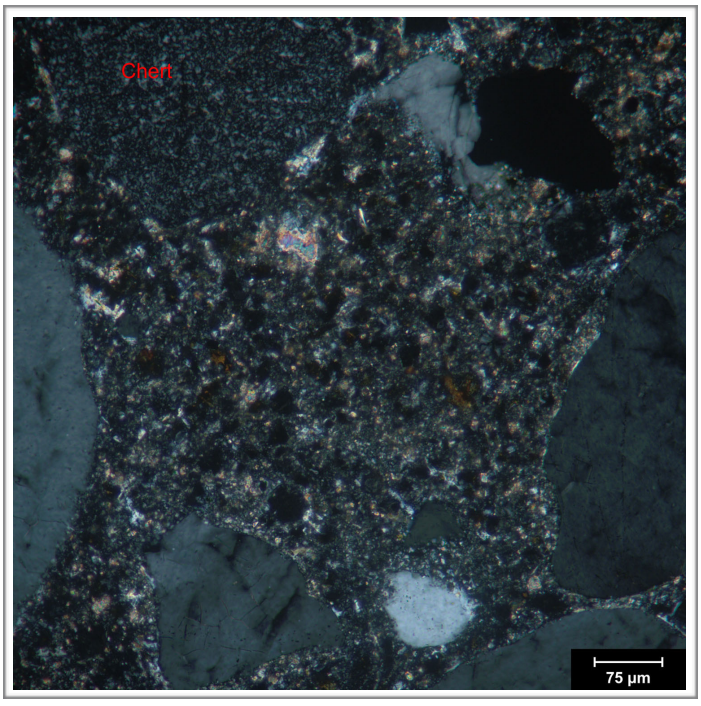

Figure D10. Transmitted light photomicrographs of thin section showing detail of paste in (a) plane-polarized and (b) cross-polarized light. The red arrows indicate RRCG in (a); also note the chert particle with internal microcracks at the top of the images.

(a)

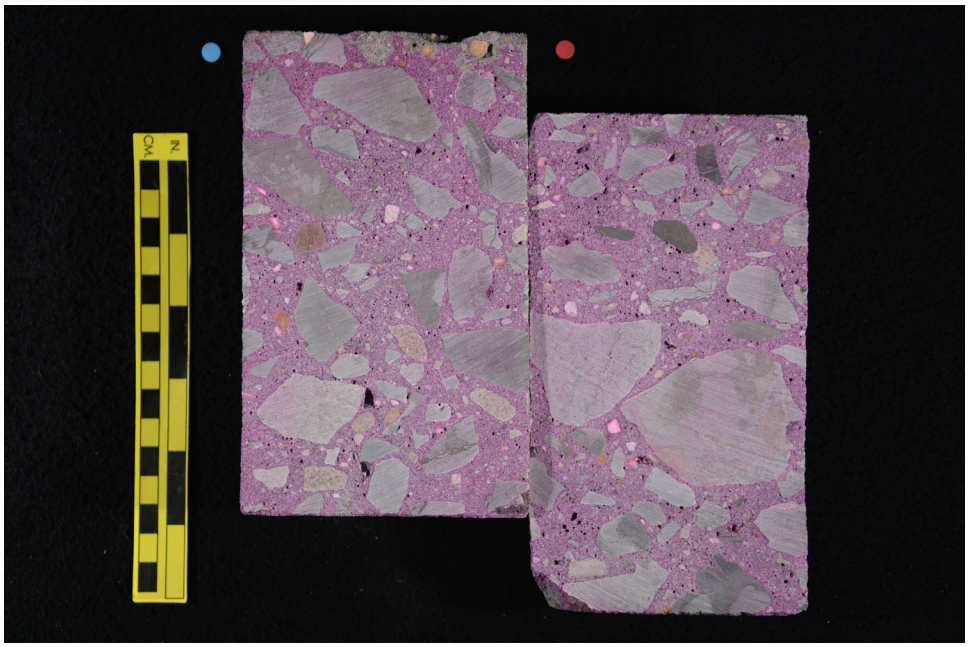

(b)

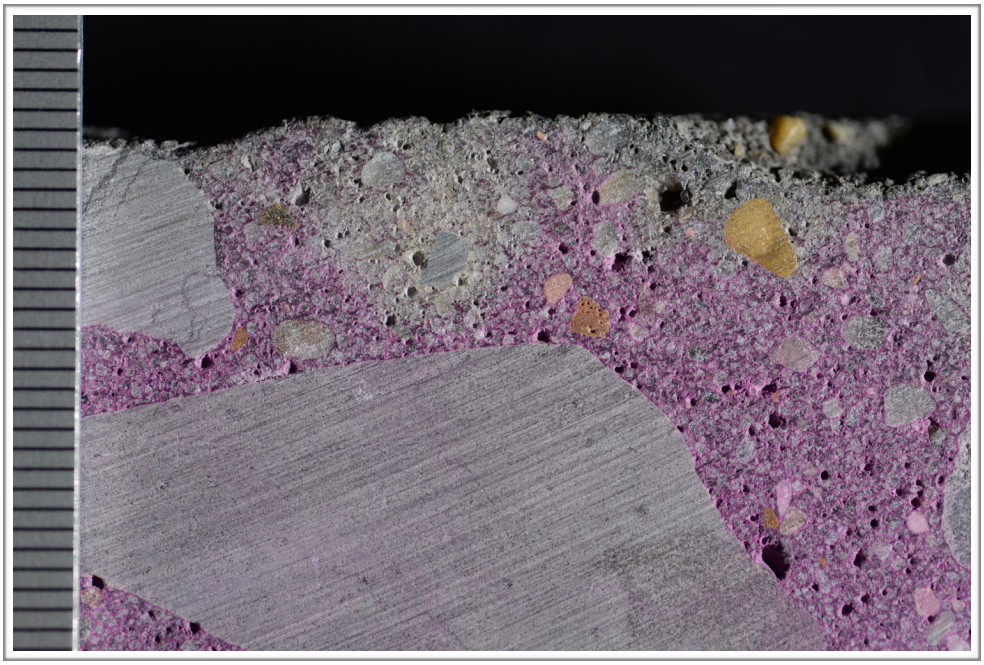

Figure D11. Photographs showing (a) overview of phenolphthalein stained surface and (b) detail of surface near the top of the core. Scale in millimeters in (b).

(a)

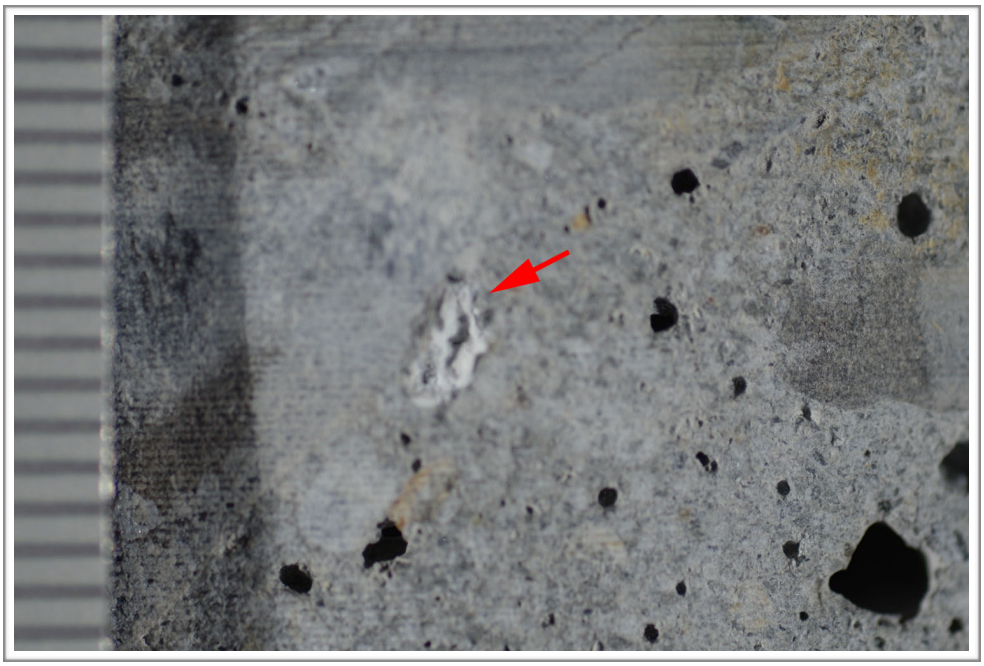

(b)

Figure D12. (a) Photograph and (b) reflected light photomicrograph of the side of the core showing a void filled with gel (red arrow in (a). Scale in millimeters in (a).

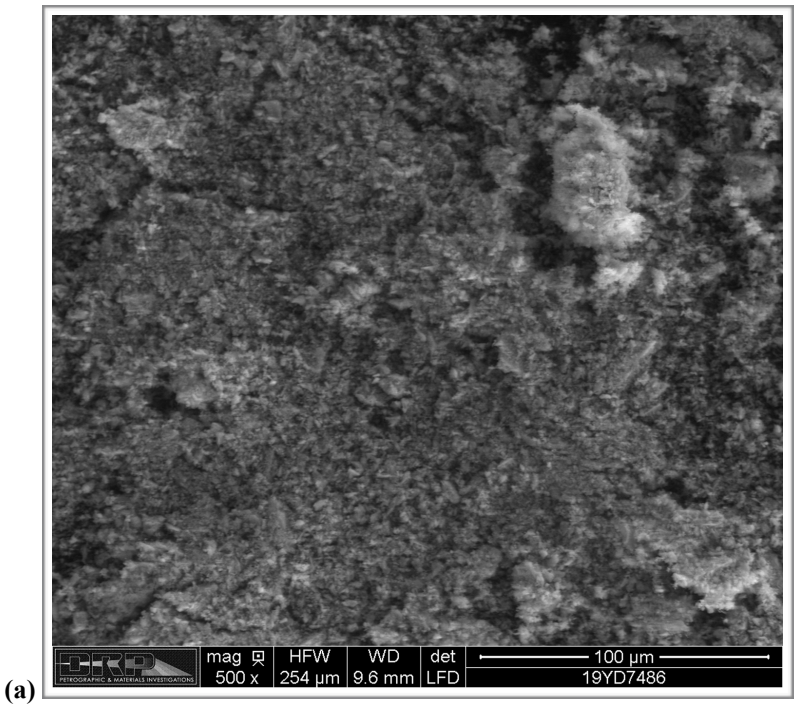

(a)

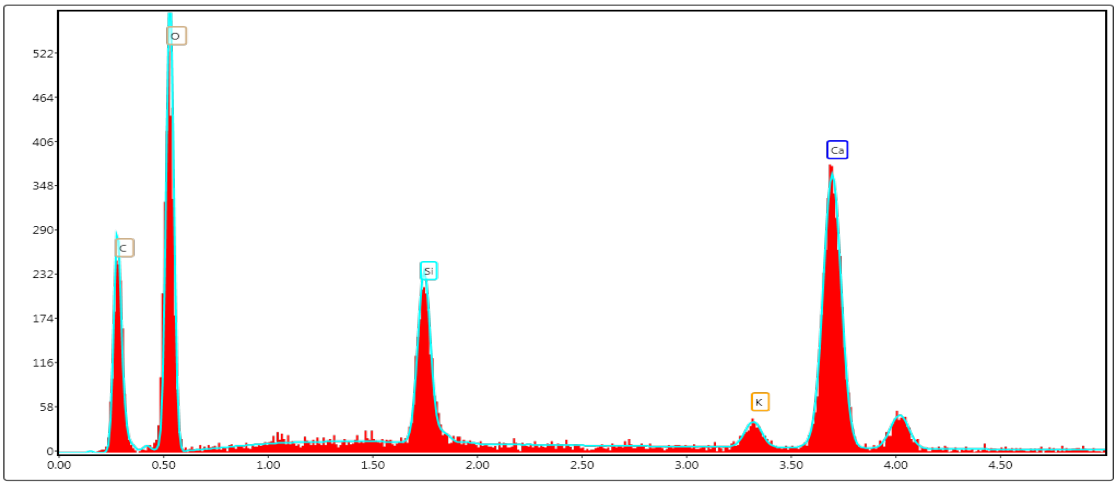

(b) Status: Idle CPS: 1491 DT: 7.3 Lsec: 10.0 0 Cnts 0.120 keV Det: Apollo X-SDD

Figure D13. (a) Backscatter electron micrograph of gel deposits scraped from void shown in D12(b) and placed on carbon tape. (b) EDS spectrum of deposit indicating composition typical of ASR gel.

1. RECEIVED CONDITION

ORIENTATION	Vertical core taken through highway pavement slab measures 100 mm (~ 4 in.) in diameter and 325 mm (~ 13 in.) long (**Figure E1, E2**).
SURFACES	The top surface shows minor wear; the tines are largely intact but numerous coarse aggregate particles are exposed and worn smooth (**Figure E3a**). The bottom surface is a saw cut such that the core represents a partial thickness of the pavement slab.
GENERAL CONDITION	The concrete is hard and compact and rings lightly when sounded with a hammer. The core was received intact in one piece.

2. EMBEDDED OBJECTS

GENERAL	None observed.

3. CRACKING

MACROSCOPIC	Linear crack cuts 100 mm (4 in.) across the top of the core; the crack is 250 µm (10 mil) wide and cuts to ~ 9.5 mm (⅜ in.; **Figure E3**). The crack cuts around aggregate particles and is free of secondary deposits. Minor internal hairline cracks observed in coarse aggregate particles. These do not propagate into the paste.
MICROSCOPIC	A microcrack that is ~ 75 µm (3 mil) wide cuts sub-vertically from the top surface to ~ 5 mm (200 mil); the microcrack is free of secondary deposits and cuts around aggregate particles (**Figure E4**). No other microcracking was observed.

4.VOIDS

VOID SYSTEM	Concrete is air-entrained (**Figure E5**) and contains 4-6% air by visual estimation (not determined following ASTM C457). The core is moderately consolidated with several larger water voids and entrapped voids that measure 6-9.5 mm (¼-⅜ in.) across observed.
VOID FILLINGS	Voids occasionally contain minor to trace deposits of ettringite.

5. COARSE AGGREGATE

PHYSICAL PROPERTIES	Crushed quarry rock with 38 mm (1 ½ in.) nominal top size (**Figure E6**). The rocks are hard and competent. The particles are sub-equant to tabular in shape with sub-angular to sub-round edges. The grading and distribution are relatively even. The sand is very fine.
ROCK TYPES*	The aggregate is carbonate in composition and consists of brown dolomitic limestone as well as tan to light brown limestones that show laminations and evidence of bioturbation as well as some oolitic limestones.
OTHER FEATURES	No deleterious coatings or incrustations observed. A few minor low w/c mortar coatings observed. Occasional particles show internal cracking and microcracking; these do not propagate into the paste.

**Modal abundance based on visual estimation.*

6. FINE AGGREGATE

PHYSICAL PROPERTIES	Natural sand consists of rocks that are hard and competent (**Figure E7**). The particles are sub-equant to tabular in shape with sub-round to sub-angular edges. The grading and distribution are relatively even.
ROCK TYPES	The sand is siliceous in composition and consists primarily of quartz and quartzite with minor amounts of granitic rocks and chert.
OTHER FEATURES	No deleterious coatings or incrustations observed and no low w/c mortar coatings observed. Particles of chert typically show reaction rims but no microcracking or deposits of gel are associated with them.

7. PASTE OBSERVATIONS

POLISHED SURFACE	Paste is gray (Munsell 2.5Y/6/1) to dark gray (2.5Y/4/1), has a smooth texture and sub-vitreous luster (**Figure E8**). The paste is hard (Mohs 3.5-4). The paste is dark gray for up to 3 mm (⅛ in.) from the top of the core.
FRESH FRACTURE	Fracture surface is light gray, has a hackly texture and a sub-vitreous luster. The fracture cuts primarily through aggregate particles (**Figure E9**). No significant secondary deposits were observed though minor deposits of ettringite commonly line voids.
THIN SECTION*	The paste contains hydrated portland cement; no fly ash, slag cement or other SCM were observed. The hydration is normal with 10-7% RRCG that consist mostly of interstitial ferrite and aluminate with occasional grains of belite (**Figure E10**). CH makes up 12-20% of the paste, is medium to coarse-grained and distributed somewhat unevenly.

** Abbreviations as follows: RRCG = relict and residual cement grains; SCM = supplemental cementitious materials; CH = calcium hydroxide; ITZ = interfacial transition zone. Modal abundances are based on visual estimations.*

8. SECONDARY DEPOSITS

PHENOLPHTHALEIN	Entire surface stains purple (**Figure E11**).
DEPOSITS	Minor carbonation observed at the top of the core and in irregularly distributed zones in the paste in thin section. Minor deposits of ettringite observed commonly in voids. No deposits of gel observed.

FIGURES

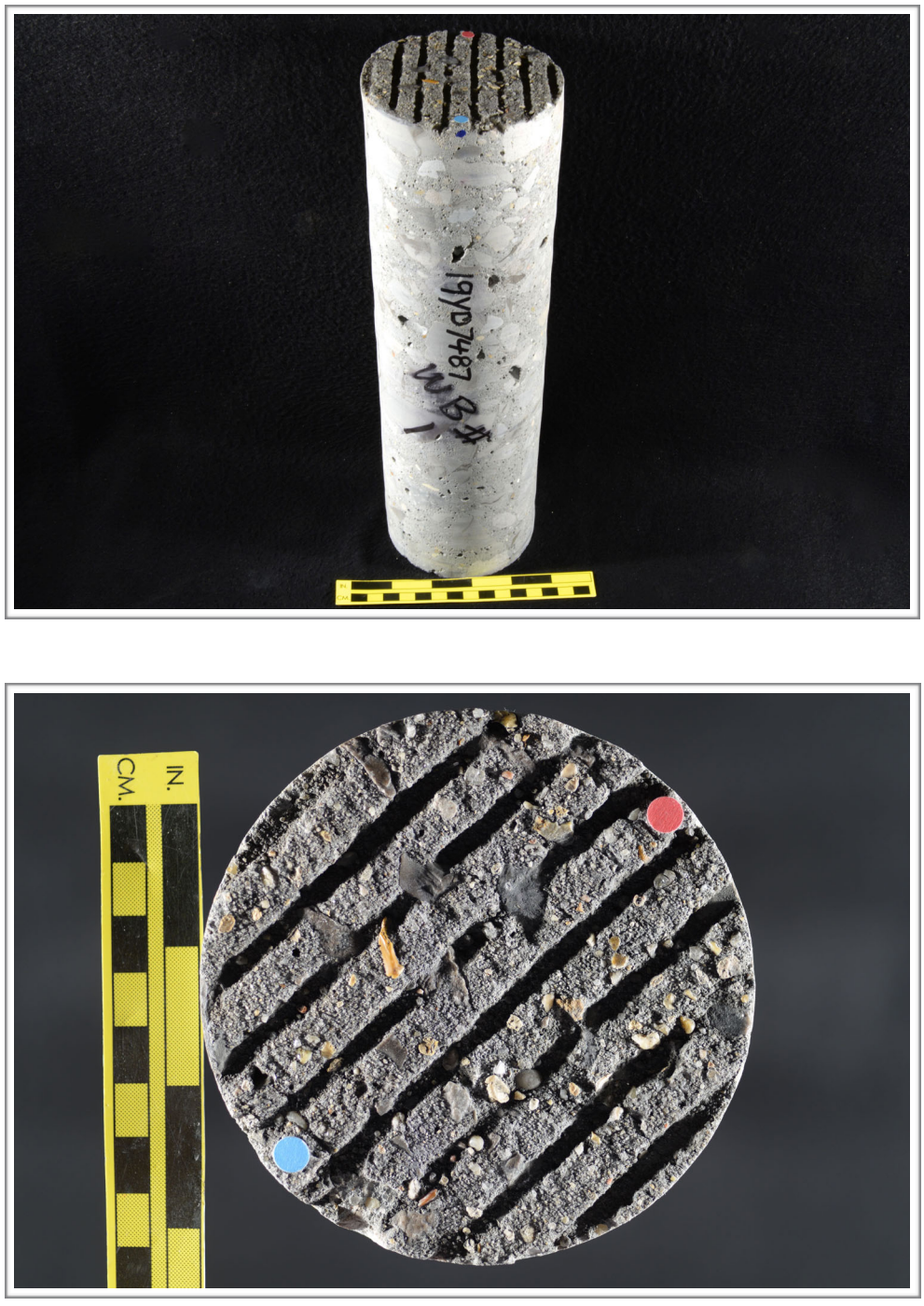

Figure E1. Photographs showing (a) oblique view of the top and side of the core with identification labels and (b) the top of the core. The red and blue dots in (a) show the orientation of the saw cuts used to prepare the sample.

(c)

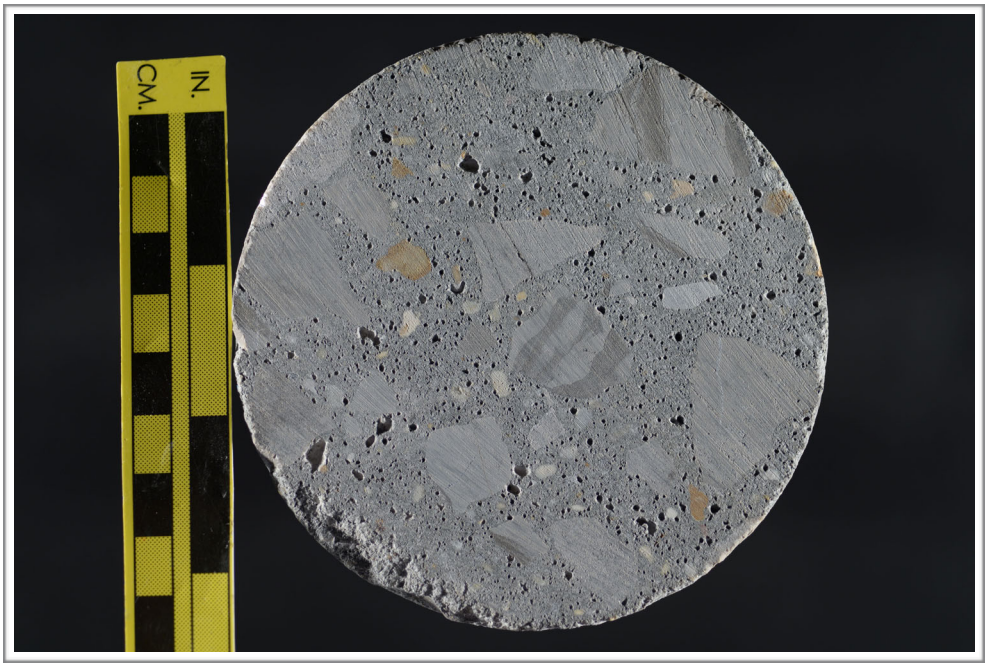

Figure E1 (cont'd). (c) Photograph showing the bottom of the core.

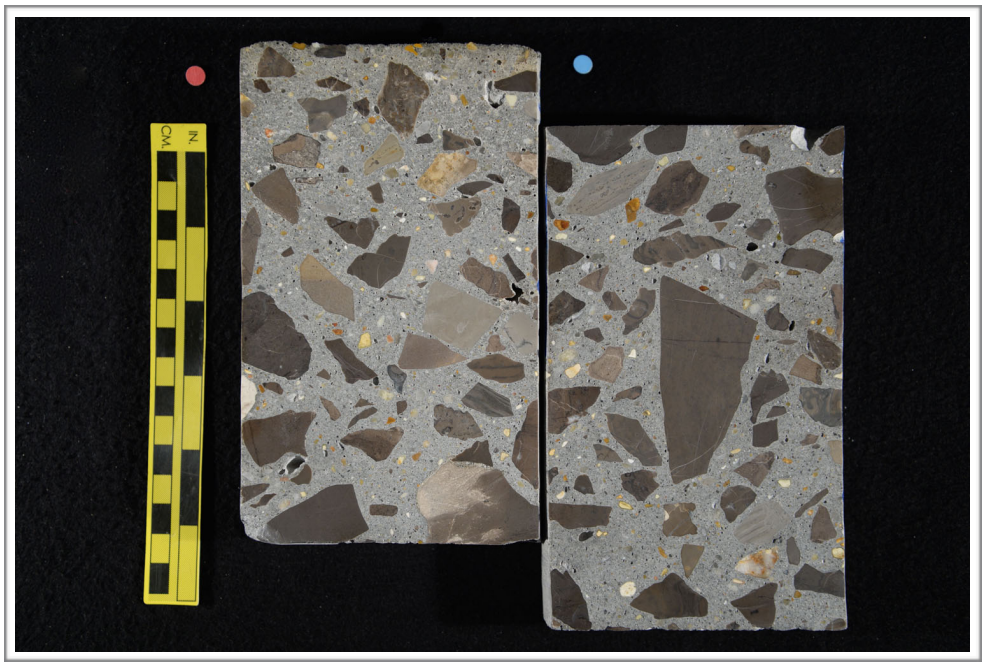

Figure E2. Photograph showing the polished surface of the core.

(a)

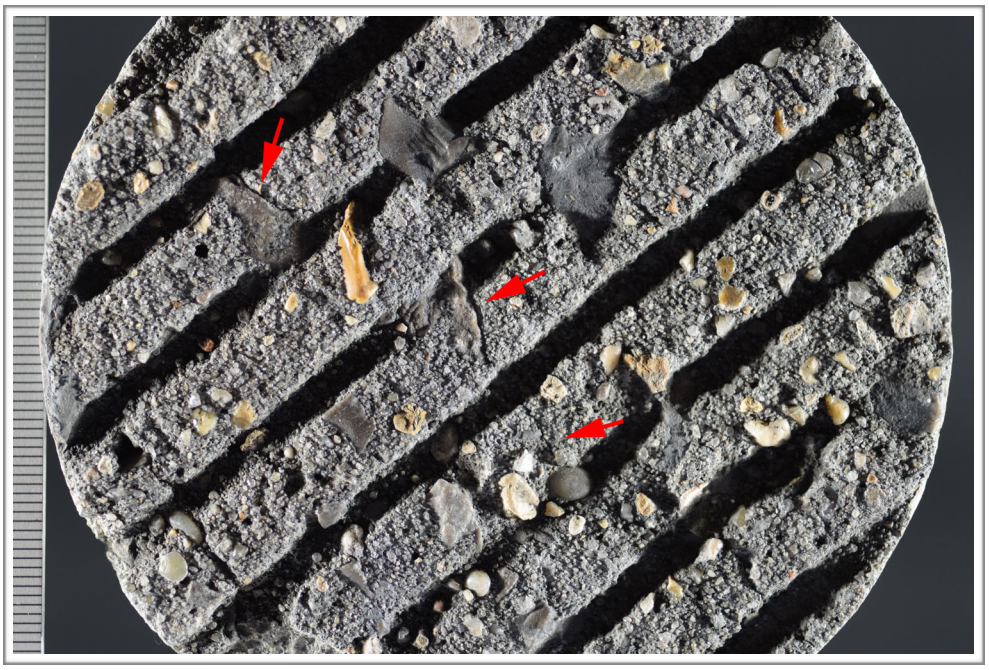

(b)

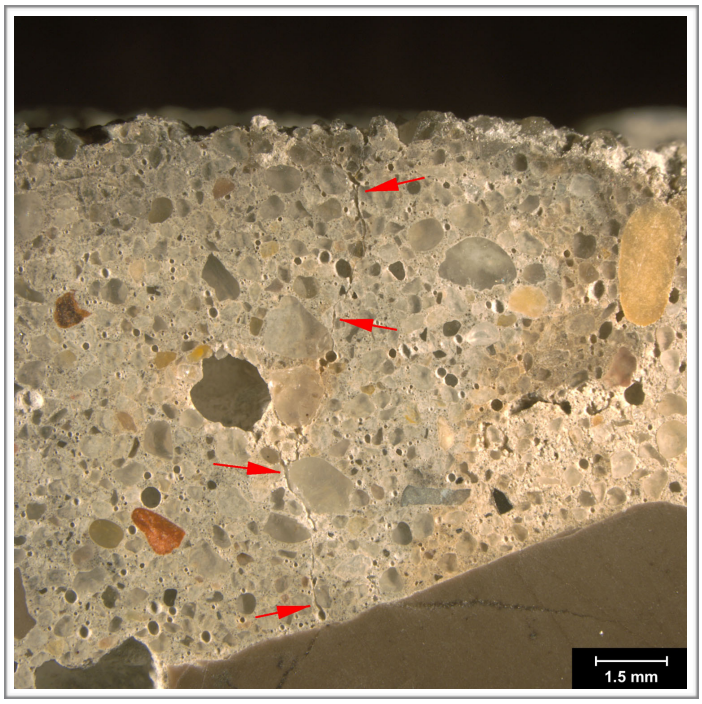

Figure E3. (a) Photograph showing crack (red arrows) on the top surface; scale in millimeters. (b) Reflected light photomicrograph showing hairline crack (red arrows) at the top of the core.

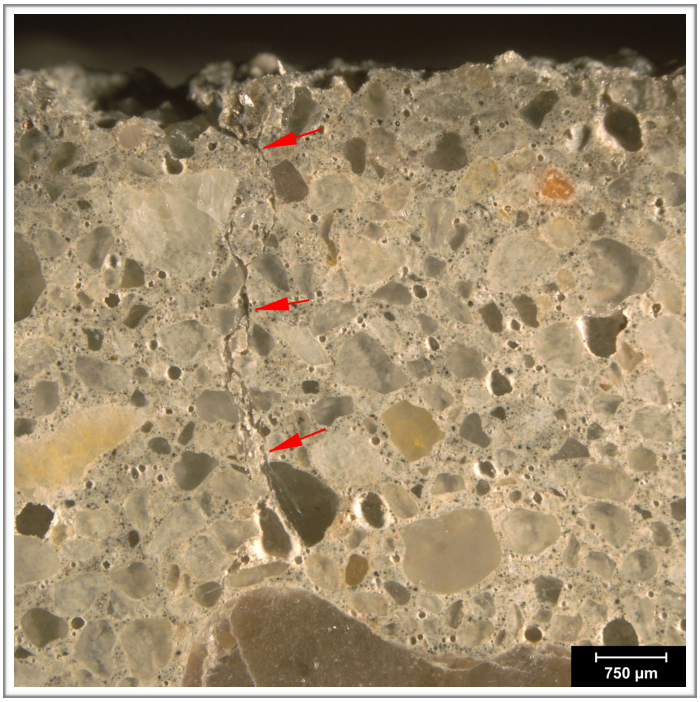

Figure E4. Reflected light photomicrograph of the polished surface showing microcrack (red arrows) at the top of the core.

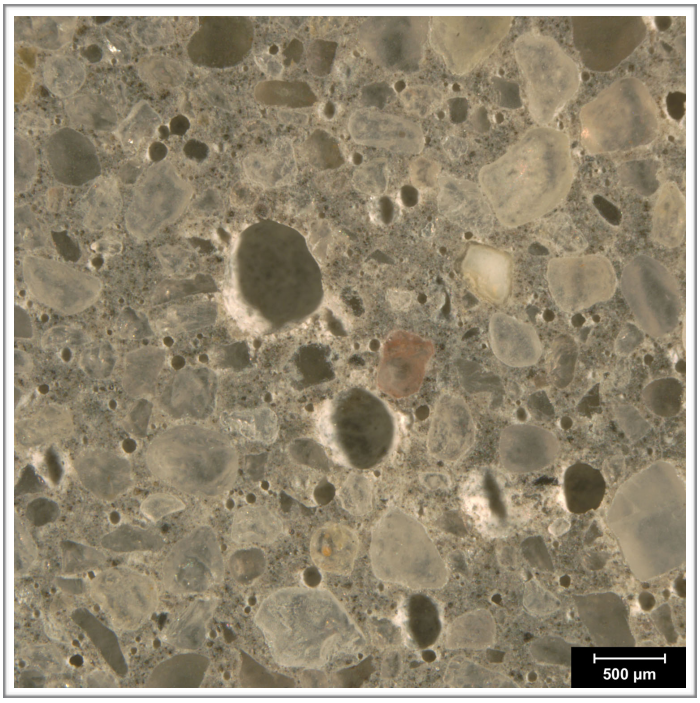

Figure E5. Reflected light photomicrograph of the polished surface showing entrained air voids (dark circles).

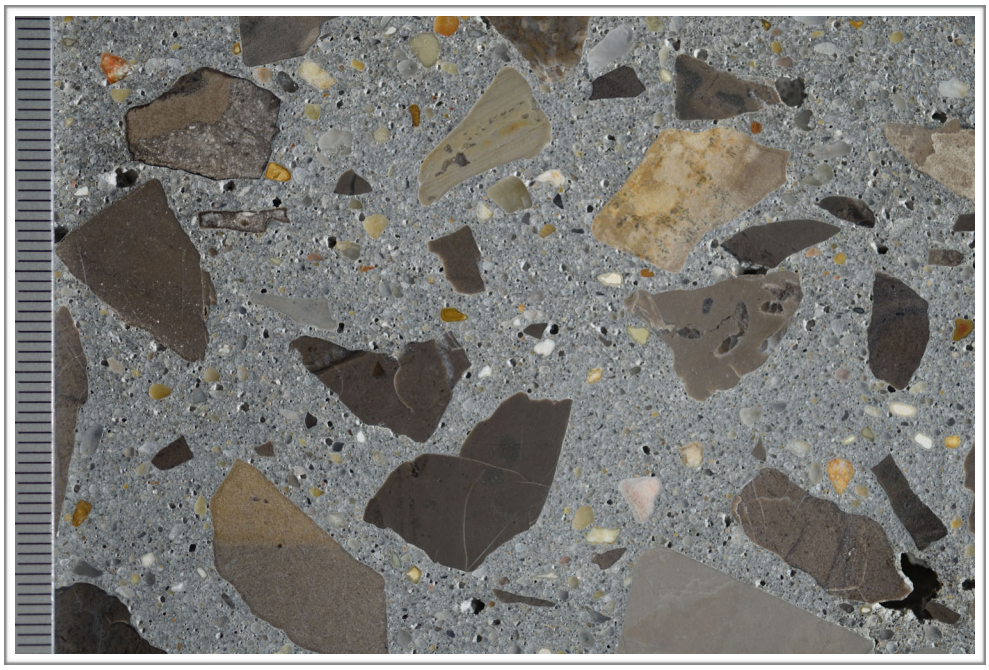

Figure E6. Photograph of the polished surface showing coarse aggregate; scale in millimeters.

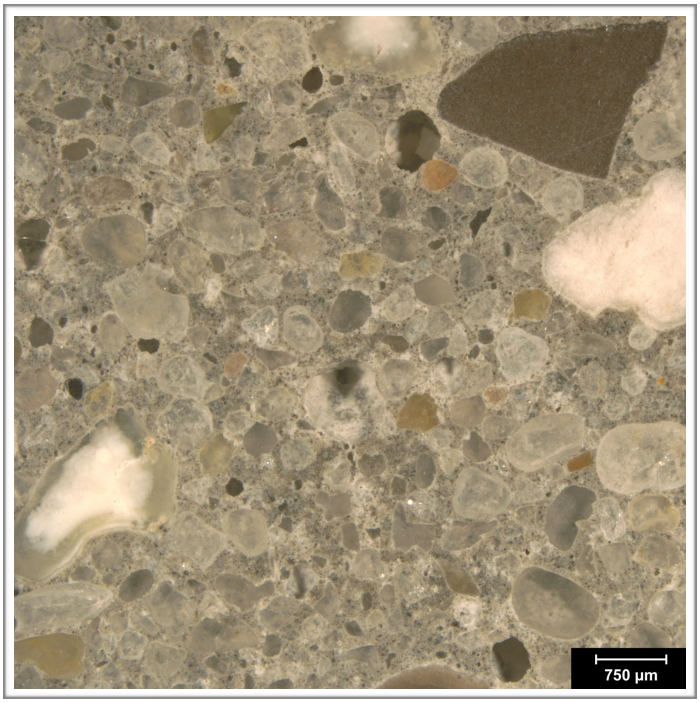

Figure E7. Reflected light photomicrograph of polished surface showing the fine aggregate.

(a)

(b)

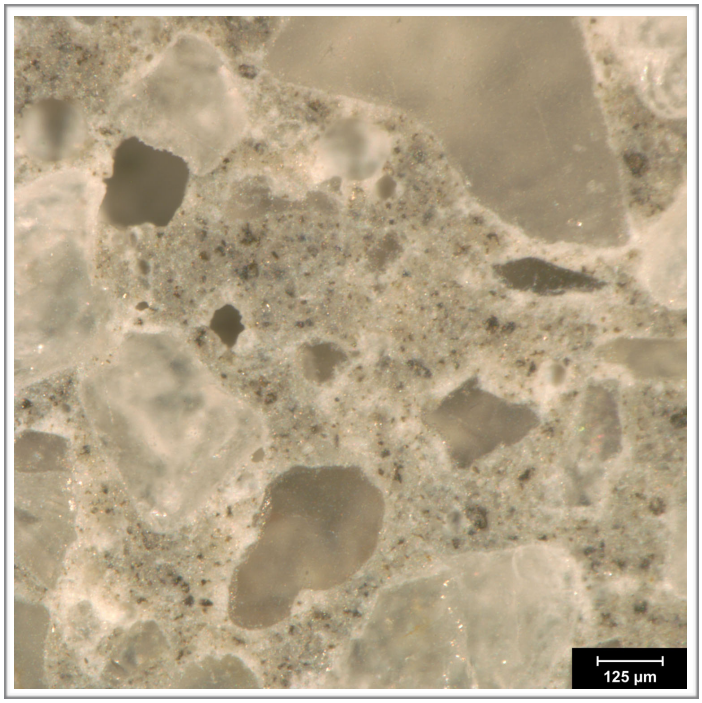

Figure E8. (a) Photograph of polished surface showing overview of paste at the top of the core. The scale is in millimeters; the red arrows indicates a water void. (b) Reflected light photomicrograph showing detail of paste color, texture and luster in the middle of the core.

(a)

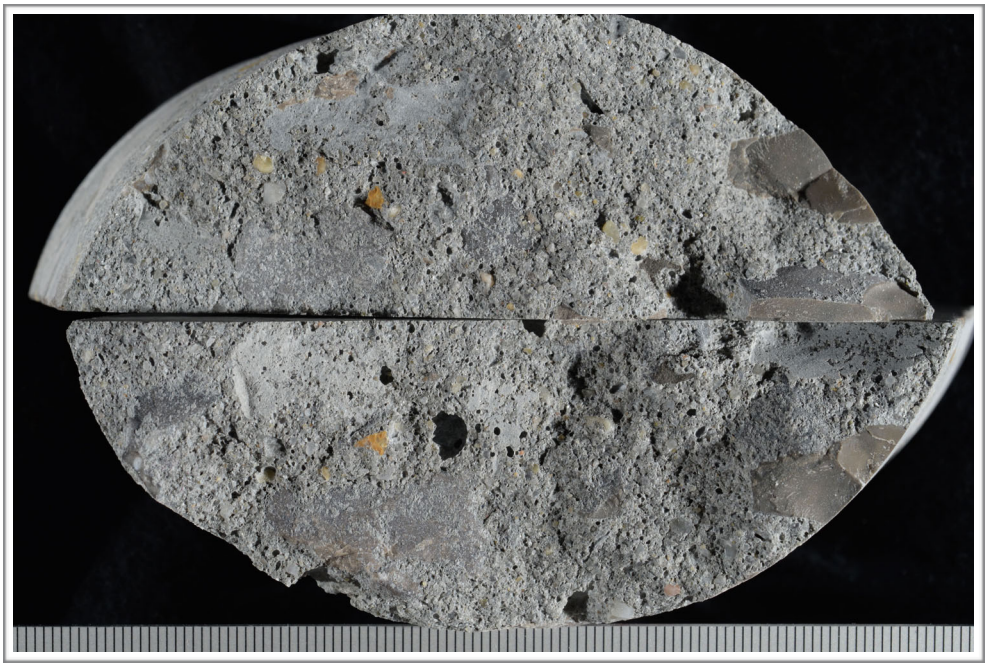

(b)

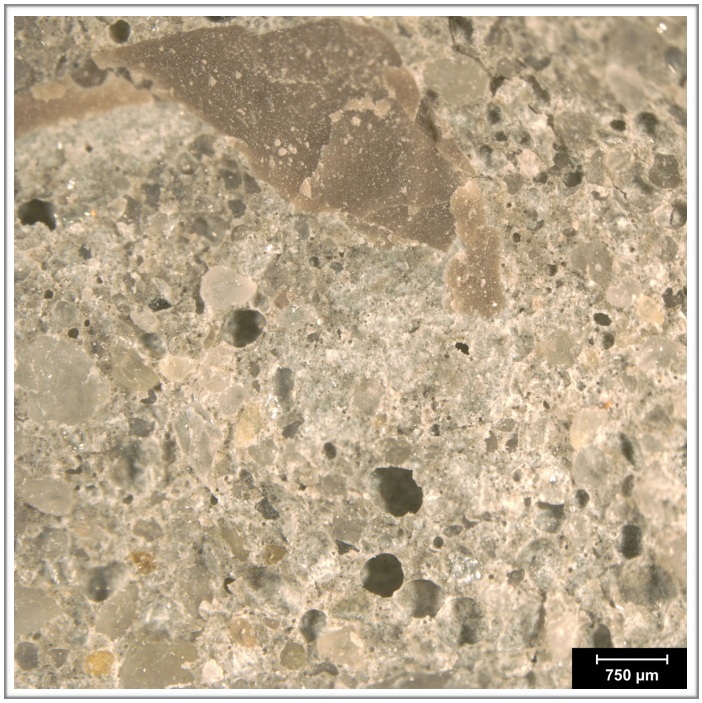

Figure E9. (a) Photograph and (b) reflected light photomicrograph of the fresh fracture surface. The scale in (a) is in millimeters.

(a)

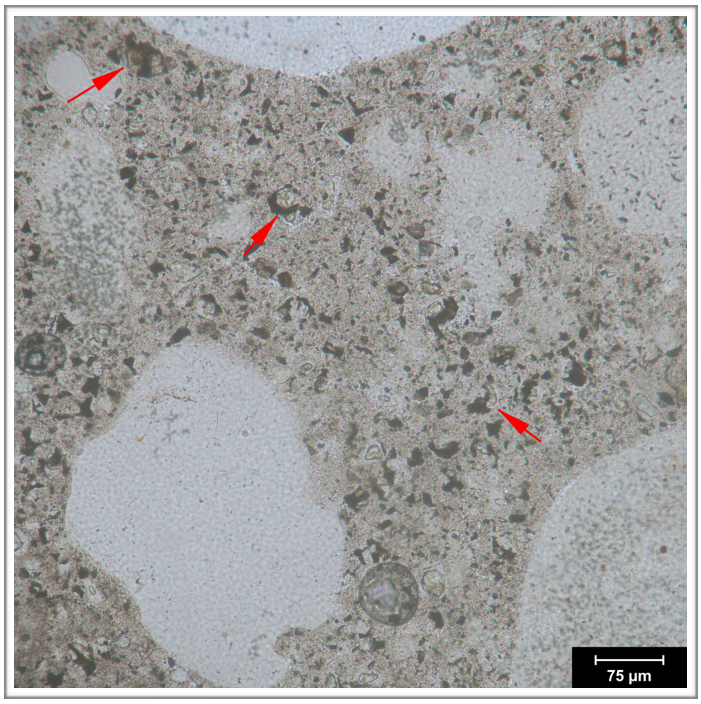

(b)

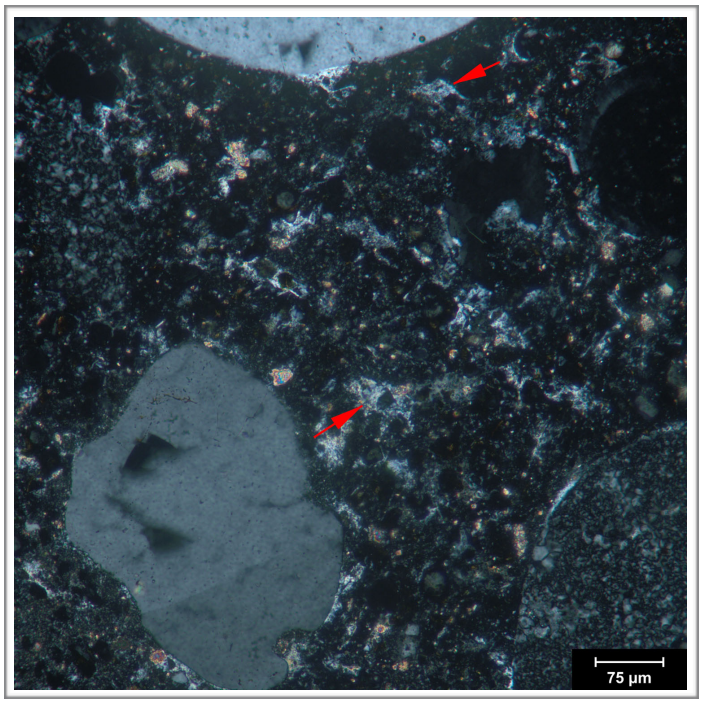

Figure E10. Transmitted light photomicrographs of thin section showing detail of paste in (a) plane-polarized and (b) cross-polarized light. The red arrows indicate RRCG in (a); in (b) they indicate coarse CH.

(a)

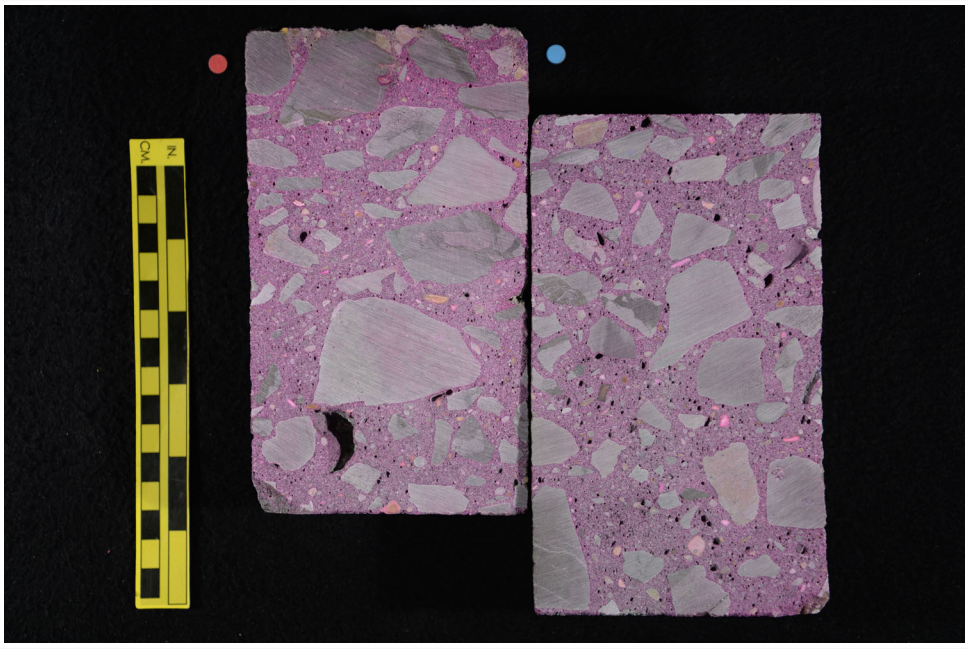

(b)

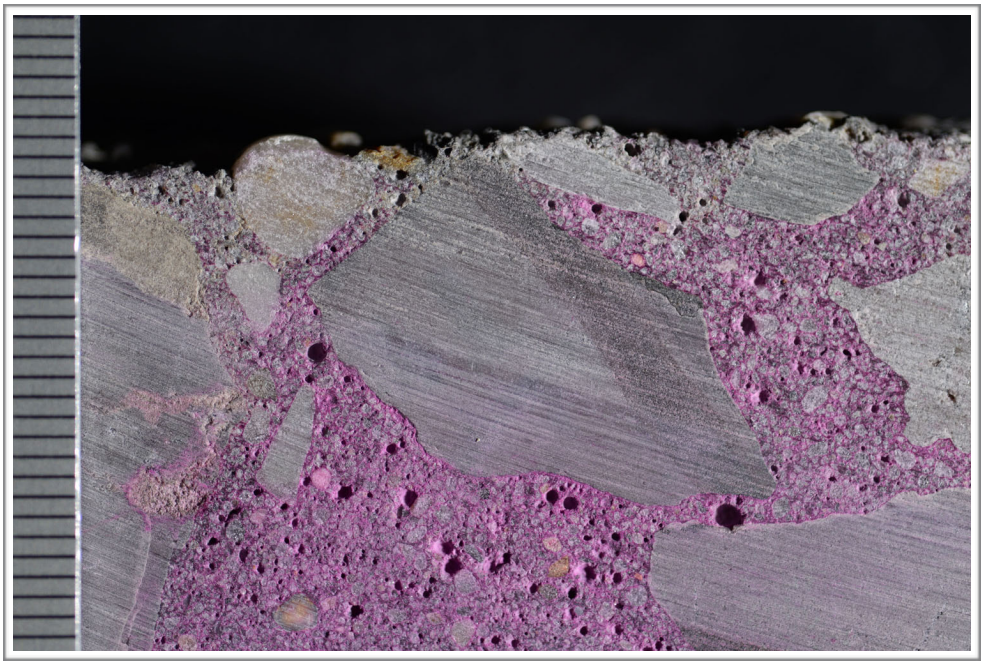

Figure E11. Photographs showing (a) overview of phenolphthalein stained surface and (b) detail of surface near the top of the core. Scale in millimeters in (b).

1. RECEIVED CONDITION

ORIENTATION	Vertical core taken through highway pavement slab measures 100 mm (~ 4 in.) in diameter and 325 mm (~ 13 in.) long (**Figure F1, F2**).
SURFACES	The top surface shows minor wear; the tines are largely intact and a few coarse aggregate particles are exposed and worn smooth (**Figure F3**). The bottom surface is a saw cut such that the core represents a partial thickness of the pavement slab.
GENERAL CONDITION	The concrete is hard and compact and rings lightly when sounded with a hammer. The core was received intact in one piece.

2. EMBEDDED OBJECTS

GENERAL	None observed.

3. CRACKING

MACROSCOPIC	Linear crack cuts 90 mm (3 ½ in.) across the top of the core; the crack is 250 µm (10 mil) wide and was not observed cutting to a significant depth on the polished surface (**Figure F4**). Minor internal hairline cracks observed in coarse aggregate particles. These do not propagate into the paste.
MICROSCOPIC	A microcrack that is ~ 75 µm (3 mil) wide cuts sub-vertically from the top surface to ~ 3 mm (⅜ in.); the microcrack is free of secondary deposits and cuts around aggregate particles (**Figure F5**). No other microcracking was observed.

4. VOIDS

VOID SYSTEM	Concrete is air-entrained (**Figure F6**) and contains 4-6% air by visual estimation (not determined following ASTM C457). The core is moderately consolidated with several larger water voids and entrapped voids that measure up to 12.5 mm (½ in.) across observed (**Figure F7**).
VOID FILLINGS	Voids commonly contain minor deposits of ettringite.

5. COARSE AGGREGATE

PHYSICAL PROPERTIES	Crushed quarry rock with 38 mm (1 ½ in.) nominal top size (**Figure F8**). The rocks are hard and competent. The particles are sub-equant to tabular in shape with sub-angular to sub-round edges. The grading and distribution are relatively even. The sand is very fine.
ROCK TYPES*	The aggregate is carbonate in composition and consists of brown dolomitic limestone as well as tan to light brown limestones that show laminations and evidence of bioturbation as well as some oolitic limestones.
OTHER FEATURES	No deleterious coatings or incrustations observed. A few minor low w/c mortar coatings observed. Occasional particles show internal cracking and microcracking; these do not propagate into the paste.

**Modal abundance based on visual estimation.*

6. FINE AGGREGATE

PHYSICAL PROPERTIES	Natural sand consists of rocks that are hard and competent (**Figure F9**). The particles are sub-equant to tabular in shape with sub-round to sub-angular edges. The grading and distribution are relatively even.
ROCK TYPES	The sand is siliceous in composition and consists primarily of quartz and quartzite with minor amounts of granitic rocks and chert.
OTHER FEATURES	No deleterious coatings or incrustations observed and no low w/c mortar coatings observed. Particles of chert typically show reaction rims but no microcracking or deposits of gel are associated with them.

7. PASTE OBSERVATIONS

POLISHED SURFACE	Paste is gray (Munsell 2.5Y/6/1) to dark gray (2.5Y/4/1), has a smooth texture and sub-vitreous luster (**Figure F10**). The paste is hard (Mohs 3.5-4). The paste is dark gray for up to 3 mm (⅛ in.) from the top of the core.
FRESH FRACTURE	Fracture surface is light gray, has a hackly texture and a sub-vitreous luster. The fracture cuts primarily through aggregate particles (**Figure F11**). No significant secondary deposits were observed though minor deposits of ettringite commonly line voids.
THIN SECTION*	The paste contains hydrated portland cement; no fly ash, slag cement or other SCM were observed. The hydration is normal with 4-8% RRCG that consist mostly of interstitial ferrite and aluminate with occasional grains of belite (**Figure F12**). CH makes up 10-17% of the paste, is fine to medium-grained and evenly distributed.

** Abbreviations as follows: RRCG = relict and residual cement grains; SCM = supplemental cementitious materials; CH = calcium hydroxide; ITZ = interfacial transition zone. Modal abundances are based on visual estimations.*

8. SECONDARY DEPOSITS

PHENOLPHTHALEIN	Entire surface stains purple (**Figure F13**).
DEPOSITS	Minor carbonation observed at the top of the core and in irregularly distributed zones in the paste in thin section. Minor deposits of ettringite observed commonly in voids. Deposits of gel observed in minor amounts in rare voids (**Figure F14-Figure F17**). No microcracking observed in association with ASR.

FIGURES

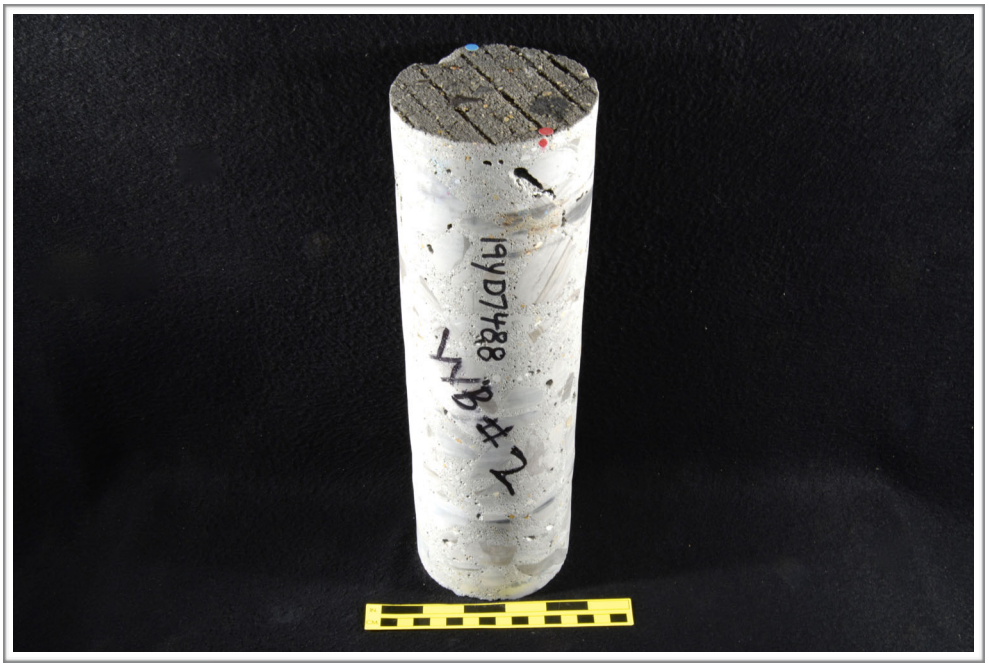

(a)

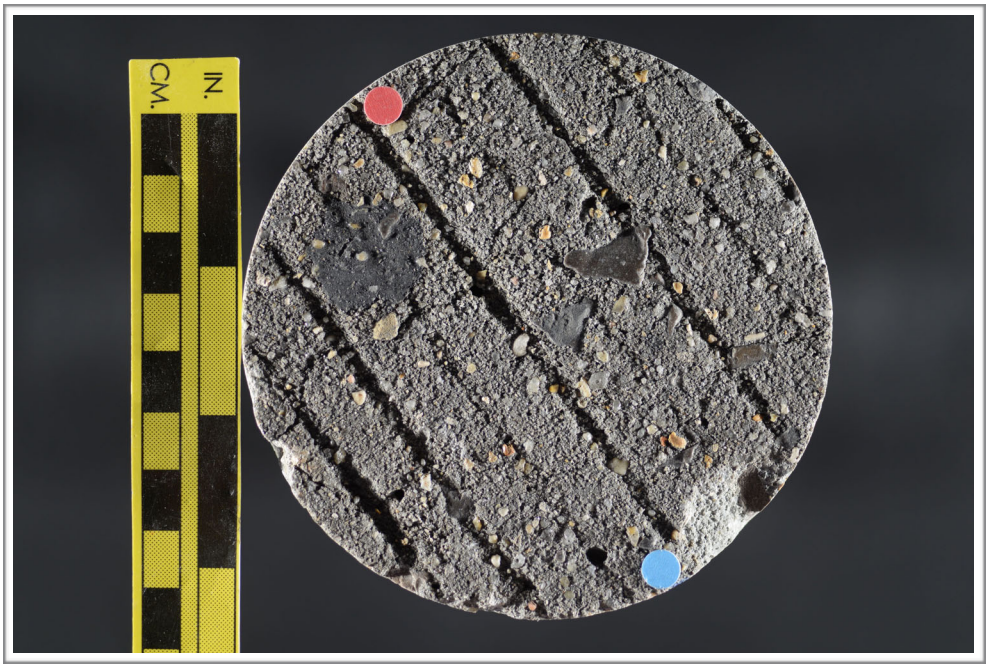

(b)

Figure F1. Photographs showing (a) oblique view of the top and side of the core with identification labels and (b) the top of the core. The red and blue dots in (a) show the orientation of the saw cuts used to prepare the sample.

(c)

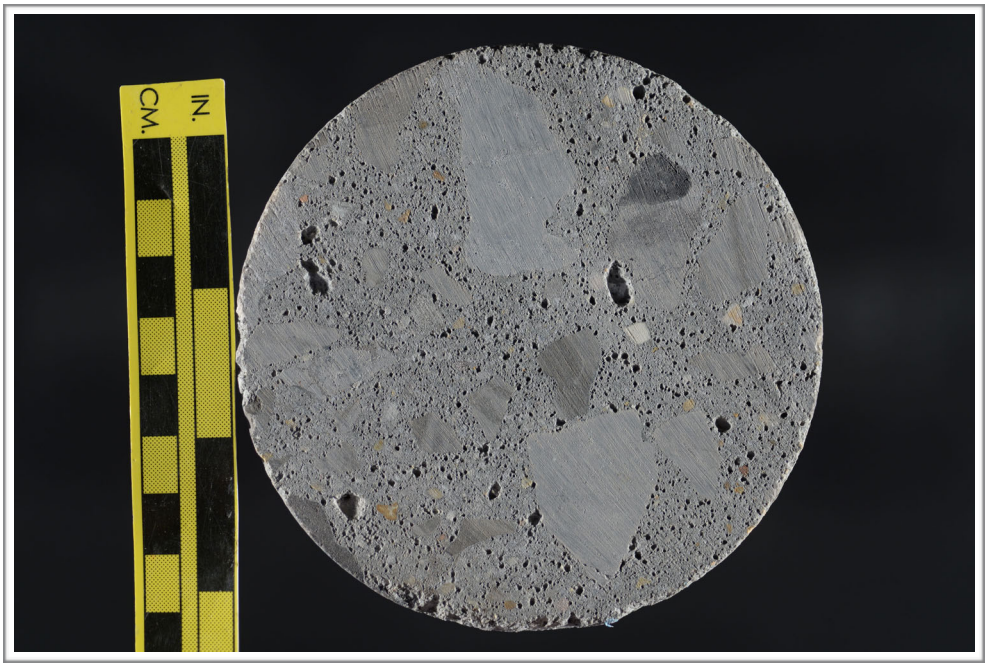

Figure F1 (cont'd). (c) Photograph showing the bottom of the core.

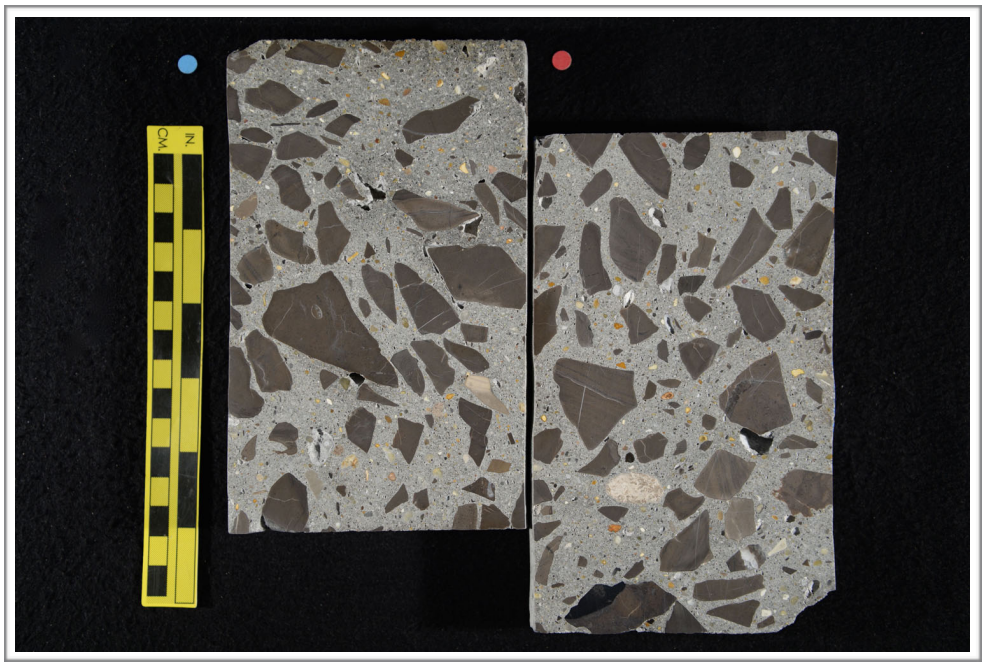

Figure F2. Photograph showing the polished surface of the core.

Figure F3. Photograph showing detail of the top surface of the core; scale in millimeters.

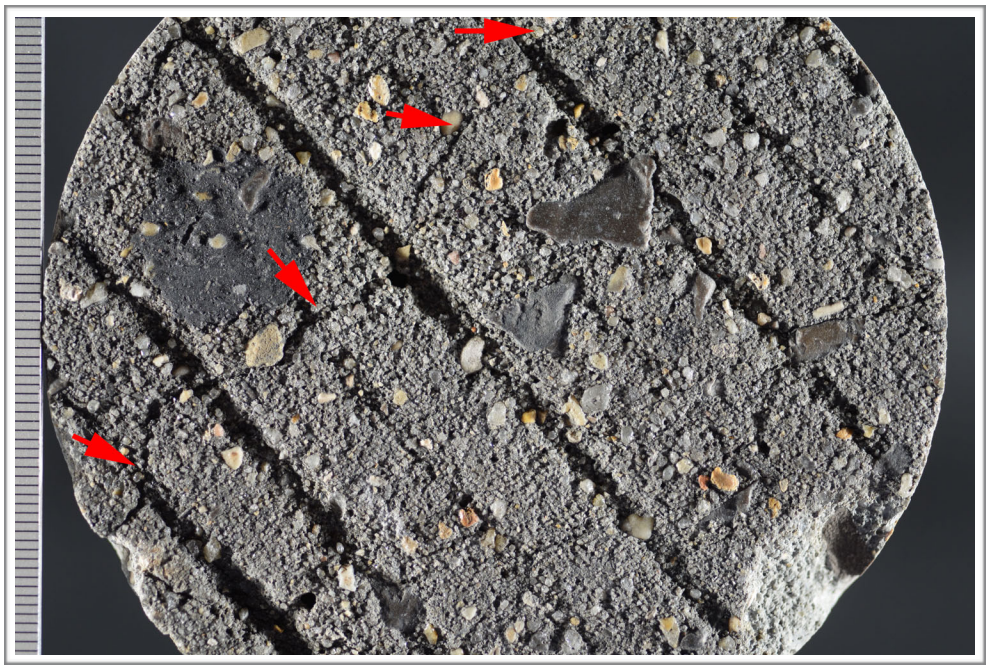

Figure F4. Photographs showing crack (red arrows) on the top surface; scale in millimeters.

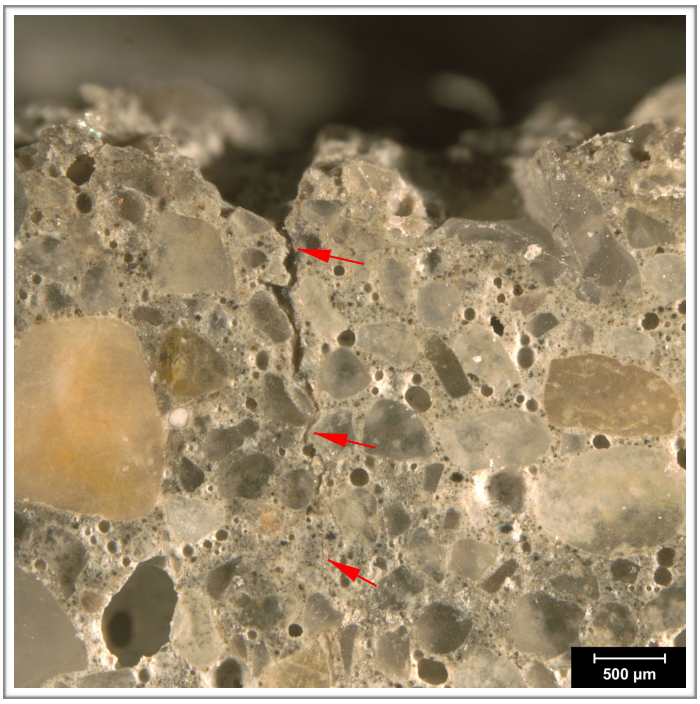

Figure F5. Reflected light photomicrograph of the polished surface showing microcrack (red arrows) at the top of the core.

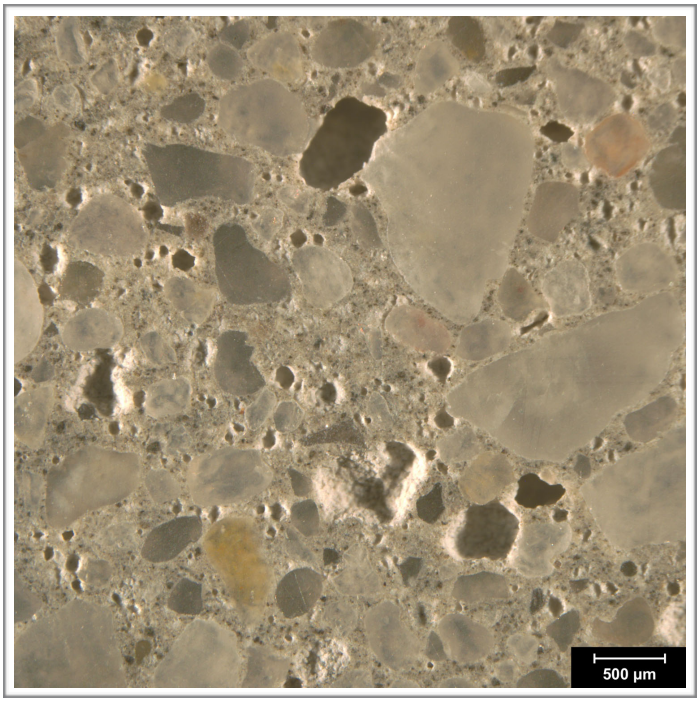

Figure F6. Reflected light photomicrograph of the polished surface showing entrained air voids (dark circles).

(a)

(b)

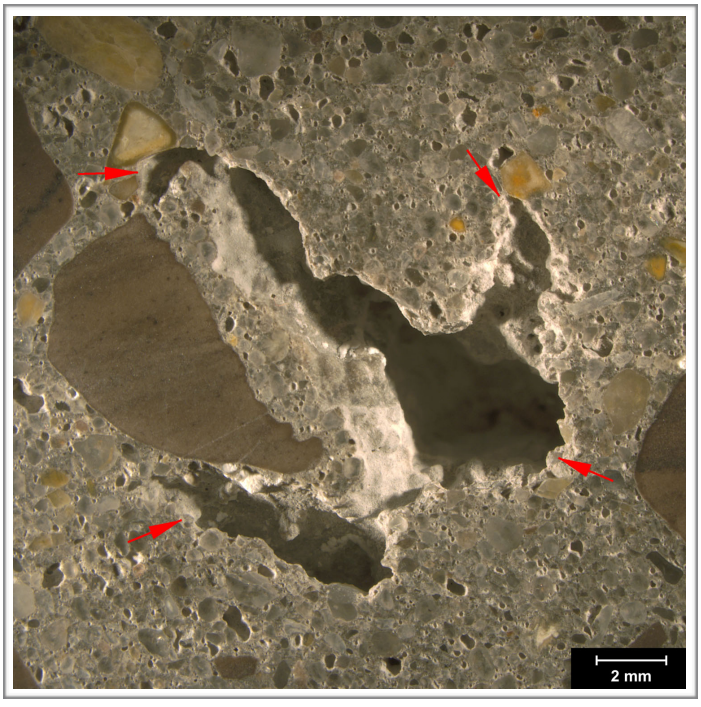

Figure F7. (a) Photograph and (b) reflected light photomicrograph of the polished surface showing overview and detail, respectively of large entrapped voids about 50 mm (2 in.) below the polished surface.

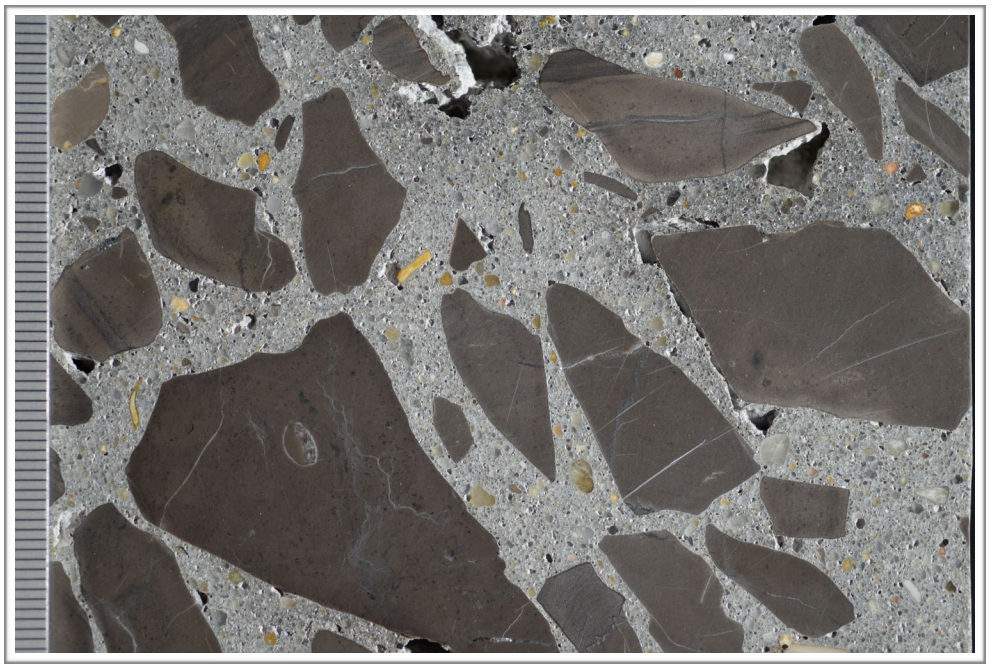

Figure F8. Photograph of the polished surface showing coarse aggregate; scale in millimeters.

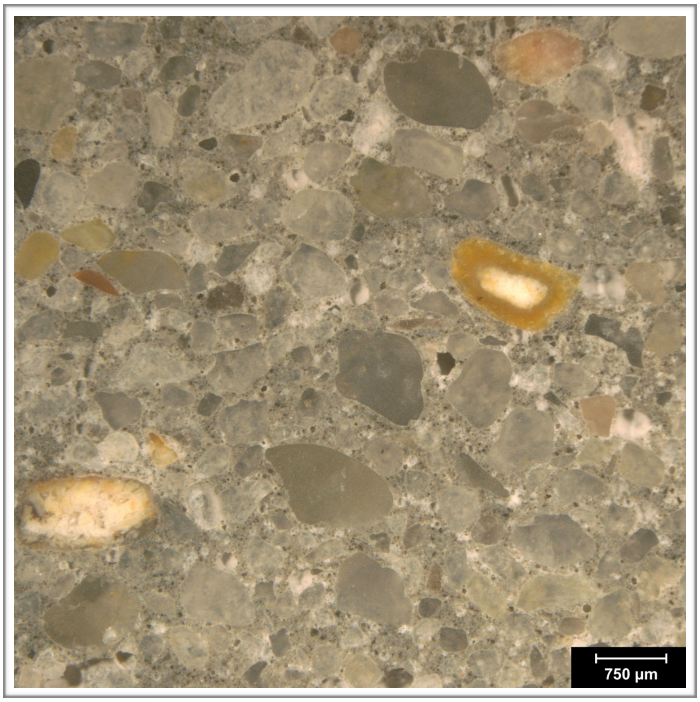

Figure F9. Reflected light photomicrograph of polished surface showing the fine aggregate.

(a)

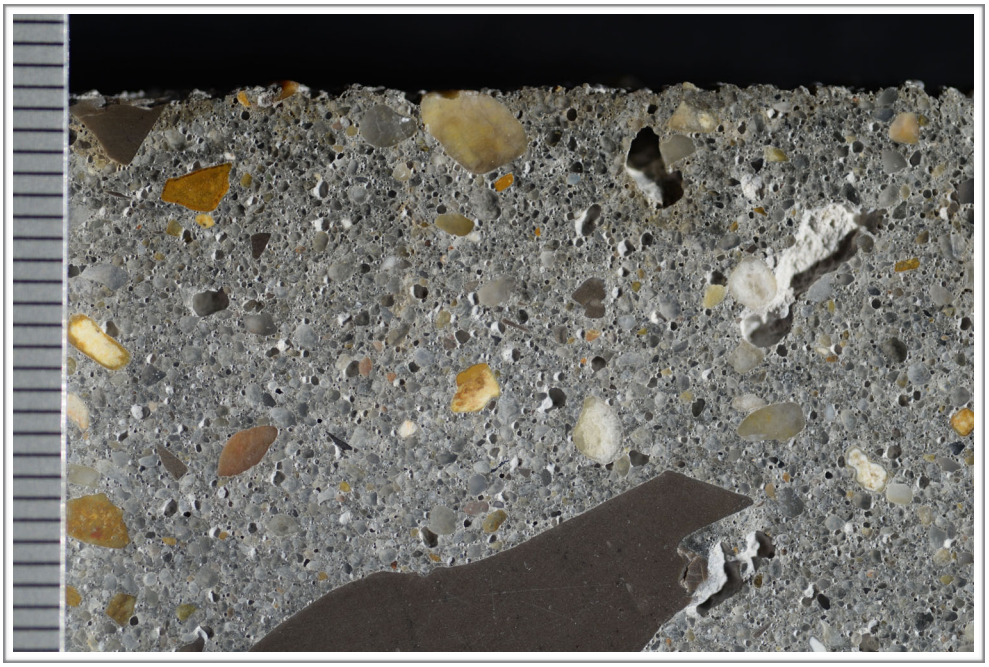

(b)

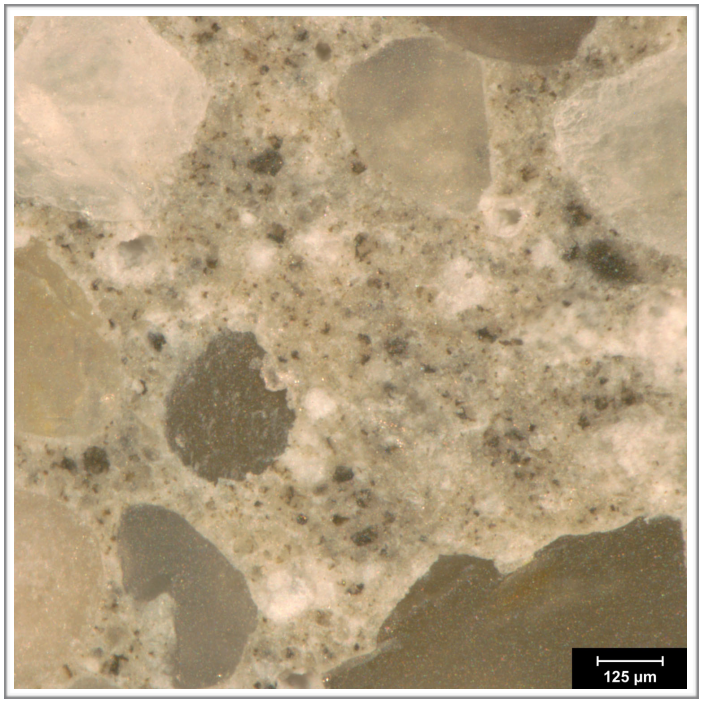

Figure F10. (a) Photograph of polished surface showing overview of paste at the top of the core. The scale is in millimeters; the red arrows indicate the hairline crack that cut across the top surface. (b) Reflected light photomicrograph showing detail of paste color, texture and luster in the middle of the core.

(a)

(b)

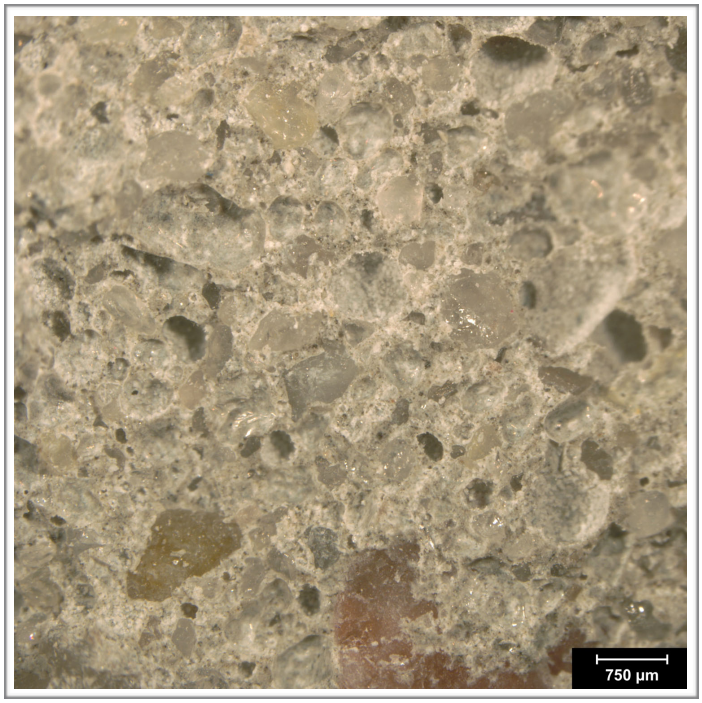

Figure F11. (a) Photograph and (b) reflected light photomicrograph of the fresh fracture surface. The scale in (a) is in millimeters.

(a)

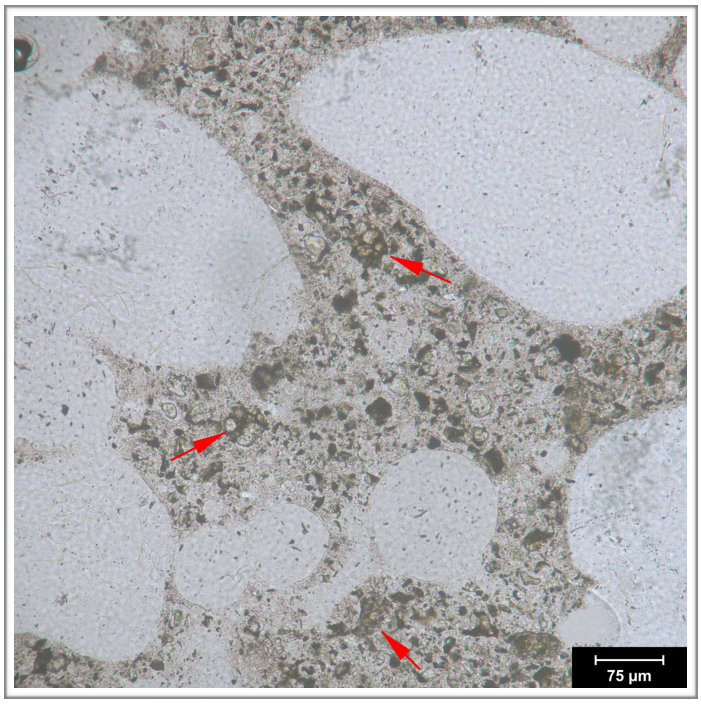

(b)

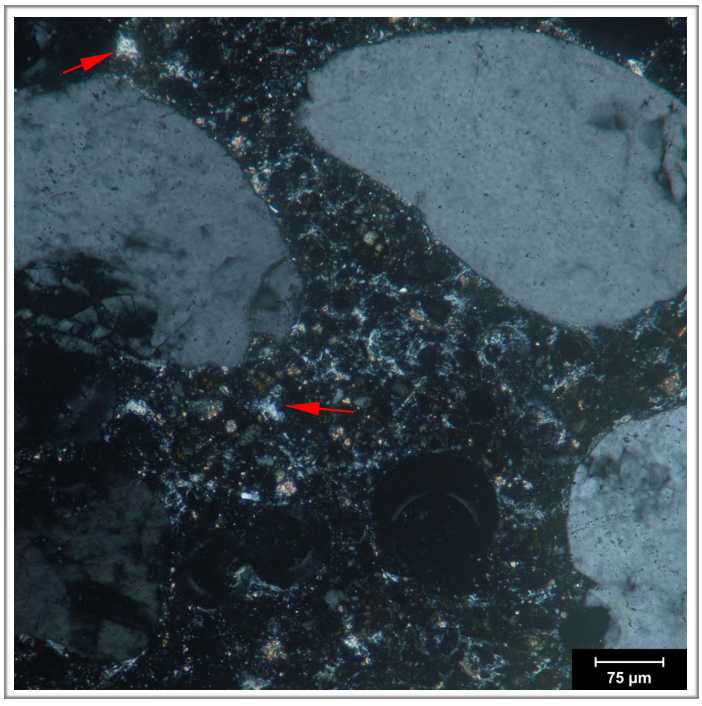

Figure F12. Transmitted light photomicrographs of thin section showing detail of paste in (a) plane-polarized and (b) cross-polarized light. The red arrows indicate RRCG in (a) and CH in (b).

(a)

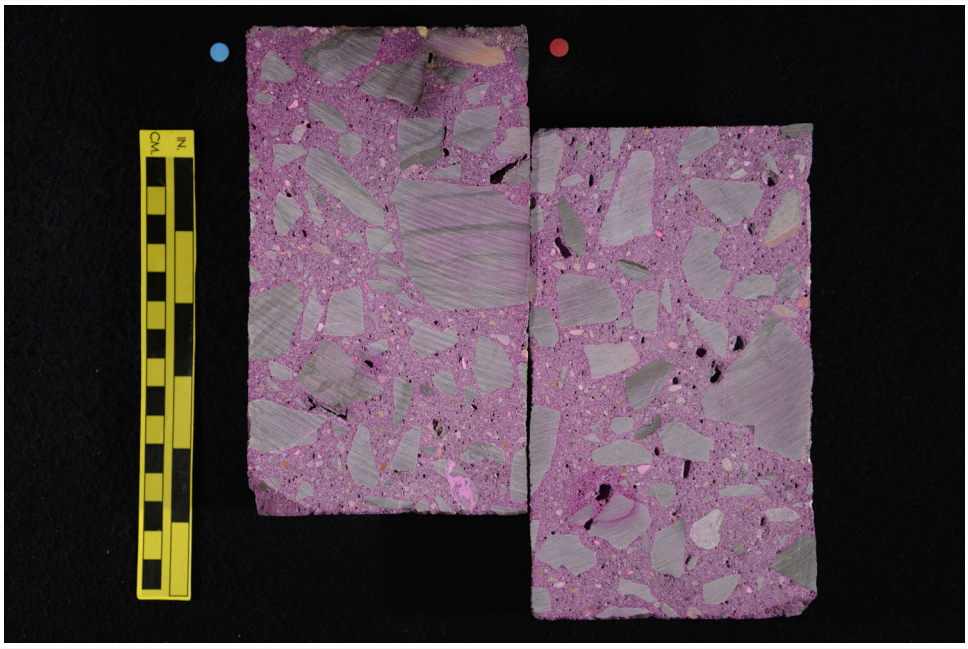

(b)

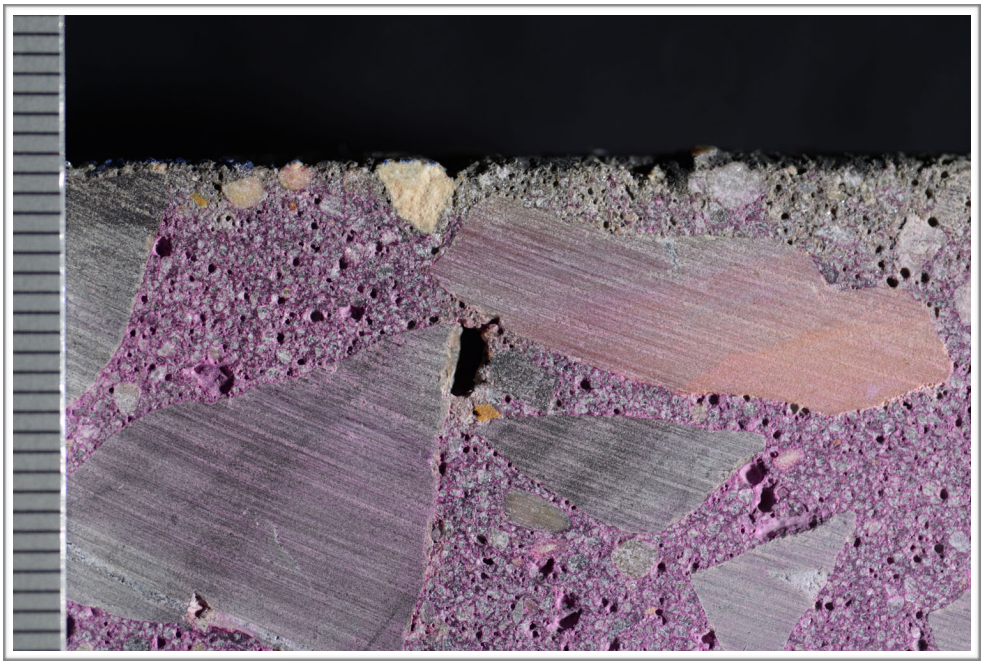

Figure F13. Photographs showing (a) overview of phenolphthalein stained surface and (b) detail of surface near the top of the core. Scale in millimeters in (b).

(a)

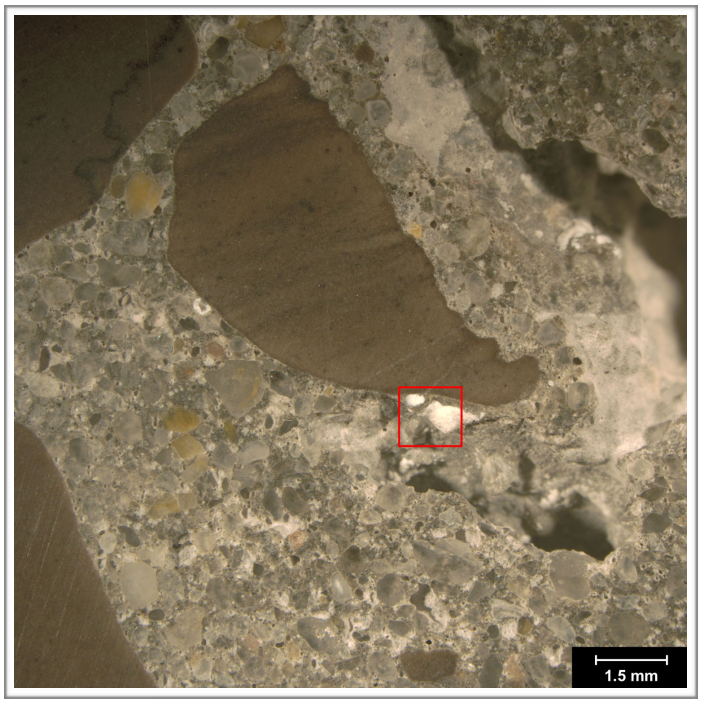

(b)

Figure F14. Reflected light photomicrographs of the polished surface showing a void filled with secondary deposits (red arrow in (b) about 50 mm (2 in.) below the top surface. The red square in (a) shows the approximate are of (b).

(a)

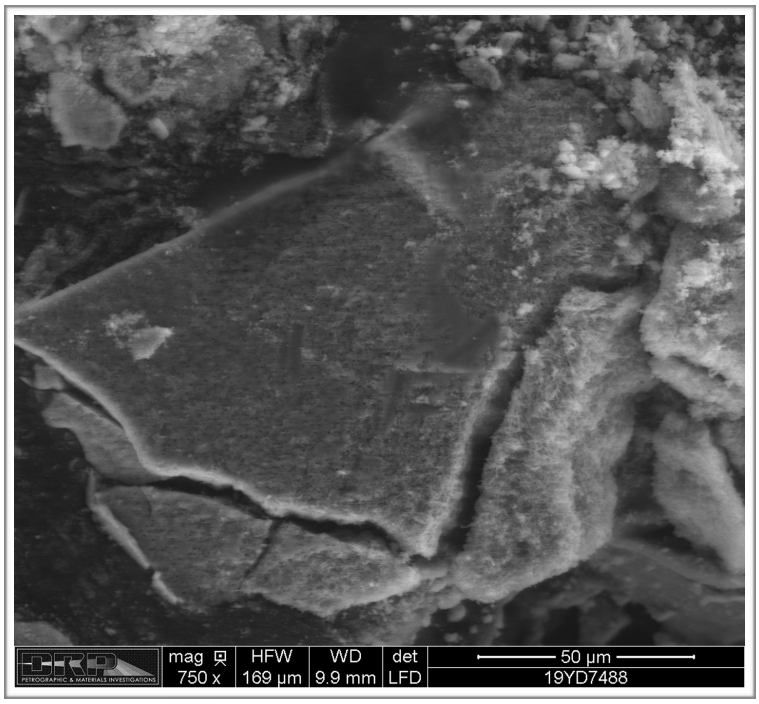

(b)

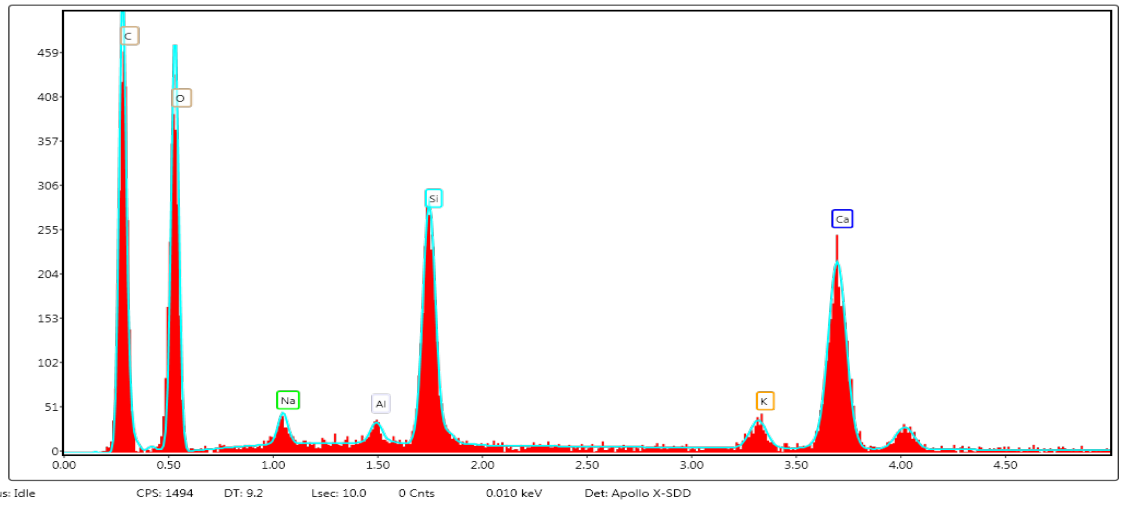

Figure F15. (a) Backscatter electron micrograph of gel deposits scraped from void shown in F12(b) and placed on carbon tape. (b) EDS spectrum of deposit indicating composition typical of ASR gel.

(a)

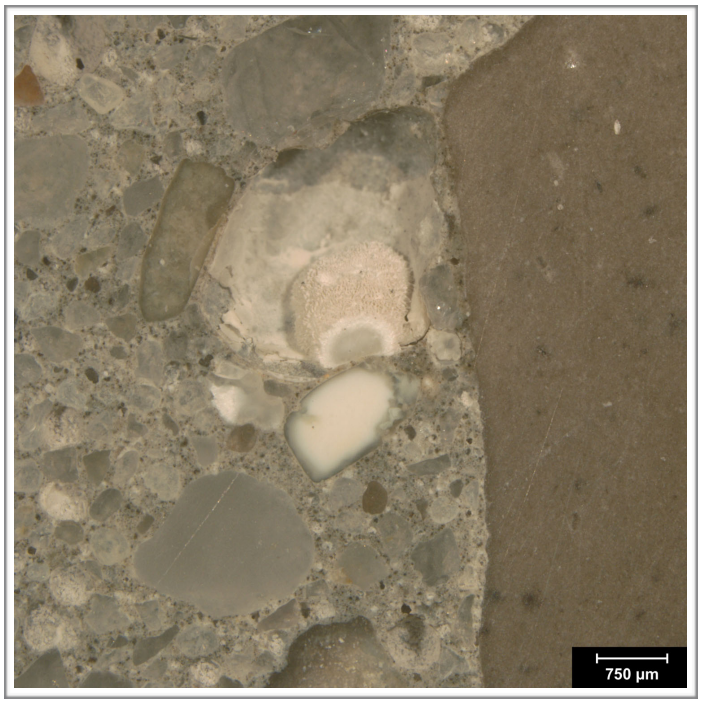

(b)

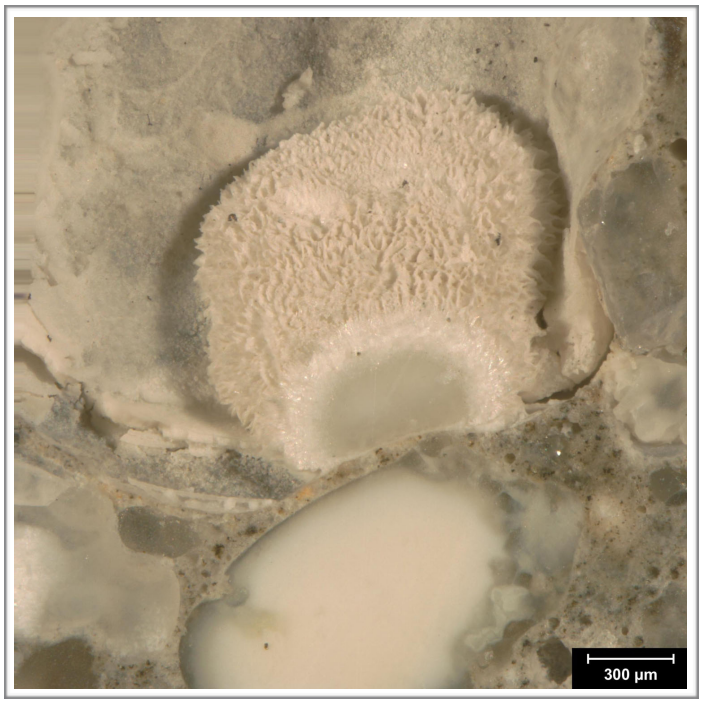

Figure F16. Reflected light photomicrographs of the polished surface showing a void filled with secondary deposits about 195 mm (7 ¾ in.) below the top surface.

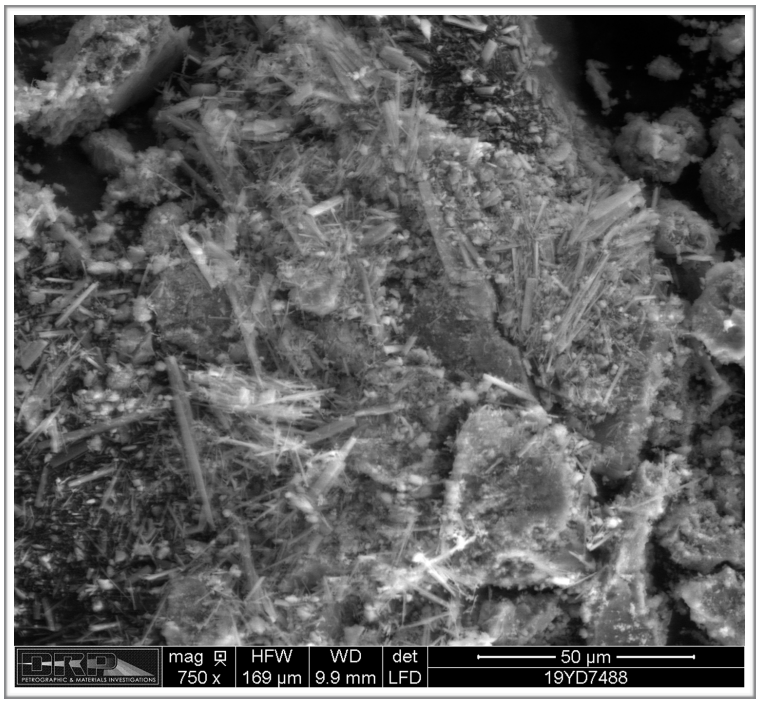

(a)

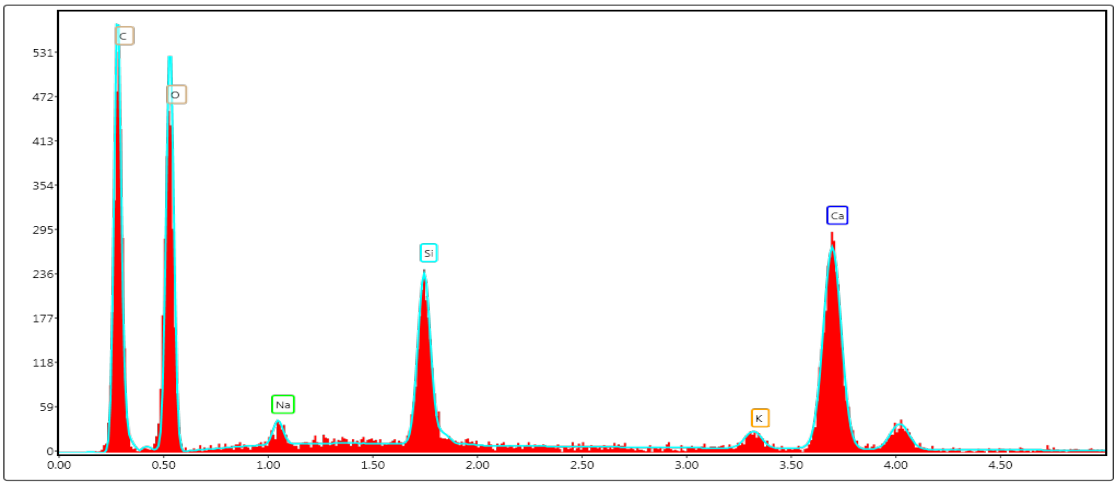

(b)

Figure F17. (a) Backscatter electron micrograph of gel deposits scraped from void shown in F14(b) and placed on carbon tape. (b) EDS spectrum of deposit indicating composition typical of ASR gel.

1. RECEIVED CONDITION

ORIENTATION	Vertical core taken through highway pavement slab measures 100 mm (~ 4 in.) in diameter and 325 mm (~ 13 in.) long (**Figure G1, G2**).
SURFACES	The top surface shows wear that exposes smooth coarse aggregate particles but the tines are largely intact (**Figure G3**). The bottom surface is a saw cut such that the core represents a partial thickness of the pavement slab.
GENERAL CONDITION	The concrete is hard and compact and rings lightly when sounded with a hammer. The core was received intact in one piece.

2. EMBEDDED OBJECTS

GENERAL	None observed.

3. CRACKING

MACROSCOPIC	Linear crack that is up to 500 µm (20 mil) wide cuts 100 mm (4 in.) across the top of the core and cuts sub-vertically ~15 mm (⅝ in.) down the side of the core (**Figure G4**). On the polished surface the crack cuts around aggregates to ~ 19 mm (¾ in.) below the top surface (**Figure G5**). Minor internal hairline cracks observed in coarse aggregate particles. These do not propagate into the paste. No other cracks were observed.
MICROSCOPIC	No significant microcracks observed.

4.VOIDS

VOID SYSTEM	Concrete is air-entrained (**Figure G6**) and contains 4-6% air by visual estimation (not determined following ASTM C457). The core is well consolidated with no significant entrapped voids or water voids observed.
VOID FILLINGS	Voids commonly contain minor deposits of ettringite.

5. COARSE AGGREGATE

PHYSICAL PROPERTIES	Crushed quarry rock with 38 mm (1 ½ in.) nominal top size (**Figure G7**). The rocks are hard and competent. The particles are sub-equant to tabular in shape with sub-angular to sub-round edges. The grading and distribution are somewhat uneven with some gap grading and segregation of large particles toward the bottom of the core. The sand is very fine.
ROCK TYPES*	The aggregate is carbonate in composition and consists of brown dolomitic limestone as well as tan to light brown limestones that show laminations and evidence of bioturbation as well as some oolitic limestones.
OTHER FEATURES	No deleterious coatings or incrustations observed. A few minor low w/c mortar coatings observed. Occasional particles show internal cracking and microcracking; these do not propagate into the paste.

**Modal abundance based on visual estimation.*

6. FINE AGGREGATE

PHYSICAL PROPERTIES	Natural sand consists of rocks that are hard and competent (**Figure G8**). The particles are sub-equant to tabular in shape with sub-round to sub-angular edges. The grading and distribution are relatively even.
ROCK TYPES	The sand is siliceous in composition and consists primarily of quartz and quartzite with minor amounts of granitic rocks and chert.
OTHER FEATURES	No deleterious coatings or incrustations observed and no low w/c mortar coatings observed. Particles of chert typically show reaction rims but no microcracking or deposits of gel are associated with them.

7. PASTE OBSERVATIONS

POLISHED SURFACE	Paste is gray (Munsell 2.5Y/6/1) to dark gray (2.5Y/4/1), has a smooth texture and sub-vitreous luster (**Figure G9**). The paste is hard (Mohs 3.5-4).
FRESH FRACTURE	Fracture surface is light gray, has a hackly texture and a sub-vitreous luster. The fracture cuts primarily through aggregate particles (**Figure G10**). Minor deposits of gel observed.
THIN SECTION*	The paste contains hydrated portland cement; no fly ash, slag cement or other SCM were observed. The hydration is normal with 4-8% RRCG that consist mostly of interstitial ferrite and aluminate with occasional grains of belite (**Figure G11**). CH makes up 10-17% of the paste, is fine to medium-grained and evenly distributed.

** Abbreviations as follows: RRCG = relict and residual cement grains; SCM = supplemental cementitious materials; CH = calcium hydroxide; ITZ = interfacial transition zone. Modal abundances are based on visual estimations.*

8. SECONDARY DEPOSITS

PHENOLPHTHALEIN	Entire surface stains purple (**Figure G12**).
DEPOSITS	Minor carbonation observed at the top of the core and in irregularly distributed zones in the paste in thin section. Minor deposits of ettringite observed commonly in voids. Deposits of gel observed in minor amounts in rare voids (**Figure G13, Figure G14**). No microcracking was observed in association with ASR.

FIGURES

(a)

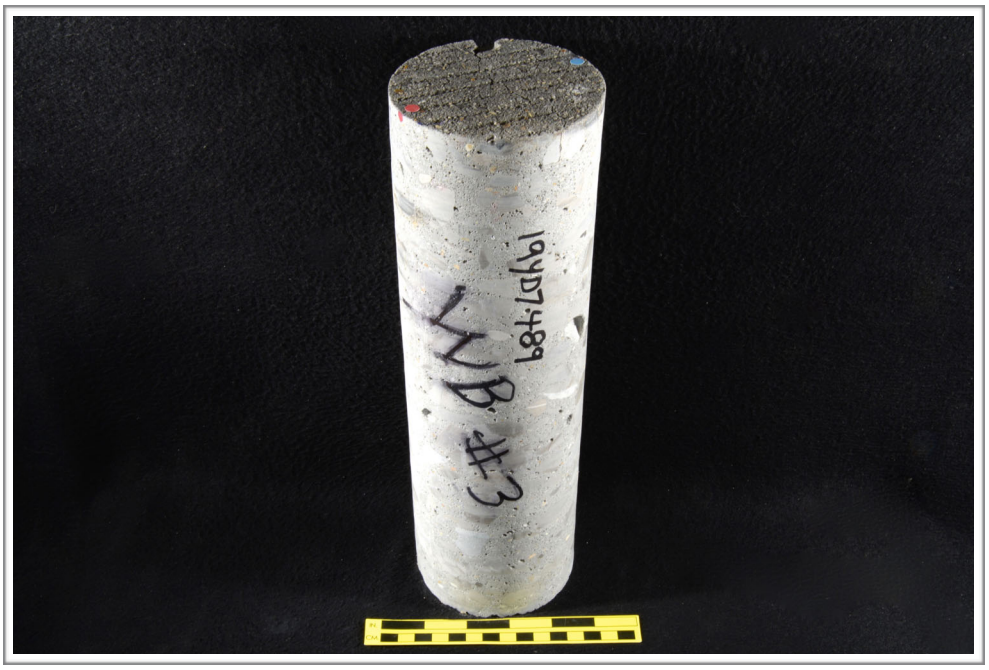

(b)

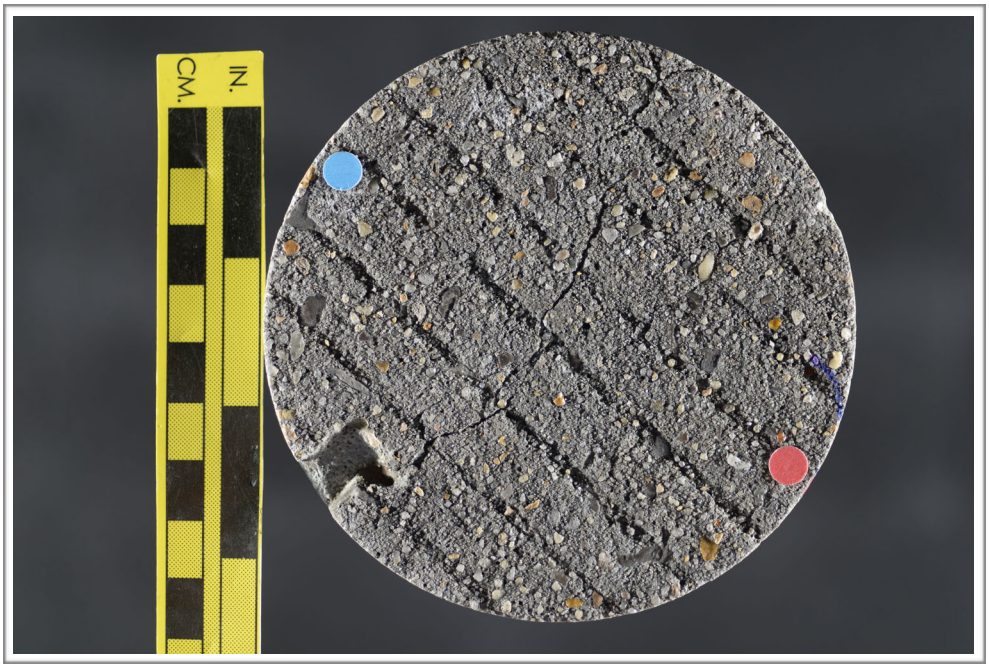

Figure G1. Photographs showing (a) oblique view of the top and side of the core with identification labels and (b) the top of the core. The red and blue dots in (a) show the orientation of the saw cuts used to prepare the sample.

(c)

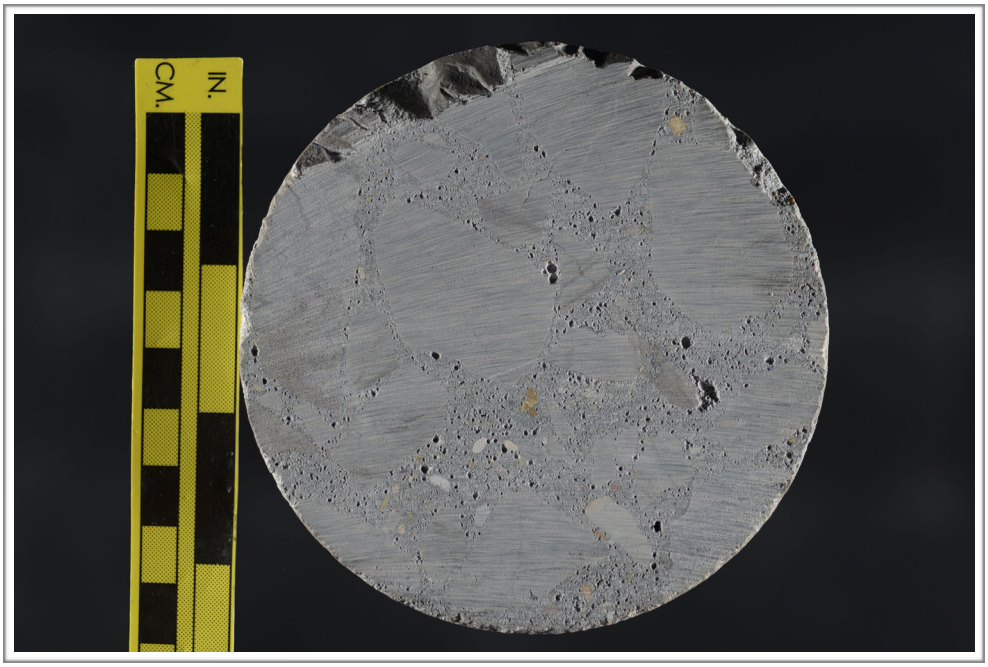

Figure G1 (cont'd). (c) Photograph showing the bottom of the core.

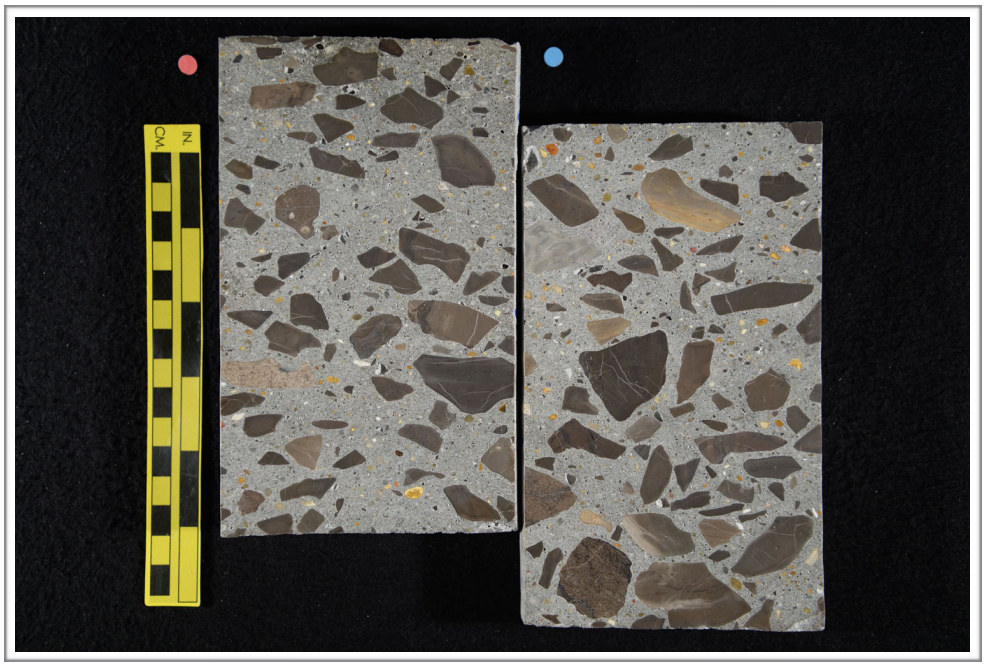

Figure G2. Photograph showing the polished surface of the core.

Figure G3. Photograph showing detail of the top surface of the core; scale in millimeters.

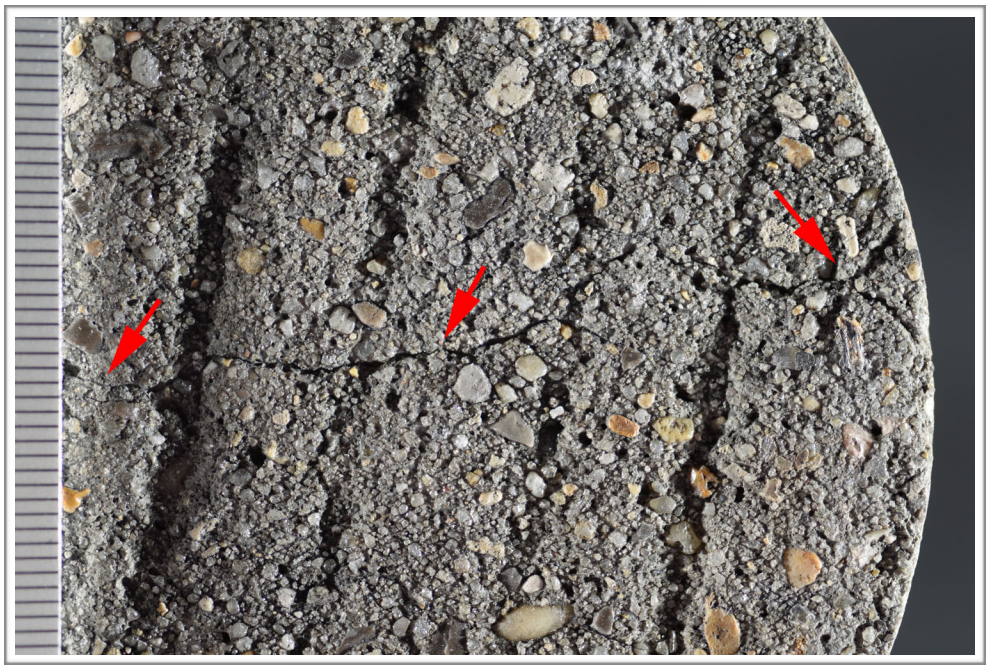

Figure G4. Photographs showing crack (red arrows) on the top surface; scale in millimeters.

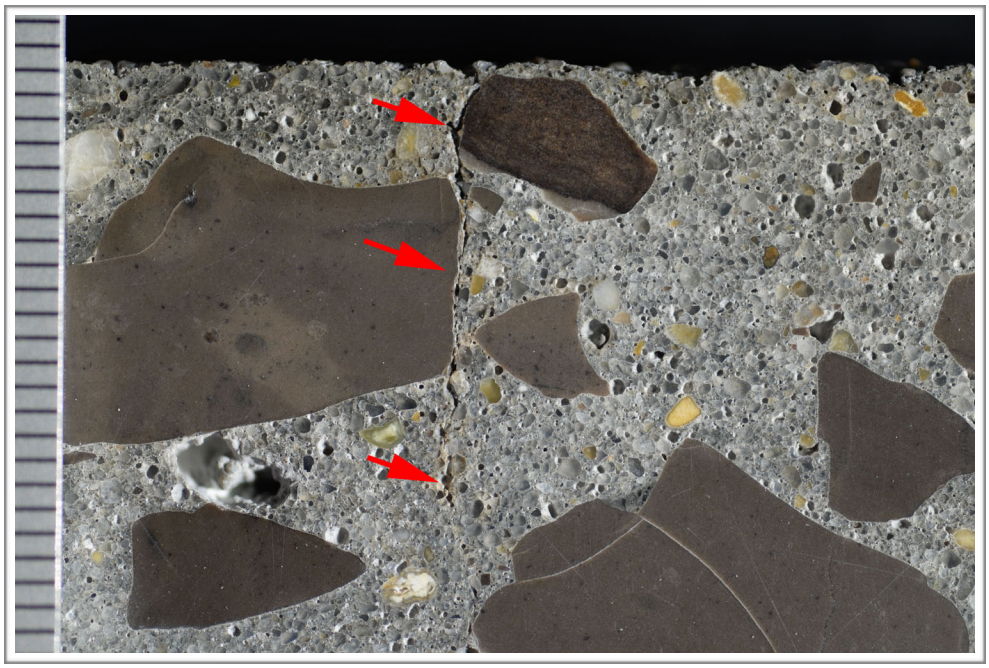

Figure G5. Reflected light photomicrograph of the polished surface showing microcrack (red arrows) at the top of the core.

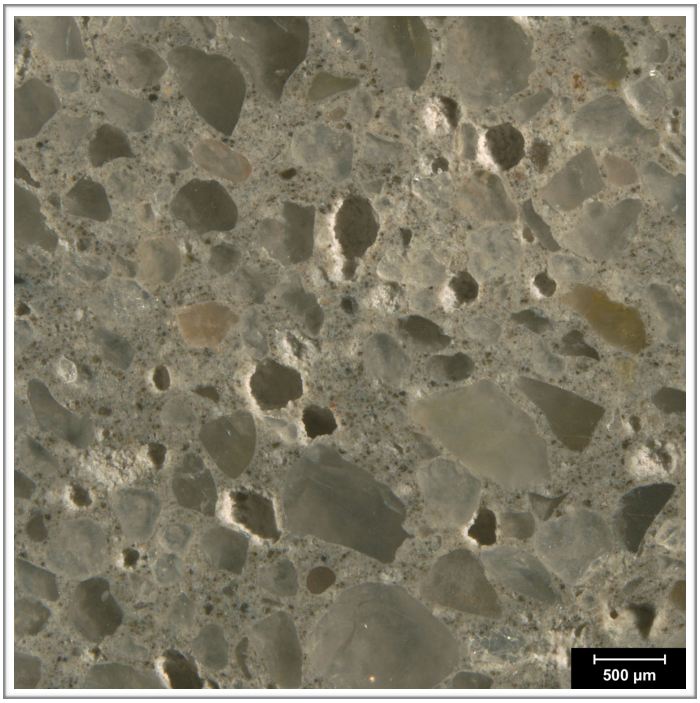

Figure G6. Reflected light photomicrograph of the polished surface showing entrained air voids (dark circles).

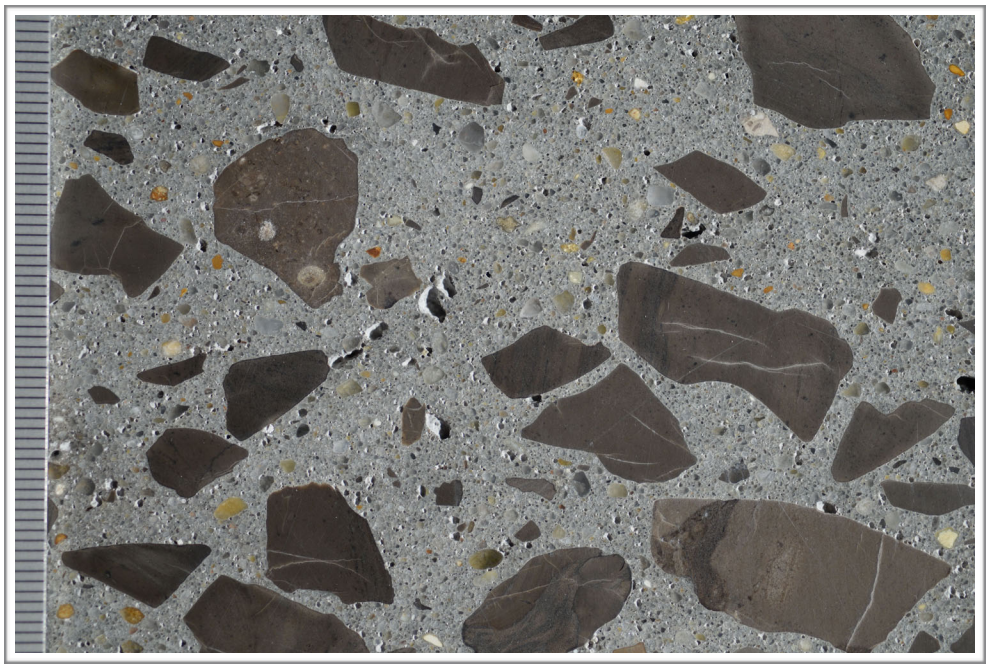

Figure G7. Photograph of the polished surface showing coarse aggregate; scale in millimeters.

Figure G8. Reflected light photomicrograph of polished surface showing the fine aggregate.

(a)

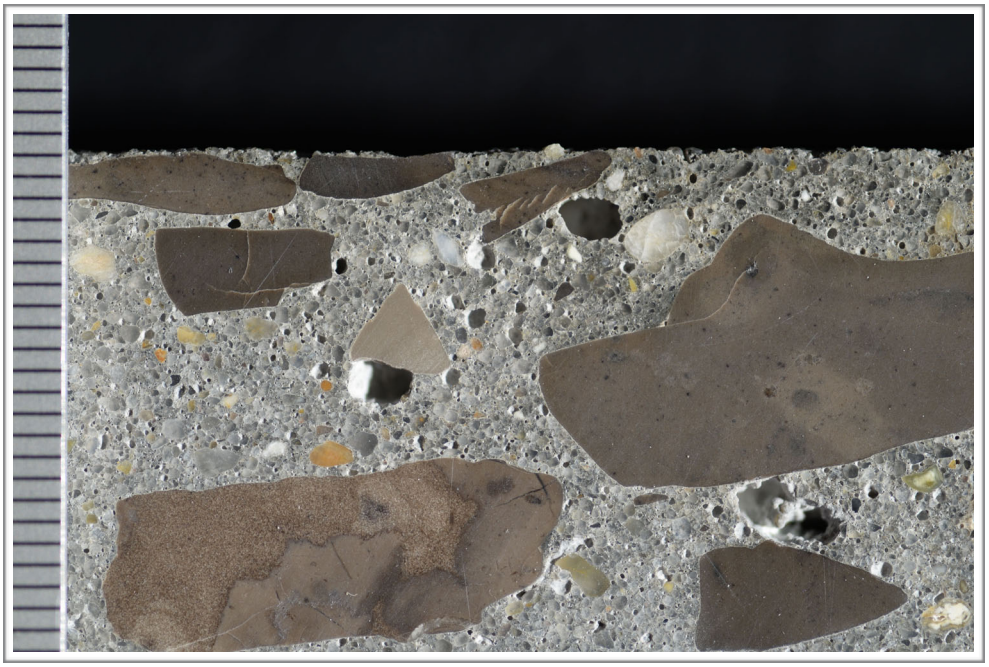

(b)

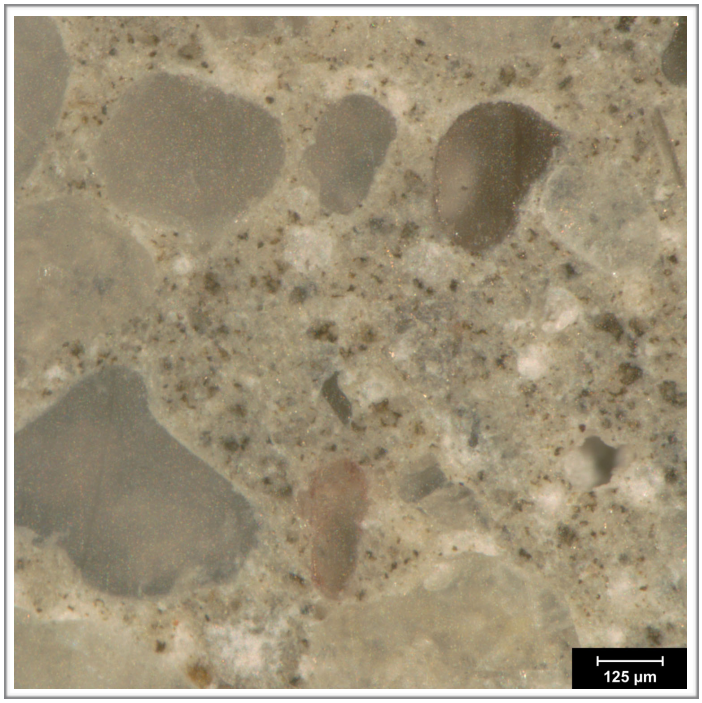

Figure G9. (a) Photograph of polished surface showing overview of paste at the top of the core. The scale is in millimeters. (b) Reflected light photomicrograph showing detail of paste color, texture and luster in the middle of the core.

(a)

(b)

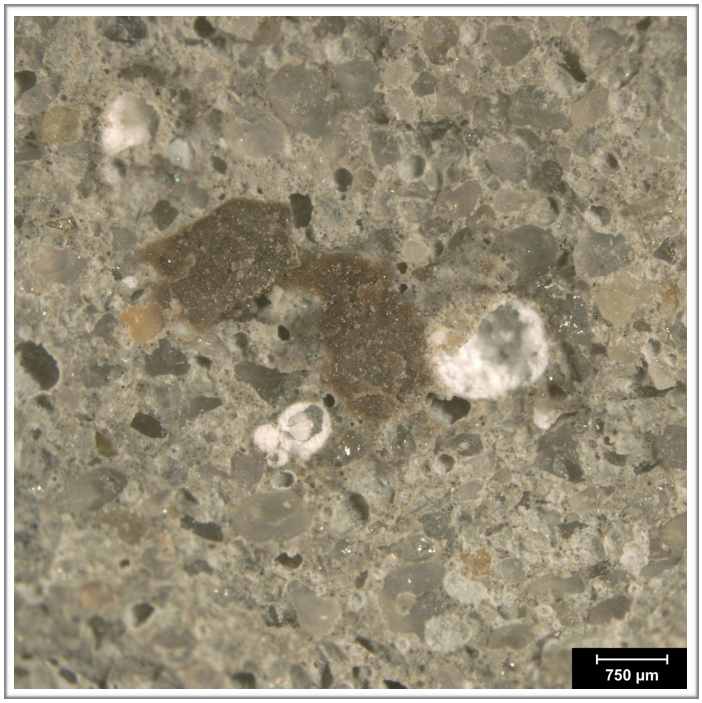

Figure G10. (a) Photograph and (b) reflected light photomicrograph of the fresh fracture surface. The scale in (a) is in millimeters. The white deposits in voids consist of ASR gel.

(a)

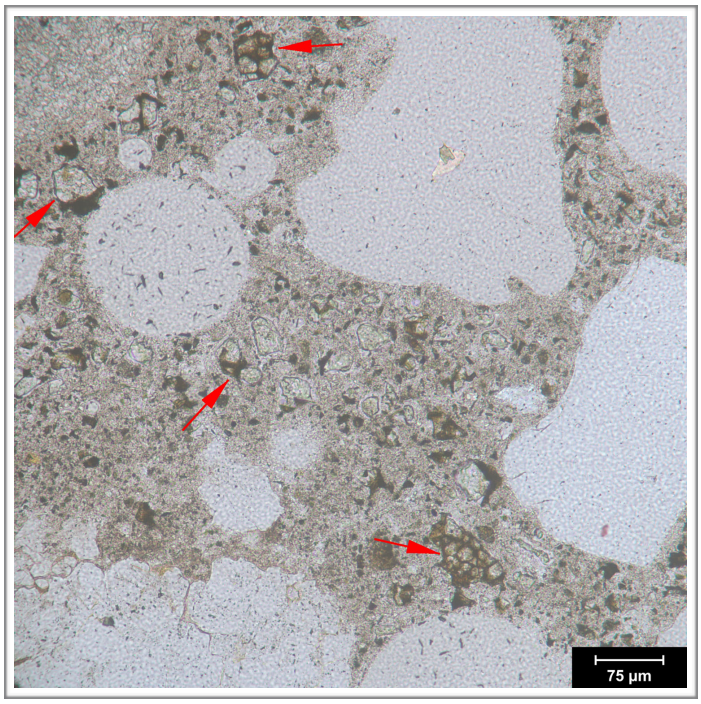

(b)

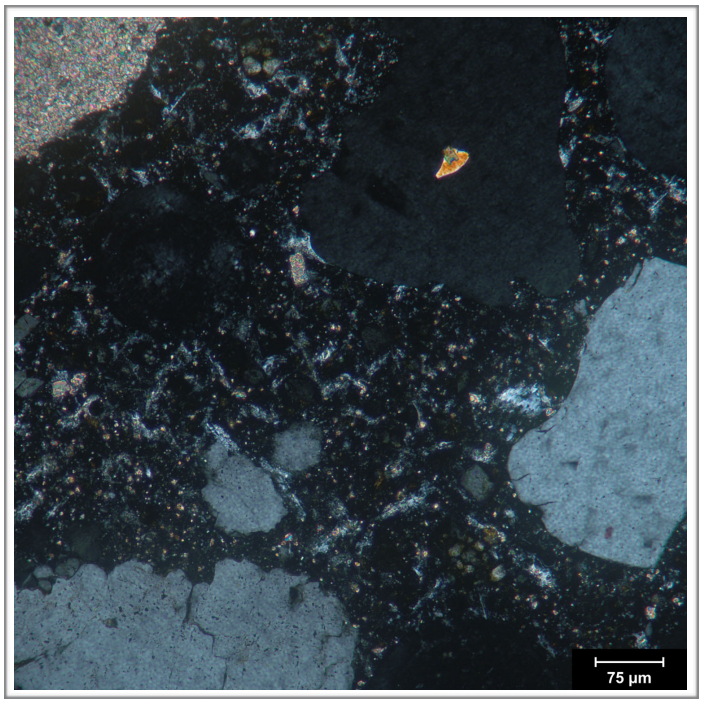

Figure G11. Transmitted light photomicrographs of thin section showing detail of paste in (a) plane-polarized and (b) cross-polarized light. The red arrows indicate RRCG in (a).

(a)

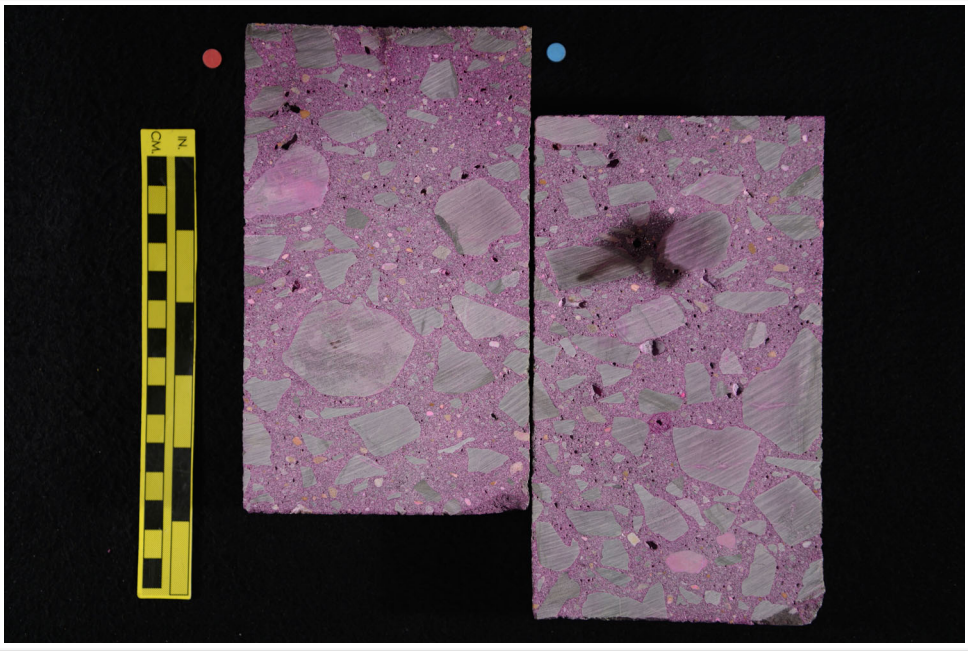

(b)

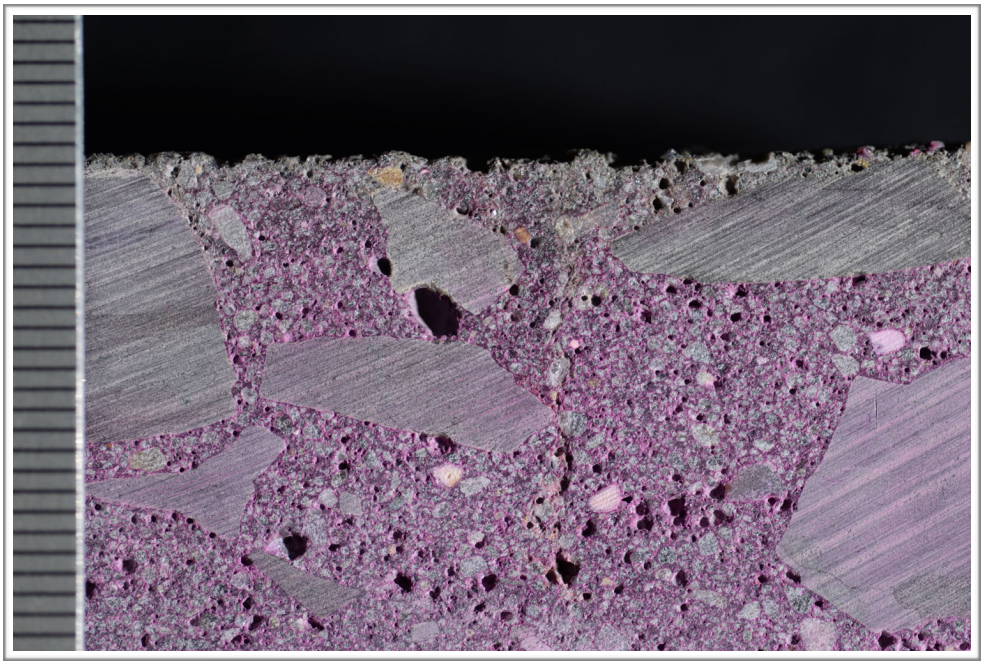

Figure G12. Photographs showing (a) overview of phenolphthalein stained surface and (b) detail of surface near the top of the core. Scale in millimeters in (b).

(a)

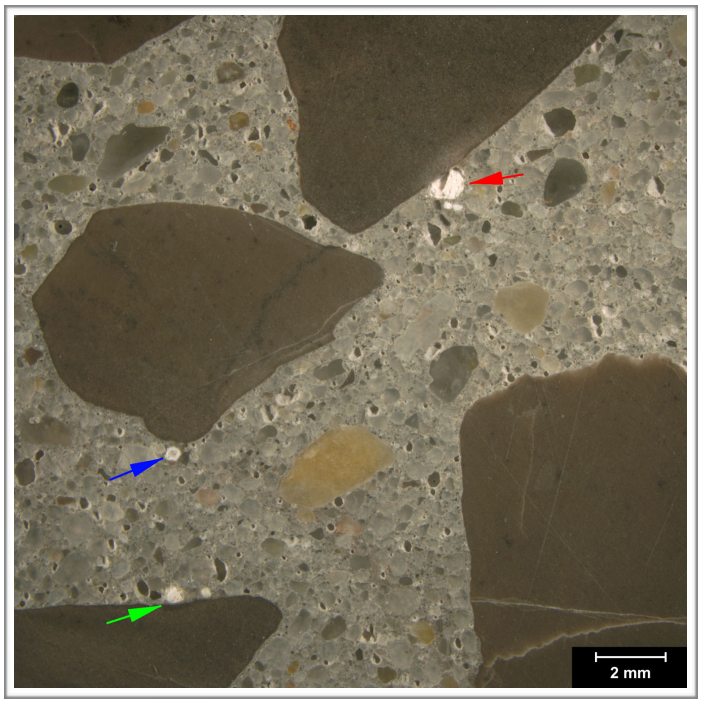

(b)

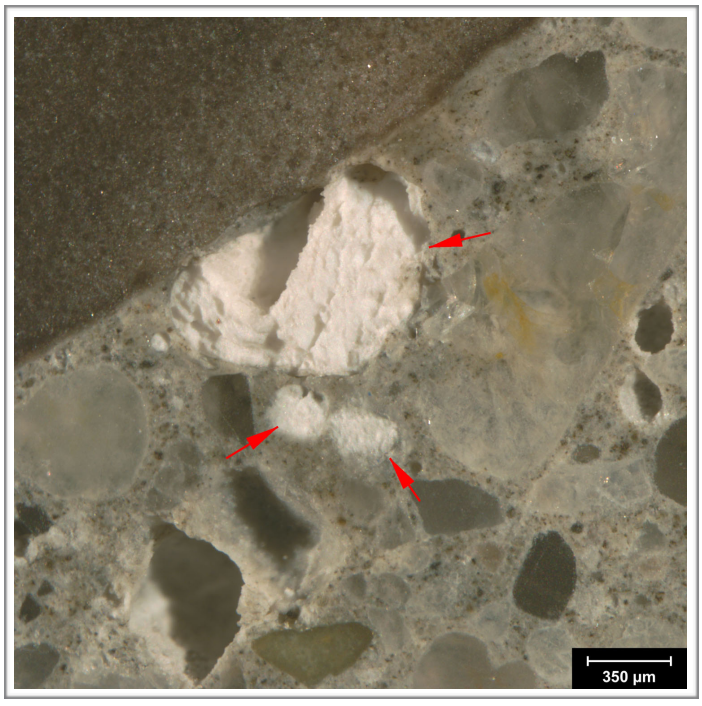

Figure G13. Reflected light photomicrographs of the polished surface showing several voids filled with ASR gel about 80 mm (3 ⅛ in.) below the top surface. The red, blue and green arrows indicate voids that are shown in more detail in (b), (c) and (d), respectively.

(c)

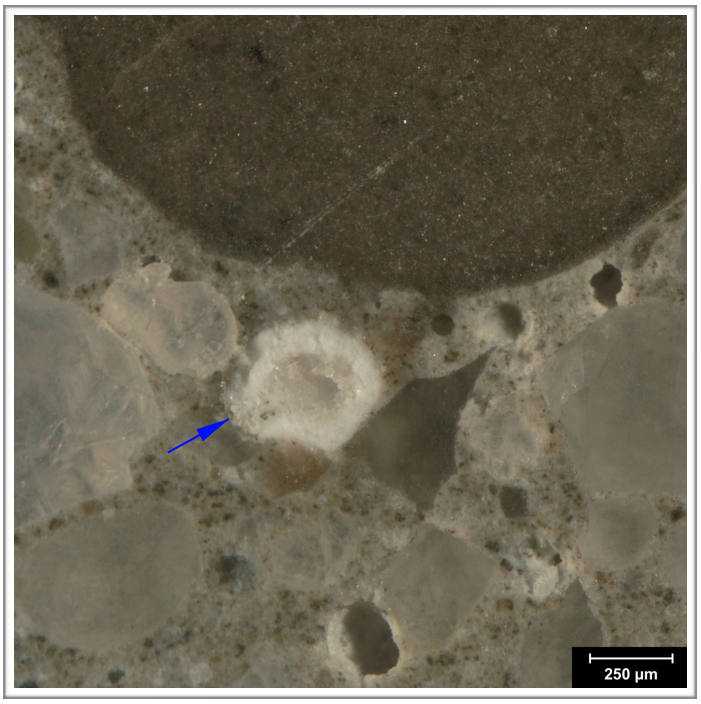

(d)

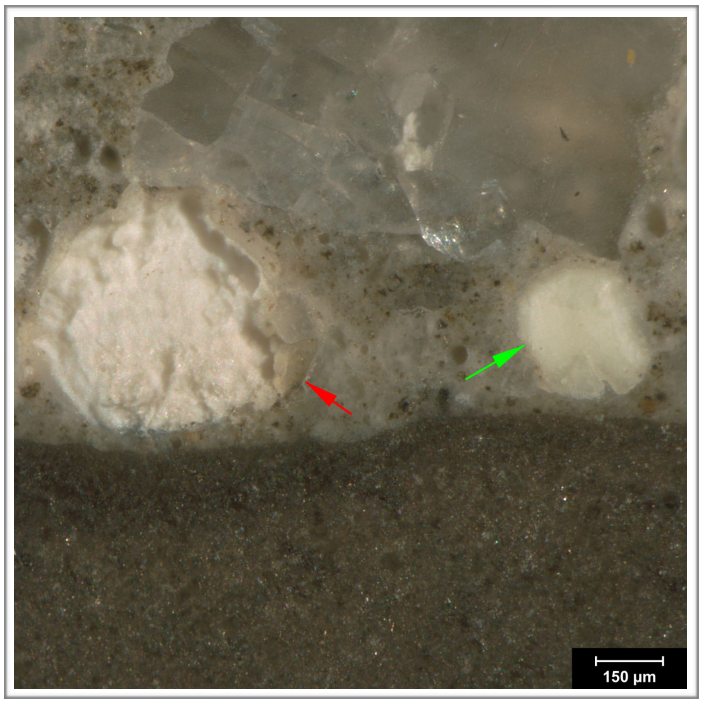

Figure G13 (cont'd). Reflected light photomicrographs of the polished surface showing detail of voids filled with gel indicated by the blue and green arrows in (c) and (d), respectively. The red arrow in (d) indicates a void filled with ettringite.

(a)

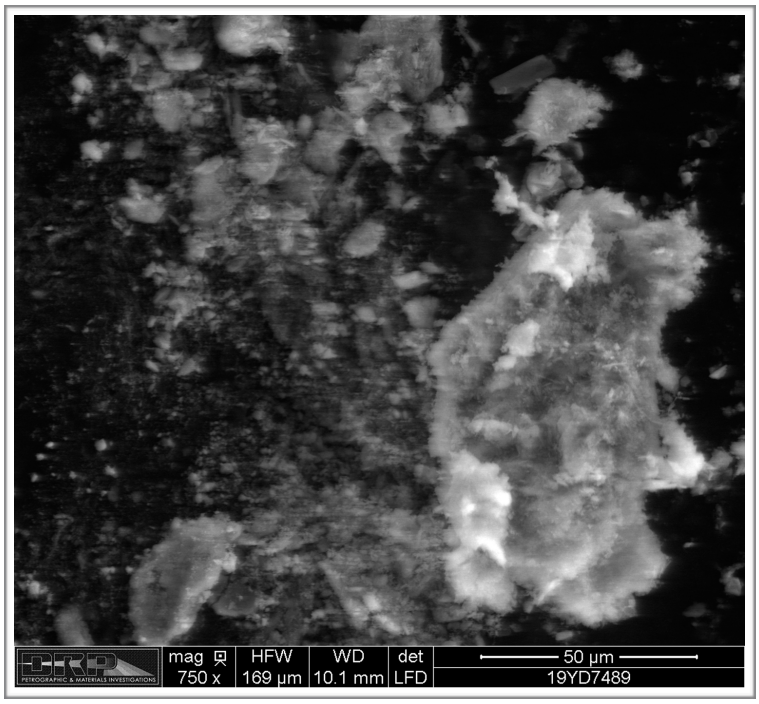

(b)

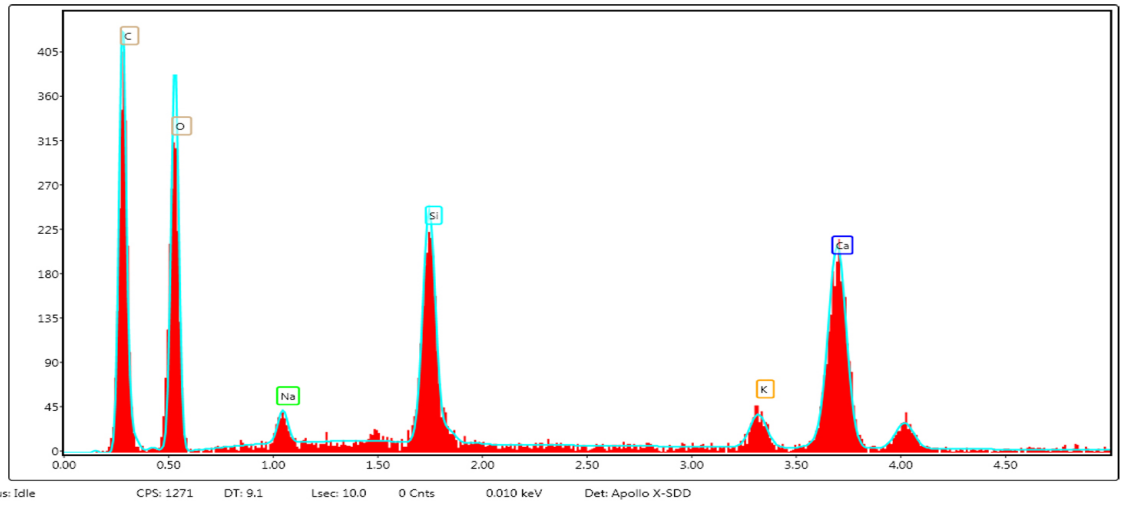

Figure G14. (a) Backscatter electron micrograph of gel deposits scraped from void shown in Figure G13(b) and placed on carbon tape. (b) EDS spectrum of deposit indicating composition typical of ASR gel.

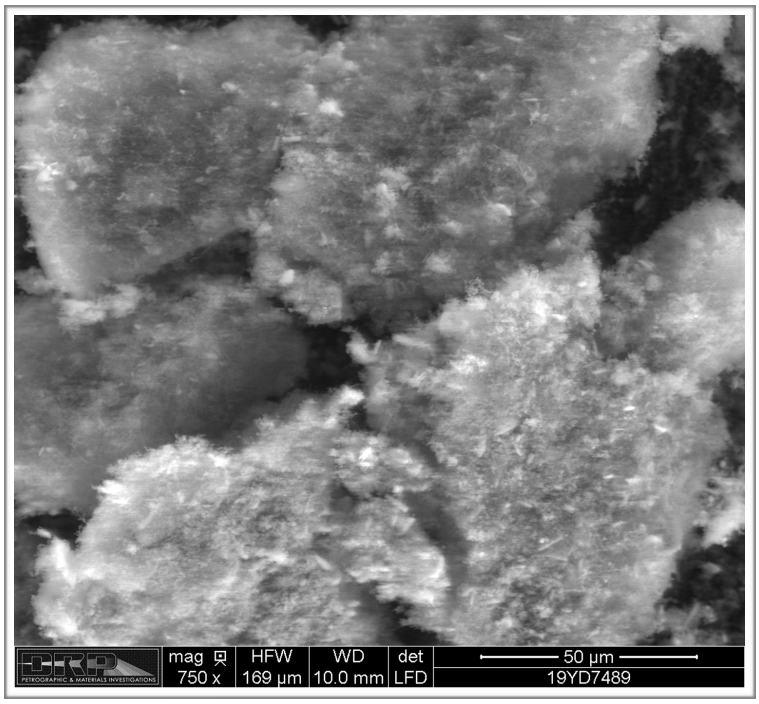

(a)

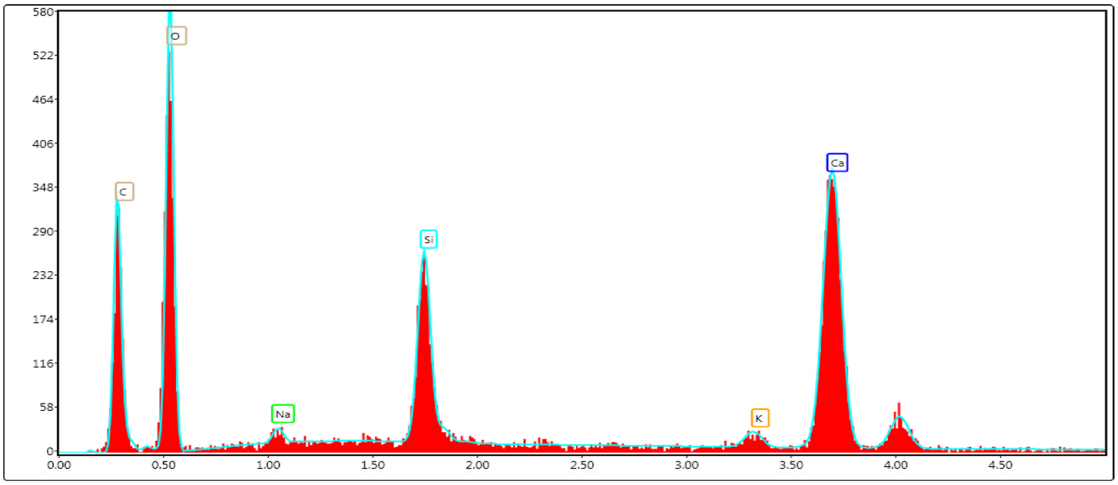

(b)

Figure G15. (a) Backscatter electron micrograph of gel deposits scraped from void on fresh fracture surface shown in G10(b) and placed on carbon tape. (b) EDS spectrum of deposit indicating composition typical of ASR gel.

1. RECEIVED CONDITION

ORIENTATION	Vertical core taken through highway pavement slab measures 100 mm (~ 4 in.) in diameter and 325 mm (~ 13 in.) long (**Figure H1, H2**).
SURFACES	The top surface shows wear that exposes smooth coarse aggregate particles but the tines are largely intact (**Figure H3**). The bottom surface is a saw cut such that the core represents a partial thickness of the pavement slab.
GENERAL CONDITION	The concrete is hard and compact and rings lightly when sounded with a hammer. The core was received intact in one piece.

2. EMBEDDED OBJECTS

GENERAL	None observed.

3. CRACKING

MACROSCOPIC	A few cracks were observed on the top surface that range up to 500 µm (20 mil) wide and 70 mm (2 ¾ in,) long; these cracks form a triple point pattern (**Figure H4**). These cracks do not penetrate the concrete significantly. No other cracks were observed.
MICROSCOPIC	No significant microcracks observed. A couple of microcracks cut from the top surface to a depth of 1-2 mm (40-80 mil); these microcracks represent extensions of the triple point cracks described above and cut around aggregate particles and are free of secondary deposits (**Figure H5**).

4. VOIDS

VOID SYSTEM	Concrete is air-entrained (**Figure H6**) and contains 4-6% air by visual estimation (not determined following ASTM C457). The core is well consolidated with no significant entrapped voids or water voids observed.
VOID FILLINGS	Voids commonly contain minor deposits of ettringite.

5. COARSE AGGREGATE

PHYSICAL PROPERTIES	Crushed quarry rock with 38 mm (1 ½ in.) nominal top size (**Figure H7**). The rocks are hard and competent. The particles are sub-equant to tabular in shape with sub-angular to sub-round edges. The grading is relatively even. The gradation is uneven with gap grading and an abundance of sand that is very fine.
ROCK TYPES*	The aggregate is carbonate in composition and consists of brown dolomitic limestone as well as tan to light brown limestones that show laminations and evidence of bioturbation as well as some oolitic limestones.
OTHER FEATURES	No deleterious coatings or incrustations observed. A few minor low w/c mortar coatings observed. Occasional particles show internal cracking and microcracking; these do not propagate into the paste.

**Modal abundance based on visual estimation.*

6. FINE AGGREGATE

PHYSICAL PROPERTIES	Natural sand consists of rocks that are hard and competent (**Figure H8**). The particles are sub-equant to tabular in shape with sub-round to sub-angular edges. The grading and distribution are relatively even.
ROCK TYPES	The sand is siliceous in composition and consists primarily of quartz and quartzite with minor amounts of granitic rocks and chert.
OTHER FEATURES	No deleterious coatings or incrustations observed and no low w/c mortar coatings observed. Particles of chert typically show reaction rims but no microcracking or deposits of gel are associated with them.

7. PASTE OBSERVATIONS

POLISHED SURFACE	Paste is gray (Munsell 2.5Y/6/1) to dark gray (2.5Y/4/1), has a smooth texture and sub-vitreous luster (**Figure H9**). The paste is hard (Mohs 3.5-4).
FRESH FRACTURE	Fracture surface is light gray, has a hackly texture and a sub-vitreous luster. The fracture cuts primarily through aggregate particles (**Figure H10**). Minor deposits of gel and ettringite observed.
THIN SECTION*	The paste contains hydrated portland cement; no fly ash, slag cement or other SCM were observed. The hydration is normal with 4-8% RRCG that consist mostly of interstitial ferrite and aluminate with occasional grains of belite (**Figure H11**). CH makes up 10-17% of the paste, is fine to medium-grained and evenly distributed.

** Abbreviations as follows: RRCG = relict and residual cement grains; SCM = supplemental cementitious materials; CH = calcium hydroxide; ITZ = interfacial transition zone. Modal abundances are based on visual estimations.*

8. SECONDARY DEPOSITS

PHENOLPHTHALEIN	Entire surface stains purple (**Figure H12**).
DEPOSITS	Minor carbonation observed at the top of the core and in irregularly distributed zones in the paste in thin section. Minor deposits of ettringite observed commonly in voids. Deposits of gel observed in minor amounts in rare voids (**Figure H13-Figure H15**).

FIGURES

(a)

(b)

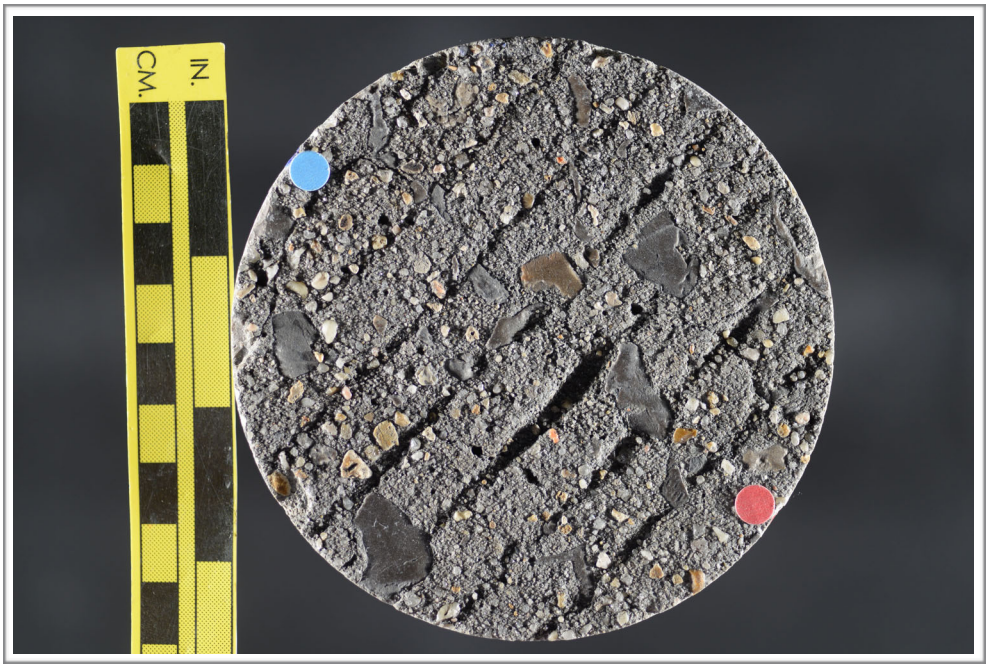

Figure H1. Photographs showing (a) oblique view of the top and side of the core with identification labels and (b) the top of the core. The red and blue dots in (a) show the orientation of the saw cuts used to prepare the sample.

(c) 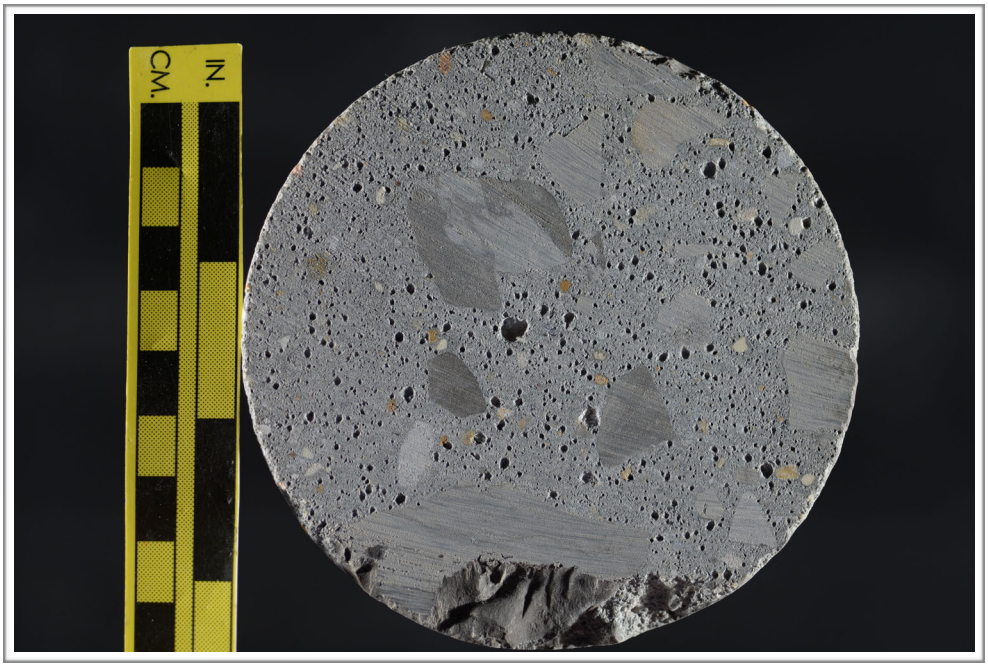

Figure H1 (cont'd). (c) Photograph showing the bottom of the core.

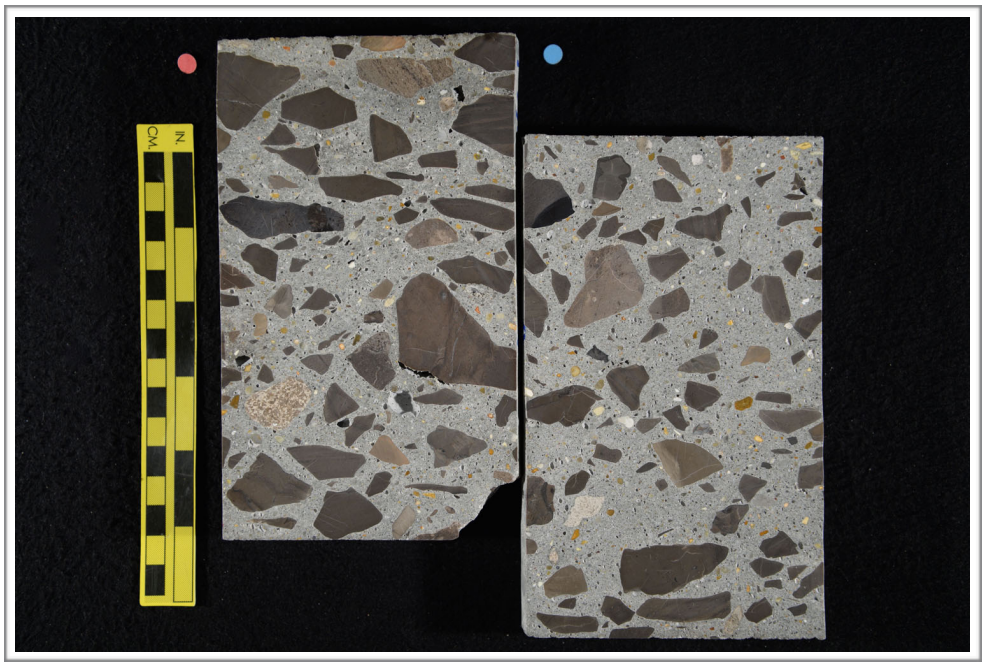

Figure H2. Photograph showing the polished surface of the core.

Figure H3. Photograph showing detail of the top surface of the core; scale in millimeters.

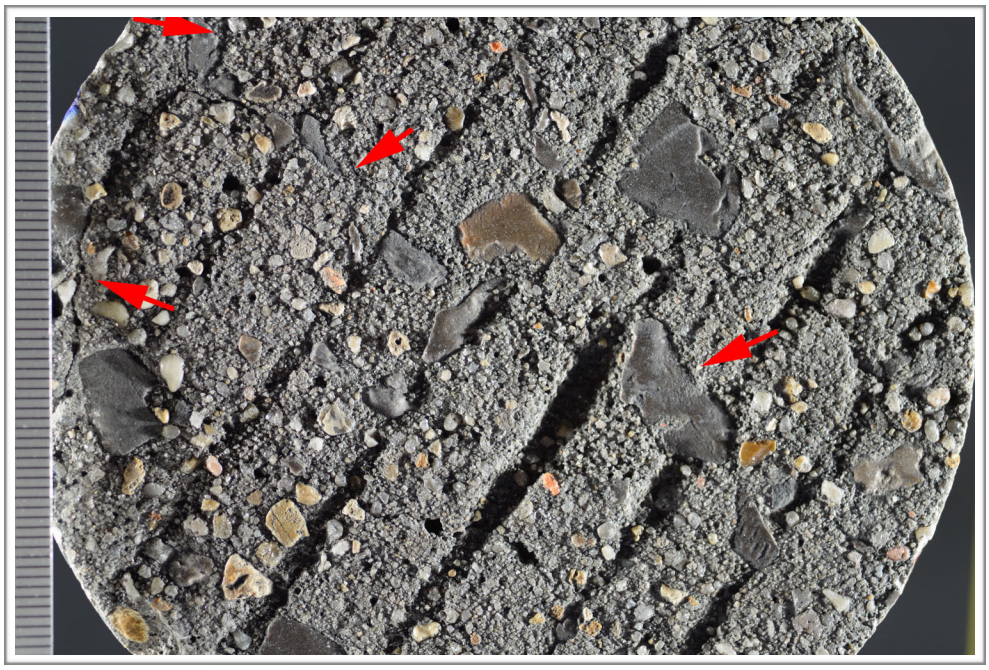

Figure H4. Photographs showing crack (red arrows) on the top surface; scale in millimeters.

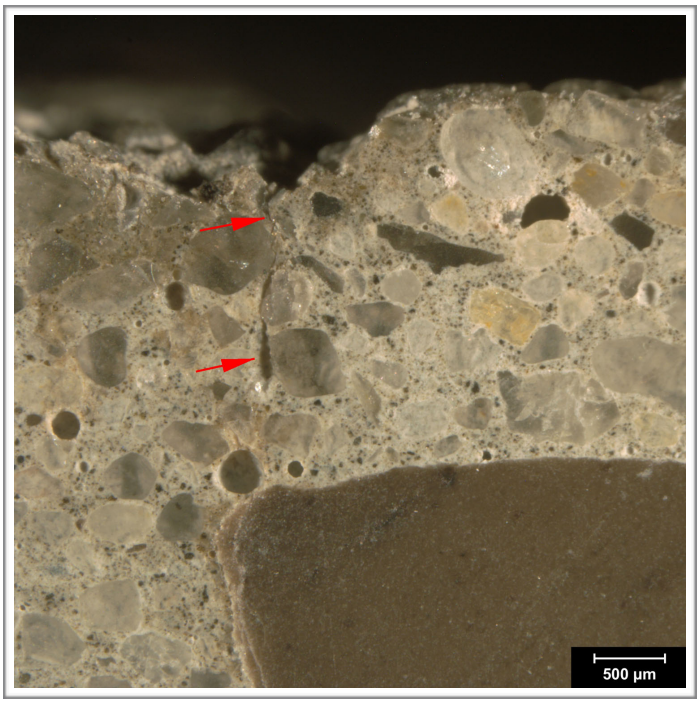

Figure H5. Reflected light photomicrograph of the polished surface showing microcrack (red arrows) at the top of the core.

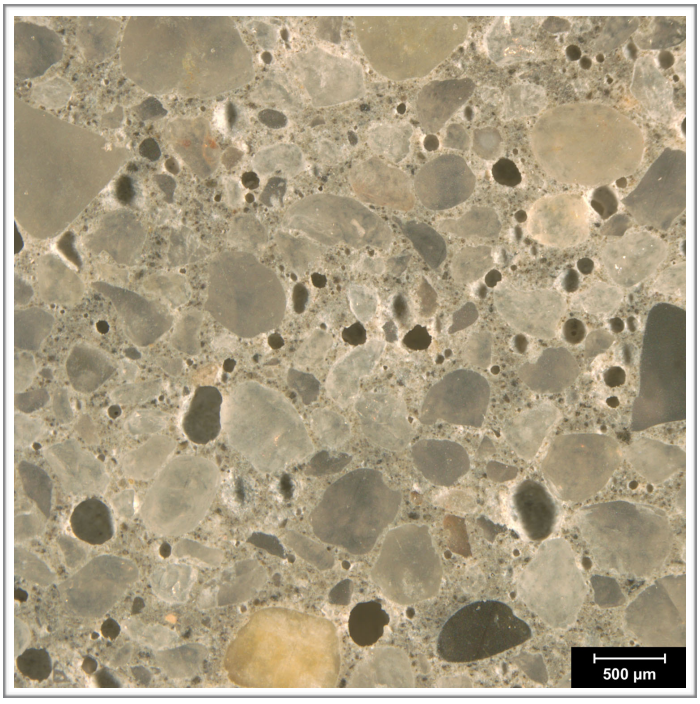

Figure H6. Reflected light photomicrograph of the polished surface showing entrained air voids (dark circles).

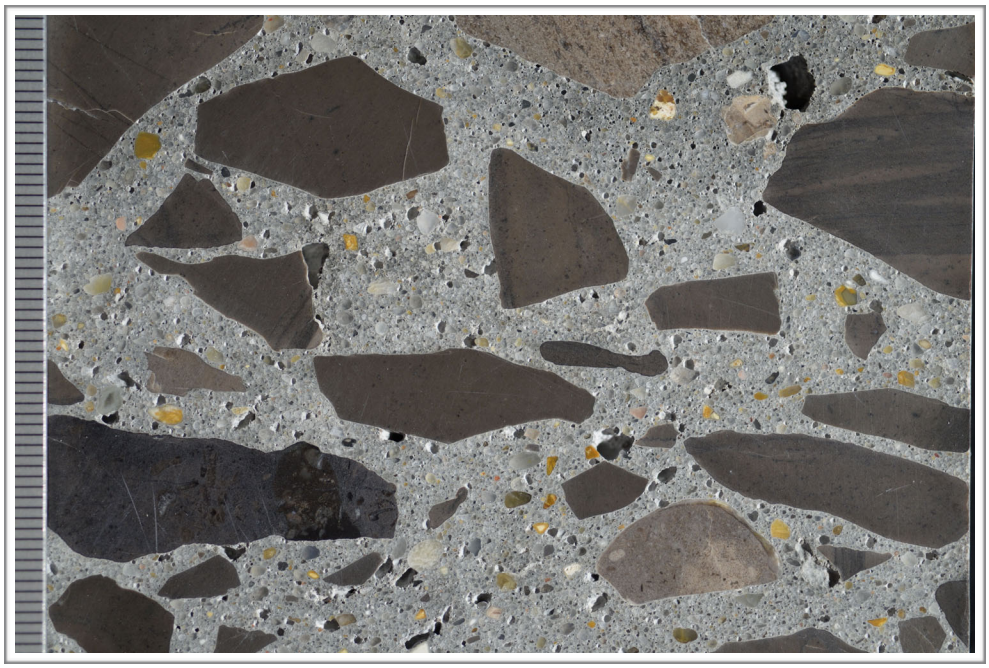

Figure H7. Photograph of the polished surface showing coarse aggregate; scale in millimeters.

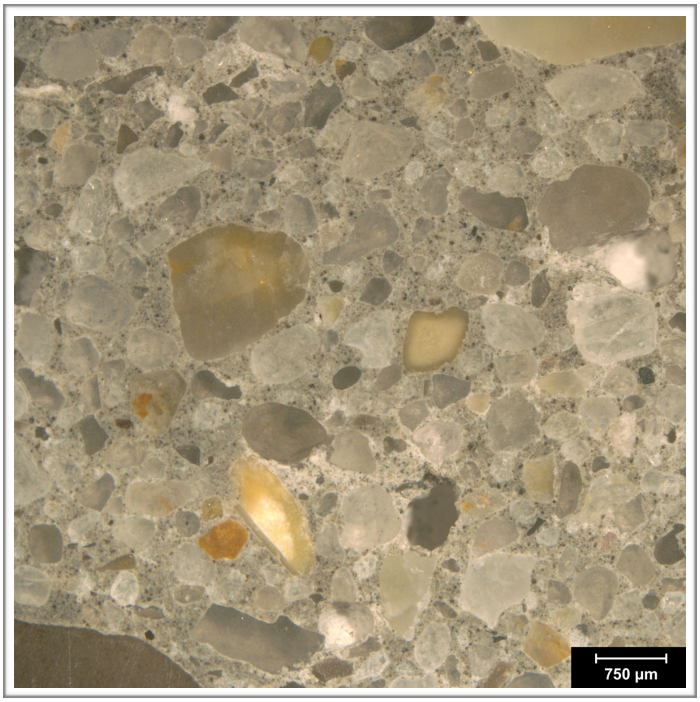

Figure H8. Reflected light photomicrograph of polished surface showing the fine aggregate.

(a)

(b)

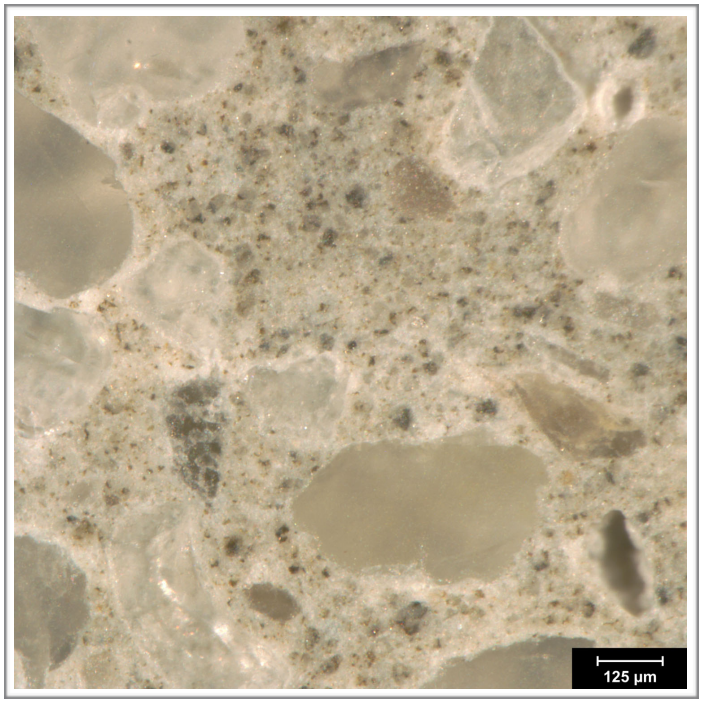

Figure H9. (a) Photograph of polished surface showing overview of paste at the top of the core. The scale is in millimeters; the red arrows indicate the hairline crack that cut across the top surface. (b) Reflected light photomicrograph showing detail of paste color, texture and luster in the middle of the core.

(a)

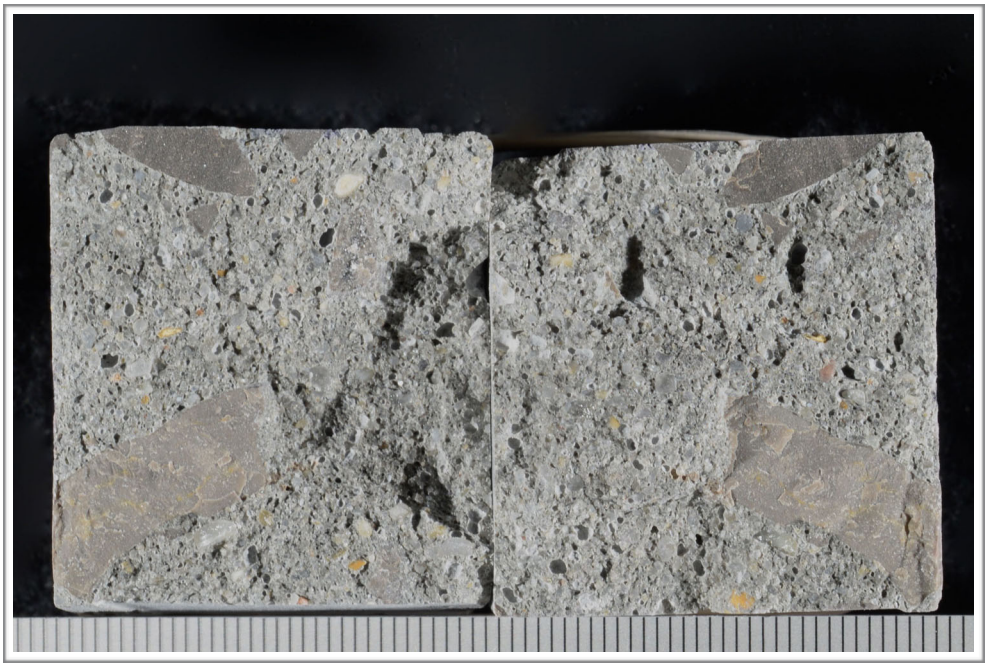

(b)

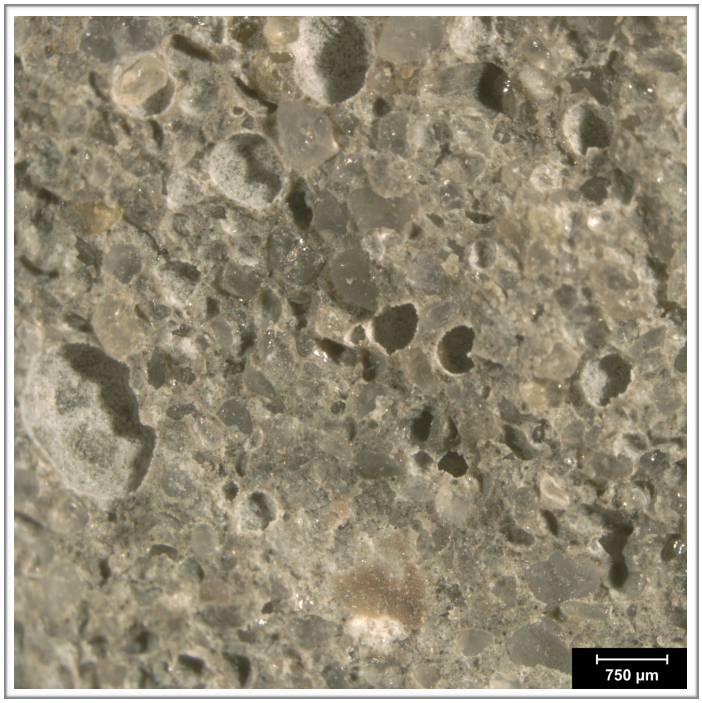

Figure H10. (a) Photograph and (b) reflected light photomicrograph of the fresh fracture surface. The scale in (a) is in millimeters.

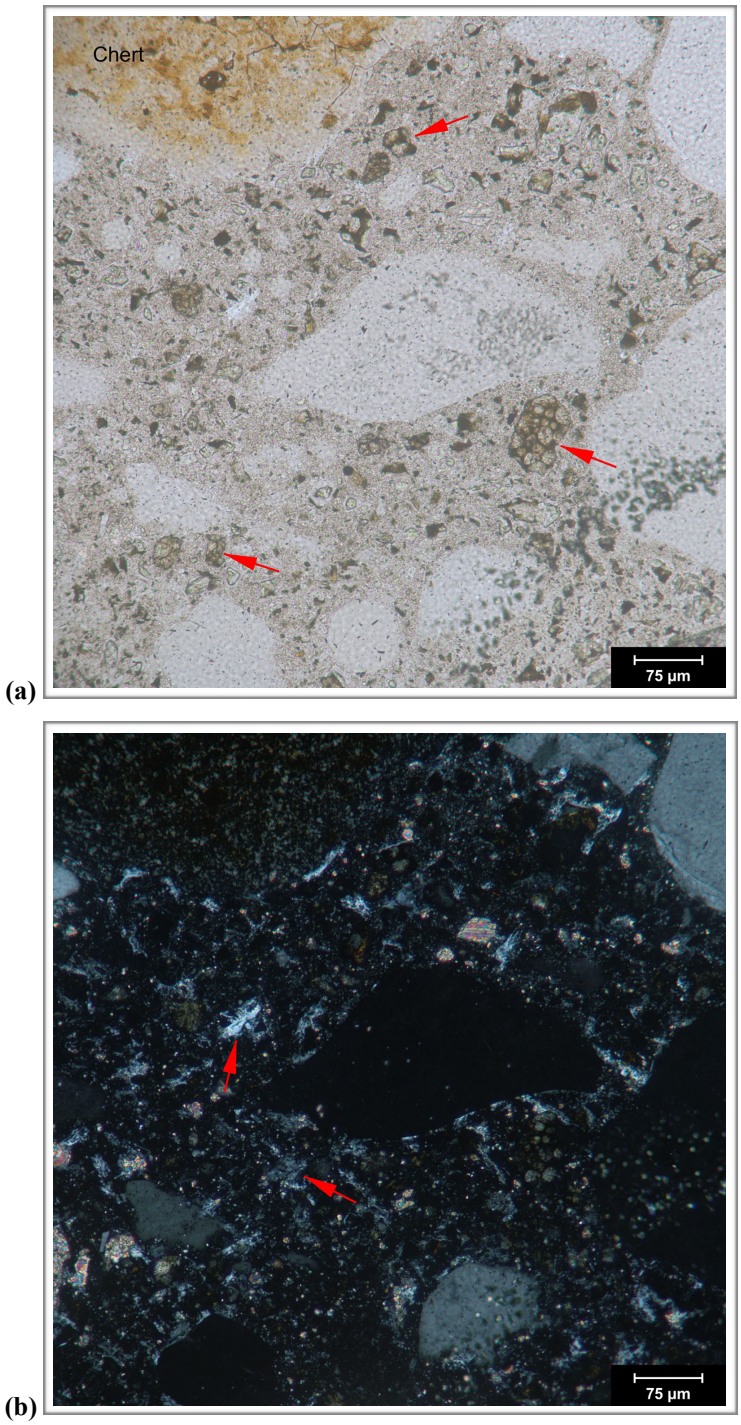

Figure H11. Transmitted light photomicrographs of thin section showing detail of paste in (a) plane-polarized and (b) cross-polarized light. The red arrows indicate RRCG in (a) and CH in (b).

(a)

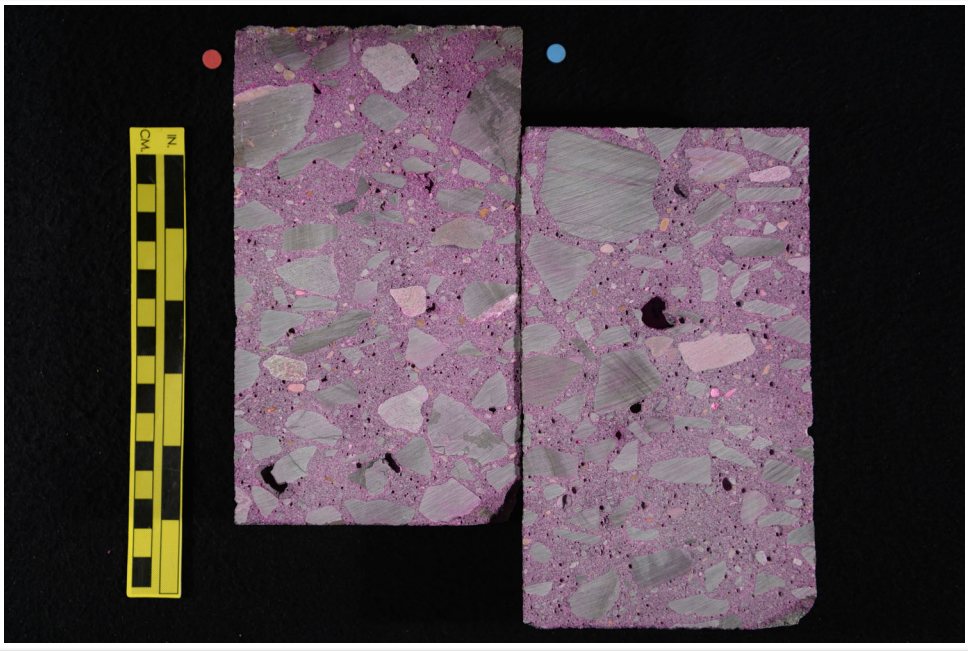

(b)

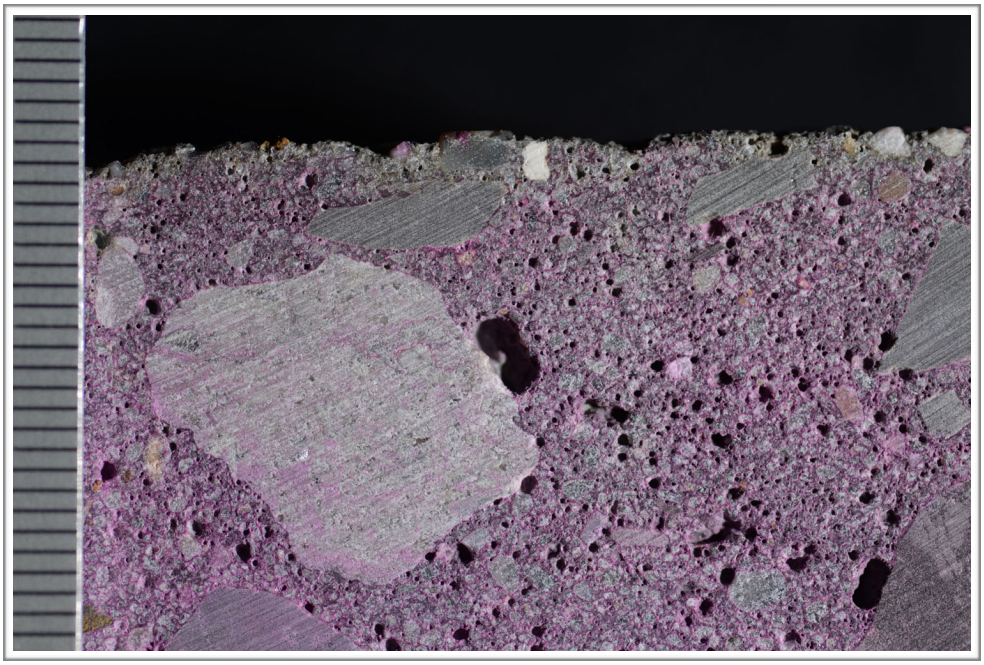

Figure H12. Photographs showing (a) overview of phenolphthalein stained surface and (b) detail of surface near the top of the core. Scale in millimeters in (b).

(a)

(b)

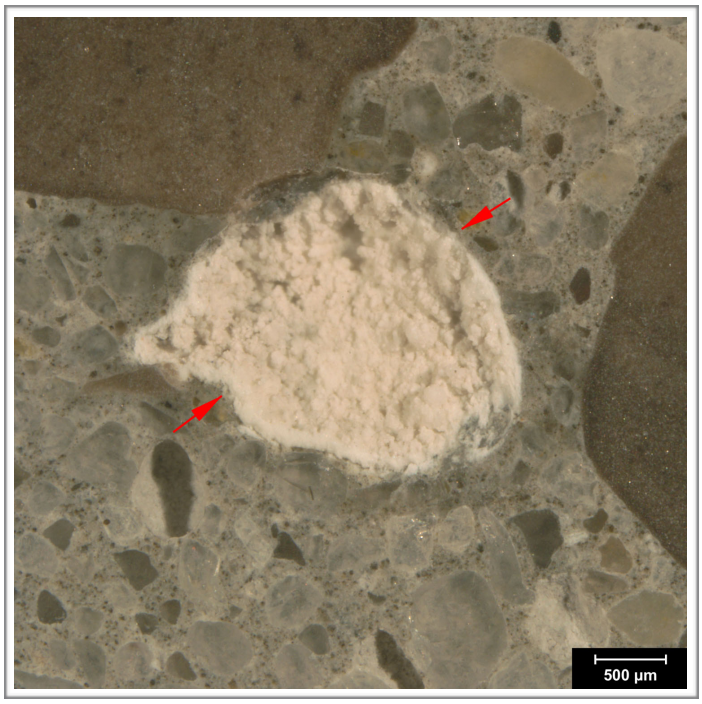

Figure H13. Reflected light photomicrographs of the polished surface showing voids filled with gel (red arrows) about (a) 220 mm (8 ¾ in.) and (b) 225 mm (9 in.) below the top surface.

(a)

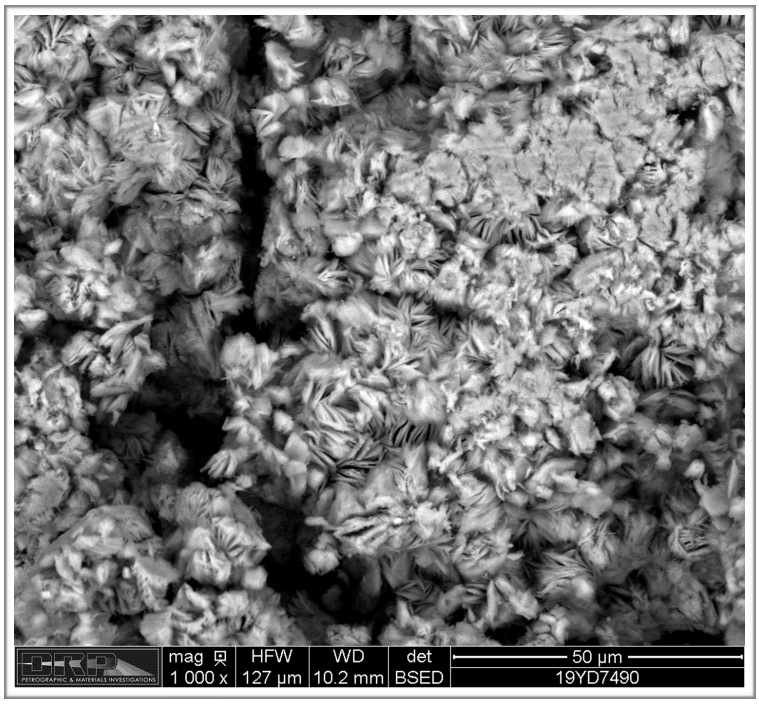

(b)

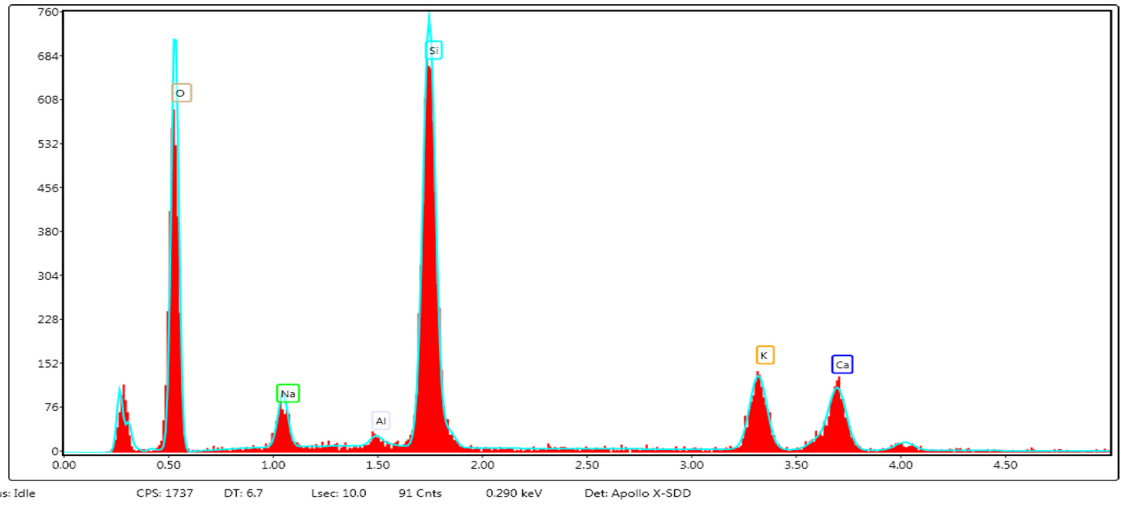

Figure H14. (a) Backscatter electron micrograph of gel deposits scraped from void shown in H13(a) and placed on carbon tape. (b) EDS spectrum of deposit indicating composition typical of ASR gel.

(a)

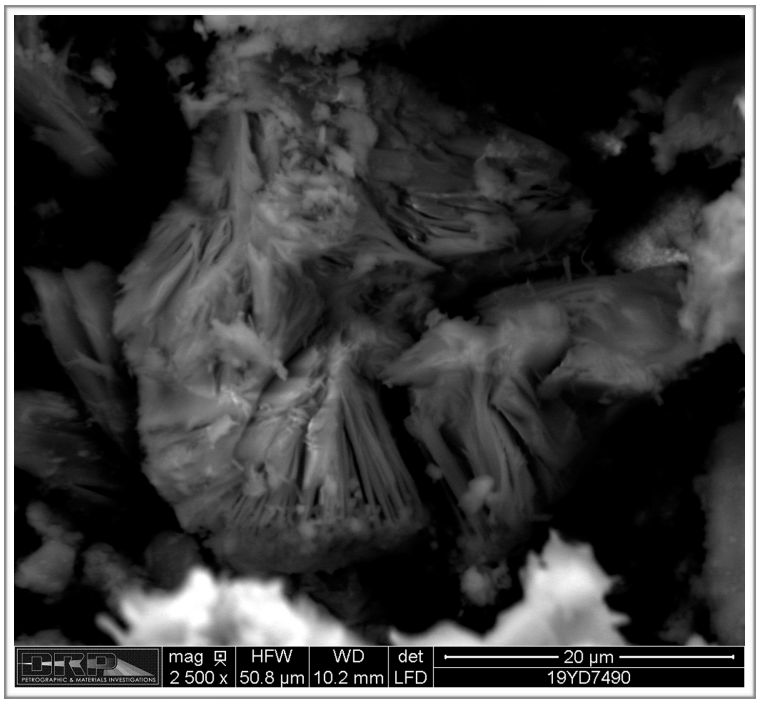

(b)

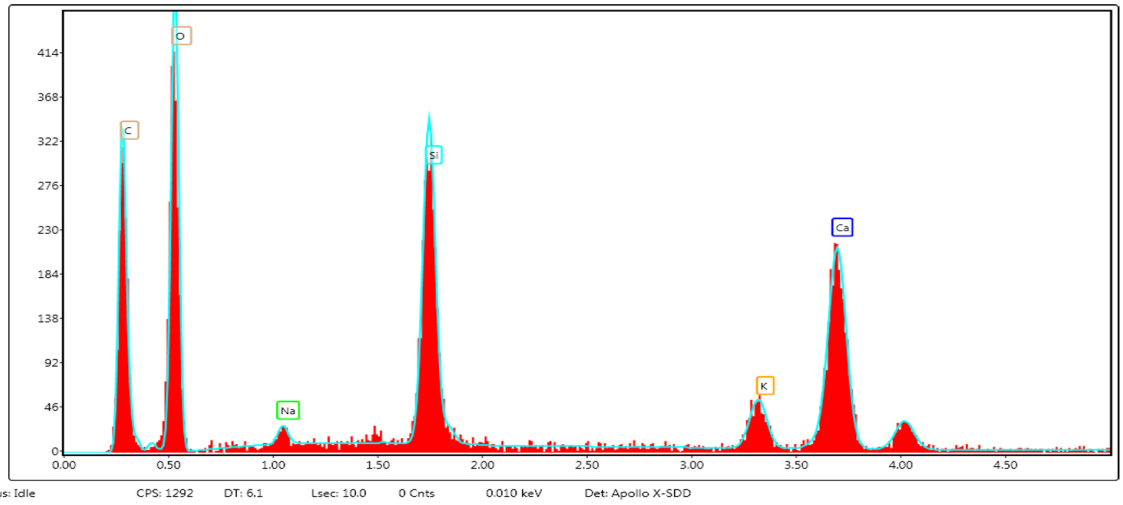

Figure H15. (a) Backscatter electron micrograph of gel deposits scraped from void shown in H13(b) and placed on carbon tape. (b) EDS spectrum of deposit indicating composition typical of ASR gel.

Table I1. Summary of Point Count Data

Aggregate Stops	218	290	229	257	249	261
Air Stops (S_a)	61	15	60	19	24	30
Calculated Parameters	**P#1 Top**	**P#1 Middle**	**P#2 Top**	**P#2 Middle**	**Wall #1 Top**	**Wall #1 Middle**
Traverse Length (T_t; in.)	26.9	28.9	27.0	28.5	26.3	27.2
Traverse Length (T_t; mm)	427	458	428	452	418	431
Aggregate Content	60.7%	75.3%	63.6%	67.6%	70.9%	72.1%
Paste Content (p)	22.3%	20.8%	19.7%	27.4%	22.2%	19.6%
Air Content (A)	17.0%	3.9%	16.7%	5.0%	6.8%	8.3%
Paste-Air Ratio (p/A)	1.3	5.3	1.2	5.5	3.3	2.4

Note: Analysis done via the Point-Count Method (Method B) in ASTM C457 using a stepping distance of 1.905 mm (0.075 in.) at 125x magnification.

Table I1. Summary of averaged point count data for top sections and middle sections of three cores.

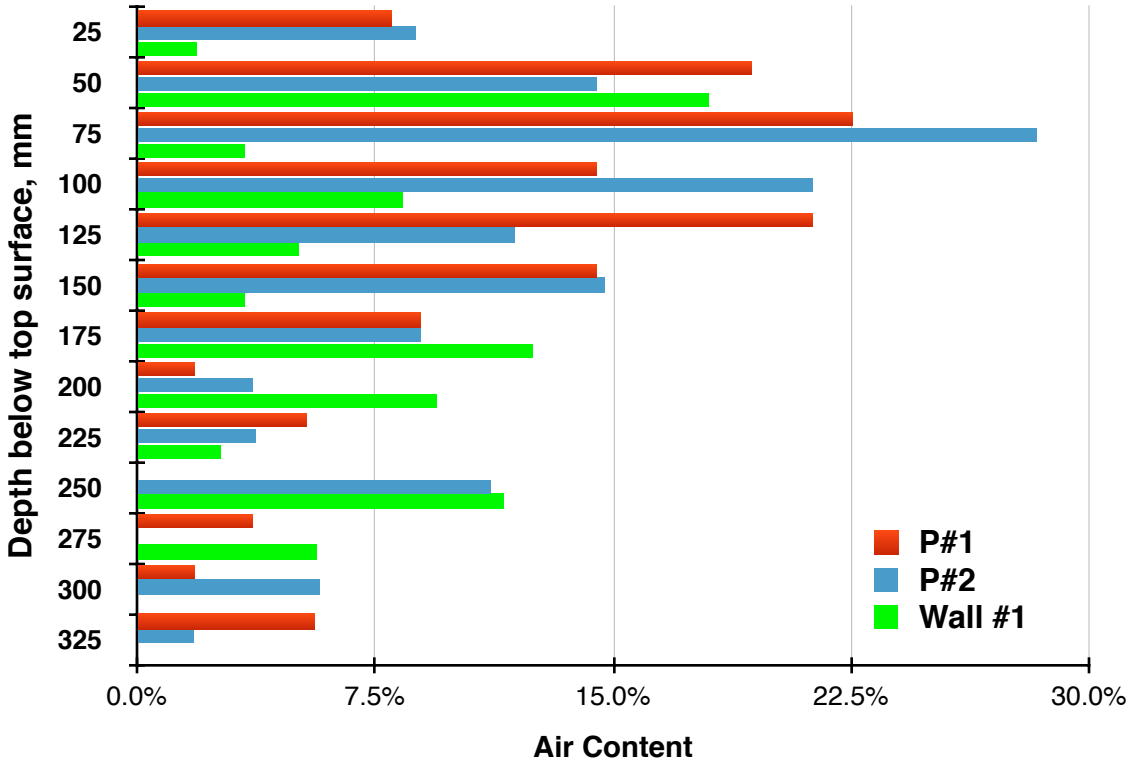

Chart 1. Summary of air content data for cores determined from point count analysis. Note that 0% air was measured at 275 mm in Core P#2.

FIGURES

(a)

(b)

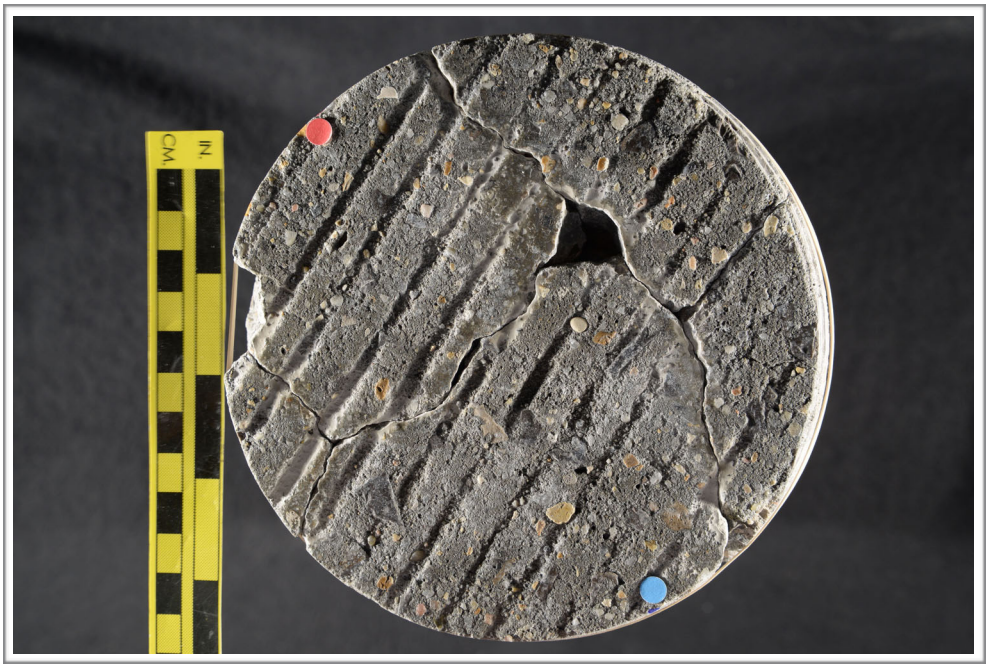

Figure I1. Photographs showing (a) oblique view of the top and side of Core P#1 with identification labels and (b) the top of Core P#1. The red and blue dots in (a) show the orientation of the saw cuts used to prepare the sample.

(c)

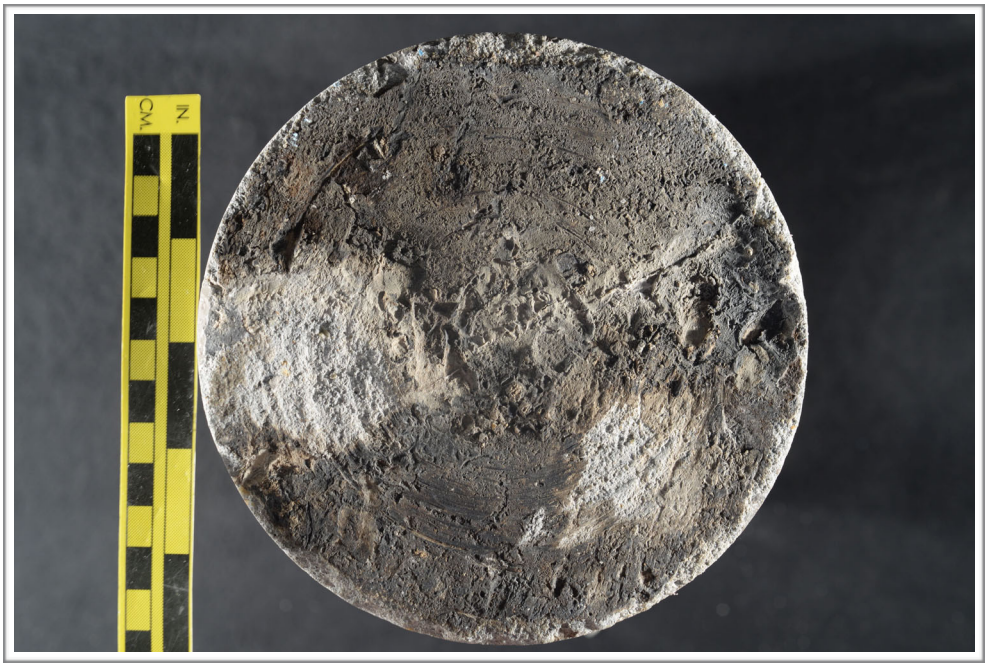

Figure I1 (cont'd). (c) Photograph showing the bottom of Core P#1.

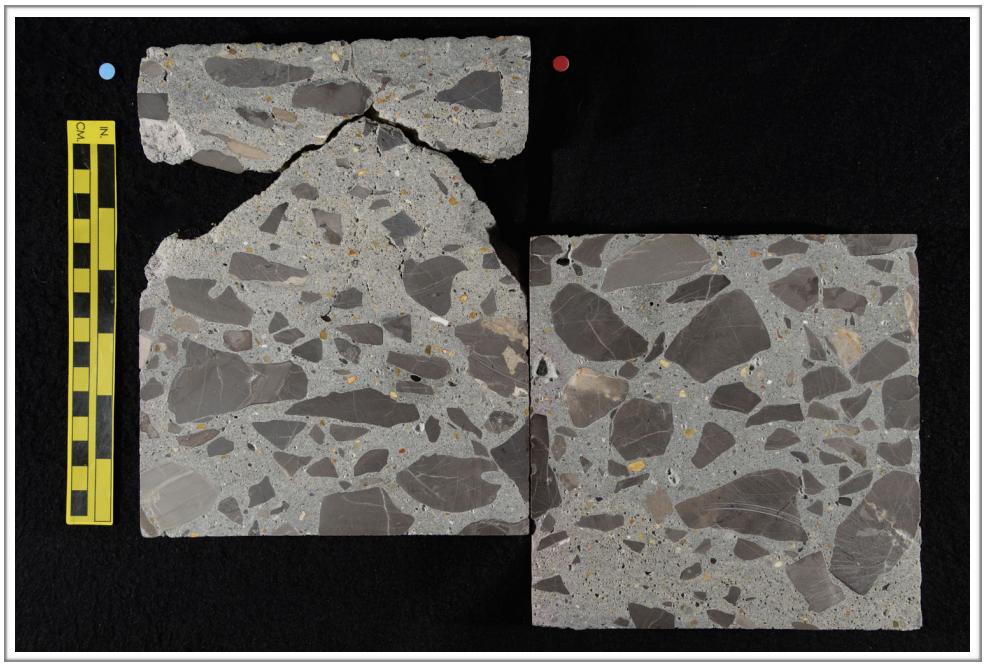

Figure I2. Photograph showing the polished surface of Core P#1.

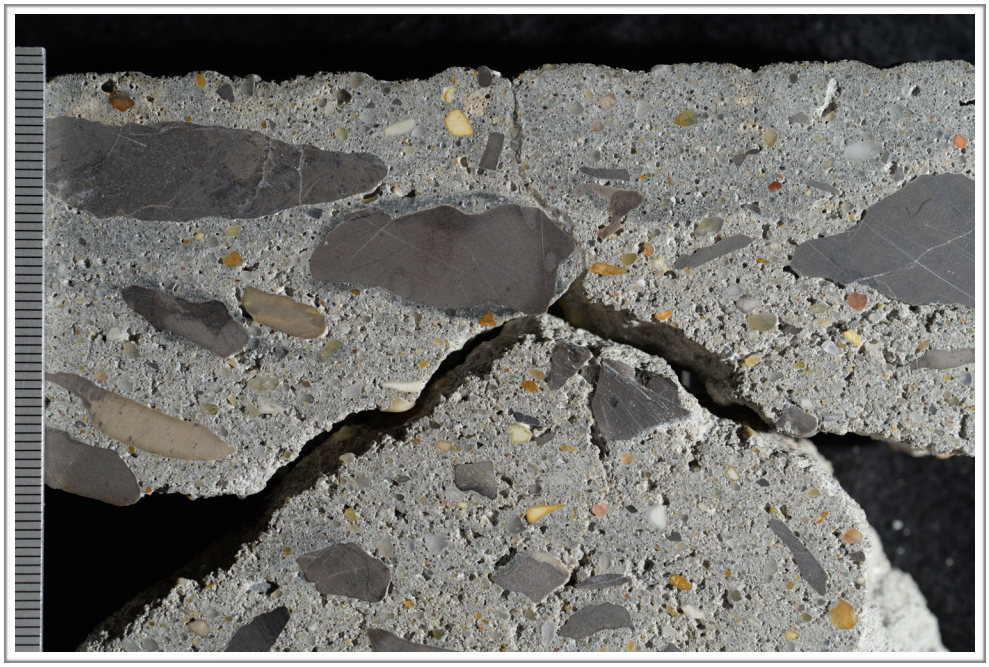

Figure I3. Photograph showing overview of polished surface at the top of Core P#1; scale in millimeters.

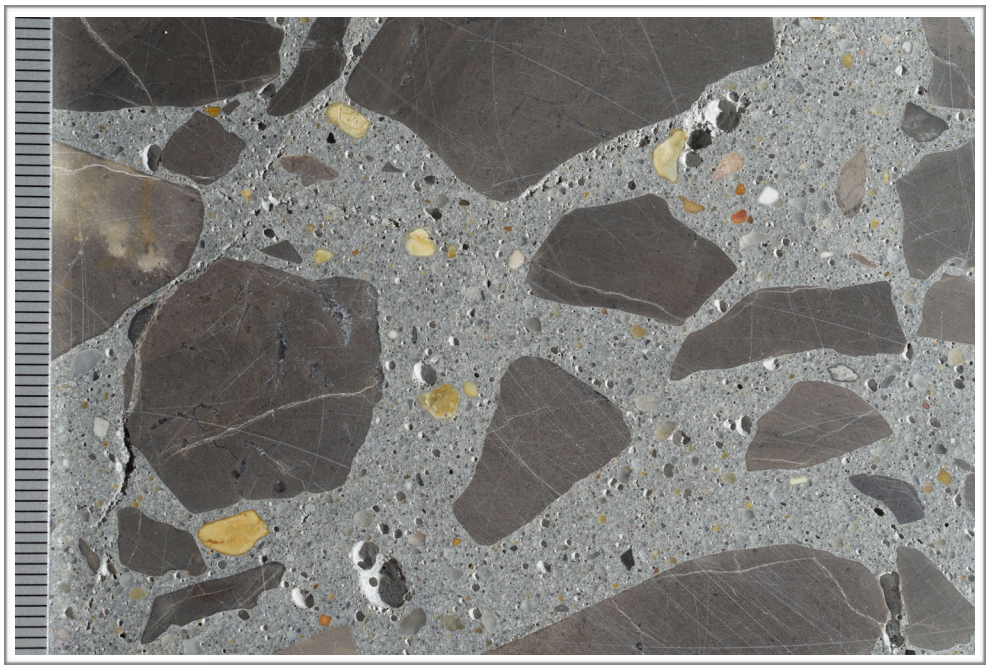

Figure I4. Photographs showing overview of polished surface in the middle of Core P#1; scale in millimeters.

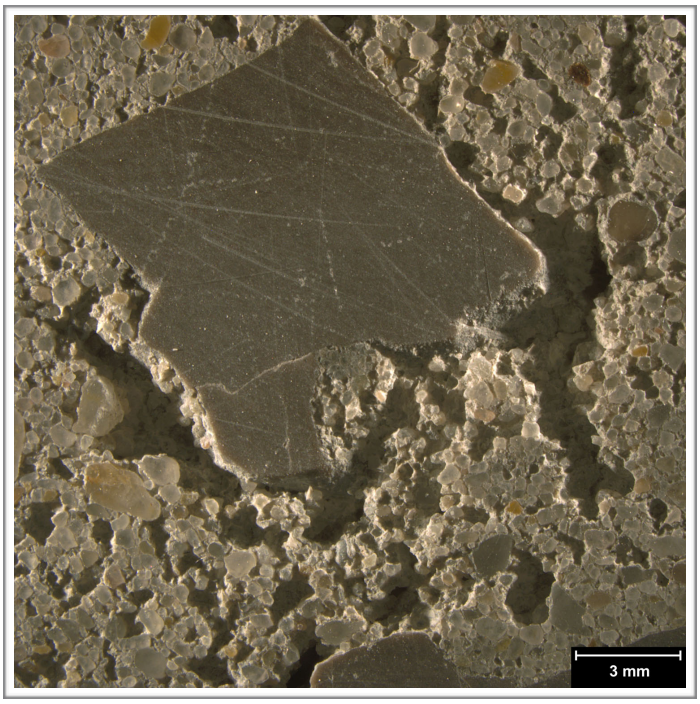

Figure I5. Reflected light photomicrograph of the polished surface showing voids and rough texture of the polished surface at the top of Core P#1.

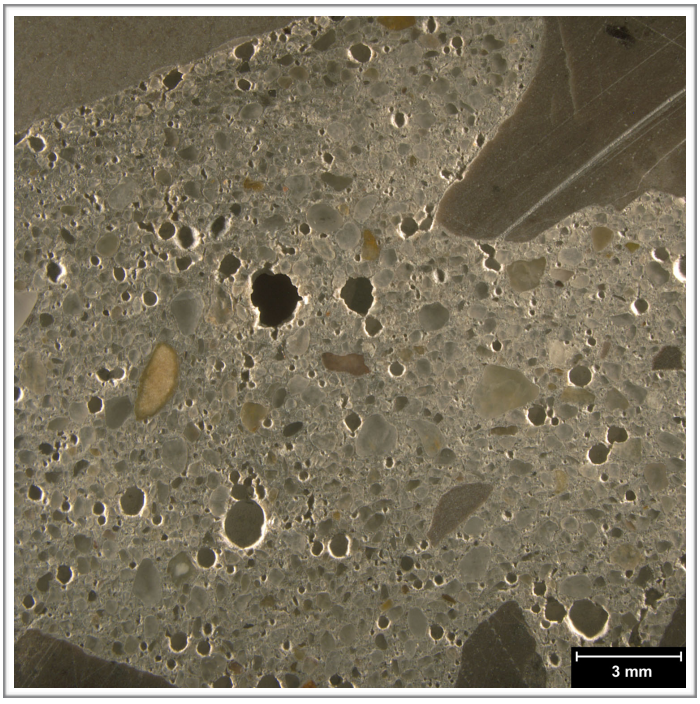

Figure I6. Reflected light photomicrograph of the polished surface showing voids and smooth texture of the polished surface in the middle of Core P#1.

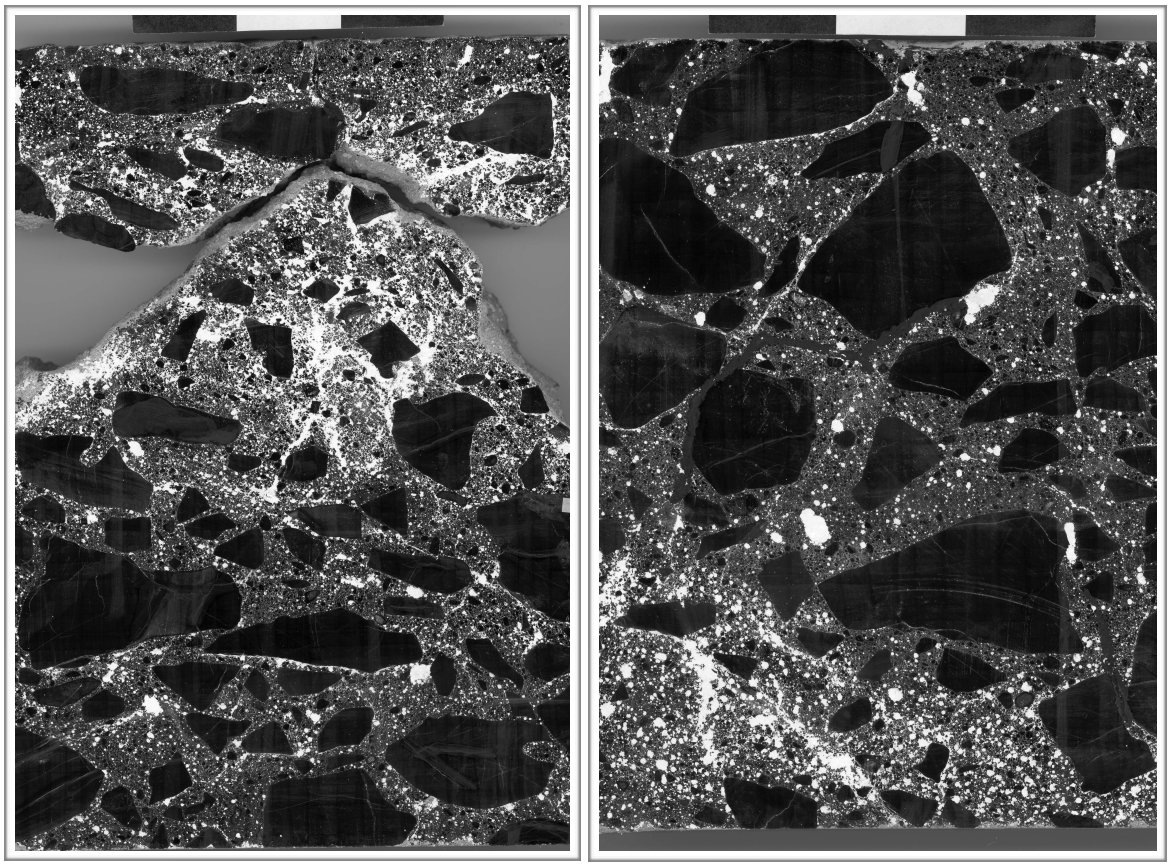

(a) (b)

Figure I7. Scanned images of polished surface of Core P#1 after slab was prepared for enhanced contrast image analysis. The images represent areas at the (a) top of the core and (b) at the bottom of the core. In these images white areas represent voids and black areas represent paste and aggregate. The black and white bars at the top of each image are 75 mm (3 in.) across. Note that near the bottom of (a) the abundance of voids (white areas) is markedly lower than at the top. Also note that at the bottom of (b) there is a zone of high void content.

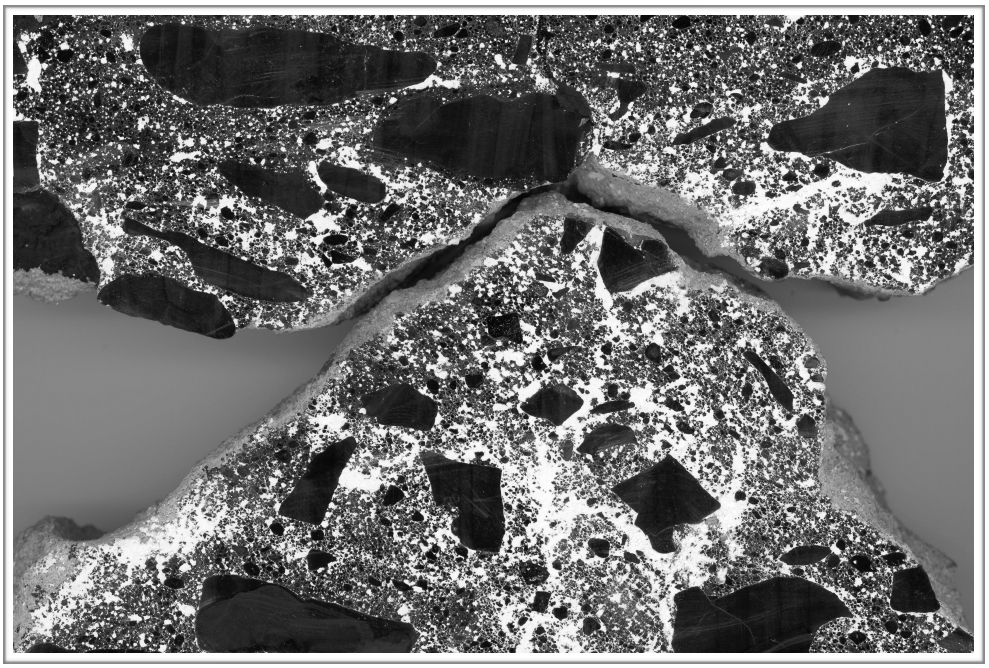

(a)

Figure I8. Cropped scanned image of enhanced contrast slab at the top of Core P#1 showing detail of area with high air content. The horizontal field width (HFW) is ~ 135 mm (5 ¼ in.).

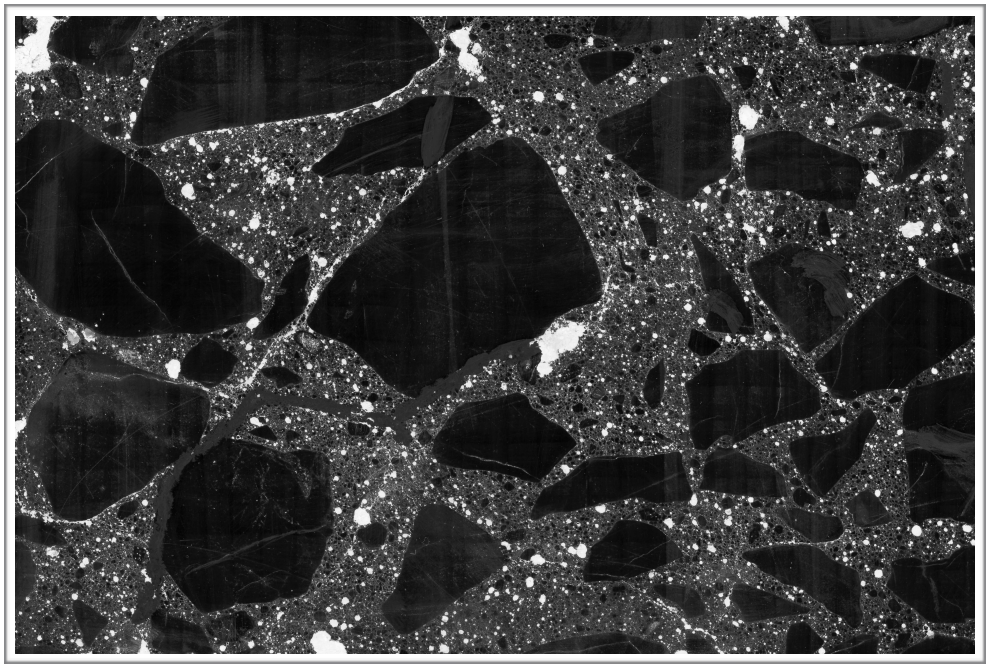

Figure I9. Cropped scanned image of enhanced contrast slab at the bottom of Core P#1 showing detail of area with low air content. The HFW is ~ 135 mm (5 ¼ in.).

(a)

(b)

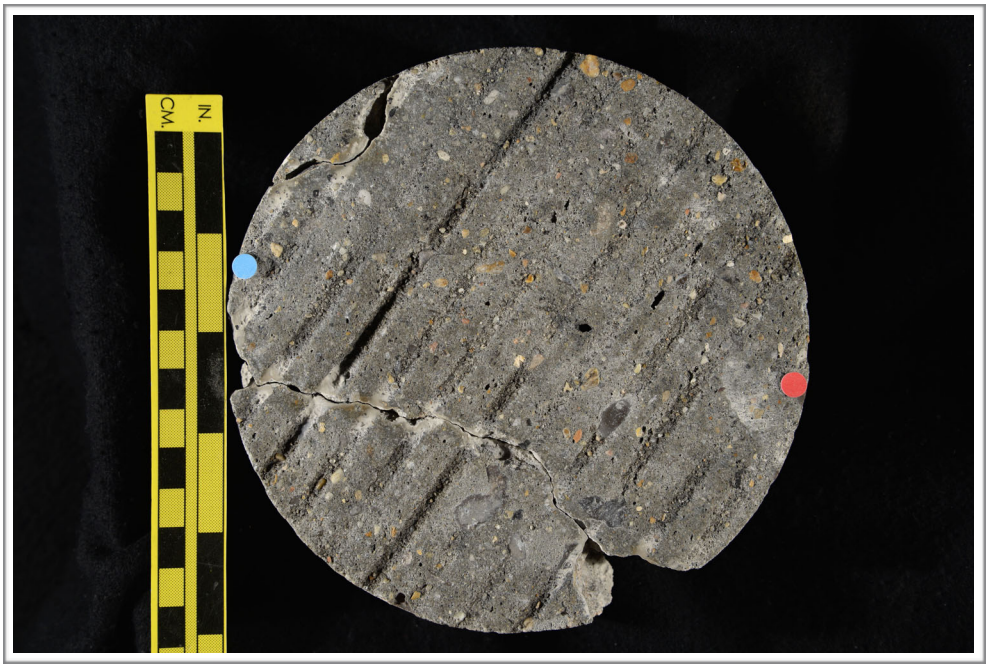

Figure I10. Photographs showing (a) oblique view of the top and side of Core P#2 with identification labels and (b) the top of Core P#2. The red and blue dots in (a) show the orientation of the saw cuts used to prepare the sample.

(c)

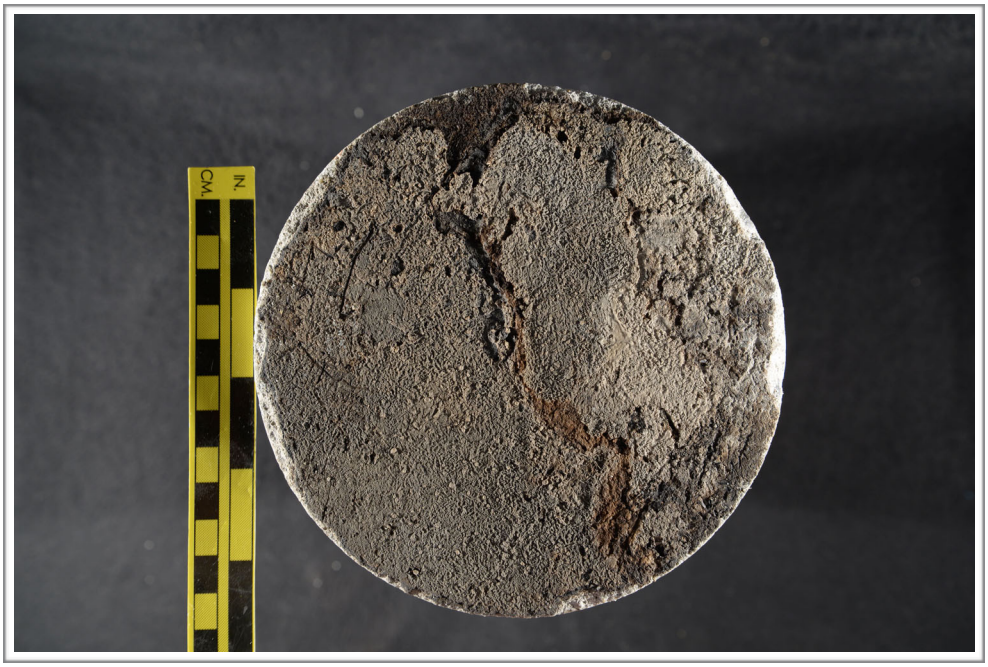

Figure I10 (cont'd). (c) Photograph showing the bottom of Core P#2.

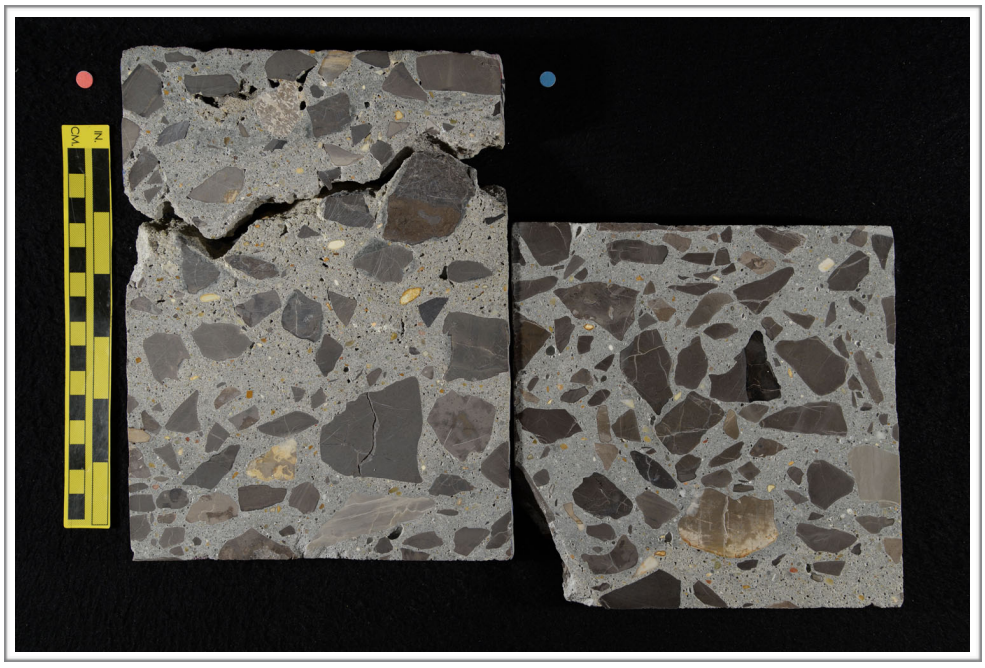

Figure I11. Photograph showing the polished surface of Core P#2.

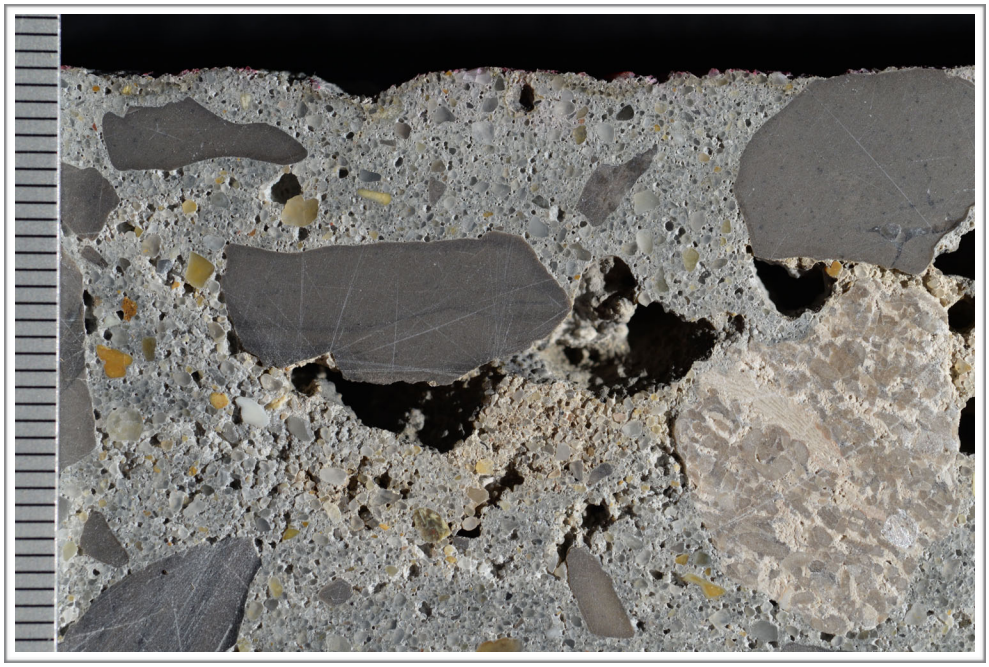

Figure I12. Photograph showing overview of polished surface at the top of Core P#2; scale in millimeters.

Figure I13. Photographs showing overview of polished surface in the middle of Core P#2; scale in millimeters.

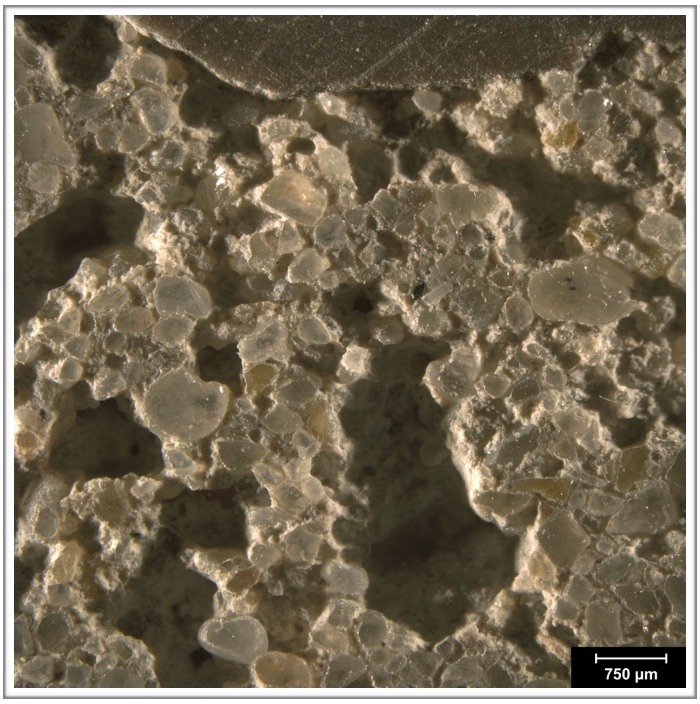

Figure I14. Reflected light photomicrograph of the polished surface showing voids and rough texture of the polished surface at the top of Core P#2.

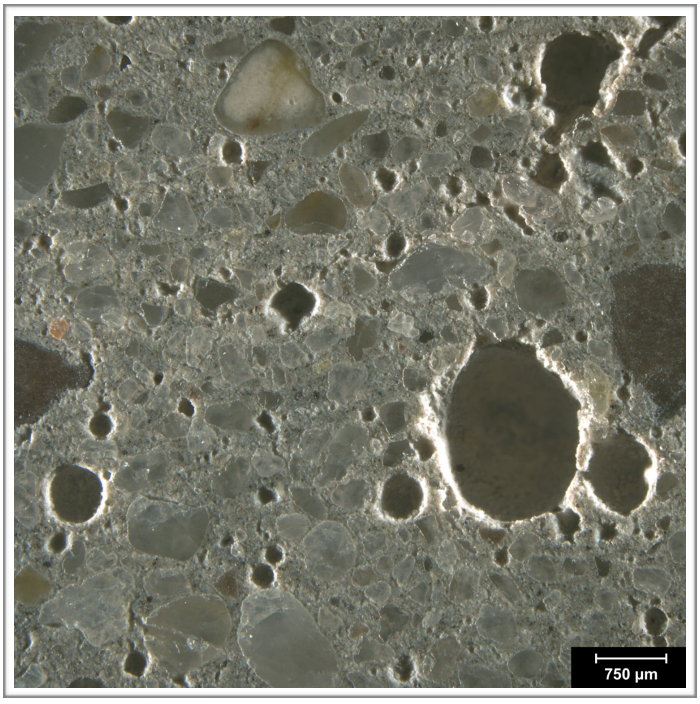

Figure I15. Reflected light photomicrograph of the polished surface showing voids and smooth texture of the polished surface in the middle of Core P#2.

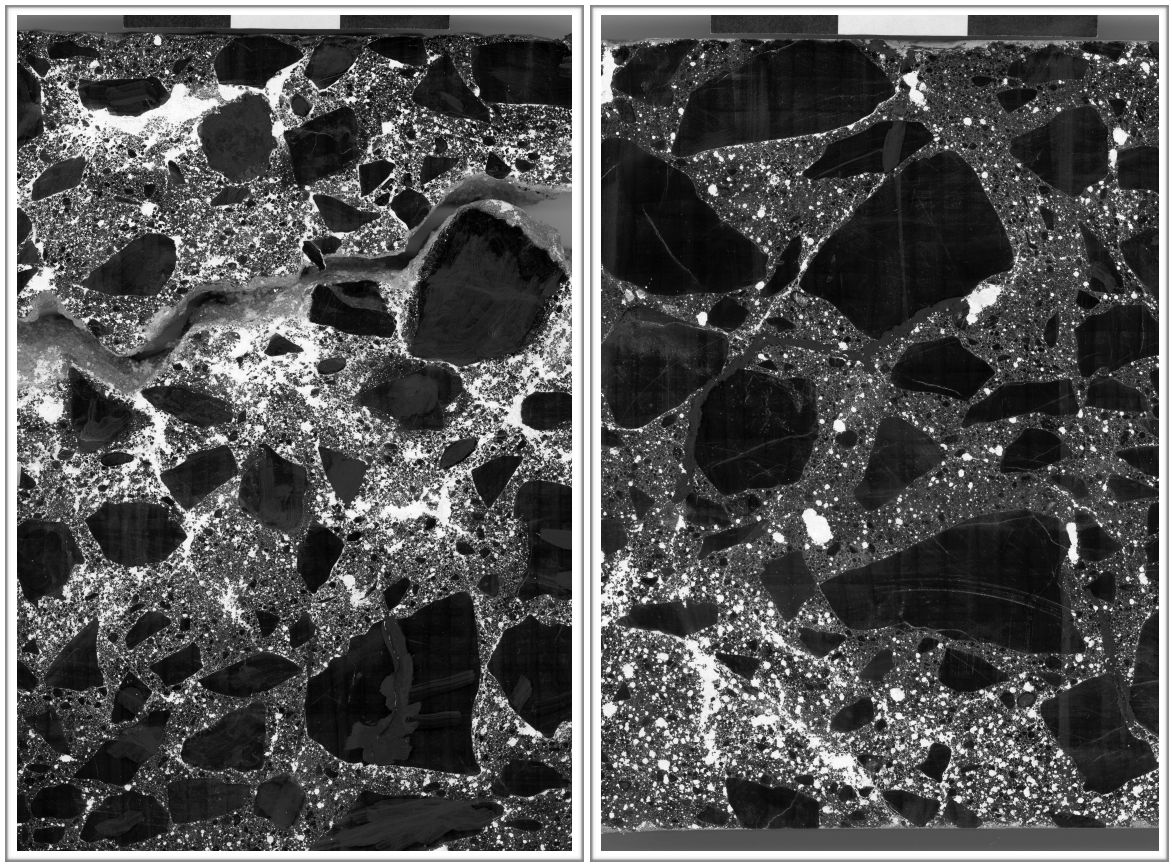

(a) (b)

Figure I16. Scanned images of polished surface Core P#2 after slab was prepared for enhanced contrast image analysis. The images represent areas at the (a) top of the core and (b) at the bottom of the core. In these images white areas represent voids and black areas represent paste and aggregate. The black and white bars at the top of each image are 75 mm (3 in.) across. Note that near the bottom of (a) the abundance of voids (white areas) is markedly lower than at the top. Also note that at the bottom of (b) there is a zone of high void content.

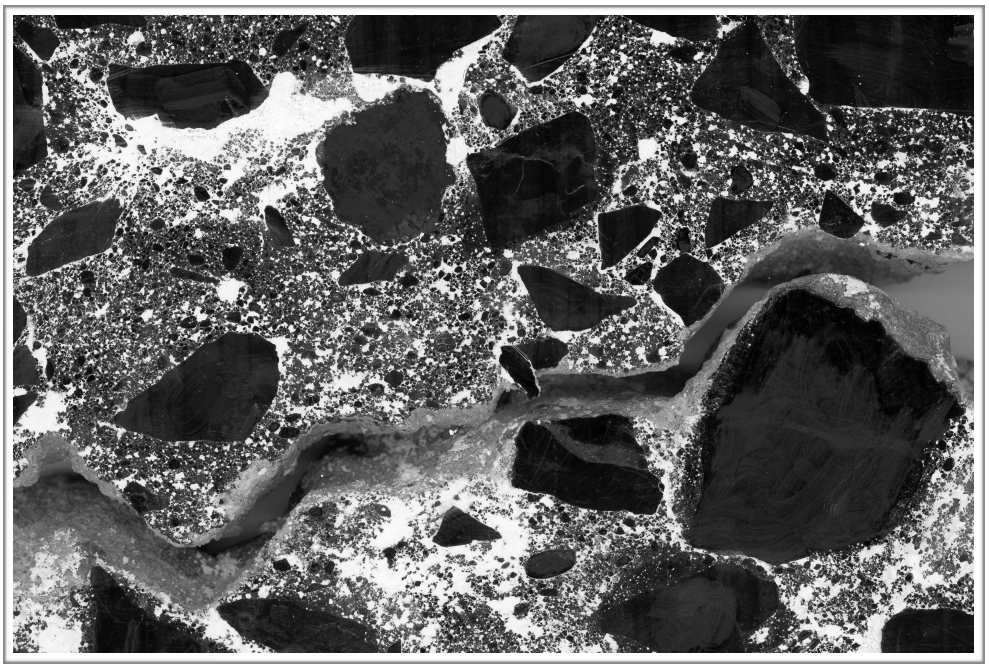

(a)

Figure I17. Cropped scanned image of enhanced contrast slab at the top of Core P#2. The HFW is ~ 135 mm (5 ¼ in.).

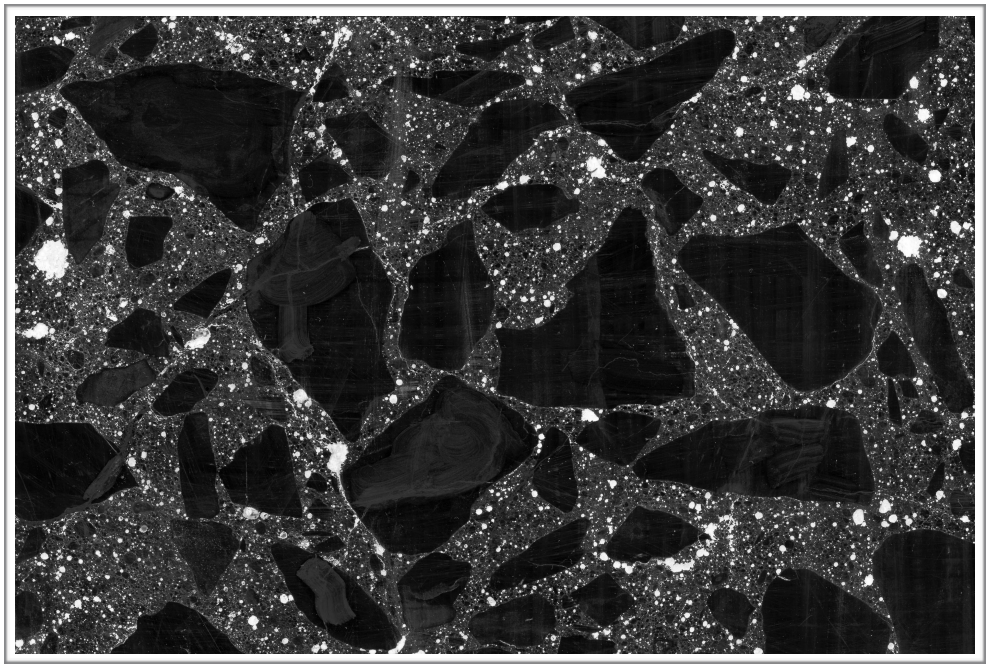

Figure I18. Cropped scanned image of enhanced contrast slab at the bottom of Core P#2. The HFW is ~ 135 mm (5 ¼ in.).

(a)

(b)

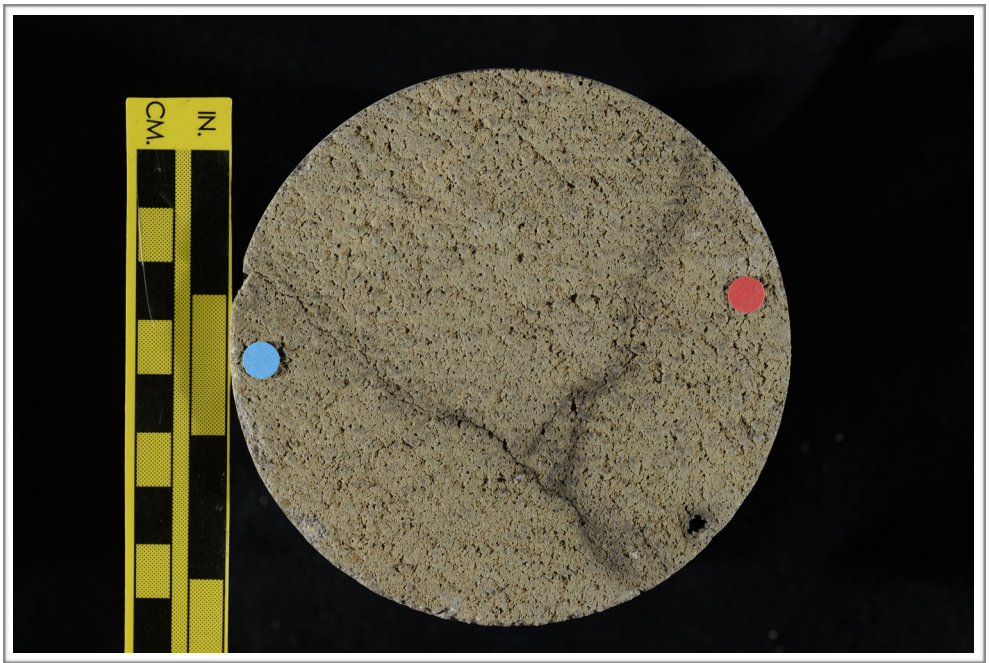

Figure I18. Photographs showing (a) oblique view of the outer surface and side of Core Wall #1 with identification labels and (b) the outer surface of Core Wall #1. The red and blue dots in (a) show the orientation of the saw cuts used to prepare the sample.

(c)

Figure I18 (cont'd). (c) Photograph showing the inner surface of Core Wall #1.

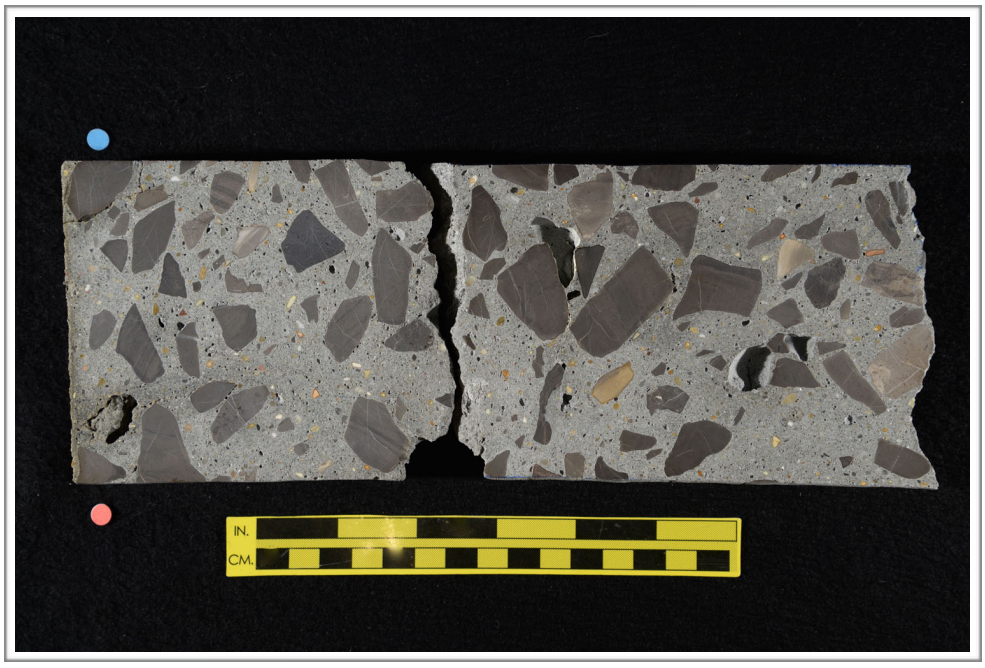

Figure I19. Photograph showing the polished surface of Core Wall #1.

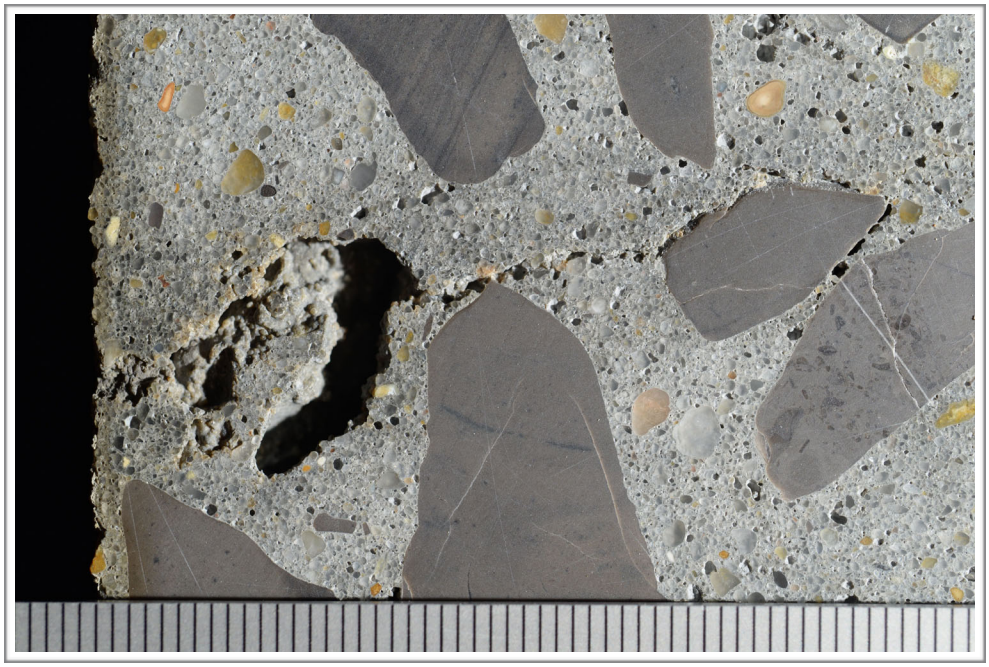

Figure I20. Photograph showing overview of polished surface at the outer end of Core Wall #1; scale in millimeters.

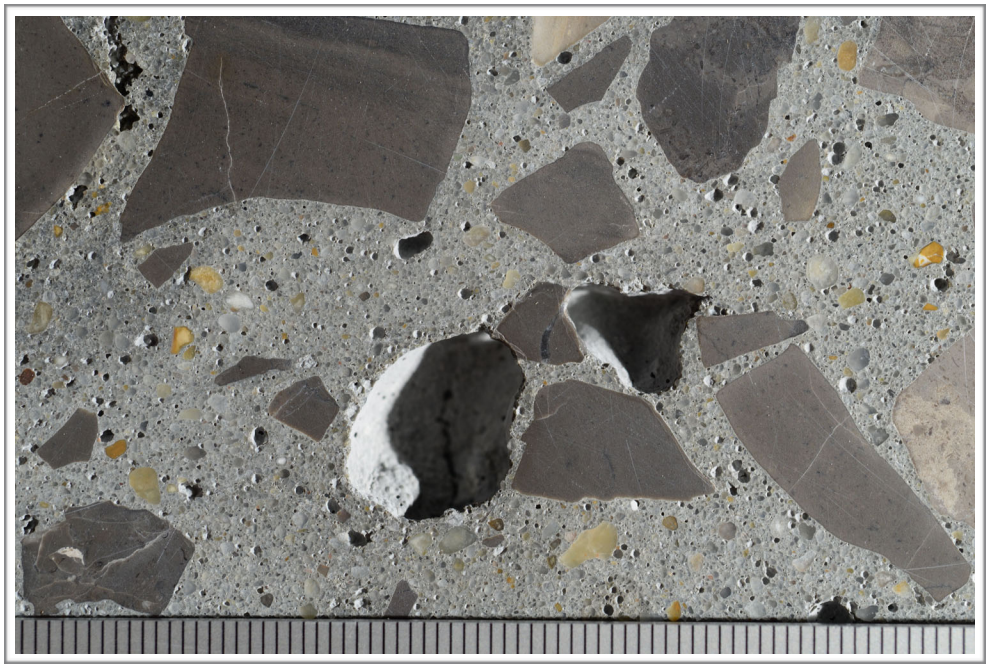

Figure I21. Photographs showing overview of polished surface in the middle of Core Wall #1; scale in millimeters.

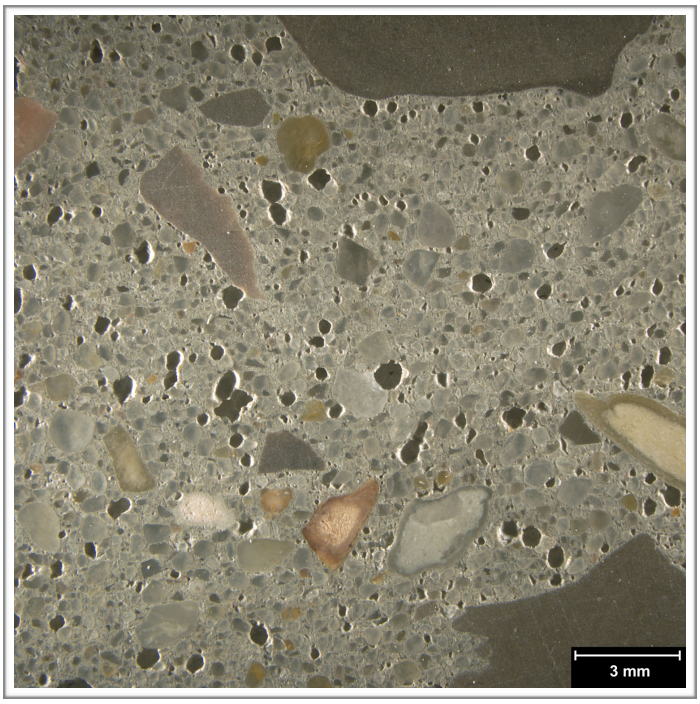

Figure I22. Reflected light photomicrograph of the polished surface showing voids and smooth texture of the polished surface at the outer end of Core Wall #1.

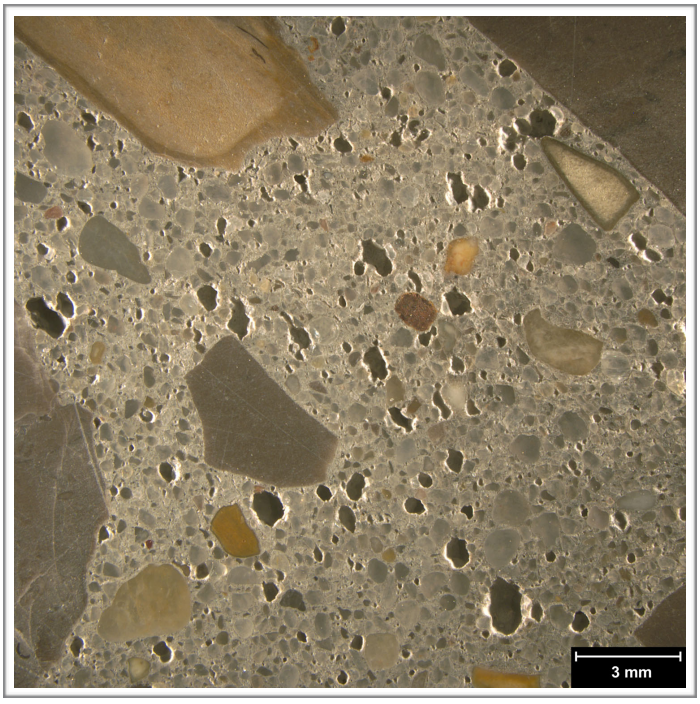

Figure I23. Reflected light photomicrograph of the polished surface showing voids and smooth texture of the polished surface in the middle of Core Wall #1.

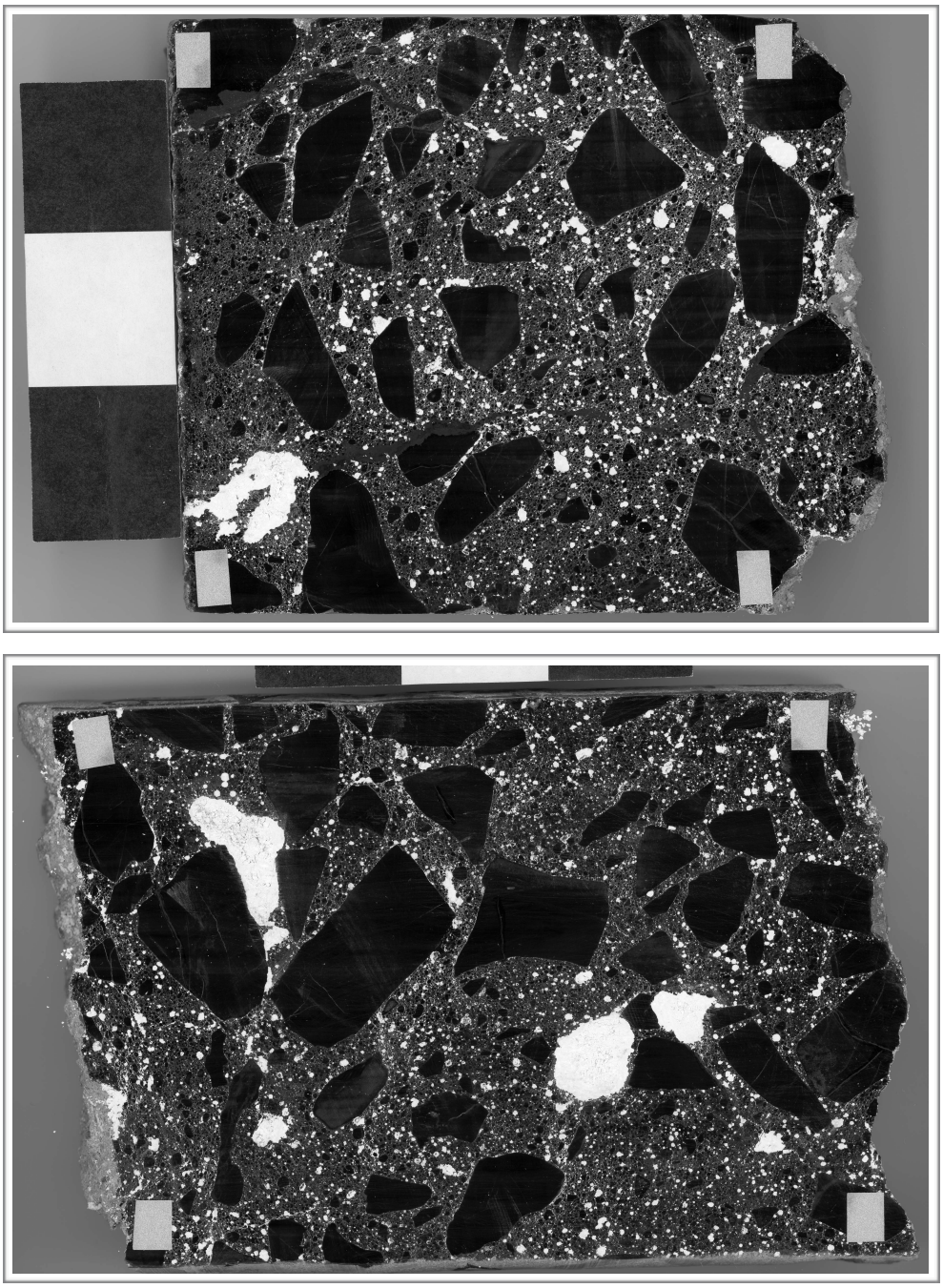

(a)

(b)

Figure I24. Scanned images of polished surface Core Wall #1 after slab was prepared for enhanced contrast image analysis. The images represent areas at the (a) outer end of the core and (b) at the middle of the core. In these images white areas represent voids and black areas represent paste and aggregate. The black and white bars shown in each image are 75 mm (3 in.) long.

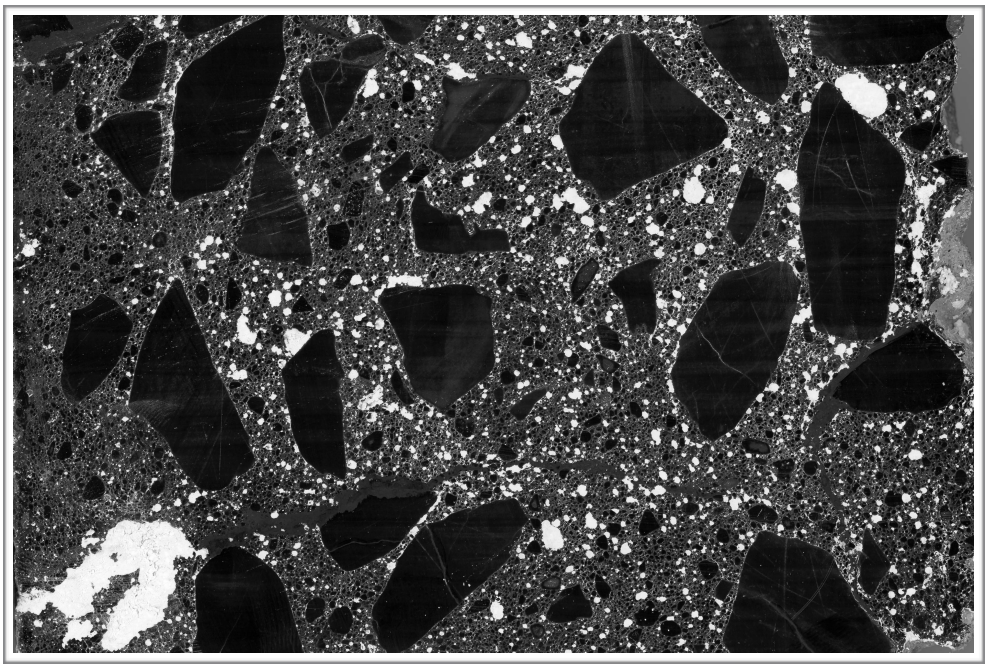

(a)

Figure I25. Cropped scanned image of enhanced contrast slab at the outer end of Core wall #1. The HFW is ~ 115 mm (4 ½ in.).

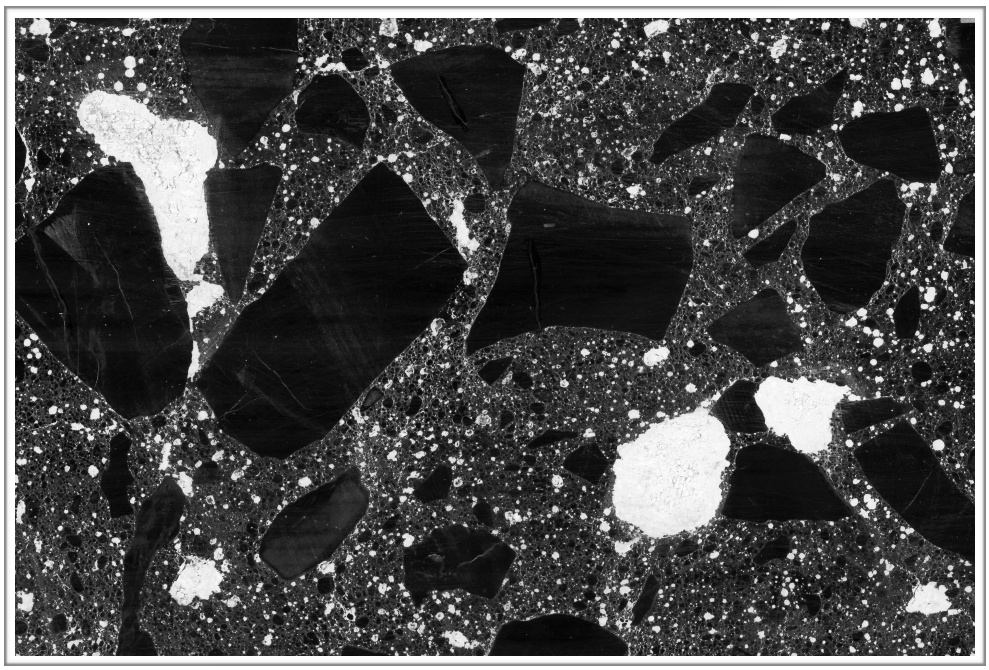

Figure I26. Cropped scanned image of enhanced contrast slab at the bottom of Core P#2. The HFW is ~ 100 mm (4 in.).

PROCEDURES

ASTM C856--Petrographic Analysis The petrographic work was done following ASTM C856 [**1**] with sample preparation done at **DRP** in the following manner. After writing the unique **DRP** sample number on each sample near the received label, the samples were measured and inspected visually and with a hand lens. The orientation of the saw cuts used to prepare the samples was then indicated on each sample with blue and red dots. The samples were then photographed in their as-received condition.

A slab representing a longitudinal cross section of each sample was cut from the central portion of the core using a Diamond Pacific® TR-24, a 24-inch diameter oil-lubricated saw. This produced three (3) longitudinal sections for each core. These sections were rinsed in an aqueous solution with a detergent to remove the cutting oil and oven dried overnight in a Gilson® Bench Top laboratory oven at ~ 40°C (~ 105°F) to remove remaining traces of the oil. After drying, each piece was labelled with the appropriate **DRP** sample number. One piece was set aside for phenolphthalein staining and the other was set aside for thin section preparation.

The central slab was then lapped and polished on a Diamond Pacific® RL-18 Flat Lap machine. This machine employs an 18-inch diameter cast iron plate onto which Diamond Pacific® Magnetic Nova Lap discs with progressively finer grits are fixed. The Nova Lap discs consist of a $^1/_{16}$ in. backing of solid rubber containing magnetized iron particles that is coated with a proprietary Nova resin-bond formula embedded with industrial diamonds of specific grit. The slab preparation involved the use of progressively finer wheels to a 3000 grit (~4 μm) final polish following procedures outlined in ASTM C457 [**2**]. An aqueous lubricant is used in the lapping and polishing process. The polished slab from each sample was examined visually and with a Nikon® SMZ-1500 stereomicroscope with 3-180x magnification capability following to the standard practice set forth in ASTM C856.

Phenolphthalein was applied to a freshly saw-cut surface from each sample to assess the extent of carbonation, along with thin section analysis. Phenolphthalein is an organic stain that colors materials with pH of greater than or equal to ~ 9.5 purple. Portland cement concrete generally has a pH of ~ 12.5. Carbonation lowers the pH of the paste below 9.5, so areas not stained by phenolphthalein are an indicator of carbonation. The depth of paste not stained by phenolphthalein was measured from each exposed surface.

Petrographic thin sections were prepared by cutting billets from the remaining longitudinal section. Outlines marking the area of the billets were drawn with a marker on the saw-cut surface after visual and microscopical examination of saw-cut and polished surfaces. The billets were labeled with the unique **DRP** number assigned to the sample and impregnated with epoxy. The impregnated billets

1 *Standard Practice for Petrographic Examination of Hardened Concrete.* Annual Book of ASTM Standards, Vol. 4.02., ASTM C856-14.

2 *Standard Test Method for Microscopical Determination of Parameters of the Air-Void System in Hardened Concrete*, Annual Book of ASTM Standards, Vol. 4.02, ASTM C457-12.

were then fixed to glass slides with epoxy. After the epoxy cured, the slide was trimmed and ground on a Buehler® Petro-Thin device to a thickness of ~ 30 µm (1.2 mil). The slide was then moved to a Buehler® Beta-Vector machine and polished to a final thickness of ~ 20 µm. The grinding and polishing of the thin sections were done in a non-aqueous environment. The thin sections were examined with a Nikon® E-Pol 600 petrographic microscope equipped to provide a 50-1000x magnification range following the standard practice set forth in ASTM C856.

ASTM C1723 Electron Microscopy A FEI™ Quanta 250 Environmental Scanning Electron Microscope (ESEM) was used to supplement the petrographic methods described above (see ASTM C1723 [**3**]). The Quanta 250 is capable of operation in three different vacuum modes: high vacuum (< 6 e^{-4} Pa) for conductive or conventionally prepared specimens; low vacuum (10-130 Pa) for non-conductive specimens without preparation; and ESEM™ mode (10-2600 Pa) for specimens such as hydrous materials (cement paste) that are incompatible with high vacuum. The instrument is equipped with several detectors for imaging: an Everhardt Thornley secondary electron detector (SED), a Large Field, Low vacuum SED, a high-sensitivity, low kV solid state backscatter electron detector (BSED), and gaseous SED and BSED for ESEM conditions.

The instrument uses a Tungsten hairpin filament mounted within a tetrode gun assembly and operates with an accelerating voltage of 200 V to 30 kV with beam currents up to 2 µA. The instrument has a magnification range from 6 to more than 1,000,000 x. The resolution of the instrument is as follows (measured as particle separation on a carbon substrate):

High vacuum mode: 3.0 nm at 30 kV and 8.0 nm at 3 kV for SED
4.0 nm at 30 kV for BSED

Low vacuum mode: 3.0 nm at 30 kV and 10.0 nm at 3 kV for SED
4.0 nm at 30 kV for BSED

Extended vacuum mode (ESEM): 3.0 nm at 30 kV for SED

The Quanta is also with an equipped with an EDAX® Apollo X Silicon Drift Detector for Energy Dispersive X-ray (EDX) analysis. The Apollo X is equipped with a 10 mm^2 window and has a resolution of 131 eV or better with peak to background ratios that are greater than 10,000:1. The detector is capable of handling input count rates up to 850,000 cps and throughput of more than 350,000 cps. The detector is capable of detecting all chemical elements down to Beryllium and is capable of quantitative analyses down to and including Boron. The EDX has a take-off angle of 35º at a 10 mm working distance.

---

3 *Standard Guide for Examination of Hardened Concrete Using Scanning Electron Microscopy,* Annual Book of ASTM Standards, Vol. 4.02, ASTM C1723-10.

Sections are prepared for the ESEM/EDX work in the following manner. After visual and microscopic examination of the polished surface used for stereomicroscopy, a coupon measuring ~ 50 mm x 50 mm (2 x 2 in.) in area and ~ 15 mm (⅝ in.) in thickness is cut out of one of the hemicylindrical sections from the core. The sample is then lapped and polished using rigid polishing wheels (Buehler Meta-Di Supreme™) embedded with the following sequence of progressively finer grits of industrial diamonds: 165 µm, 45 µm, 15 µm, 9 µm, 3 µm and 0.5 µm. A 0.05 µm diamond suspension and polishing cloth is used for the final polishing step. None of the abrasive wheels or suspensions contain silicon, aluminum or cesium.

For the present investigation, uncoated polished samples were examined in the low vacuum (~ 70 Pa) mode using an accelerating voltage of 15 kV and a spot size of 5, which gives a count rate of ~ 3,000 counts per second. Counting times of 10 seconds were used for the EDX analyses.

ASTM C457 Air Content Determinations The air void analyses were done using the modified point-count method outlined in ASTM C457. The point counts were done under oblique illumination at a magnification of 125 with a stepping distance of 1.9 mm (0.075 in.) between traverse points. Each point was tabulated and recorded as aggregate, paste or a void to allow the measurement of the volumetric proportions of air, paste, and aggregate. Note that the point counts did not conform to the number of points required by ASTM C457, but were done to provide key data (paste content) for the image analysis as well as an informal check on the image analysis.

The samples were also analyzed using the enhanced contrast method described in Petersen et al. [**4**] This method is currently a ballot item for approval by ASTM. It is similar to methods used internationally such as Rapid-Air™. The polished slab is blackened with a wide-tipped black permanent marker. Several coats are applied, changing the orientation of the lines 90º between coats. Wollastonite powder is then worked into the samples and the excess is scraped away, which leaves the powder embedded in the voids. The residual powder is removed using an oiled fingertip. The slab is inspected under the stereoscopic microscope and pores within aggregate particles and cracks in the paste are darkened with a fine-tipped black permanent marker. The specimen was scanned at 16 bit resolution using a conventional desktop flatbed Epson photo scanner. The image is scanned at a resolution of 3200 dpi and saved in TIFF format. The image is then processed using the open source software program Bubble Counter (https://github.com/mtu-most/bubblecounter). This software acts as a plugin for the widely available Image J image analysis program that was developed by the National Institute of Health (at http://imagej.nih.gov/ij/). Each core was analyzed using bubble counter and results compared to the data obtained manually. There was excellent agreement between the point count data and the image analysis data.

4 Petersen, K., Sutter, L., and Radlinski, M., 2009, *The Practical Application of a Flatbed Scanner for Air-Void Characterization of Hardened Concrete,* Journal of ASTM International, vol. 6, no. 9, p. 1-15.

This public document is published at a total cost of $250
42 copies of this public document were published in this first printing at a cost of $250. The total cost of all printings of this document including reprints is $250. This document was published by Louisiana Transportation Research Center to report and publish research findings as required in R.S. 48:105. This material was duplicated in accordance with standards for printing by state agencies established pursuant to R.S. 43:31. Printing of this material was purchased in accordance with the provisions of Title 43 of the Louisiana Revised Statutes.